



Dublin City University  
Ollscoil Chathair Bhaile Átha Cliath  
School of Chemical Sciences.

Development of fast ion chromatography.

Damian Connolly

PhD 2005.

# **Development of fast ion chromatography.**

by

**Damian Connolly B.Sc. (Hons), AMRSC.**

**A thesis submitted to Dublin City University in part fulfilment for the degree of**

**DOCTOR OF PHILOSOPHY**

**Dublin City University.  
School of Chemical Sciences.  
Supervisor: Dr. Brett Paull.**

**February 2005**

**Volume 1 of 2.**

For my parents

### **Authors declaration**

*I hereby certify that this material, which I now submit for assessment on the programme of study leading to the award of Doctor of Philosophy is entirely my own work and has not been taken from the work of others' save and to the extent that such work has been cited and acknowledged within the text of my work.*

Signed: Damian Connolly

I.D. no: 95050299

Date: 31 Jan 2005

This copy of the thesis has been supplied on condition that anyone who consults it is understood to recognise that its copyright rests with the author and that no quotation from the thesis and no information derived from it may be published without the author's prior consent.

## **Abstract.**

Fast ion chromatography has been applied to short (3 cm) silica based ODS columns with a view to achieving rapid determinations of selected inorganic anions. The use of smaller stationary phase particle sizes (3  $\mu\text{m}$ ) allowed higher flow rates (2.0 – 2.5 ml/min) to be used while maintaining chromatographic efficiency due to the favorable Van Deemter curves obtained as particle size decreases. Using ion-interaction chromatography and direct UV detection, eight anions were separated in under four minutes with the first five anions separated in < 50 seconds; this separation was subsequently applied to the rapid analysis of nitrite and nitrate in tap water. With the addition of a peristaltic pump and in-line filter, up to 60 analyses per hour could be carried out unattended using an on-line system, which matches the analysis rate possible with traditional FIA based methods. This mobile phase was further modified such that nitrate, nitrite and thiocyanate could be rapidly determined in urine samples as a means to quantitatively evaluate smoking behavior.

Subsequently, the same column was permanently coated using didodecyldimethylammonium bromide (DDAB) and anion exchange chromatography used for the isocratic separation of nine common anions in 160 seconds, with the first seven anions, including phosphate, chloride and sulphate, separated within only 65 seconds using a simple phthalate eluent. The high capacity, highly hydrophobic ion exchange coating demonstrated excellent stability over time, even at elevated temperatures (45 °C). The developed chromatography was successfully applied to the rapid analysis of river water, tap water and relatively high ionic strength seawater samples with minimal sample preparation required.

Multi-valent eluents were briefly applied to this column with a view to achieving faster separations, with further studies also involved the use of dipicolinic acid eluents, which allowed the simultaneous separation of chloride, sulphate, nitrate, carbonate, magnesium and calcium, in less than 180 seconds.

Short monolithic silica ODS columns were used with a tetrabutylammonium-phthalate eluent and direct conductivity detection for the rapid analysis of six

common inorganic anions in < 60 seconds. Van deemter curves for this monolithic column showed that considerably higher flow rates could be used without adversely affecting efficiency relative to 3  $\mu\text{m}$  particulate columns due to the improved permeability of these phases. Finally, two short  $\text{C}_{18}$  monoliths were coated with DDAB and DOSS and individually used to separate eight anions in 100 seconds and five cations in 100 seconds using a common phthalate/ethylenediamine eluent. By subsequently coupling the columns in parallel, the with the eluent delivered using a flow splitter from a single isocratic pump, the simultaneous analysis of anions and cations was also possible, based on a single conductivity detector.

## Acknowledgements.

Firstly, I would like to thank my parents for having supported me through almost ten years of university to get me to this stage.

My thanks to the entire chemistry technician staff for all their help over the last five years, in particular, Ambrose May, Maurice Burke and Mary Ross.

I would like to especially thank the members of my research group for lightening my mood during dark times, and for the *countless* times in which they dispensed technical advice; Colman, Edel, Danielle, Wasim, Johnny, Leon, Marion and Eadaoin. I would like to particularly thank Leon, for his patience and understanding every time I commandeered his LC instrument!! Thanks also to Marion King and Keiran Nolan for their kind donation of biological samples for study. My thanks to Kathleen for keeping me awake during those long late nights of typing, to Liam, John, Ray and Brendan Duffy for helping to calm my last-minute nerves with their computer know-how, and to Aoife Morrin and Blathnaid White for advice and equipment. I would like to thank Marianne for being there for me and for calming my nerves before (and after) my viva. Thanks Marianne!! I would especially like to thank all the DCU chemistry postgrad community, particularly those who have become good friends.

I would like to thanks Swords Laboratories for funding my research over these last five years.

Finally, and most importantly, I would like to offer my sincerest thanks to my supervisor, Dr. Brett Paull. Performing my research as a part-time student was a huge challenge for me, which was made bearable by having Brett as a supervisor, who always showed endless patience and boundless enthusiasm. He was always there to offer advice and suggestions, and afforded me the opportunity to travel to a number of research symposia, from Nice to Chicago. The last five years were not half as traumatic as one might expect, due in no small part to Brett's supervision. Thanks Brett!!

<b><u>Contents</u></b>	<b><u>Page</u></b>
Author's Declaration.....	v
Copyright statement.....	vi
Abstract.....	vii
Acknowledgements.....	ix
List of contents (volume 1 of 2).....	x
Abbreviations.....	xiv
List of figures (volume 1 of 2).....	xvii
List of tables (volume 1 of 2).....	xxvii
Publications, conferences and oral presentations.....	xxviii
<b>1 Introduction to fast liquid chromatography.....</b>	<b>1-1</b>
<b>1.1 The effect of smaller particles on efficiency.....</b>	<b>1-2</b>
<b>1.2 Advantages of fast LC.....</b>	<b>1-7</b>
<b>1.3 Applications of fast LC.....</b>	<b>1-11</b>
1.3.1 Pharmaceuticals.....	1-11
1.3.2 Protein and peptide separations.....	1-13
<b>1.4 Monolithic columns.....</b>	<b>1-17</b>
1.4.1 Preparation of monoliths.....	1-19
1.4.2 Control of macropore size during synthesis.....	1-20
1.4.3 Control of mesopore size during synthesis.....	1-21
1.4.4 Coupling of monolithic columns in series.....	1-22
1.4.5 Flow gradients with monolithic columns.....	1-23
1.4.6 Separation impedance of monoliths relative to particulate columns.....	1-23
1.4.7 Evaluation of separation efficiency of monolithic columns..	1-24
<b>1.5 Instrumental considerations for fast LC.....</b>	<b>1-27</b>
1.5.1 Data acquisition for fast LC.....	1-29
1.5.2 Signal-to-noise ratio determinations.....	1-31
1.5.3 Autosamplers in fast LC.....	1-32
<b>1.6 Elevated column temperature for fast LC.....</b>	<b>1-33</b>
1.6.1 Effect of temperature on selectivity in ion-exchange	

chromatography.....	1-38
<b>1.7 Ion interaction chromatography.....</b>	<b>1-41</b>
1.7.1 The ion-pair model.....	1-45
1.7.2 The dynamic ion-exchange model.....	1-46
1.7.3 The ion-interaction model.....	1-47
<b>1.8 Detection methods for ion-exchange and ion-interaction chromatography.....</b>	<b>1-52</b>
1.8.1 Conductivity detection.....	1-52
1.8.1.1 <i>Effect of temperature upon conductivity detection.</i>	1-58
1.8.2 Spectrophotometric detection.....	1-58
1.8.2.1 <i>System peaks</i> .....	1-61
<b>1.9 References.</b>	<b>1-62</b>
<b>2 Fast Separation of UV-Absorbing Anions Using Ion-interaction Chromatography.....</b>	<b>2-1</b>
<b>2.1 Introduction.....</b>	<b>2-1</b>
<b>2.2 Experimental.....</b>	<b>2-3</b>
2.2.1 Equipment.....	2-3
2.2.2 Reagents and chromatographic conditions.....	2-3
<b>2.3 Results and discussion.....</b>	<b>2-4</b>
2.3.1 Mobile phase optimization.....	2-4
2.3.2 Optimization of column temperature.....	2-15
2.3.3 Effect of flow rate.....	2-20
2.3.4 Data acquisition in rapid chromatography.....	2-24
2.3.5 Speciation studies.....	2-25
<b>2.4 Conclusions.....</b>	<b>2-30</b>
<b>2.5 References.....</b>	<b>2-30</b>

<b>3 Rapid online determination of nitrate and nitrite in drinking water using ion-interaction liquid chromatography.....</b>	<b>3-1</b>
<b>3.1 Introduction.....</b>	<b>3-1</b>
<b>3.2 Experimental.....</b>	<b>3-10</b>
3.2.1 Equipment.....	3-10
3.2.2 Reagents.....	3-10
<b>3.3 Results and discussion.....</b>	<b>3-11</b>
3.3.1 Determination of nitrate/nitrite in water samples.....	3-12
3.3.2 On-line determination of nitrate and nitrite in drinking water.....	3-17
3.3.3 Analytical performance characteristics.....	3-22
3.3.3.1 <i>System precision</i> .....	3-22
3.3.3.2 <i>Detector linearity</i> .....	3-24
3.3.3.3 <i>Sensitivity</i> .....	3-28
3.3.3.4 <i>Interferences</i> .....	3-31
3.3.3.5 <i>System accuracy/comparative analysis</i> .....	3-32
<b>3.4 Conclusions.....</b>	<b>3-37</b>
<b>3.5 References.....</b>	<b>3-37</b>

<b>4 Determination of urinary thiocyanate, nitrate and nitrite using fast ion-interaction chromatography.....</b>	<b>4-1</b>
<b>4.1 Introduction.....</b>	<b>4-1</b>
4.1.1 Thiocyanate in biological fluids.....	4-1
4.1.2 Nitrate and nitrite in biological fluids.....	4-5
<b>4.2 Experimental.....</b>	<b>4-9</b>
4.2.1 Equipment.....	4-9
4.2.2 Reagents and chromatographic conditions.....	4-9
4.2.3 Sample pre-treatment.....	4-9
<b>4.3 Results and discussion.....</b>	<b>4-10</b>

4.3.1	Preliminary studies of saliva analysis.....	4-10
4.3.2	Mobile phase optimisation for analysis of urine.....	4-11
4.3.3	Optimisation of detection parameters.....	4-15
4.3.4	Precision, linearity and detection limits.....	4-16
4.3.5	Analysis of real samples.....	4-21
4.3.6	Additional spike linearity data and working range studies...	4-25
4.3.7	Comparative analysis using anion exchange chromatography.....	4-33
	4.3.7.1 <i>Mobile phase optimisation</i> .....	4-34
	4.3.7.2 <i>System precision</i> .....	4-35
	4.3.7.3 <i>Linearity studies</i> .....	4-35
	4.3.7.4 <i>Sensitivity</i> .....	4-38
	4.3.7.5 <i>Analysis of real samples; thiocyanate spike linearity</i> .....	4-40
	4.3.7.6 <i>Use of an AG17 guard column to reduce analysis times</i> .....	4-42
<b>4.4</b>	<b>Conclusions</b> .....	4-43
<b>4.5</b>	<b>References</b> .....	4-43

## Abbreviations.

<b>ACN</b>	<b>Acetonitrile.</b>
<b>ASRS</b>	<b>Anion self-regenerating suppressor.</b>
<b>AU</b>	<b>Absorbance units.</b>
<b>CE</b>	<b>Capillary electrophoresis.</b>
<b>CSRS</b>	<b>Cation self-regenerating suppressor.</b>
<b>CTA+</b>	<b>Cetyltrimethylammonium cation.</b>
<b>CTAB</b>	<b>Cetyltrimethylammonium bromide.</b>
<b>CTAC</b>	<b>Cetyltrimethylammonium chloride.</b>
<b>CZE</b>	<b>Capillary zone electrophoresis.</b>
<b>DAN</b>	<b>2,3-diaminonaphthalene</b>
<b>DCTA</b>	<b><i>trans</i>-1,2-diaminecyclohexane-<i>N,N,N',N'</i>-tetraacetic acid</b>
<b>DDA+</b>	<b>Didodecyldimethylammonium cation.</b>
<b>DDAB</b>	<b>Didodecyldimethylammonium bromide.</b>
<b>DLPC</b>	<b>1,2-dilauroyl-<i>sn</i>-phosphatidylcholine</b>
<b>DMF</b>	<b>Dimethylformamide.</b>
<b>DOSS</b>	<b>Diocylsulphosuccinate.</b>
<b>EDA</b>	<b>Ethylenediamine.</b>
<b>EDTA</b>	<b>Ethylenediaminetetraacetic acid</b>
<b>EDTA-2K</b>	<b>Ethylenediaminetetraacetic acid dipotassium salt.</b>
<b>EOF</b>	<b>Electro-osmotic flow.</b>
<b>EU</b>	<b>European Union.</b>
<b>FIA</b>	<b>Flow injection analysis.</b>
<b>GC</b>	<b>Gas chromatography.</b>
<b>HDTMA</b>	<b>Hexadecyltrimethylammonium.</b>
<b>HETP</b>	<b>Height equivalent of a theoretical plate.</b>
<b>HPLC</b>	<b>High pressure liquid chromatography.</b>
<b>I.D.</b>	<b>Internal diameter.</b>
<b>IIR</b>	<b>Ion interaction reagent.</b>
<b>L.O.D.</b>	<b>Limit of detection.</b>
<b>LC</b>	<b>Liquid chromatography.</b>
<b>Li-DS</b>	<b>Lithium dodecylsulphate.</b>

<b>MCL</b>	<b>Maximum contaminant level.</b>
<b>MCLG</b>	<b>Maximum contaminant level goal.</b>
<b>3,4-MDMA</b>	<b>3,4-methylenedioxymethamphetamine.</b>
<b>MeOH</b>	<b>Methanol.</b>
<b>MQC</b>	<b>Minimum quantifiable change.</b>
<b>MS</b>	<b>Mass spectrometry.</b>
<b>MSA</b>	<b>Methanesulphonic acid.</b>
<b>MW</b>	<b>Molecular weight.</b>
<b>NAT</b>	<b>2,3-naphthotriazole</b>
<b>1,5-NDS</b>	<b>Naphthalene-1,5-disulphonate.</b>
<b>NGB</b>	<b>Naphthol green B.</b>
<b>NO</b>	<b>Nitric oxide.</b>
<b>NPS-RP</b>	<b>Non-porous silica reversed phase.</b>
<b>O.D.</b>	<b>Outer diameter.</b>
<b>ODS</b>	<b>Octadecylsilane.</b>
<b>PDCA</b>	<b>Pyridine dicarboxylic acid.</b>
<b>PEEK</b>	<b>Polyether-ether-ketone.</b>
<b>PEG</b>	<b>Poly(ethylene glycol).</b>
<b>phen</b>	<b>Phenyl.</b>
<b>PS-DVB</b>	<b>Polystyrene divinylbenzene.</b>
<b>PTFE</b>	<b>Polytetrafluoroethylene.</b>
<b>rFIA</b>	<b>Reversed flow injection analysis.</b>
<b>RMS</b>	<b>Root mean square.</b>
<b>RSD</b>	<b>Relative standard deviation.</b>
<b>S/N</b>	<b>Signal/noise.</b>
<b>SAX</b>	<b>Strong anion exchange.</b>
<b>SCX</b>	<b>Strong cation exchange.</b>
<b>SPE</b>	<b>Solid phase extraction.</b>
<b>TBA</b>	<b>Tetrabutylammonium.</b>
<b>TBA-Cl</b>	<b>Tetrabutylammonium chloride.</b>
<b>TBA-OH</b>	<b>Tetrabutylammonium hydroxide.</b>
<b>TEA</b>	<b>Tetraethylammonium</b>
<b>TFA</b>	<b>Trifluoroacetic acid.</b>

<b>THA</b>	<b>Tetrahexylammonium</b>
<b>TMA</b>	<b>Tetramethylammonium.</b>
<b>TPA</b>	<b>Tetrapropylammonium</b>
<b>TPA-OH</b>	<b>Tetrapropylammonium hydroxide.</b>
<b>TPeA</b>	<b>Tetrapentylammonium.</b>
<b>USEPA</b>	<b>United States Environmental Protection Agency.</b>
<b>UV</b>	<b>Ultraviolet.</b>
<b>UV-Vis</b>	<b>Ultraviolet-Visible.</b>

## List of figures.

- Figure 1-1.** *Typical Van Deemter plot.*
- Figure 1-2.** *Van Deemter's curves showing how efficiency is inversely proportional to particle size for 10  $\mu\text{m}$ , 5  $\mu\text{m}$  and 3  $\mu\text{m}$  columns.*
- Figure 1-3.** *Analysis of caffeine by fast LC.*
- Figure 1-4.** *Analysis of phenol priority pollutants by fast LC.*
- Figure 1-5.** *Ultra fast separation of a five-component mixture by fast LC.*
- Figure 1-6.** *Rapid chlorthalidone HPLC assay by fast LC.*
- Figure 1-7.** *Rapid separation of six proteins on a short Micra NPS-RP column.*
- Figure 1-8.** *Rapid separation of a tryptic digest of haemoglobin A on a Micra NPS-RP column at 70 °C.*
- Figure 1-9.** *Macroporous structure of monolithic silica.*
- Figure 1-10.** *Mesoporous structure of monolithic silica.*
- Figure 1-11.** *Van Deemter plots for a C<sub>18</sub> monolith (closed symbols) and a Capcellpak C<sub>18</sub> SG 5  $\mu\text{m}$  column (open symbols) with amylbenzene (●,○) and insulin (■,□) as solutes.*
- Figure 1-12.** *Comparison of different detector response times on peak shape in fast LC.*
- Figure 1-13.** *Van Deemter curves showing decreased plate height with increasing column temperature.*
- Figure 1-14.** *The effect of thermally mismatched mobile phase temperatures and column temperatures upon peak efficiency.*
- Figure 1-15.** *Chromatograms showing the effect of increased column temperature*

*upon the rapid separation of a mixture of alkylphenones.*

**Figure 1-16.** *Effect of increased column temperature upon selectivity for a separation of nine cations.*

**Figure 1-17.** *Schematic of the “ion-pair retention model” for ion-interaction chromatography.*

**Figure 1-18.** *Schematic of the “dynamic ion-exchange model” for ion-interaction chromatography.*

**Figure 1-19.** *Schematic of the “ion-interaction model” for ion-interaction chromatography.*

**Figure 1-20.** *Mechanism of suppression in suppressed IC.*

**Figure 2-1.** *Effect of % MeOH upon the retention of UV absorbing anions.*

**Figure 2-2.** *Effect of IIR concentration upon the retention of UV absorbing anions.*

**Figure 2-3.** *Effect of IIR concentration upon the retention of weakly retained UV absorbing anions.*

**Figure 2-4.** *Schematic showing the test mobile phases within the chosen experimental search area. Each green symbol represents a mobile phase preparation with the concentrations of methanol and TBA indicated.*

**Figure 2-5.** *Response surface for mobile phase optimisation showing normalised resolution production (R) as a function of mobile phase IIR concentration and % MeOH for a standard mixture of bromate, nitrite, bromide, nitrate, thiosulphate, iodide and benzoate.*

**Figure 2-6.** *Optimised mobile phase for determination of eight UV absorbing*

anions by ion-interaction chromatography on a short 3 cm 3  $\mu$ m column.

**Figure 2-7.** *Response surface for mobile phase optimisation showing normalised resolution product (R) as a function of mobile phase IIR concentration and % MeOH for a standard mixture of bromate, nitrite, bromide and nitrate, the weakly retained subgroup of anions.*

**Figure 2-8.** *Optimised mobile phase for determination of five “weakly retained” UV absorbing anions by ion-interaction chromatography on a short 3 cm 3  $\mu$ m column.*

**Figure 2-9.** *Effect of temperature upon the retention of UV absorbing anions in ion-interaction chromatography on a short 3 cm 3  $\mu$ m column.*

**Figure 2-10.** *Separation of eight anions by ion-interaction chromatography on a short 3 cm 3  $\mu$ m column at the optimum column temperature.*

**Figure 2-11.** *Effect of temperature in ion-interaction chromatography upon the normalised resolution product for a test mixture of eight UV absorbing anions and for the “weakly retained subgroup”.*

**Figure 2-12.** *Effect of temperature upon the separation efficiency of a test mixture of eight UV absorbing anions in ion-interaction chromatography.*

**Figure 2-13.** *Effect of flow rate upon the separation efficiency of a test mixture of “weakly retained” anions in ion-interaction chromatography.*

**Figure 2-14.** *Optimised separation of five inorganic UV-absorbing anions by fast ion-interaction chromatography on a short 3 cm 3  $\mu$ m column.*

**Figure 2-15.** *Effect of flow rate upon the separation efficiency of a test mixture of eight UV absorbing anions by ion-interaction chromatography on a*

*short 3 cm 3  $\mu$ m column.*

**Figure 2-16.** *Effect of flow rate upon the normalised resolution product of a test mixture of eight UV absorbing anions in ion-interaction chromatography.*

**Figure 2-17.** *Optimised separation of eight UV absorbing anions by fast ion-interaction chromatography on a short 3 cm 3  $\mu$ m column.*

**Figure 2-18.** *Data acquisition rate for a rapidly eluting peak (bromide) by fast ion-interaction chromatography on a short 3 cm 3  $\mu$ m column.*

**Figure 2-19.** *Ultra-fast separation of iodate and iodide by ion-interaction chromatography on a short 3 cm 3  $\mu$ m column.*

**Figure 2-20.** *Ultra-fast separation of 5 mg/L bromate and bromide by ion-interaction chromatography on a short 3 cm 3  $\mu$ m column.*

**Figure 2-21.** *Ultra-fast separation of nitrite and nitrate by ion-interaction chromatography on a short 3 cm 3  $\mu$ m column.*

**Figure 3-1.** *Rapid separation of five inorganic UV-absorbing anions by ion interaction chromatography on a short 3  $\mu$ m C<sub>18</sub> column.*

**Figure 3-2.** *Optimisation of detector wavelength for the determination of nitrate and nitrite by fast ion interaction chromatography.*

**Figure 3-3.** *Comparison of noise generated by the injection of a water blank compared with a mobile phase blank by ion interaction chromatography.*

**Figure 3-4.** *Rapid determination of nitrate/nitrite by ion interaction chromatography on a short 3  $\mu$ m C<sub>18</sub> column.*

- Figure 3-5.** *Rapid determination of nitrate/nitrite levels in river water by ion interaction chromatography on a short 3  $\mu\text{m}$   $\text{C}_{18}$  column.*
- Figure 3-6.** *Rapid determination of nitrate/nitrite levels in tap water by ion interaction chromatography on a short 3  $\mu\text{m}$   $\text{C}_{18}$  column.*
- Figure 3-7.** *Instrumental set-up for online analysis of tap water by fast ion interaction chromatography.*
- Figure 3-8.** *Plot of nitrate and nitrite concentration versus sampling/analysis time.*
- Figure 3-9.** *Overlay of chromatograms collected 22, 23 and 24 minutes into the sampling period.*
- Figure 3-10.** *Determination of system precision by thirty consecutive injections of a 3.9 mg/L nitrate standard.*
- Figure 3-11.** *Linearity study for nitrite by fast ion interaction chromatography.*
- Figure 3-12.** *Linearity study for nitrate by fast ion interaction chromatography.*
- Figure 3-13.** *Linearity study for  $\mu\text{g/L}$  nitrite spikes in a 5 mg/L nitrate matrix by fast ion interaction chromatography.*
- Figure 3-14.** *Overlay of  $\mu\text{g/L}$  nitrite spikes in a 5 mg/L nitrate matrix by fast ion interaction chromatography.*
- Figure 3-15.** *Overlay of  $\mu\text{g/L}$  nitrite spikes in a 5 mg/L nitrate matrix on a 25 cm anion exchange column.*
- Figure 3-16.** *Linearity study for  $\mu\text{g/L}$  nitrite spikes in a 5 mg/L nitrate matrix on a*

*conventional (25 cm) anion exchange column.*

**Figure 3-17.** *Optimization of injection volume for the determination of nitrate and nitrite by fast ion interaction chromatography.*

**Figure 3-18.** *Chromatogram showing overlays of a blank, with a standard containing 25 µg/L nitrate and nitrite determined by fast ion-interaction chromatography.*

**Figure 3-19.** *Chromatogram showing overlays of a blank, with a standard containing 25 µg/L nitrate and nitrite determined by anion exchange chromatography.*

**Figure 3-20.** *Separation of common inorganic anions by anion exchange chromatography with suppressed conductivity detection.*

**Figure 3-21.** *Determination of optimum detection wavelength for nitrite/nitrate analysis by anion exchange chromatography.*

**Figure 3-22.** *Separation of 1.0 mg/L nitrate and nitrite by anion exchange chromatography.*

**Figure 3-23.** *Linearity of nitrate on an anion exchange AS17 column.*

**Figure 3-24.** *Linearity of nitrite on an anion exchange AS17 column.*

**Figure 3-25.** *Overlay of the analysis of a validation sample taken at 50 minutes with a 1 mg/L nitrate and nitrite standard, on a 25 cm anion exchange column.*

**Figure 4-1.** *Comparison of sample preparation with, and without the use of C<sub>18</sub> SPE cartridges for saliva analysis by ion-interaction chromatography.*

- Figure 4-2.** *Initial mobile phase conditions for the separation of nitrate, nitrite and thiocyanate by ion interaction chromatography.*
- Figure 4-3.** *Chromatogram showing the analysis of nitrate, nitrite and thiocyanate by ion interaction chromatography with a mobile phase containing phosphate as a counter-ion.*
- Figure 4-4.** *Optimised chromatographic conditions for the analysis of nitrate, nitrite and thiocyanate by ion interaction chromatography.*
- Figure 4-5.** *Optimisation of detector wavelength for the analysis of nitrate, nitrite and thiocyanate by ion interaction chromatography.*
- Figure 4-6.** *Baseline noise versus detection wavelength for a TBA-phosphate/MeOH mobile phase.*
- Figure 4-7.** *Overlay of six consecutive injections of a nitrate, nitrite and thiocyanate standard.*
- Figure 4-8.** *Linearity studies for the determination of nitrite by ion interaction chromatography.*
- Figure 4-9.** *Linearity studies for the determination of thiocyanate by ion interaction chromatography.*
- Figure 4-10.** *Linearity studies for the determination of nitrate by ion interaction chromatography.*
- Figure 4-11.** *Sensitivity studies for the determination of nitrite, nitrate and thiocyanate by ion interaction chromatography.*
- Figure 4-12.** *Effect of increased injection volume upon the separation of nitrate,*

*nitrite and thiocyanate.*

**Figure 4-13.** *Analysis of urine for thiocyanate by ion interaction chromatography on a short 3  $\mu\text{m}$   $\text{C}_{18}$  column.*

**Figure 4-14.** *Expanded view of Figure 4-13.*

**Figure 4-15.** *Overlay of the thiocyanate peak in the analysis of each of the three urine samples.*

**Figure 4-16.** *Analysis of urine for nitrate and nitrite by ion interaction chromatography.*

**Figure 4-17.** *Proposed mechanism resulting in increased retention of nitrate, nitrite and thiocyanate on a 3  $\mu\text{m}$  Hypersil stationary phase relative to a 3  $\mu\text{m}$  Kingsorb stationary phase.*

**Figure 4-18.** *Thiocyanate spike linearity study on a short column by ion interaction chromatography.*

**Figure 4-19.** *Nitrite spike linearity study on a short column by ion interaction chromatography.*

**Figure 4-20.** *Nitrate spike linearity study on a short column by ion interaction chromatography.*

**Figure 4-21.** *Overlay of nitrate, nitrite and thiocyanate linearity spikes in a single urine sample diluted 1/40.*

**Figure 4-22.** *Expanded view of Figure 4-21 showing nitrate and nitrite linearity spikes.*

- Figure 4-23.** *Expanded view of Figure 4-21 showing thiocyanate linearity spikes.*
- Figure 4-24.** *Initial separation of a nitrite/nitrate/thiocyanate standard mix on an anion exchange column.*
- Figure 4-25.** *Overlay of consecutive injections of a nitrate, nitrite and thiocyanate standard on an anion exchange column.*
- Figure 4-26.** *Nitrite linearity study on an AS17 anion exchange column.*
- Figure 4-27.** *Nitrate linearity study on an AS17 anion exchange column.*
- Figure 4-28.** *Thiocyanate linearity study on an AS17 anion exchange column.*
- Figure 4-29.** *Overlay of nitrate, nitrite and thiocyanate linearity standards on an AS17 anion exchange column.*
- Figure 4-30.** *Expansion of Figure 4-29 showing an overlay of nitrite and nitrate linearity standards on an AS17 anion exchange column.*
- Figure 4-31.** *Sensitivity study for a 5 µg/L nitrite standard determination by anion exchange chromatography.*
- Figure 4-32.** *Sensitivity study for a 50 µg/L nitrate standard determination by anion exchange chromatography.*
- Figure 4-33.** *Sensitivity study for a 500 µg/L thiocyanate standard determination by anion exchange chromatography.*
- Figure 4-34.** *Analysis of a heavy smokers' urine sample by anion exchange chromatography diluted 1/40 and spiked with thiocyanate.*

**Figure 4-35.** *Thiocyanate standard addition linearity study for a heavy smokers' urine sample diluted 1/40 as determined by anion exchange chromatography.*

**Figure 4-36.** *Preliminary rapid separation of nitrite, nitrate and thiocyanate on an AG17 anion exchange guard column.*

## List of tables.

- Table 1-1.** *Comparison of the characteristics and performance of fast LC and conventional columns. Performance based on the rapid chlorthalidone assay by fast LC.*
- Table 1-2.** *Experimental conditions of ion-interaction methods based on C<sub>18</sub> and C<sub>8</sub> stationary phases.*
- Table 1-3.** *Limiting equivalent ionic conductances for anions and cations at 25 °C.*
- Table 2-1.** *UV transmittance of acetonitrile and methanol.*
- Table 2-2.** *USEPA drinking water regulations.*
- Table 3-1.** *Comparison of sample throughput for the analysis of nitrate and nitrite for various instrumental analytical methodologies.*
- Table 4-1.** *System precision study for nitrate, nitrite and thiocyanate by ion interaction chromatography.*
- Table 4-2.** *Typical urinary thiocyanate levels (mg/L) as determined by different analytical methodologies.*
- Table 4-3.** *Effect of C<sub>18</sub> stationary phase type on the retention of nitrate, nitrite and thiocyanate in ion interaction chromatography.*
- Table 4-4.** *Characteristics of Hypersil and Kingsorb C<sub>18</sub> stationary phases.*
- Table 4-5.** *Spike linearity studies for nitrate, nitrite and thiocyanate on a short column by ion interaction chromatography.*

## **Publications, conferences and oral presentations.**

### **Publications resulting from this study;**

*“Rapid, low pressure, and simultaneous ion chromatography of common inorganic anions and cations on short permanently coated monolithic columns.”* Damian Connolly, Danielle Victory and Brett Paull, Journal of Separation Science, 27 (2004) 912.

*“Fast ion chromatography of common inorganic anions on a short ODS column permanently coated with didodecyldimethylammonium bromide.”* Damian Connolly and Brett Paull, Journal of Chromatography A, 953 (2002) 299.

*“Determination of urinary thiocyanate and nitrate using fast ion-interaction chromatography.”* Damian Connolly and Brett Paull, Journal of Chromatography B, 767 (2002) 175.

*“Fast separation of UV absorbing anions using ion-interaction chromatography.”* Damian Connolly and Brett Paull, Journal of Chromatography A, 917 (2001) 355.

*“Rapid determination of nitrate and nitrite in drinking water samples using ion-interaction liquid chromatography.”* Damian Connolly and Brett Paull, Analytica Chimica Acta, 441 (2001) 53.

### **Conferences attended during this study;**

13<sup>th</sup> International Ion Chromatography Symposium 2000, Nice, France, September 2000.

Environ 2001, Dublin City University, January 2001.

53<sup>rd</sup> Irish Universities Chemistry Research Colloquium 2001, University College Dublin, 2001.

Analytical Research Forum (Incorporating Research and Development Topics), University of East Anglia, Norwich, England, 2001.

14<sup>th</sup> International Ion Chromatography Symposium 2001, Chicago, Illinois, USA, September 2001.

Analytical Research Forum (Incorporating Research and Development Topics), University of Kingston, London, England, 2002.

54<sup>th</sup> Irish Universities Chemistry Research Colloquium 2001, Queens University, Belfast, 2002.

2<sup>nd</sup> Biennial Conference on Analytical Sciences in Ireland, Tallaght Institute of Technology, 2002.

Analytical Research Forum (Incorporating Research and Development Topics), University of Sunderland, Sunderland, England, 2003.

Analytical Research Forum (Incorporating Research and Development Topics), University of Central Lancashire, Preston, England, 2004.

56<sup>th</sup> Irish Universities Chemistry Research Colloquium 2001, University of Limerick, 2004.

3<sup>rd</sup> Biennial Conference on Analytical Sciences in Ireland, University College Cork, September 2004.

**Oral presentations given during this study;**

*“Rapid online analysis of a flowing tap-water stream for nitrate and nitrite by ion-interaction chromatography”* Presented at Environ 2001, January 2001, Dublin City University.

*“Rapid ion-interaction and ion-exchange chromatography...rapid separation of inorganic anions using short dynamically and permanently coated columns.”* Presented at the 14<sup>th</sup> International Ion Chromatography Symposium, Chicago, Illinois, USA, September 2001.

*“High speed ion chromatography of inorganic anions using short C<sub>18</sub> 3 μm particulate columns.”* Presented at the 54<sup>th</sup> Irish Universities Chemistry Research Colloquium, Queens University, Belfast, 2002.

## **1 Introduction to fast liquid chromatography.**

Modern liquid chromatography (LC) techniques form the backbone of most analytical methodologies in a myriad of industries such as pharmaceuticals, the power industry, petrochemicals and environmental analysis. LC has been proven to be a precise, accurate, and quantitative technique. Since its inception, the theoretical principles which govern the retention behaviour of analytes within a given mobile phase/stationary phase system have been well studied and have allowed retention models to be used to customise chromatographic separations to suit a specific need with a high degree of accuracy. LC has been demonstrated to be compatible with a wide range of universal or highly selective detection modes such as UV-Vis detection, fluorescence detection, electrochemical detection, conductivity detection (suppressed or non-suppressed), refractive index detection and mass-selective detection.

Modern LC instrumentation has become highly automated and is capable of analysing multiple samples, unattended, with for example many modern autosamplers even capable of relatively complex sample preparation steps prior to injection. Most chromatographic separations (for example, a binary gradient separation) can be successfully repeated in different laboratories, on instruments produced by different manufacturers, eg: Waters and Agilent Technologies, by a simple adjustment to the gradient program to account for slight differences in system delay volumes.

Despite the fact that highly precise and accurate instrumentation is available to today's laboratory manager, including very well validated data processing software and excellent technical support from the leading vendors in the field, a simple problem will quite often remain; that samples pile up. Many modern analytical laboratories can often have tens of LC instruments and a large team of analysts to operate them, but if the choice of chromatographic method is poorly considered, then laboratory productivity suffers.

Unfortunately, many analysts may operate in a controlled GMP environment (particularly in the pharmaceutical industry) where a reconsideration of an unnecessarily time-consuming method may require a full method revalidation; particularly if this involves a major change such as the use of a shorter column. The use of fast LC as an option for improving laboratory productivity must therefore be considered at the earliest stage of method development.

### **1.1 The effect of smaller particles upon efficiency.**

Fast LC is rapidly receiving more and more interest in the field of chromatography, born out of the necessity for methods which increase overall sample throughput in a modern laboratory. It has also been called "rapid", "high-speed", or "ultra-fast", but of course in all cases, it essentially involves the use of a short analytical column (3-5 cm) with a small particle size (3  $\mu\text{m}$ ) stationary phase. Moderate flow rates may be used (1-3 ml/min), and ordinarily the operational column backpressure is not unduly excessive. The main advantage is obviously a considerable decrease in the overall analysis time for a given group of analytes, but peak efficiency can also improve as will be discussed in more detail.

Chromatographic efficiency is a measure of the relative narrowness of a solute band as it moves through the column. Ideally, peaks will be very narrow, meaning that there is very little "band broadening" within the chromatographic system. Classical plate theory postulates that the efficiency of a chromatographic separation can be considered in terms of "theoretical plates". Liquid chromatography may be considered as being a process in which a solute traverses a column packed with a stationary phase, across or through which a mobile phase is pumped. Each molecule of solute will "partition" between the stationary phase and the mobile phase based on its affinity for the two respective phases. Residence time in either phase is irregular. The residence time is short for some molecules and longer for others. Movement down the column can occur only while the molecule is in the mobile phase. Hence certain molecules travel rapidly by virtue of their inclusion in the mobile phase for a majority of the time, whereas others lag behind because they are incorporated in the stationary phase for a greater than average period. Therefore a

solute will not elute as an infinitely narrow band but will rather broaden due to the cumulative effect of a number of reasons.

A solute molecule partitions between both phases, and this partitioning at equilibrium is described by a simple equation:



$$K = \frac{A_{stat}}{A_{mobile}} \quad \text{Equation 1-2}$$

$A_{mobile}$  = the equilibrium concentration of solute A in the mobile phase.

$A_{stat}$  = the equilibrium concentration of solute A in the stationary phase.

$K$  = partition coefficient.

The concept of a theoretical plate describes the site of a single equilibrium. Plate theory assumes that there are many thousands of these equilibria established as the solute traverses the column. An acceptable separation is one in which the efficiency, measured in the number of theoretical plates, is in the tens of thousands of plates/metre. For a column of length  $L$ , the "height equivalent to a theoretical plate" ( $H$ ) is given by:

$$H = \frac{L}{N} \quad \text{Equation 1-3}$$

$H$  is the distance a solute molecule moves while undergoing one partition. Ideally  $H$  should be small and  $N$  large. Plate theory is based on the assumptions that: (1) There is rapid equilibration between stationary phase and mobile phase. (2) Equilibration is independent of analyte concentration. (3) There is constant mobile phase flow. (4) There is negligible axial diffusion of solute molecules.

There are a number of factors contributing to plate height, many of which can be minimised up to a certain point. It will become clear that in several instances, the

use of shorter columns packed with smaller particles combined with the use of higher flow rates (as is common in rapid LC) can be effective in counteracting these effects.

*Longitudinal diffusion* results in molecular diffusion of the analyte in all directions. This effect is only significant at low mobile phase velocities, and when there is a relatively high sample diffusion coefficient (particularly evident when mobile phases of low viscosity are used). Then the high diffusion rates of the solute in the mobile phase can cause the solute molecules to diffuse axially (at right angles to the mobile phase flow) while slowly migrating through the column. If this happens, peak broadening occurs, but *the effect can be minimised by increasing the flow rate.*

*Eddy diffusion.* Since the column is packed with small stationary phase particles, the solute molecules must ideally find the shortest pathway through the bed as they travel along the column with the mobile phase. However, not all of the solute molecules will find a direct pathway through the bed and will undergo several diversions along the way, whereas others leave the column having travelled in roughly a straight line. This concept is known as eddy diffusion. The result is that the solute band will have broadened relative to the initial width of the band upon entering the column bed.

*Flow distribution.* The mobile phase passes in a laminar flow between the stationary phase particles. The flow is faster in the intra-particle "channel" centre than it is near a particle. Thus solute molecules occupying a position within this channel that is close to a particle will move slower and lag behind those solute molecules which happen to be incorporated in the faster flowing centre of this channel. Eddy diffusion and flow distribution may be reduced by packing the column with even sized particles, i.e. the column packing should be composed of particles with as narrow a size distribution as possible. *This multiple path term is minimised by reducing particle size and obviously decreases with decreasing column length.*

*Mass transfer.* In the pore structure of a stationary phase particle, the channels are both narrow and wide, some pass through the whole particle and others form "dead ends" or are closed off. The importance of these pores is that analytes can

diffuse into and out of these pores and therefore interact with the stationary phase. It is because of the presence of these pores that silica phases have such a high bonded surface area, that is, most of the surface area and bonded phase is located in these pores. For most HPLC silica packings, the pore diameter ranges from 80-120 angstroms. When the column is equilibrated with mobile phase the pores are filled with mobile phase that is stagnant, i.e., it does not move. A sample molecule entering a pore will cease to be transported by the flowing mobile phase and is in effect, trapped in the pore while the other solute molecules in the intra-particle channels outside the pores are carried forward by the flowing mobile phase. The trapped molecules can only return to the bulk flowing mobile phase by diffusion. *The resulting band broadening is smaller the shorter are these pores, i.e. the smaller are the stationary phase particles.* Some silica gels have been produced which are non-porous, such that stagnated pockets of mobile phase within the pores is no longer an issue. Also *diffusion rates of solute molecules in and out of the pores are higher when the viscosity of the mobile phase is reduced.* Methods for reducing mobile phase viscosity will be discussed in more detail later. In the case of mass transfer, band broadening increases with mobile phase flow velocity, the sample molecules in the moving solvent becoming further removed from the sample molecules in the stagnant pockets of mobile phase the faster is the solvent flux. High analysis speed is achieved at the expense of resolution (and vice versa). However, this effect is much less pronounced with smaller particles (1.5 – 3 μm) than with larger particles (5 – 10 μm), because smaller particles are much less resistant to mass transfer, and yield flatter van Deemter's curves, allowing the use of higher flow rates.

The van Deemter equation is a composite of the three components contributing to band broadening and is a plot of H against μ (the linear velocity of the mobile phase in cm/sec) according to the equation:

$$H = A + \frac{B}{\mu} + C\mu \quad \text{Equation 1-4}$$

The linear velocity of the mobile phase is used because it can be directly related to the speed of analysis whereas the flow rate depends on the column cross

section and the column volume occupied by the packing material.  $A$  is the eddy diffusion and flow distribution component of band broadening and are little effected if at all by mobile phase velocity. As would be expected from the previous discussion, the longitudinal diffusion component  $B$  rises sharply with a decrease in mobile phase flow velocity. The mass transfer term  $C$ , also increases steadily with flow rate. The optimum flow rate ( $\mu_{opt}$ ) is reached at the point in the curve where  $H$  is minimised and  $N$  therefore optimised. In HPLC, we normally operate at flow rates higher than  $\mu_{opt}$ , in order to achieve separations in a reasonable time frame. A typical plot is illustrated in Figure 1-1.

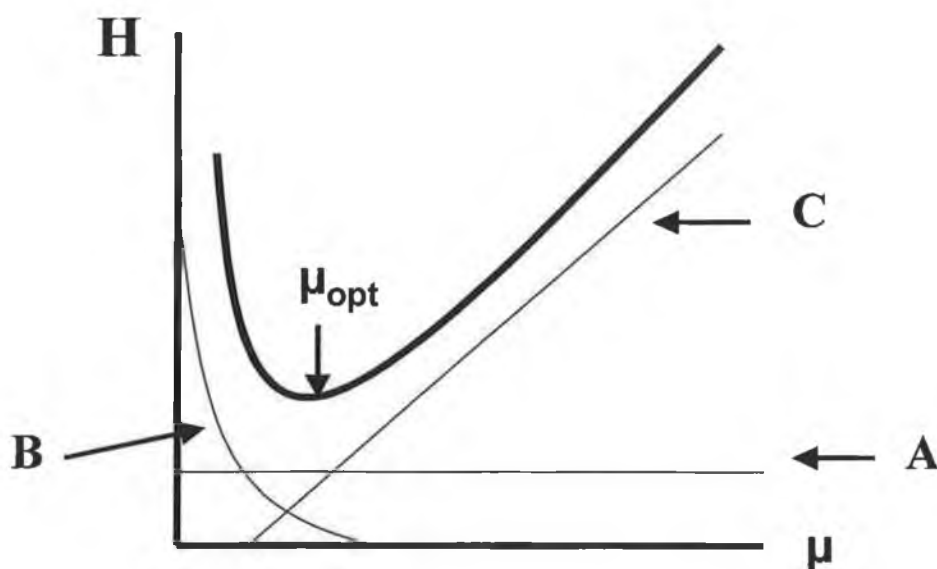


**Figure 1-1.** Typical van Deemter plot.  $A$  = eddy diffusion and flow distribution component of band broadening.  $B$  = longitudinal diffusion component.  $C$  = mass-transfer component.  $\mu_{opt}$  = the optimum mobile phase flow velocity at which  $H$ , the height equivalent to a theoretical plate is minimised.

The influence of particle size on the shape of the van Deemter plot is profound. Firstly, smaller particle sizes reach their  $\mu_{opt}$  at higher flow rates than larger sizes, allowing an equivalent efficiency to be achieved at a faster rate. Also, these smaller particles yield flatter curves, illustrating that the efficiency of smaller packings have less tendency to be adversely affected by increased flow rates. This effect can be seen in Figure 1-2. The  $C$  component has a lower slope, illustrating that smaller packings are less resistant to mass transfer than larger particles.

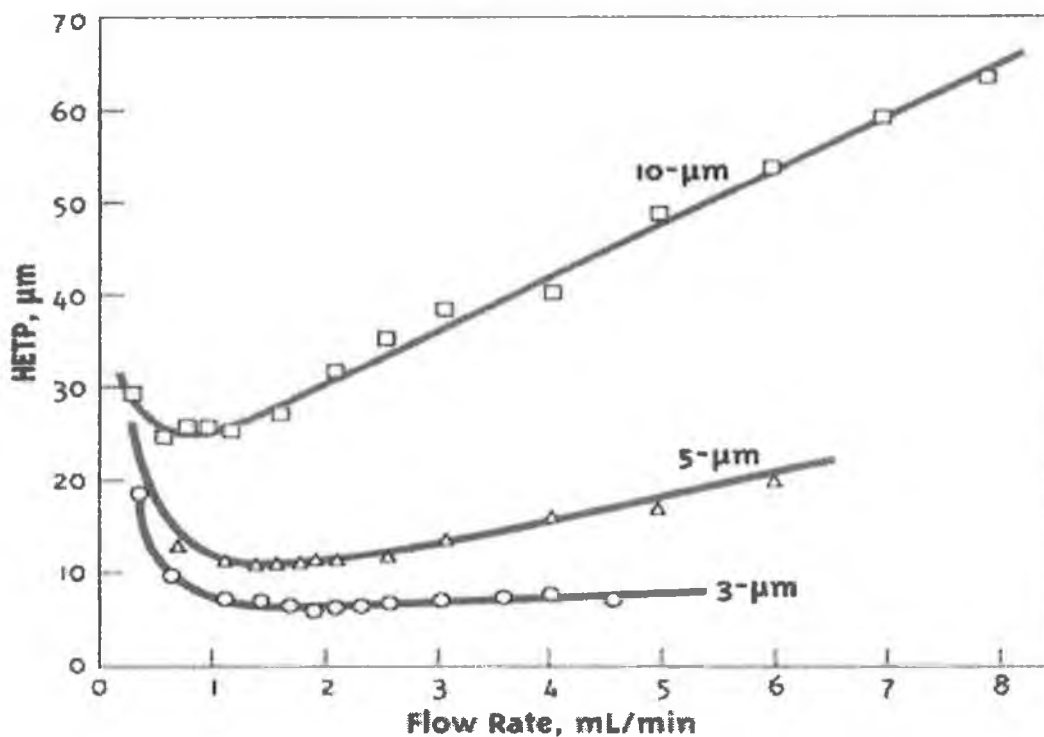


**Figure 1-2.** Van Deemter's curves showing how efficiency is inversely proportional to particle size for 10  $\mu\text{m}$ , 5  $\mu\text{m}$  and 3  $\mu\text{m}$  columns. Column I.D.: 4.6 mm; mobile phase: 65% ACN/H<sub>2</sub>O; sample: *t*-butylbenzene. Reproduced from M. Dong, *Today's Chemist at Work* 9 (2000) 46.

## 1.2 Advantages of fast LC.

There are many advantages of fast LC over chromatography performed on columns of more conventional length (15–25 cm).

Faster analysis times. A very obvious advantage is the faster analysis times resulting in the use of fast LC. Figure 1-3 illustrates the rapid isocratic separation of caffeine and related substances in < 45 seconds [2]. The use of a Pecosphere 3 X 3 C<sub>18</sub> (33 X 4.6 mm I.D.) column allowed the use of an elevated flow rate of 3 ml/min without compromising efficiency.

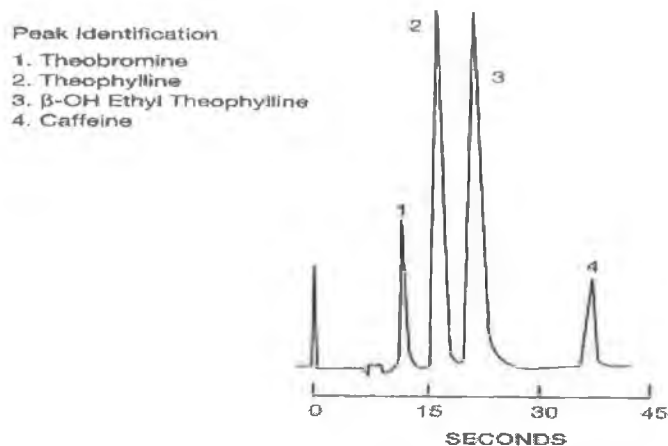


**Figure 1-3.** Analysis of caffeine by fast LC. Chromatographic conditions: Column: Pecosphere 3 X 3  $C_{18}$  (33 X 4.6 mm I.D.) Detection: UV at 273 nm. Mobile phase: 11 %  $CH_3CN$  in  $H_2O$ . Flow rate: 3.0 ml/min. Injection volume: 6  $\mu L$ . Analyte concentrations: 1-10 mg/L. Reproduced from "Fast LC", Perkin Elmer Technical Bulletin (1996).

Rapid gradient analysis is also possible with fast LC, provided the system has a low delay volume. Figure 1-4 shows the rapid gradient separation of 11 priority phenol pollutants in only five minutes [2]. Fast between-run column equilibration is possible due to the decreased bed volume.

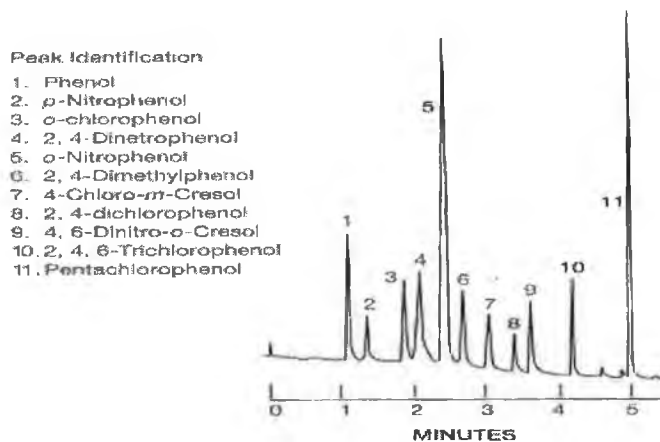


**Figure 1-4.** Analysis of phenol priority pollutants by fast LC. Chromatographic conditions: Column: Pecosphere 3  $C_{18}$  (33 X 4.6 mm I.D., 3  $\mu m$ ) Mobile phase: Linear gradient of 35 % ACN/ $H_2O$  (pH 2.2) to 100 % ACN in 4 minutes. Flow rate: 2.5 ml/min. Injection volume: 6  $\mu L$ . Detection: UV at 254 nm. Analyte concentrations: 0.1-0.2 mg/mL. Reproduced from "Fast LC", Perkin Elmer Technical Bulletin (1996).

Increased sample throughput. Figure 1-3 would suggest a sample throughput of > 60 samples/hour. The very fast runtime depicted in Figure 1-5, might well

permit a sample throughput in excess of 720 samples/hour, although this figure may need to be reduced for the injection of standards or retention time markers for system calibration.

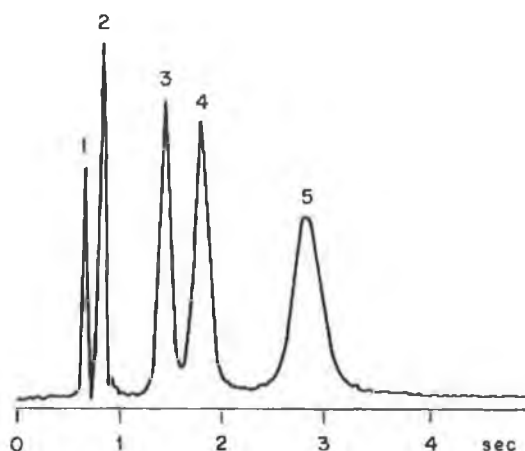


**Figure 1-5.** Ultra fast separation of a five-component mixture by fast LC. Conditions: Column: 2.5 cm X 2.6 mm I.D. Hypersil 3.4  $\mu$ m, Mobile phase: 13 ml/min pentane containing 2.2 % methyl acetate ( $\mu = 3.3$  cm/sec), UV detector: 254 nm; cell volume: 1.4 mL; Data acquisition: 100 points/second, Peaks: 1 = p-xylene, 2 = anisole, 3 = nitrobenzene, 4 = acetophenone, 5 = dipropyl phthalate. Reproduced from V.R. Meyer, "Practical high performance liquid chromatography", 1993 Wiley 298.

Economy – lower reagent consumption. Taking the example in Figure 1-3, reagent consumption per analysis is only 3 mL, (given a runtime of one minute.) This means that mobile phase costs are reduced, as are the costs of waste disposal, since less mobile phase waste is generated.

Economy – lower column cost. The cost of shorter columns is reduced relative to a longer column of equivalent stationary phase.

Faster method development and validation. To a certain extent, method development is performed using a system of trial and error; a mobile phase is tried, and if found to be inadequate, is replaced by a second and third and so on. With the use of shorter columns, equilibration is rapid and feedback is almost immediate. Also, standard method evaluation parameters such as linearity, precision and sensitivity can be established in a matter of minutes.

The advantages of rapid chromatography are illustrated further in Figure 1-6 and in the following Table 1-1 [2]. Here an impurities assay of the pharmaceutical, chlorthalidone is performed in only three minutes [2], and several evaluation parameters are compared with columns of more conventional length.

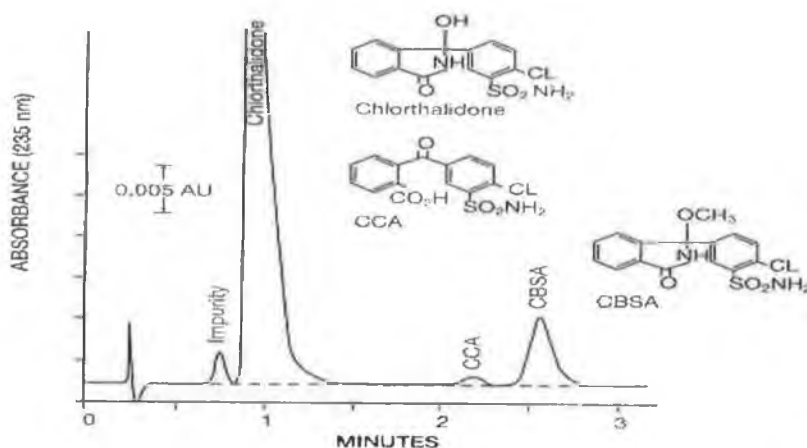


**Figure 1-6.** Rapid chlorthalidone HPLC assay by fast LC. Chromatographic conditions: Column: Reduced-activity  $C_{18}$  (33 X 4.6 mm I.D.) Mobile phase: MeOH/H<sub>2</sub>O/CH<sub>3</sub>COOH (34:65:1). Flow rate: 1.5 ml/min. Column temperature: 30 °C. Detection: UV at 235 nm. Reproduced from "Fast LC", Perkin Elmer Technical Bulletin (1996).

**Table 1-1.** Comparison of the characteristics and performance of Fast LC and conventional columns. Performance based on the rapid chlorthalidone assay by fast LC. Reproduced from "Fast LC", Perkin Elmer Technical Bulletin (1996).

<b>Type</b>	<b>Fast LC</b>		<b>Conventional LC</b>	
<b>Particle (<math>\mu\text{m}</math>)</b>	3 $\mu\text{m}$	3 $\mu\text{m}$	5 $\mu\text{m}$	10 $\mu\text{m}$
<b>Dimension (mm)</b>	33 X 4.6	83 X 4.6	150 X 4.6	250 x 4.6
<b>Column volume (mL)</b>	0.3	0.8	1.5	2.5
<b>Efficiency (plates)</b>	4,000	12,000	10,000	10,000
<b>Performance</b>				
<b>Analysis time (min)</b>	2	5	10	25
<b>Methods validation (week)</b>	1	2	3	5
<b>Solvent use (mL/assay)</b>	5	10	15	25
<b>Detection limit (ng)</b>	0.1	0.15	0.4	0.5

### 1.3 Applications of fast LC.

#### 1.3.1 Pharmaceuticals.

The use of fast LC for the rapid analysis of pharmaceuticals has received much attention due to the ever increasing requirement for high sample throughput in the field of drug discovery. Gomis *et al.* [4] used a 50 mm X 4.6 mm i.d, 2.0  $\mu$ m TSK Gel Super ODS column for the rapid determination of a  $\beta$ -lactam antibiotic (sulbactam) and its synthetic precursors. With a mobile phase of A: 5 mM TBA-OH and 15 mM KCl, pH 6.0 with H<sub>3</sub>PO<sub>4</sub> and B: 100 % acetonitrile, a rapid gradient was used at 1.5 ml/min, whereby the acetonitrile concentration increased from 15 % to 40 % in 1.8 minutes allowing the separation of six peaks including sulbactam in 2.5 minutes. The column temperature of 40 °C was used to reduce the pressure drop across the column. Compared to a conventional column, the separation time was reduced by a factor of five while resolution between adjacent peaks was still maintained.

A 45 mm X 4.6 mm Ultrasphere Cyano column with a particle size of 5  $\mu$ m was used by Macek *et al.* [5] to separate citalopram (an antidepressant drug) from its metabolites (didesmethylcitalopram and *N*-desmethylcitalopram) and an internal standard of verapamil in under 2.5 minutes. The mobile phase was acetonitrile – 30 mM phosphate buffer, pH 6.0 (50:50 v/v), and the flow rate was 2.0 ml/min at 30 °C, allowing about 200 samples to be analysed in one day. This method demonstrates that despite the fact that small particles ( $\leq 3.0 \mu$ m) are usually required for most fast LC analyses, for many applications, the moderate efficiencies obtained with 5  $\mu$ m particles are sufficient<sup>1</sup>.

Yu and Balogh [6] compared traditional HPLC with fast LC for the separation of six drugs (betamethsone, prednisolone, diphenhydramine, amitriptyline, ibuprofen and naproxen) and demonstrated that the cycle time per analysis could be reduced from over 20 minutes to 2.5 minutes. The separation was initially optimised on a Waters Symmetry C<sub>18</sub> (50 mm X 2.1 mm) column with a 3.5  $\mu$ m particle size

---

<sup>1</sup> The column efficiency calculated on the citalopram peak was approximately 2000 theoretical plates which corresponds to 45,000 plates/m.

using an ammonium acetate / acetonitrile gradient at 0.3 ml/min with a column temperature of 30 °C. By subsequently using a shorter (20 mm X 2.1 mm) Waters Xterra C<sub>18</sub> column of particle size 2.6 µm with a modified gradient at 1.0 ml/min and 40 °C the separation could be achieved in 1.4 minutes. The total cycle time per analysis of 2.5 minutes was due to the extra time required for the autosampler to perform needle washes, and for column equilibration after the gradient program.

Dong and Gant [7] reported the rapid separation of theobromine, theophylline, β-OH ethyl theophylline and caffeine in less than 45 seconds. For this separation a Pecosphere 33 mm X 4.6 mm, 3.0 µm column was used with a mobile phase of 11 % acetonitrile in water at a flow rate of 3.0 ml/min. The same column was also used for the separation of eleven phenol priority pollutants within five minutes using a linear gradient of 35 % acetonitrile / water (pH 2.2) to 100 % acetonitrile in four minutes with a flow rate of 2.5 ml/min [2]. Finally, Dong and Gant [7] baseline resolved four antimicrobial parabenes (methyl paraben, ethyl paraben, propyl paraben and butyl paraben) within 25 seconds, using the same column with a mobile phase of 50 % acetonitrile in water at 4.0 ml/min.

Heinig and Henion [8] used a short SB-C<sub>18</sub> Mac Mod Rapid Resolution 15 X 2.1 mm cartridge packed with 3 µm particles to perform rapid separations of selected groups of compounds of pharmaceutical interest (flavones, benzodiazepines and tricyclic amines). In all cases, gradient elution was avoided since as discussed, it is often not desirable for the fast cycle times required for high throughput analysis. Isocratic elution does not require a re-equilibration time after the run, and so despite runtimes often being longer, overall cycle times can be shortened. Five flavones<sup>2</sup> were resolved in 30 seconds, (with the first four peaks separated within 15 seconds), using a mobile phase of acetonitrile-ammonium acetate (3 mM, pH 5.5) (31:69) at 2 ml/min. Five benzodiazepines<sup>3</sup> were separated within 15 seconds using a mobile phase of acetonitrile-3 mM ammonium acetate, pH 3.3 (35:65) at 1.35 ml/min. Finally, a mixture of five tricyclic amines<sup>4</sup> together with propranolol and

---

<sup>2</sup> Daidzein, genistein, 7-hydroxy-flavone, 7-hydroxy-methoxyisoflavone and flavone

<sup>3</sup> Bromazepam, carbamazepine, estazolam, norfludiazepam and delorazepam.

<sup>4</sup> Doxepin, desipramine, imipramine, amitriptyline and trimipramine.

carbamazepine was separated within 30 seconds with a mobile phase of acetonitrile-3 mM ammonium acetate, pH 3.3 (32:68) at 1.2 ml/min.

Later, Zweigenbaum and Henion [9] separated a group of six estrogen receptor modulators<sup>5</sup> on a 30 mm X 1 mm Luna C<sub>18</sub> column packed with 3 µm particles. The mobile phase was 32 % methanol, 28 % acetonitrile, 30 % water and 3 mM ammonium acetate at pH 4.6; and by using a flow rate of 0.5 ml/min with a column temperature of 80 °C, the separation was complete in less than 25 seconds.

### 1.3.2 Protein and peptide separations.

Silica based packing materials with dimensions smaller than 3 µm were developed some time ago, and despite the high back-pressures associated with these reduced particle sizes, such columns have been shown to be applicable to the determination of a wide range of molecules including large biomolecules. In 1987, Danielson and Kirkland [10] developed 2 µm C<sub>4</sub> wide-pore silica microspheres as column packings for the rapid determination of peptides and proteins. The synthesized particles has a relatively narrow size distribution with the average particle size being  $2.0 \pm 0.9$  µm with at least 75 % of the particles being in the size range of 1.5 – 3.0 µm. The average pore size was 200 Å. These particles were found to be particularly suited to the analysis of large molecules such as peptides and proteins, because the smaller particle size leads to shortened diffusion pathlengths and greatly improved mass transfer (particularly since biomolecules have much lower diffusion coefficients). Using a 33 mm X 6.2 mm column packed with the aforementioned particles, Danielson and Kirkland achieved a number of rapid separations of biomolecules. A mixture of five peptides<sup>6</sup> were baseline resolved in 60 seconds using a mobile phase of 24:76 acetonitrile/water with 0.1 % TFA and a flow rate of 4.0 ml/min. Column back-pressure was 370 bar. The separation of an eight

---

<sup>5</sup> Raloxifene, 4-hydroxytamoxifen, nafoxidene, tamoxifen, idoxifene and d5-idoxifene.

<sup>6</sup> Oxytocin (MW = 1,007), bradykinin (MW = 1,060), angiotensin II (MW = 1,046), neurotensin (MW = 1,296) and angiotensin I (MW = 1,673)

component protein mixture<sup>7</sup> ranging in molecular weight from 6,500 to 100,000 was achieved in under 2.5 minutes using a three minute gradient of 25:75 acetonitrile/water/TFA (0.1 %) to 100 % acetonitrile/TFA (0.1 %) and a flow rate of 3.0 ml/min.

Later, Moriyama *et al.* [11] used a TSKgel Super-ODS, 50 mm X 4.6 mm column packed with 2  $\mu\text{m}$  porous silica particles to separate six peptides within 60 seconds using a short gradient time and a high flow rate. By employing a mobile phase of 13 mM HClO<sub>4</sub>/acetonitrile with a 2 minute linear gradient of acetonitrile from 23 % to 56 % and a flow rate of 2 ml/min, a mixture of oxytocin,  $\alpha$ -endorphin, bombesin, leu-enkephalin,  $\gamma$ -endorphin and somatostatin were baseline resolved in less than 60 seconds. Moriyama *et al.*, also extended their studies to include a comparison of separation efficiency across four different columns; one column incorporating a 2.3  $\mu\text{m}$  particle size, one with 2.5  $\mu\text{m}$  particles and two columns both with 5  $\mu\text{m}$  particles. Higher resolution values were found on the columns with the 2.3  $\mu\text{m}$  and 2.5  $\mu\text{m}$  particle sizes as expected.

Particle sizes have been reduced further still to 1.5  $\mu\text{m}$  dimensions. The 1.5  $\mu\text{m}$  non-porous silica reversed phase columns developed by Micra Scientific were evaluated by Issaeva *et al.* [12] for rapid separations of proteins and peptides. There is an inherent constraint in separation speeds with traditional porous particles because of the relatively long diffusion times required for macro molecules to traverse the porous structure inside the particles. By reducing the particle size, this diffusion distance is lowered, resulting in faster separations. Alternatively, non-porous silica phases of 1.5  $\mu\text{m}$  yield even flatter van Deemter curves since the mass transfer limitations are reduced still further. However, a disadvantage of 1.5  $\mu\text{m}$  non-porous silica phases is that they have limited sample loading capabilities because of the lower surface area available for sample interaction. Nevertheless, Issaeva *et al.* achieved an extremely rapid baseline separation of six proteins (ribonuclease, cytochrome C, lysosyme, bovine serum albumin, catalase and ovalbumin) within only 6 seconds as shown in Figure 1-7. The column used was a Micra NPS-RP 15

---

<sup>7</sup> Aprotinin (MW = 6,500), cytochrome C (MW = 12,400), protease (MW = 20,000), trypsinogen (MW = 24,000), lactalbumin (MW = 17,400), chymotrypsin (MW = 21,600), carbonic anhydrase (MW = 29,000) and hexokinase (MW = 100,000).

mm X 4.6 mm (1.5  $\mu$ m) column at a flow rate of 4 ml/min resulting in a column backpressure of 405 bar. A rapid gradient program of 30 % to 100 % acetonitrile in water with 0.1 % TFA in 5 seconds was used.

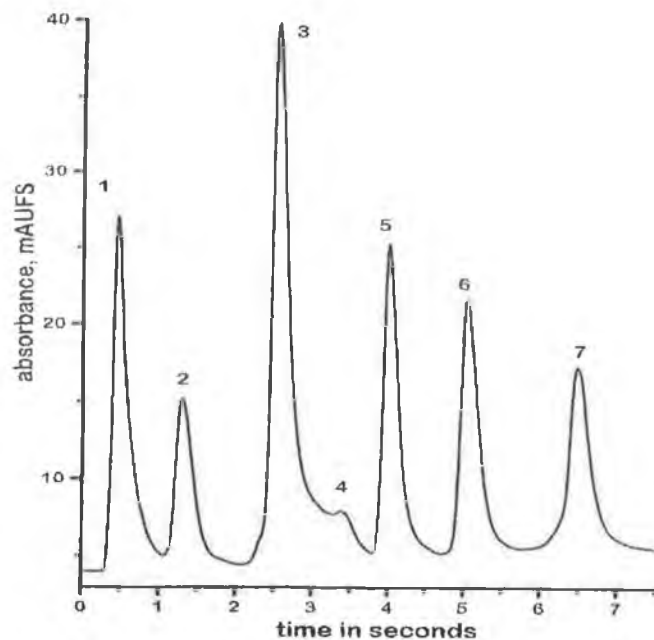


**Figure 1-7.** Rapid separation of six proteins on a short Micra NPS-RP column. Chromatographic conditions: Column: Micra NPS-RP 1.5  $\mu$ m 15 X 4.6 mm, Flow rate: 4 ml/min, Column back-pressure: 405 bar, Gradient program: 30 % to 100 % acetonitrile in water with 0.1 % TFA in 5 seconds, Peaks: [1]: ribonuclease A, [2]: cytochrome C, [3]: lysozyme, [4]: unknown, [5]: bovine serum albumin, [6]: catalase, [7]: albumin egg (ovalbumin). Reproduced from T. Issaeva et al. *J. Chromatogr. A* 890 (2000) 3.

Tryptic digest of protein is a widely used tool for the recovery of protein structure. However, separation of a single sample can last many hours [12]. However, using a 1.5  $\mu$ m Micra NPS-RP 33 mm X 4.6 mm column, a tryptic digest of haemoglobin A containing up to 40 components could be resolved within 70 seconds using a column temperature of 70  $^{\circ}$ C [12]. At this column temperature, the back-pressure was reduced from 495 bar (room temperature) to 250 bar (70  $^{\circ}$ C) allowing a flow rate of 2.5 ml/min to be used. The gradient program for the percentage of acetonitrile in water containing 0.1 % TFA (in seconds) was 1 % 0 sec; 20 % 20 sec; 30 % 90 sec; 40 % 100 sec; 40 % 120 sec; 60 % 130 sec, such that the total cycle time per analysis was 130 seconds to separate 40 components within a retention time window of 70 seconds as shown in Figure 1-8.

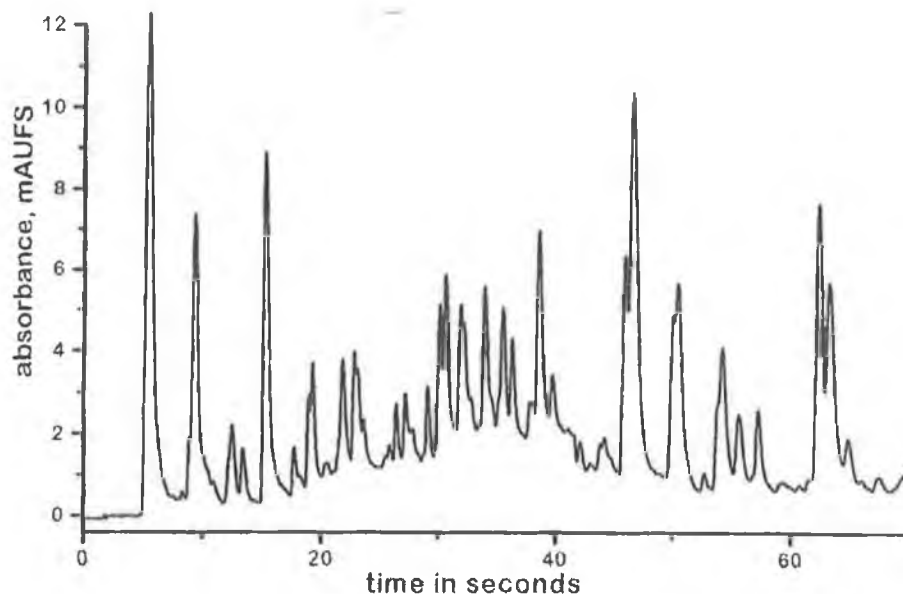


**Figure 1-8.** Rapid separation of a tryptic digest of haemoglobin A on a Micra NPS-RP column at 70 °C. Chromatographic conditions: Column: Micra NPS-RP 1.5  $\mu\text{m}$  33 X 4.6 mm, Flow rate: 2.5 ml/min, Column back-pressure: 250 bar, Gradient program: acetonitrile in water with 0.1 % TFA according to program (% acetonitrile, time in seconds): 1 % 0 sec; 20 % 20 sec; 30 % 90 sec; 40 % 100 sec; 40 % 120 sec; 60 % 130 sec. Reproduced from T. Issaeva *et al.* *J. Chromatogr. A* 890 (2000) 3.

Since a disadvantage of totally porous silica particles is the relatively longer diffusion pathlengths relative to non-porous particles and since a disadvantage of non-porous particles is the relatively lower surface area, a viable compromise between the two has recently been proposed. Superficially porous silica particles (“Poroshell”) have been synthesized by Kirkland *et al.* [13] comprising a 5  $\mu\text{m}$  ultra-pure solid silica core with a thin 0.25  $\mu\text{m}$  porous shell. The synthetic method for the preparation of these stationary phases is discussed in detail in a paper by Kirkland, Truszkowski, Dilks and Engel [13]. These superficially porous stationary phases deliver separation efficiencies which are intermediate between < 2  $\mu\text{m}$  non-porous particles and conventional totally porous particles. Therefore, rapid separations are possible for large macromolecules with nine proteins<sup>8</sup> baseline resolved in less than two minutes using a 5  $\mu\text{m}$  Poroshell 300 SB-C18, 0.25  $\mu\text{m}$  porous shell column of

<sup>8</sup> Met-enkephalin, leu-enkephalin, angiotensin II, neurotensin, insulin, ribonuclease, lysozyme, myoglobin and carbonic anhydrase.

dimensions 75 mm X 2.1 mm. The mobile phases were A = acetonitrile/0.1 % aqueous TFA (5:95); B = acetonitrile/0.1 % aqueous TFA (95:5) with a gradient program of 2 % B to 65 % B in 2.0 minutes. The flow rate used was 2.0 ml/min with a column temperature of 35 °C.

By increasing the column temperature to 80 °C and the flow rate to 4.0 ml/min, five proteins<sup>9</sup> were resolved in about 20 seconds on the same column. In this instance the mobile phase was: A = acetonitrile with 0.1% TFA, B = 0.1 % TFA with a gradient program switching from 25 % acetonitrile to 65 % acetonitrile in 6 seconds.

#### 1.4 Monolithic columns.

As has been previously discussed, reducing runtimes by the use of shorter columns necessitates the use of smaller particle sizes such that chromatographic efficiency is maintained. Columns with 3  $\mu\text{m}$  particle sizes (and smaller) are generally more expensive than columns with 5  $\mu\text{m}$  particle sizes because of the difficulty of producing uniform particles of such small diameters with a narrow size distribution and packing them in a column. In addition, the smaller the particles, the higher will be the resulting column pressure drop which is proportional to the reciprocal of the square of  $d_p$ . HPLC operation at high backpressures over long time periods can cause damage to conventional columns as well as to the instrumentation. Gerber *et al.* [14] found that some manufacturers pack their columns with 3  $\mu\text{m}$  particles at pressures lower than 400 bar. By operating the column at 330 bar, Gerber *et al.* observed a drastic deterioration in peak shape after only about 90 injections. After opening the column at the column head, a void was visible because the pressure had compressed the packing. Evidently the backpressure problems commonly experienced with traditional particulate columns is the limiting factor when high flow rates are used ( $\geq 2.5 - 3.0$  ml/min).

---

<sup>9</sup> Ribonuclease, cytochrome C, lysozyme, carbonic anhydrase and ovalbumin

Monolithic columns have been developed which address these backpressure problems such that higher flow rates can be used at much reduced backpressures due to the considerably higher permeability of the stationary phase. A monolith is a column made of a single continuous piece of silica with thin interconnected porous skeletons and a relatively high fraction of interconnected flow paths (through-pores) through these skeletons for solvent flow. Thus a monolithic silica rod possesses a biporous structure typically consisting of 2  $\mu\text{m}$  macropores and 13 nm mesopores and a high interconnectivity between these two sets of pores. The larger 2  $\mu\text{m}$  macropores (shown in Figure 1-9) serve as through-pores and form a flow channel network outside the monolithic skeleton. Solute molecules are rapidly transported (via the through-pores) through the column by convection under low pressure to the 13 nm mesopores inside the silica skeleton, (shown in Figure 1-10) where chromatographic separation takes place. The total surface of the interconnected silica skeleton has an area of approximately 300  $\text{m}^2/\text{g}$  made available by the mesopores. By virtue of the 2  $\mu\text{m}$  through-pores, the overall porosity of the monolithic silica matrix is greater than 80 %, allowing the user to perform separations with a significantly lower backpressure than with conventional particulate columns which exhibit total porosity of just approximately 65 %.

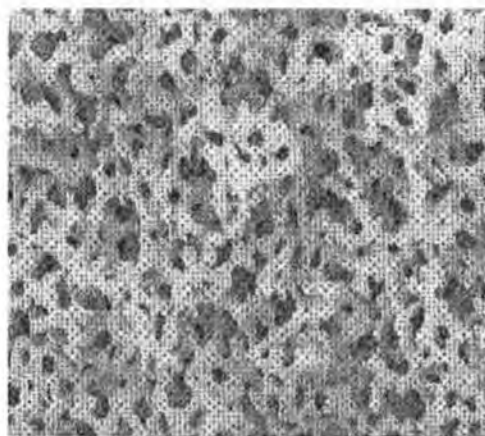


**Figure 1-9.** *Macroporous structure of monolithic silica. Reproduced from K. Cabrera et al. Application Note, Am. Lab. (February 2001) 40.*



**Figure 1-10.** *Mesoporous structure of monolithic silica. Reproduced from K. Cabrera et al. Application Note, Am. Lab. (February 2001) 40.*

#### 1.4.1 Preparation of monoliths.

Monoliths are prepared by a unique “sol-gel” method involving the hydrolytic polymerisation of highly pure metal-free alkoxy-silanes in the presence of water-soluble organic polymers. Monolith preparation using this methodology was first reported by Minakuchi *et al.* [16] in 1996, and has been adopted by other workers with some minor modifications since then [16-23]. A typical methodology is as follows: tetramethoxysilane (or tetraethoxysilane) is added to a solution of poly(ethylene glycol) (PEG)<sup>10</sup> and urea in 0.01 M acetic acid and stirred at 0 °C for 45 minutes. The resultant homogeneous solution is charged into a polycarbonate (or glass) mould and allowed to react at 40 °C to form monolithic silica rods having macro-pores around 2 µm across. This gelation process occurs in approximately 2 hours and the gel is then aged overnight in the mould at the same temperature. The temperature is then raised and the gel treated for 3 hours at 120 °C to complete the formation of mesopores using ammonia<sup>11</sup> generated by the hydrolysis of urea, followed by water and methanol washes. After drying, heat treatment is carried out at 330 °C for 25 hours resulting in the decomposition of organic moieties in the mould. Surface modification of the monolithic silica is carried out on-column by

---

<sup>10</sup> See Section 1.6.2 “Control of macropore size during synthesis”.

<sup>11</sup> See Section 1.6.3 “Control of mesopore size during synthesis”.

continuously recycling a solution of octadecyldimethyl-*N,N*-diethylaminosilane in 8 ml toluene under a pressure of 50 mbar at 60 °C for 3 hours.

#### 1.4.2 Control of macropore size during synthesis.

In a conventional packed column the interstitial voids between particles provide the flow path, and the size of the particles determines the size of the interstitial voids, the relative ratio generally being 0.25 – 0.40. Independent control of the size of particles and the size of the interstitial void volume is not possible with conventional particle-packed columns. In contrast, the size of the through-pores in silica rods can be controlled independently from the size of the skeletons, and can be reduced in size by increasing the amount of PEG in the reaction mixture. For example, Tanaka *et al.* [21] achieved pore sizes of 1.3, 1.7, 2.3 and 3.4 µm corresponding to the amounts of PEG 10.4, 10.2, 9.8 and 9.4 g per 100 ml aqueous acetic acid in the starting mixture. As the through-pore size decreases, there is a resulting decrease in the permeability of the monolith, as expected. Permeability (*K*) is calculated by Equation 1-5:

$$K = \frac{\mu\eta L}{\Delta P} \quad \text{Equation 1-5.}$$

where  $\mu$  is the linear velocity of the mobile phase, *L* is the length of the column/monolith,  $\Delta P$  is the backpressure and  $\eta$  is the mobile phase viscosity. The (through-pore size) / (skeleton size) ratio of monoliths can be 2 – 4 which is much greater than 0.25 – 0.40 found in a column packed with particles [22]. For example, a column packed with 5 µm particles has a permeability of  $\sim 4 \times 10^{-14} \text{ m}^2$ , whereas a monolith typically has a permeability of  $\sim 1 \times 10^{-12} \text{ m}^2$  [24].

In order to achieve high efficiency at high flow rates, it is necessary to have a reduced through-pore size although it will be accompanied with a reduction in permeability. Tanaka *et al.* [21] found that in a manner similar to particle-packed columns, higher column efficiency was obtained with monolithic columns of smaller domain size (resulting in higher back-pressures however). The monolithic columns having domain size of 5.8, 3.8, 2.9, and 2.3 µm showed minimum plate heights of 15,

7, 8, and 5  $\mu\text{m}$  respectively. Other workers have made similar observations [21,23] reasoning that the steepness of the van Deemter curves for monoliths with large through-pores (2-8  $\mu\text{m}$ ) is due a large  $A$ -term component of the van Deemter equation. The contribution of eddy diffusion becomes very large as the through-pore size increases because of inefficient exchange of solute molecules between streamlines. Essentially, solutes can be carried away much further from the active surface area of the silica skeleton by virtue of the relatively large and straight through-pores, resulting in greater band-broadening due to the eddy diffusion term. In the case of monolithic columns with smaller through-pores, more efficient mixing occurs such that the effects of eddy diffusion are reduced.

#### 1.4.3 Control of mesopore size during synthesis.

The mesopore structure of the wet gel is tailored by exchanging the fluid phase with an external solution of aqueous ammonium hydroxide [16-19], [21]. The size of the mesopores mainly depends on the temperature and pH of the exchanged solution. The chromatographically important size range of mesopores between 5 and 25 nm diameter can be covered by adopting a 0.001  $M$  to 1.0  $M$  ammonium hydroxide solution at 120  $^{\circ}\text{C}$ . Tanaka *et al.* [21] for example found that mesopore sizes of 16 nm to 24 nm were obtained by treating the gels with 0.01  $M$  and 1.0  $M$  ammonium hydroxide solutions respectively resulting in surface areas of 340  $\text{m}^2/\text{g}$  and 140  $\text{m}^2/\text{g}$  respectively.

Other workers have since prepared mesopores by utilising the hydrolysis of urea to produce ammonia [22,23]. The addition of urea to the starting mixture has made the process simpler since the mesopores are formed just by heating the reaction mixture in the mould without having to introduce aqueous ammonium hydroxide solution.

#### 1.4.4 Coupling of monolithic columns in series.

The mould used for preparation of monoliths can be a 6 - 9 mm I.D. glass or polycarbonate tube. The preparation in a mould is accompanied by the volume reduction of the whole structure. The diameters of the products are 4.6 mm and 7.0 mm when one uses a mould of 6 mm or 9 mm I.D. respectively [21]. The fragile porous rods are removed from their polycarbonate mould and coated with polyether ether ketone (PEEK) tubing so that they can be used for pressure driven flow in HPLC. The preparation of monolithic silica columns in a mould limits the length of a column to be less than 15 cm or so, otherwise a straight monolithic rod cannot be prepared causing problems in the subsequent column fabrication process that includes cladding with PEEK [23]. Therefore the monolithic silica columns (4 – 6 mm I.D.) prepared in a mould can provide high separation speed while the maximum number of theoretical plates per column is rather limited due to the limited length. A number of such columns can be connected in series, however, producing a column with a plate count significantly higher than particulate columns while producing very low backpressures. Apers *et al.* [25] linked two 100 mm X 4.6 mm Chromolith Performance RP-18e monolithic columns in series with a flow rate of 3 ml/min and achieved the same selectivity but much improved efficiency for later eluting peaks than with a LiChrospher RP-18 250 mm X 4.6 mm (5  $\mu$ m) column at a flow rate of 1 ml/min.

Lubda *et al.* [26] linked fourteen 100 mm X 4.6 mm Chromolith Performance columns in series, producing a column with a combined length of 1.4 metres. Using a mobile phase of 80:20 acetonitrile – water, a mixture of alkyl-benzenes was well resolved and a column plate number of 108,000 plates was achieved. The runtime was not rapid (at just under 60 minutes) but it was demonstrated nevertheless that column efficiency can be increased by increasing the column length without a prohibitively high back-pressure (117 bar), which is not possible with conventional particulate columns.

#### 1.4.5 Flow gradients with monolith columns.

Another benefit of the low back-pressure from monolithic columns is that flow gradients can be used to decrease retention times for strongly retained analytes. Unlike mobile phase gradients, there is no need to re-equilibrate the column before the next injection but instead, the flow rate is simply returned to the initial conditions prior to the next injection. For the separation of ten  $\beta$ -blockers on a 100 mm X 4.6 mm Chromolith Performance RP-18e, Lubda *et al.* [26] reduced the total runtime by a factor of two (from 11.5 minutes with an isocratic flow to 5.75 minutes with a flow gradient).

Cabrera *et al.* [27] used a flow gradient from 3 ml/min to 9 ml/min to separate four K-vitamins on a SilicaROD RP-18e (83 X 7.2 mm) with a mobile phase of acetonitrile/water (95:5). The original separation using a flow rate of 1 ml/min took 45 minutes, whereas with the flow gradient the runtime was reduced to 6.5 minutes.

To separate a mixture of isoflavones from soy extracts, Apers *et al.* [25] used a flow gradient at the end of a run which also incorporated a mobile phase gradient at an elevated flow rate of 3 ml/min. The flow gradient went from 3 ml/min to 4 ml/min at the end of the run for washing the column. This flow gradient was applied to two 100 mm X 4.6 mm Chromolith Performance RP-18e monolithic columns connected in series, but was not possible with a LiChrospher RP-18 250 mm X 4.6 mm (5  $\mu$ m) column due to back-pressure restrictions.

#### 1.4.6 Separation impedance of monoliths relative to particulate columns.

In addition to the construction of van Deemter plots for direct comparison between monolithic columns and particulate columns, many workers [17], [21-23] have used *separation impedance* ( $E$ ) as a measure of total column efficiency.

$$E = \frac{t_o \Delta P}{N^2 \eta} \quad \text{Equation 1-6.}$$

where  $t_o$  is the time taken for an unretained solute to elute,  $N$  is the number of theoretical plates per column,  $\Delta P$  is the backpressure and  $\eta$  is the mobile phase viscosity. As well as the plate height  $H$ , separation impedance also takes pressure drop into account, allowing comparison of phases of different particle size. The impedance for a particulate column rises steeply relative to that of a monolith as the flow rate increases, such that at high flow rates,  $E$  can be as much as an order of magnitude higher for particulate columns [18]. Because of the low pressure drop and better efficiency of monolithic columns, they provide significantly higher  $E$  values than particulate columns. Therefore, at a similar pressure-drop, one can use a longer monolithic column to produce a greater number of theoretical plates than with a column packed with particles.

#### 1.4.7 Evaluation of separation efficiency of monolithic columns.

When making comparisons between stationary phases in terms of column efficiency and van Deemter curves, the stationary phase particle size has been used as the parameter for direct comparisons to be made. In the case of monolithic columns which obviously do not have particles, by analogy the domain size (combined skeleton size and through-pore size) has been used as an equivalent dimension [17,28]. To measure the domain size, the sum of the through-pore size and the size of the silica skeleton at narrow (saddle) portions is taken, and this represents the repeating unit length when considering band broadening effects relative to particulate columns.

The size of interstitial void spaces between spherical particles is commonly 0.25 – 0.40 times the particle size. Therefore, the size of interstitial voids in 5  $\mu\text{m}$  particulate columns should be approximately similar to monolithic silica columns with 2  $\mu\text{m}$  through-pores [17,27]. In this respect, a number of workers have chosen 5  $\mu\text{m}$  particulate phases for the purposes of comparison with regard to the effect of high flow rates upon band broadening [16,19,21,23,26].

As illustrated in Figure 1-11, Minakuchi *et al.* [16,19] found that a monolithic provided much lower plate heights for amylbenzene particularly at higher flow rates than a Capcellpak C<sub>18</sub> SG 5  $\mu\text{m}$  column. In addition, the difference in column

efficiency for a monolithic column at high flow rates relative to a 5  $\mu\text{m}$  particulate column for a large biomolecule such as insulin was more pronounced than for the smaller amylobenzene molecule.

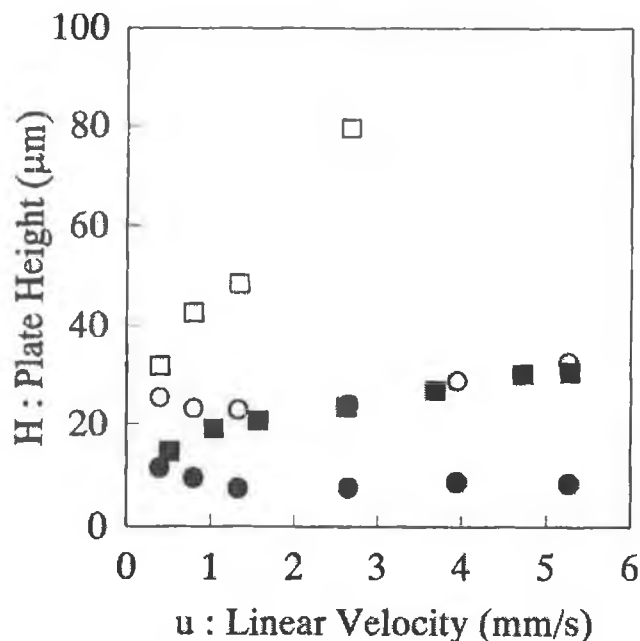


**Figure 1-11.** Van Deemter plots for a  $C_{18}$  monolith (closed symbols) and a Capcellpak  $C_{18}$  SG 5  $\mu\text{m}$  column (open symbols) with amylobenzene ( $\bullet, \circ$ ) and insulin ( $\blacksquare, \square$ ) as solutes. Columns: monolithic silica 83 mm X 7.0 mm and Capcellpak  $C_{18}$  SG (5  $\mu\text{m}$ ) 150 X 4.6 mm. Mobile phase: 80 % methanol with amylobenzene and acetonitrile – water mixture with insulin (30:70, v/v) for monolithic column and (32:68, v/v) for Capcellpak  $C_{18}$  SG in the presence of 0.1 % TFA. Reproduced from H. Minakuchi et al. *J. Chromatogr. A* 828 (1998) 83.

Monolithic phases have been used for the rapid analysis of a range of analytes, with the majority of work to date focusing on reversed-phase separations of pharmaceuticals [14,26,27,29], compounds of forensic interest (opiates, barbiturates, steroids) [30], biomolecules [16,19,21,25,27] and alkyl-benzenes [16,17,21,23,29].

Gerber *et al.* [14] demonstrated that the separation of a Novartis development compound ( $M_r = 330.4$ ) from its by-products, which was initially optimised on a LiChrospher 100 column (RP-18, 5  $\mu\text{m}$ , 250 mm X 4.6 mm), could be successfully transferred to a 100 mm X 4.6 mm Chromolith column resulting in a reduction in total runtime by a factor of about six. The flow rate was increased from 1 ml/min on

the LiChrospher column to 5 ml/min on the Chromolith column. An equivalent separation of all peaks was achieved. Gerber also demonstrated that the impurity assay for another development compound initially ran on a Symmetry Shield column (RP18, 3.5  $\mu$ m, 150 mm X 3 mm) at 1 ml/min could be run at 3 ml/min on a 100 mm X 4.6 mm Chromolith column, reducing the runtime from 20 minutes to 5.5 minutes.

Lubda *et al.* [26] separated five  $\beta$ -blockers in 30 seconds using a flow rate of 9 ml/min on a 50 mm X 4.6 mm Chromolith column with a mobile phase of 20:80 acetonitrile – 1 % trifluoroacetic acid in water. At this flow rate, the column back pressure was only 72 bar.

Nimesulide and five impurities were baseline resolved in 1.5 minutes by van Nederkassel *et al.* [29] who used a 50 mm X 4.6 mm Chromolith SpeedROD and an acetonitrile/ammonium phosphate mobile phase at a flow rate of 9 ml/min. This represented a reduction in runtime by a factor of up to 40 compared to a LiChrospher 100 RP-18 (250 mm X 4.6 mm, 5  $\mu$ m) column at 1.3 ml/min.

Cabrera *et al.* [27] reduced the runtime for the determination of three parabenes by a factor of eight by using a flow rate of 9 ml/min instead of 1 ml/min. The three analytes were baseline resolved within one minute with a resulting back-pressure of 100 bar using a mobile phase of 40/60 acetonitrile/water on a SilicaROD RP-18e (83 X 7.2 mm) column.

Pihlainen *et al.* [30] used a 50 mm X 4.6 mm Chromolith SpeedROD and a flow rate of 2.5 ml/min with gradient elution and MS-MS detection to determine 14 illicit drugs of forensic interest<sup>12</sup> within 5 minutes. Although many of the compounds were not fully separated, the use of MS-MS detection allowed the unambiguous detection of all compounds.

---

<sup>12</sup> Amphetamine, 3,4-MDMA, Buprenorphine, Clenbuterol, Salbutamol, LSD, Methandienone, Nandrolone, Stanozolol, Testosterone, Morphine, Phenobarbital, Psilocybine, Temazepam.

Van Nederkassel *et al.* [29] separated a mixture of uracil, toluene, ethylbenzene, butylbenzene, *o*-terphenyl, amylbenzene and triphenylene in under 45 seconds on a 50 mm X 4.6 mm Chromolith SpeedROD RP-18e column with a mobile phase of methanol/water (70/30) and a flow rate of 9 ml/min. M<sup>c</sup> Calley [31] separated a mixture of weak bases (uracil, pyridine, aniline, ethylaniline) and benzene on a 100 X 4.6 mm Chromolith RP-18e column in less than 60 seconds, with a mobile phase of acetonitrile-water (40:60, v/v) and a flow rate of 5 ml/min.

Monolithic columns have been shown to be particularly suitable for analysis of large biomolecules which typically have low diffusion coefficients. In conventional porous particles, most of the absorptive surface located inside the particles is accessible by slow molecular diffusion through stagnant mobile phase. Through-pores are relatively round and straight compared to interstitial voids in particle packed columns, and so diffusion path lengths are reduced, which is particularly noticeable for larger molecules which have lower diffusion coefficients. Since the diffusion path length is shortened by virtue of the large through-pores, efficient separations of peptides and other large biomolecules is possible relative to particulate columns, which typically exhibit steeper van Deemter curves due to a reduction in mass transfer effects. Minakuchi *et al.* [17] found that column efficiencies of C<sub>18</sub> silica monoliths for insulin of MW ~ 5800 were much better than that of wide-pore C<sub>18</sub> packings prepared from 5 μm silica particles having 30 nm pores, especially at high flow rates. Tanaka *et al.* [21] demonstrated that for the separation of a polypeptide mixture, the efficiency of a monolithic column was similar to or higher than that of 1.5 μm non-porous silica based particles, and much higher than that of conventional porous 5 μm particles.

### 1.5 Instrumental considerations for fast LC.

The total band broadening ( $\sigma_{\text{total}}^2$ ) of a peak is the sum of all possible band broadening processes:

$$\sigma_{\text{total}}^2 = \sigma_{\text{column}}^2 + \sigma_{\text{injector}}^2 + \sigma_{\text{tubing}}^2 + \sigma_{\text{detector}}^2 \quad \text{Equation 1-7.}$$

Since the ratio of the extra column volume to the column volume itself is critical, extra column band broadening can become more of a dominant factor in fast LC as column length is reduced. Therefore, in fast LC, all sources of extra-column band broadening should be minimised or eliminated where possible. Connecting tubing from the injector to the column and from the column to the detector should be as short as possible, and should ideally be of 0.005 – 0.007 inch I.D. tubing. Particular attention should be paid to the manner in which ferrules are fitted such that the introduction of additional system dead volume is avoided. Unnecessary components like column switching devices and connectors must be avoided where possible, since they also contribute to the extra column volume.

The most significant contributor to the total extra column band broadening in fast LC is the detector flow cell. Where possible, a micro flow cell with a volume less than 3  $\mu\text{L}$  should be fitted. However, an associated disadvantage of the use of such micro flow cells is that in the case of UV detection, a flow cell of such dimensions can negatively impact upon the sensitivity of the method due to the reduced optical light path.

As previously discussed, the use of gradients in fast LC can increase total cycle time per analysis due to the necessary column re-equilibration time; but there is also a further factor which places a constraint on the speed of an analysis. The dwell volume of a gradient system is the volume between solvent blending and the column, so that a finite time is required for a particular solvent blend (as dictated by the gradient program) to reach the column. For example, a dwell volume of 1 ml will cause a one minute gradient delay with a conventional column operated at 1 ml/min<sup>13</sup>. When operating fast LC, a system with a low dwell volume should be used. A solution to excessive dwell volume is the use of binary high pressure pumps which have much lower dwell volumes.

---

<sup>13</sup> Agilent HP1100 and Dionex DX500 GP50 pumps have dwell volumes of ~1 mL.

### 1.5.1 Data acquisition in fast LC.

Most modern detectors possess the option of setting a response time or time constant, which controls the “reaction speed” of the detector. The response time is defined as the time the system needs to reach 63 % of the input signal. As chromatographic peaks become narrower, the number of data points per peak decreases for a given response time. If a peak is defined by too few data points, band broadening of the peak can occur as peak heights are reduced and peak widths increase. The effect of detector response time on peak variance is given by Equation 1.8.

$$\sigma_{V,\text{det}}^2 = (F\tau)^2 \quad \text{Equation 1-8.}$$

where  $\sigma_V^2$  is the variance due to detector response time,  $F$  is the flow rate and  $\tau$  is the detector response time. The response time of the detector should be at least ten times smaller than the width of the narrowest analyte peak at half height, such that a minimum of ten data points are used to reconstruct the peak shape.

For a very rapidly eluting peak of peak width  $W_{50\%} = 0.62$  seconds, van Nederkassel *et al.* [29] observed that a response time of 0.1 seconds (10 Hz) was not adequate to reconstruct the peak properly. A decreased detector response time of 0.0125 seconds (80 Hz) resulted in better peak definition allowing a better measurement of peak parameters as shown in Figure 1-12. Similarly, Hatsis and Lucy [32] found that the data acquisition rate of conventional conductivity detectors (eg Dionex CDM-3, max. 5 Hz) was insufficient to monitor the peaks in a rapid separation of eight anions within 15 seconds. The first six anions, phosphate, chloride, nitrite, bromide, nitrate and chlorate were separated within a window of ~ 5 seconds.<sup>14</sup> Therefore, a prototype ED-50A detector was used to enable data collection at 20 Hz.

---

<sup>14</sup> Chromatographic conditions: *Column*: Chromolith SpeedROD RP-18e (50 X 4.6 mm), *Mobile phase*: 1.5 mM TBA – 1.1 mM phthalate with 5 % (v/v) acetonitrile, *Flow rate*: 16 ml/min split 3:1 before the detector cell, *Injection volume*: 20  $\mu$ L.

Unfortunately, high speed chromatograms tend to be noisier than routine chromatograms because of a higher data acquisition rate that passes more of the detector noise into the data system [14], and so where possible, a compromise should be made between good peak definition to avoid band broadening, and sensitivity by keeping baseline noise to a minimum.

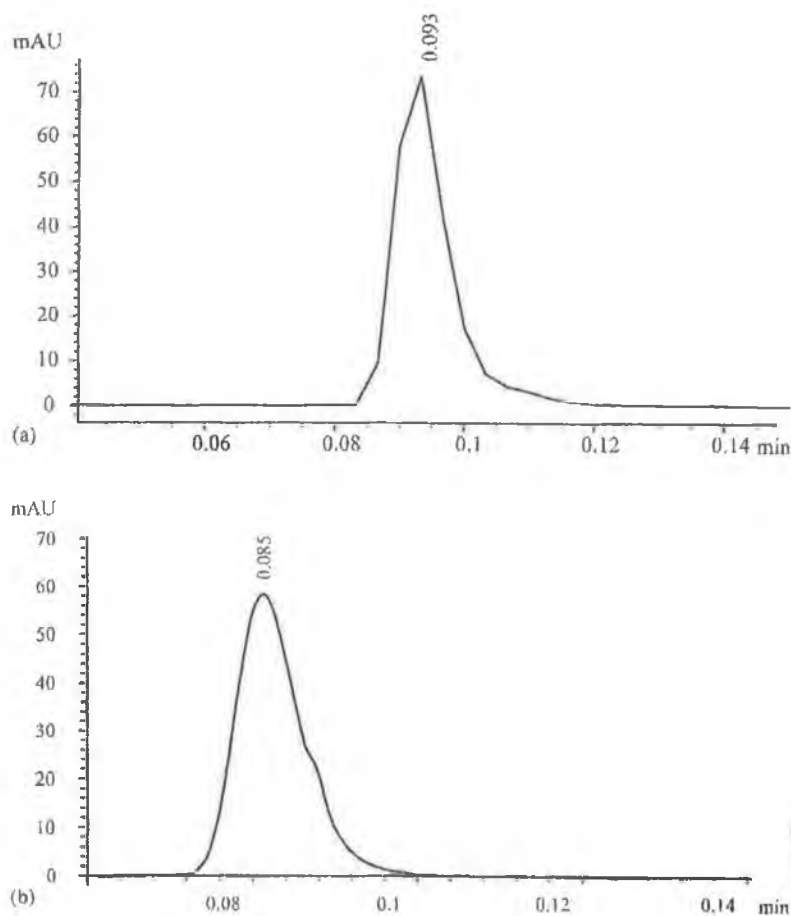


**Figure 1-12.** Comparison of different detector response times on peak shape in fast LC. The upper trace represents a response time of 0.1 seconds (10 Hz) and the lower trace represents a response time of 0.0125 seconds (80 Hz). Chromatographic conditions: Column: Chromolith SpeedROD RP-18e (50 X 4.6 mm), Mobile phase: methanol/water (70:30), Flow rate: 9 ml/min, Column temperature: 30 °C, Analyte: uracil. Reproduced from A.M. van Nederkassel et al. *J. Pharm. Biomed. Anal.* 32 (2003) 233.

### 1.5.2 Signal-to-noise ratio determinations.

Chromatography detectors respond to variations in the concentrations of molecules to which they are sensitive. A chromatographic signal in the context of signal-to-noise ratio measurement can be defined as any change in detector output attributable to the analyte. Noise can be defined as random variations in detector output due to other response provoking molecules in the background, or due to electronic noise from within the instrument or from external sources. High levels of noise can contribute uncertainty to peak areas or heights, particularly at low concentration levels of analyte. The ability of a chromatographic system to distinguish between signals and noise is usually expressed as a signal to noise ratio (S/N) calculated as the average signal amplitude divided by the average noise amplitude. The higher the S/N ratio the better is the limit of detection (L.O.D.). The L.O.D. is the concentration of analyte that gives a signal significantly different from that of the background noise. Generally, L.O.D. has been defined as an S/N ratio of three (the amplitude of the signal should be three times that of the noise), but S/N ratios of two have also been used in the literature.

S/N ratios should be calculated by measuring the peak height at a sample concentration close to the lowest detectable level. Testing at high levels and scaling the signal down to represent lower levels could cause problems with non-linear detection response at the bottom of the linear range, yielding inaccurate results.

There are two different ways to measure noise on a baseline. Peak to peak noise is the difference between the highest and lowest data point during a noise measurement interval. Root mean square noise is equal to the square root of the average of the squares of the data points' deviations from their mean value shown in the equation below in which  $m$  is the mean value of the  $n$  data points  $v_n$  spanning the noise measurement interval.

$$RMS = \sqrt{\frac{\sum (v_n - m)^2}{n}} \quad \text{Equation 1-9}$$

Occasional spikes on the baseline can increase the value of peak to peak noise, which increases to include the amplitude of the largest spike, whereas RMS noise de-emphasizes the influence of such spikes. However, if the section of baseline noise includes a visible drift, RMS noise will be higher than peak to peak noise, because for peak to peak determinations, the drift is bounded by slanted lines which essentially remove the influence of the diagonal drift.

### 1.5.3 Autosamplers in fast LC.

When runtimes of  $< 1$  minute are achieved in fast LC, conventional autosamplers can cause a bottleneck in terms of high throughput analysis because they require at least a one minute cycle time. In fast LC, a full gradient analysis cycle includes sample injection, needle wash, the actual gradient, system and column equilibration. Total cycle times can be reduced if one or more of these actions can be performed in parallel. In the case of fast LC, runtimes must be long enough to allow vial access, needle insertion, syringe draw and needle wash procedures to be performed if these actions are to occur simultaneously in the parallel mode, otherwise the instrument will have to wait for these actions to be completed. For the rapid reversed-phase analysis of six drugs (amitriptyline, betamethasone, diphenhydramine, ibuprofen, naproxen and prednisolone) Yu and Balogh [6] performed the needle wash and sample draw during the time the gradient was processed. Another approach is to use the time taken for the system to re-equilibrate after the gradient cycle.

An example of high sample throughput by eliminating autosampler delays is the high speed analysis developed by Heinig and Henion [8] who detailed an IC-MS-MS analysis of five benzodiazepines in human urine in under 15 seconds. The feasibility of injecting 240 samples per hour was investigated by filling a 10 mL syringe pump with urine extract and pumping at a rate of 120  $\mu\text{L}/\text{min}$  to keep the 5  $\mu\text{L}$  sample loop filled at all times. This allowed injections to be made automatically at discrete time intervals via a programmable Rheodyne valve.

The autosampler vial capacity might be insufficient for processing large numbers of samples with short analysis times, and so to fully realise the high throughput potential of fast LC, autosamplers with a large vial capacity should be used. Examples of commercially available autosampler vial capacities are: Agilent HP1050: 21 vials, Waters 717: 48 vials, Dionex AS50 autosampler: 100 vials, Agilent HP1100: 100 vials.

Increased autosampler capacity was demonstrated by Zweigenbaum *et al.* [33] who used four autosamplers connected sequentially to one column. Samples were injected from the sample wells of twelve 96 well plates (totalling 1152 samples). The use of four autosamplers connected in series eliminated delays between the completion of data acquisition and the injection of the next sample because of the time needed for needle washes and injector loop loading. To ensure that data collection and sample injection remained synchronous, a feedback loop was used such that each autosampler was ready to inject as soon as it received a “ready signal” from the detector, when data collection was complete from the preceding autosampler injection.

## 1.6 Elevated column temperature for fast LC.

Most of the efforts to reduce analysis times in LC have focused on using smaller particle sizes and/or shorter columns in conjunction with higher flow rates. However as discussed, the use of smaller particle sizes increases the column back-pressure which in turn places a constraint on the use of high flow rates. Also, by using shorter columns, there is an inherent loss in resolution that must occur since the number of theoretical plates is directly proportional to the length of the column. This then translates into a loss in resolution according to the following equation where  $N$  is the number of theoretical plates,  $\alpha$  is the separation factor and  $k'$  is the capacity factor.

$$R_s = \frac{\sqrt{N}}{4} \left( \frac{\alpha - 1}{\alpha} \right) \left( \frac{k'}{1 + k'} \right) \quad \text{Equation 1-10}$$

However, the use of temperature as a means of reducing analysis times for rapid LC has only recently begun to receive attention. The main challenge in the past to the use of high temperatures ( $> 60\text{ }^{\circ}\text{C}$ ) for LC was the stability of the stationary phase. At temperatures over  $60\text{ }^{\circ}\text{C}$  most silica based columns degrade very quickly, and so for high temperature HPLC, thermally stable supports such as zirconia ( $\text{ZrO}_2 \cdot n\text{H}_2\text{O}$ ) should be used [34]. For example, a Diamondbond<sup>®</sup>-C<sub>18</sub> phase manufactured by ZirChrom Separations [35] consists of a carbon clad zirconia particle covalently bonded with C<sub>18</sub> ligand and is thermally stable up to  $200\text{ }^{\circ}\text{C}$ , with a pH range of 1 to 14. Another challenge to the use of high temperatures is thermal mismatch broadening caused by a radial inequality of temperature across the diameter of the column. This phenomenon will be discussed in more detail shortly. However, there are two main advantages to the use of elevated temperatures in HPLC. Firstly, the viscosity of the mobile phase is decreased so that column back-pressure is reduced, allowing higher flow rates to be used. For example, for a temperature change from  $25\text{ }^{\circ}\text{C}$  to  $200\text{ }^{\circ}\text{C}$ , Yan *et al.* [34] reported that the viscosity of acetonitrile decreases by a factor of three and that of water decreases by a factor of eight. Secondly, the diffusion rates of analytes increase and the kinetics of the interactions between analytes and the stationary phase are faster, resulting in an overall reduction in the C-term of the van Deemter equation. Therefore, at higher temperatures, higher flow rates can be used without compromising separation efficiency due to flatter van Deemter curves. In addition, at elevated temperatures, the optimum flow rate ( $\mu_{\text{opt}}$ ) dictated by the van Deemter curve is higher, resulting in faster separations. (See Figure 1-13).

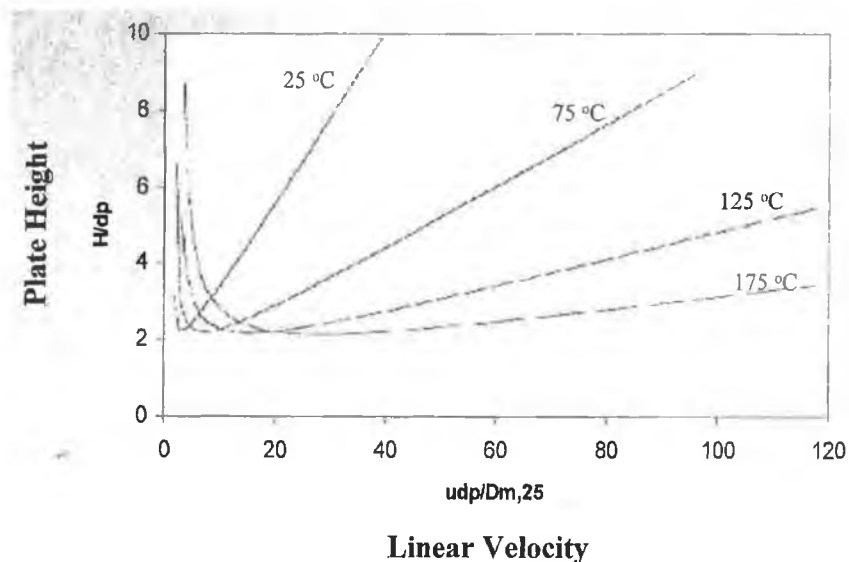


**Figure 1-13.** Van Deemter curves showing decreased plate height with increasing column temperature. Reproduced from F.D. Antia, C.S. Horvath, *J. Chromatogr.* 435 (1988) 1.

There are three main system requirements for the use of elevated column temperatures in LC such that chromatographic efficiency is not compromised.

1. Matching of mobile phase temperature with column temperature. Mayr and Welsch [37] and later, Yan *et al.* [34] studied the band broadening effect of thermostating the column at high temperatures, but leaving the eluent at room temperature. If the incoming eluent is significantly lower in temperature ( $> 5\text{ }^{\circ}\text{C}$ ) than the column temperature, the mobile phase temperature on the column will be higher at the column wall than it is at the centre of the column. This will cause a radial viscosity gradient in the column resulting in increased solute diffusion near the column wall where the mobile phase viscosity is lower. The difference in solute velocities across the viscosity gradient can cause peak broadening and splitting as illustrated by Figure 1-14. To counteract this effect, the eluent must be preheated to the same temperature as the column. Mayr and Welsch [37] pumped the eluent through some 50 cm X 0.5 mm stainless steel tubing immersed in a water bath. Due to the heat conductivity and heat capacity of the injection valve, this was also thermostatted in the same water bath. Yan *et al.* [34] noted that the use of a liquid bath for high temperature LC instead of an air bath is much more superior because heat transfer through a liquid is better than that through air. At high flow rates, the

length of thermal equilibration tubing needs to be very much longer in an air bath. An alternative to a liquid bath is a block heater, used by Chong *et al.* [38] to preheat their eluent by using a 30 cm long piece of 0.005 in. I.D. PEEK tubing wrapped around the mobile phase pre-heater.

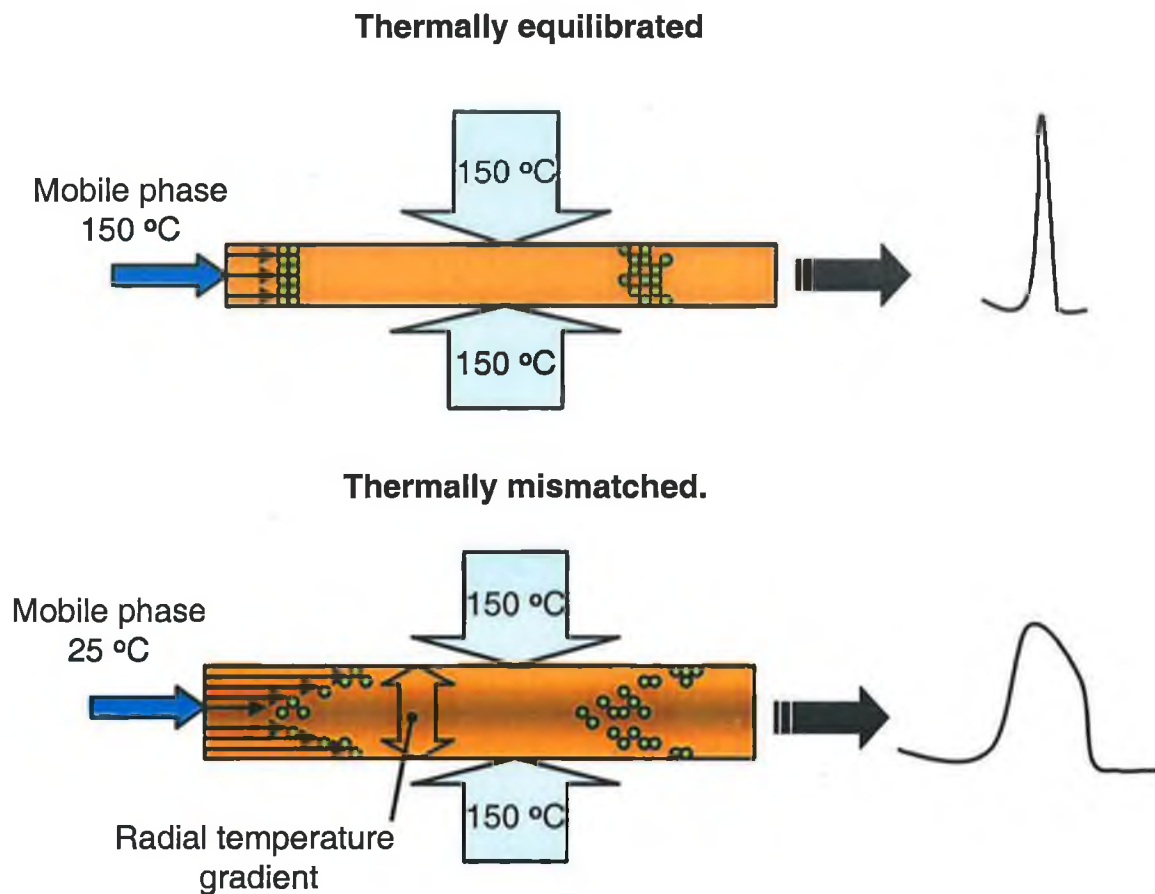


**Figure 1-14.** The effect of thermally mismatched mobile phase temperatures and column temperatures upon peak efficiency. The upper figure shows that when the mobile phase temperature is the same as the column temperature, good peak efficiency is obtained. The lower figure shows that when the mobile phase temperature is lower than the column temperature, the resulting radial temperature gradient across the column causes peak broadening.

2. Temperature reduction of column effluent to protect the detector. Yan *et al.* [34] found that at high column temperatures of 150 °C the UV detector used could not tolerate the high temperature and so the hot eluent from the column outlet had to be cooled before entering the detector by using a 20 cm length of narrow bore tubing [1/16 in. (O.D.) X 0.004 in. (I.D.)] immersed in an ice bath. Chong *et al.* [38] used a similar setup to protect their suppressor during suppressed conductivity IC, but since

the maximum column temperature used in this case was 60 °C, 10 cm of post column PTFE tubing (0.007 in. I.D.) immersed in a beaker of room temperature water was considered sufficient.

3. Prevention of mobile phase boiling using post-column back pressure coils. At higher temperatures, there is a danger that the mobile phase could boil in the column. However, since the boiling point of solvents is increased at the extremely high pressure in a HPLC column, this boiling is less likely to occur. As an additional safety feature, Yan *et al.* [34] used a backpressure regulator after the UV detector to keep about 30 bar of pressure on the system, to prevent the mobile phase from boiling.

Reversed phase separations at high temperatures have been reported using thermally stable zirconia-based stationary phases. Sixteen aromatic hydrocarbons<sup>15</sup> have been separated within six minutes on a 150 mm X 4.6 mm ZirChrom-PS<sup>16</sup> column at 125 °C with a flow rate of 3.0 ml/min. The mobile phases were A: water and B: acetonitrile. The gradient program increased the acetonitrile content from 10 % up to 50 % over the first seven minutes, with a 0.5 minute hold at this acetonitrile level [39].

A mixture of nine nitrosamines was separated in three minutes on a 100 mm X 4.6 mm zirconia-based DiamondBond-C<sub>18</sub> column at 75 °C using a flow rate of 4.0 ml/min. In this instance, the mobile phases were A: 10 mM ammonium hydroxide, pH 9.5 and B: acetonitrile. The gradient program increased the acetonitrile content from 2.5 % up to 90 % from one to three minutes [40].

A mixture of uracil, phenol, methylparaben, ethylparaben, propylparaben and butylparaben were separated in less than 45 seconds on a 50 mm X 4.6 mm DiamondBond-C<sub>18</sub> column at 150 °C with a flow rate of 5.5 ml/min. The mobile phase was 20:80 acetonitrile / 20 mM phosphoric acid, pH 2.3 [41].

---

<sup>15</sup> Naphthalene, methylnaphthalene, acenaphthylene, acenaphthene, fluorine, decafluorobiphenyl, phenanthrene, anthracene, fluoranthene, pyrene, p-terphenyl-d14, benzo(a)anthracene, benzo(b)fluoranthene, benzo(a)pyrene, dibenzo(a,h)anthracene, benzo(g,h,i)perylene.

<sup>16</sup> This phase is created by coating the zirconia particle with a thin layer of polystyrene. It has a pH working range of 1-13 and a temperature limit of 150 °C.

The reduction in analysis time which can be achieved with elevated column temperatures is illustrated by the work of Yan *et al.* [34] who reduced the analysis time for a separation on alkylphenones by a factor of 50 from twenty minutes at 25 °C to 24 seconds at 150 °C. The flow rate that could be used for a mobile phase of 30 % acetonitrile at 25 °C was 4 ml/min, whereas at 150 °C, the flow rate could be increased to 15 ml/min. At 150 °C the concentration of acetonitrile was reduced slightly to 25 % to ensure adequate resolution.

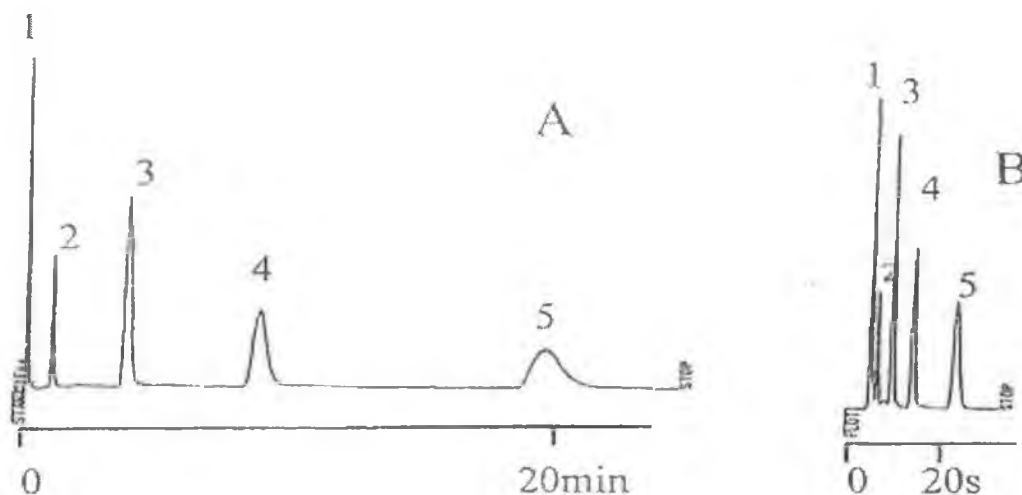


**Figure 1-15.** Chromatograms showing the effect of increased column temperature upon the rapid separation of a mixture of alkylphenones. Chromatographic conditions: Column: 50 mm X 4.6 mm PS-ZrO<sub>2</sub> (2.5 μm). Mobile phase A: 30 % acetonitrile at a flow rate of 4 ml/min at 25 °C, Mobile phase B: 25 % acetonitrile at a flow rate of 15 ml/min at 150 °C. Peaks: [1]: acetophenone, [2]: octanophenone, [3]: decanophenone, [4]: dodecanophenone, [5]: tetradecanophenone. Reproduced from B. Yan *et al.* *Anal. Chem.* 72 (2000) 1253.

### 1.6.1 Effect of temperature on selectivity in ion-exchange chromatography.

The use of elevated temperatures in anion-exchange chromatography is usually restricted to temperatures below 60 °C. More drastic increases in column temperature are not practical because of the low thermal conductivity of PEEK, the polymer used for most ion-exchange columns, the low thermal stability of quaternary ammonium exchange sites [24,38] and the endothermic retention behaviour of some anions such as sulphate and phosphate. Hatsis and Lucy [42] investigated the effect of temperatures up to 60 °C on the retention of small inorganic anions on Dionex

AS11 and AS14 anion exchange columns. Van't Hoff plots were used to determine the influence of temperature upon retention and selectivity. The van't Hoff equation describes the effect of temperature upon chromatographic retention.

$$\ln k' = A - \frac{B}{T} \quad \text{Equation 1-11}$$

where A and B are constants for a particular analyte,  $k'$  is the capacity factor and T is the temperature in Kelvin. Plots of  $\ln k'$  versus  $1/T$  were linear over the temperature range studied by Hatsis and Lucy. The slopes of the van't Hoff curves for different anions were both negative<sup>17</sup> (endothermic) and positive<sup>18</sup> (exothermic). Endothermic retention behaviour results in an increase in retention with increasing temperature whereas exothermic behaviour results in a decrease in retention with increasing temperature.

In reversed phase HPLC exothermic retention behaviour is generally observed, with the retention of all analytes decreasing at the same rate, since the slopes of the van't Hoff curves are generally all equal. However, Hatsis and Lucy observed that in anion exchange chromatography, the retention of different anions was affected to differing degrees such that large changes in selectivity for an anion exchange separation could be achieved by judicious use of column temperature. Hatsis and Lucy separated the test anions into individual subgroups based on the van't Hoff curves obtained. The retention of anions within the same subgroup was affected by temperature to the same extent, based on the approximately parallel lines of the van't Hoff curves. Therefore, changes in selectivity were not observed within a particular subgroup, but changes in temperature did result in selectivity changes between analytes from different subgroups. These subgroups were divided into three distinct groupings of retention behaviour: weakly retained anions (iodate, bromate, nitrite, bromide and nitrate), multiply charged anions (sulphate, oxalate, phosphate and thiosulphate), and strongly retained singly charged anions (iodide, thiocyanate and perchlorate). Hatsis and Lucy also found that changing the eluent type, for

---

<sup>17</sup> Iodate, bromate, nitrate, sulphate, oxalate, thiosulphate and phosphate on a Dionex AS11 column with a 12 mM hydroxide eluent.

<sup>18</sup> Bromide, nitrate, iodide, thiocyanate and perchlorate on a Dionex AS11 column with a 12 mM hydroxide eluent.

example from hydroxide to carbonate, changed the temperature dependence of these subgroups such that the slopes of the van't Hoff curves changed, and in some cases were actually reversed from endothermic behaviour to exothermic behaviour.

In the case of cation exchange resins, Chong *et al.* [38] found that they exhibited better thermal stability than anion exchange resins allowing temperatures up to 90 °C to be used. Chong *et al.* found that retention could be decreased for all cations studied<sup>19</sup> over a temperature range of 27 °C to 90 °C using a Dionex CS12A column and a 17 mM MSA eluent. Selectivity differences were most pronounced for cations of differing charge. The same observations were made by Hatsis and Lucy [43] again using a Dionex CS12A column. Even though the retention of all cations decreased with increasing temperature, the retention of alkali metals was more sensitive to increasing temperature than that of alkaline earth metals. Chong *et al.* [38] found therefore that as temperature was increased, the separation between cesium and magnesium was much improved. (See Figure 1-16). Increasing the column temperature from 27 °C to 60 °C allowed an increase in flow rate from 0.9 ml/min to 1.30 ml/min due to the decrease in the viscosity of the 17 mM MSA eluent. This resulted in a 35 % decrease in analysis time.

---

<sup>19</sup> Lithium, sodium, ammonium, potassium, rubidium, cesium, magnesium, calcium and strontium.

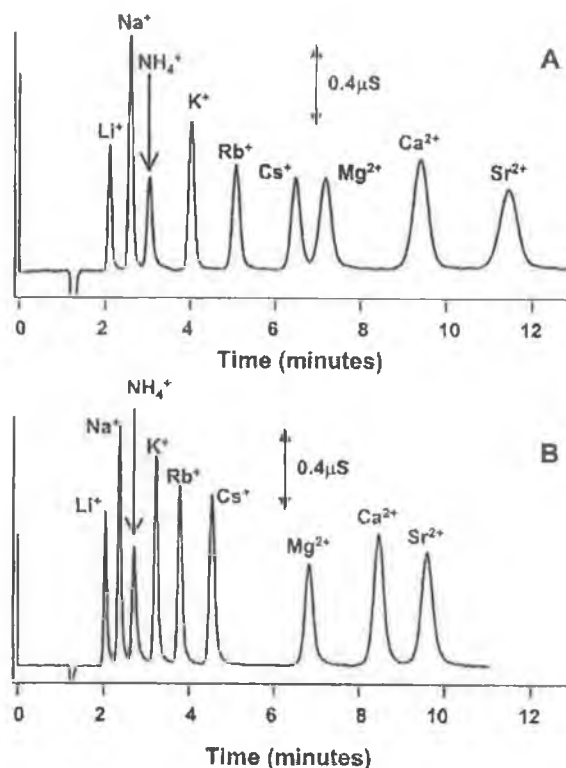


**Figure 1-16.** Effect of increased column temperature upon selectivity for a separation of nine cations. Chromatographic conditions: Column: Dionex CS12A 150 X 3 mm I.D., Mobile phase: 17 mM MSA, Flow rate: 0.5 ml/min, Injection volume: 20  $\mu$ L, Column temperature: (A) 27  $^{\circ}$ C and (B) 60  $^{\circ}$ C, Analyte concentration: 50  $\mu$ M. Reproduced from J. Chong et al. *J. Chromatogr. A.* 997 (2003) 161.

Hatsis and Lucy [43] noted that like the retention behaviour of anions with changing temperature, the retention behaviour of cations could be divided into three distinct subgroups; alkali metals, alkaline earth metals and amines. Again, selectivity was not affected between cations belonging to a particular subgroup (by virtue to the roughly parallel van't Hoff curves), but changes in temperature did result in selectivity changes between analytes from different subgroups.

### 1.7 Ion interaction chromatography.

It has been seen that silica-based packings are well suited to rapid reversed phase separations, by virtue of the manufacturer's ability to produce the small particle sizes necessary. It is possible to use reversed-phase chromatography to

separate a mixture of ionic analytes, which possess some hydrophobic character. With a suitable choice of mobile phase pH, or the use of a pH gradient, the ionisation of the analytes can be suppressed, such that they move through the column as neutral molecules, and interact with the stationary phase primarily by reversed phase hydrophobic interactions.

In the case of very hydrophilic inorganic anions (chloride, nitrate, nitrite, sulphate, phosphate etc) and cations of interest, which are derived from strong acids or bases, they are dissociated over a very wide pH range. Suppression of their ionisation is not possible within the working pH range of common silica based columns (pH 2-8). Therefore, there is little or no retention of such hydrophilic ionic solutes on lipophilic C<sub>18</sub> stationary phases when conventional reversed phase eluents are used.

Ion-exchange chromatography offers a suitable alternative and involves the use of a stationary phase containing chemically bonded charged functional groups on its surface. The mobile phase contains oppositely charged counter-ions to neutralise the charge, and sample ions of the same charge as the mobile phase counter-ion, will compete for electrostatic interaction with the stationary phase. For example, to separate a mixture of anions, a stationary phase containing positively charged ammonium groups will be used, with a mobile phase containing a negatively charged counter-ion such as hydroxide. Similarly for cation analysis the stationary phase will be functionalised with negatively charged sulphonate groups and the mobile phase will contain a positively charged counter-ion such as hydronium.

The most commonly used option for ion analysis has been ion-exchange chromatography. The determination of common anions in natural and treated waters is one of the commonest analyses routinely carried out by testing laboratories. However, despite the advances made in conventional LC separations, the rapid chromatographic separation of small inorganic/organic ions using ion-exchange resins has to-date not received much attention. This is due to the lack of commercially available bonded ion-exchange resins that possess the desired properties for rapid chromatographic separations discussed in Section 1-1.

However, this problem can be overcome by carrying out ion-interaction chromatography using the above reversed-phase materials. Ion-interaction chromatography is a powerful technique that allows conventional reversed-phase columns to be used for the separation of inorganic and organic ions, with comparable and often better efficiency and resolution to that obtained by conventional ion chromatography. The mobile phases used in ion-interaction chromatography contain a hydrophobic ion-interaction (ion-pairing) reagent of opposite charge to the analyte ions, with analyte retention being based upon the formation of a neutrally charged ion-pair between these two species. This ion-pair formation may take place predominantly in the mobile phase (as described by the so-called 'ion-pairing retention model'), or at the surface of a dynamically coated stationary phase ('dynamic ion-exchange retention model'). A third mechanism has been suggested which is considered to be a hybrid of the two other retention mechanisms. A number of reviews have been published on the subject of ion-interaction chromatography of small anions including a recent comprehensive review by Gennaro and Angelino [44], which discusses the various models put forward to explain the retention mechanism in ion-interaction chromatography.

No firm agreement has been reached as to which model best describes the mechanism for ion-interaction chromatography, but each of the three models is supported to differing extents by the experimental data gathered when certain chromatographic parameters are varied, as discussed below:

- **The nature of the ion-interaction reagent (IIR).** The IIR is typically a long chain hydrophobic molecule with a charged group at one end (typically an ammonium group for anion determinations and a sulphonate group for cation determinations). In general terms, the length of the hydrocarbon chain determines its hydrophobicity, with hydrophobicity increasing with increasing chain length. More hydrophobic IIR's in the eluent will interact with the stationary phase to a greater extent and increase the "dynamic exchange capacity" of the column, thus increasing retention for oppositely charged solute ions [45-47]. As a general rule, hydrophilic ions are best separated using a hydrophobic IIR, and hydrophobic ions are best separated using a hydrophilic IIR.

- **The concentration of the IIR.** Increased concentration of IIR in the eluent will also result in increased retention of oppositely charged analytes, again since the “dynamic exchange capacity” of the column is increased. The retention will increase up to a certain point, and will then decrease with further additions of IIR, due to the increasing concentration of the IIR counter-ion, which acts as a competing ion [48,49]. High concentrations of IIR in the eluent can cause solubility problems, especially if acetonitrile is used as an organic modifier. If this becomes an issue, then a longer chain IIR should be used. Generally, a low concentration of a long chain IIR will result in the same separation as that produced when a high concentration of a short chain IIR is used.
- **The concentration of the organic modifier.** Since the analyte/IIR ion pair has an overall neutral charge, its retention is thus governed by hydrophobic interactions by virtue of its lipophilicity. An organic solvent is added to decrease retention of the combined analyte/IIR pair or the IIR itself, and therefore reduce runtimes [48,49]. Selectivity can be adjusted by appropriate choice of the organic solvent.
- **The nature of the stationary phase.** Gennaro and Angelino compared the performance of polymeric supports versus silica based supports for ion-interaction chromatography with iron(II)-1,10-phenanthroline as IIR and found that polymeric based supports gave better results regarding (i) stability in relation to pH variation, (ii) greater efficiency, (iii) longer column life, (iv) higher IIR loading. However, for alkylammonium IIR's, silica based stationary phases resulted in higher efficiencies and were faster to equilibrate when elution conditions were changed. With silica based phases, retention increases on a more hydrophobic stationary phase, for example; C<sub>18</sub> relative C<sub>8</sub> [49]. Also, irregularity of the silica packing material can cause increased retention and tailing of peaks, because the coverage of the silica material is less homogenous than in the presence of spherical particles. This can induce secondary, non-specific interaction between the stationary phase and the analytes [49].

- **The concentration and nature of the counter ion.** Retention will decrease with an increase in IIR counter ion concentration. The “dynamic ion-exchange” retention model suggests that the stationary phase has ion-exchange character when charged IIR is adsorbed. For this reason, the IIR counter-ion, (which will have the same charge as that of the analyte) acts as a competing ion, resulting in decreased retention. In a manner similar to conventional ion-exchange chromatography, retention will be decreased when a counter-ion is chosen which has increased eluting strength (for example if a monovalent ion is replaced by a divalent ion). Of course the choice of IIR counter-ion may be dictated by the mode of detection used. For example:

- Hydroxide for suppressed conductivity detection.
- Phthalate for direct conductivity detection.
- Phosphate for direct UV detection.
- Phthalate or salicylate for indirect UV detection.

#### 1.7.1 The ion-pair model.

This model postulates that the charged IIR forms an “ion-pair” with an analyte molecule of opposite charge in the eluent. This lipophilic ion-pair, which has an overall neutral charge, partitions between the mobile and stationary phases by reversed phase hydrophobic interactions. The degree of retention occurring for an analyte is dependant on the lipophilicity of the IIR, and its concentration, with increases in both resulting in increased retention. As in classical reversed phase chromatography, increased organic modifier content will shift the partition equilibrium toward the mobile phase and result in reduced retention. An increased concentration of IIR counter-ion or some other added competing ion will result in reduced retention, since there is increased competition for ion-pair formation in the eluent.

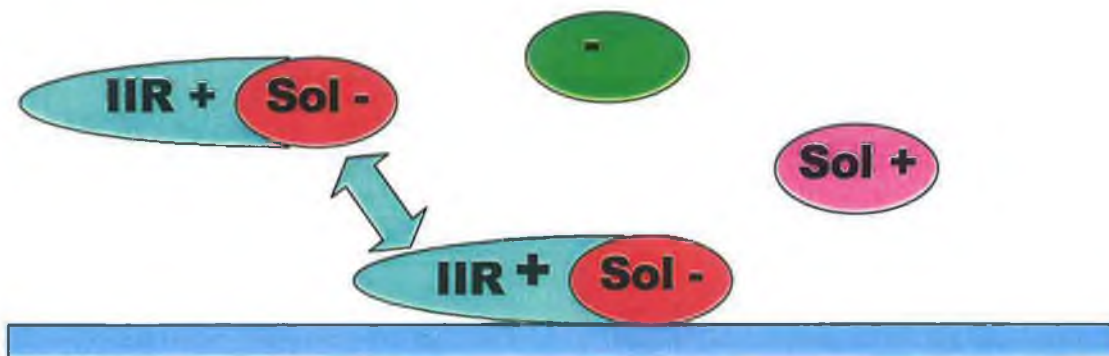


**Figure 1-17.** Schematic of the “ion-pair retention model” for ion-interaction chromatography. The blue section represents the stationary phase. In this case, the IIR is a cation and so the figure represents the determination of anions. The dark green circle is the IIR counter-ion and the pink circle is the solute counter-ion.

### 1.7.2 The dynamic ion-exchange model.

This model suggests that the charged IIR is in dynamic equilibrium between the stationary phase and mobile phase and will adsorb onto the stationary phase by virtue of its hydrophobic nature. This imparts a charge on the stationary phase such that it acts as an ion-exchanger. The charged active sites are not fixed like in a bonded ion-exchange stationary phase, but are rather constantly interchanging, since the IIR is in dynamic equilibrium between both phases. This means that the column can be considered a *dynamic ion-exchanger*. Altering the nature of the IIR, its concentration in the eluent, and the concentration of organic modifier can change the *dynamic exchange capacity* of the column. Oppositely charged solute ions will compete with the IIR counter ion (or a second competing ion which could be deliberately added) for the charged sites.

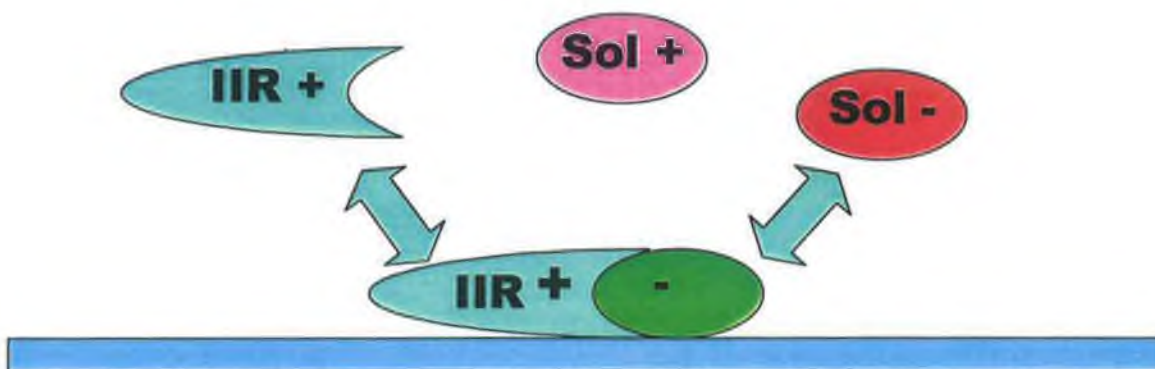


**Figure 1-18.** Schematic of the “dynamic ion-exchange model” for ion-interaction chromatography. The blue section represents the stationary phase. Again, in this case, the IIR is a cation and so the figure represents the determination of anions. The dark green circle is the IIR counter-ion and the pink circle is the solute counter-ion.

### 1.7.3 The ion-interaction model.

This model can be considered to be a hybrid of the two previously discussed models. Firstly it incorporates the theory that retention of a solute ion involves a pair of oppositely charged ions. Secondly it proposes that a charged IIR adsorbs onto the stationary phase and imparts a charge such that the stationary phase possesses a dynamic exchange capacity. This results in an electrical double layer at the charge surface. The adsorbed IIR ions on the stationary phase will be evenly spaced due to repulsive effects, and constitute the primary charged layer. A secondary oppositely charged layer is attracted to this layer and consists mainly of IIR counter-ions. The amount of charge in each layer is governed by the hydrophobicity and concentration of IIR and by the concentration of organic modifier present. Solute molecules can compete with counter-ions for a presence in the secondary layer, and when they are in this layer, they will be attracted to the primary layer by electrostatic effects and will be retained. When a solute molecule enters the primary layer, an oppositely charged IIR ion must enter the primary layer to maintain a charge balance. In this respect, one can consider the solute ion to be traversing the column as a pair of ions, but not necessarily an ion-pair.

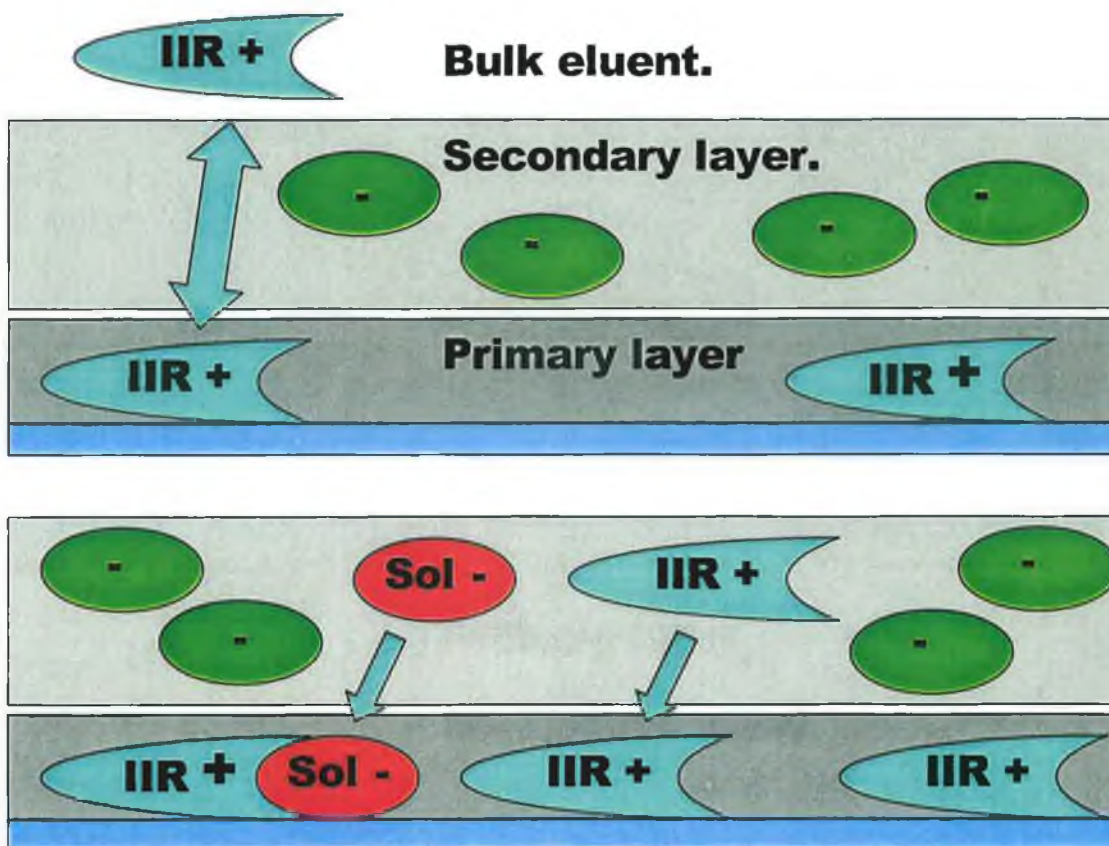


**Figure 1-19.** Schematic of the “ion-interaction model” for ion-interaction chromatography. The blue section represents the stationary phase. Again, in this case, the IIR is a cation and so the figure represents the determination of anions. The dark green circle is the IIR counter-ion.

There are two distinct modes of operation in ion-interaction chromatography. One mode known as “dynamic modification” involves the use of a mobile phase containing an IIR, which is in dynamic equilibrium with the stationary phase. The stationary phase can be considered to possess a “dynamic exchange capacity”, which is dependant on the mobile phase composition (organic modifier content, concentration and type of IIR etc).

The second mode of operation is that known as “permanent coating”, in which the stationary phase is coated with an IIR in an initial step, in effect giving the stationary phase ion-exchange properties. The advantage of this mode over “dynamic modification” is that the IIR can be removed completely from the mobile phase in subsequent analyses, and replaced by a simple counter-ion, in a manner similar to

conventional ion-exchange chromatography. The further advantage of this mode over conventional ion-exchange chromatography, is that ion-chromatography can be performed on reversed-phase packings which exhibit very high separation efficiency, while utilising similar eluents commonly used in ion-exchange chromatography. In addition, the exchange capacity of the column can be customised to suit a specific need, simply by adjusting the concentration of IIR, which has access to the stationary phase during the coating step. There has been much work done in this field utilising both modes in combination with a number of detection modes for the determination of a wide range of small ions, as detailed in Table 1-2. Permanent coating is discussed in more detail in Chapter 5, Chapter 6 and Chapter 8.

The work detailed in the following results section, illustrates the use of both modes of ion-interaction chromatography on a short column (the use of dynamic modification was initially studied, followed by permanent coating), and demonstrates the use of such modes for a wide range of environmental monitoring applications.

**Table 1-2:** Experimental conditions of ion-interaction methods based on  $C_{18}$  and  $C_8$  stationary phases.

Stationary phase	Mobile phase	Analytes	Method	Detection mode	Application.	Reference
TSK gel ODS-80T <sub>M</sub> CTR (100 X 4.6 mm) 5 μm, and SIL-C <sub>18</sub> /5B (150 X 4.6 mm) 5 μm.	Varying concs of the hydroxide forms of TMA, TEA, TPA, TBA, TPcA and THA in MeOH investigated.	Br <sup>-</sup> , NO <sub>3</sub> <sup>-</sup> , I <sup>-</sup> , Cl <sup>-</sup> , ClO <sub>3</sub> <sup>-</sup> , NO <sub>2</sub> <sup>-</sup> , SO <sub>4</sub> <sup>2-</sup> , BF <sub>4</sub> <sup>-</sup> , K <sup>+</sup> and Na <sup>+</sup>	Dynamic modification	Indirect UV at 300 nm	River, tap, rain and sea-waters.	[45]
(50 X 4.6 mm) Capcell Pack C <sub>18</sub> AG120, 5 μm	1 mM citrate, pH 7.0 with NaOH	Thiocyanate	Permanent coating with 10 mM cetyldimethylamine in 0.001 M HCl containing 10 % MeOH	UV at 210 nm	Urine and saliva.	[46]
Ultaron VX ODS, 150 X 4.6 mm)	ACN/H <sub>2</sub> O (20:80) + 6 mM TPA-OH, pH 5.0	SCN <sup>-</sup> and polythionates (S <sub>x</sub> O <sub>6</sub> <sup>2-</sup> ): x = 2,3,4,5 and 6)	Dynamic modification	UV at 230 nm	Hot spring water	[47]
Shim-Pack CLC-C <sub>8</sub> (150 X 6 mm) 5 μm	MeOH/phosphate buffer (15:85) pH 5, 3.0 mM TBA-OH and 0.1 mM EDTA	I <sup>-</sup> , S <sub>2</sub> O <sub>3</sub> <sup>2-</sup> , NO <sub>2</sub> <sup>-</sup> , SCN <sup>-</sup> , S <sup>2-</sup>	Dynamic modification	Amperometric, glassy carbon electrode (+1.0 V) vs. Ag/AgCl	Lake water	[48]
Analytical columns used: 10 μm, (250 X 4 mm) LiChrosorb RP-18, LiChrospher 100 RP-18 and LiChrospher 100 RP-8. Guard columns: 5 μm (4 X 4 mm) LiChrocart RP-18 and LiChrocart RP-8	MeOH/H <sub>2</sub> O (6:94), 7 mM hexamethonium bromide, 60 mM NaCl, pH 7.0	Tartaric, fumaric, pyruvic, maleic, phthalic, benzoic, sorbic, 4-hydroxybenzoic and toluene-4-sulphonic acids.	Dynamic modification	UV at 210 nm	Orange juices.	[49]
Spherisorb ODS, (250 X 4.6 mm) 5 μm	Micellar mobile phase. 0.018 M phosphate buffered ACN/H <sub>2</sub> O (35:65 v/v) containing 1 X 10 <sup>-2</sup> M HDTMA chloride	IO <sub>3</sub> <sup>-</sup> , NO <sub>2</sub> <sup>-</sup> , Br <sup>-</sup> , NO <sub>3</sub> <sup>-</sup> , I <sup>-</sup>	Dynamic modification	UV at 205 nm	Nitrate and nitrite in domestic water.	[50]
Zorbax C <sub>18</sub> (150 X 4.6 mm) 6 μm, and PRP-1 (150 X 4.1 mm) 10 μm	1,10-phenanthroline [Fe(phen) <sub>3</sub> ] <sup>2+</sup> , with varied concs of MeOH or ACN	Cl <sup>-</sup> , F <sup>-</sup> , Br <sup>-</sup> , BrO <sub>3</sub> <sup>-</sup> , ClO <sub>3</sub> <sup>-</sup> , IO <sub>3</sub> <sup>-</sup> , NO <sub>3</sub> <sup>-</sup> , I <sup>-</sup>	Dynamic modification	Indirect UV-Vis at 510 nm	-	[51]
Resolve C <sub>18</sub> Radial-Pak cartridge, 5 μm, (8 mm X 10 cm)	0.4 mM TBA-Salicylate, pH 4.62	NO <sub>3</sub> <sup>-</sup> , Cl <sup>-</sup> , Br <sup>-</sup> , NO <sub>2</sub> <sup>-</sup> , I <sup>-</sup> , SO <sub>4</sub> <sup>2-</sup> , S <sub>2</sub> O <sub>3</sub> <sup>2-</sup> , H <sub>2</sub> PO <sub>4</sub> <sup>-</sup>	Dynamic modification, and permanent coating with cetylpyridinium Cl	Indirect UV at 288 nm and conductivity	-	[52]
TSK gel ODS-80T <sub>M</sub> (50 X 4.6 mm) 5 μm	1 mM citrate-2.5 % MeOH, pH 6.5	NO <sub>3</sub> <sup>-</sup> , Br <sup>-</sup> , NO <sub>2</sub> <sup>-</sup> , SO <sub>4</sub> <sup>2-</sup>	Permanent coating with 0.01 M cetylpyridinium Cl in 10 % MeOH	UV at 210 nm	Human serum, saliva and urine.	[53]

Stationary phase	Mobile phase	Analytes	Method	Detection mode	Application.	Reference
Zorbax ODS (250 X 4.6 mm) 5 $\mu$ m	ACN/H <sub>2</sub> O (35:65), 2 mM cetylpyridinium Br, and 10 mM phosphate buffer.	IO <sub>3</sub> <sup>-</sup> , Br <sup>-</sup> , NO <sub>3</sub> <sup>-</sup> , I <sup>-</sup> , BrO <sub>3</sub> <sup>-</sup> , NO <sub>2</sub> <sup>-</sup> , SCN <sup>-</sup>	Dynamic modification	UV at 222 nm	NO <sub>2</sub> <sup>-</sup> /NO <sub>3</sub> <sup>-</sup> in human saliva, iodide in commercial salt.	[54]
Spherisorb ODS-2, (250 X 4.6 mm) 5 $\mu$ m	5mM octylamine at pH 6.4 with orthophosphoric acid	NO <sub>2</sub> <sup>-</sup> , NO <sub>3</sub> <sup>-</sup>	Dynamic modification	UV at 230 nm	Venice lagoon water.	[55]
TSK gel ODS-80T <sub>M</sub> (150 X 4.6 mm) 5 $\mu$ m and Capcellpak C <sub>18</sub> (150 X 4.6 mm) 5 $\mu$ m.	0.1 M NaCl with 5 mM sodium phosphate buffer (pH 5.8)	IO <sub>3</sub> <sup>-</sup> , Br <sup>-</sup> , NO <sub>3</sub> <sup>-</sup> , I <sup>-</sup> , S <sub>2</sub> O <sub>3</sub> <sup>2-</sup> , NO <sub>2</sub> <sup>-</sup> , SCN <sup>-</sup>	Permanent coating with 1 mM cetylpyridinium Cl in 20 % MeOH	UV at 225 nm and amperometric (glassy carbon working electrode (+1.0 V) vs. Ag/AgCl)	Artificial sea water.	[56]
Waters Novapak C <sub>18</sub> (150 X 3.9 mm) 4 $\mu$ m.	30 $\mu$ M potassium hexacyanoferrate	SO <sub>4</sub> <sup>2-</sup>	Permanent coating with 5 mM 1,12-diaminododecane in 10 % MeOH pH 4.2 (H <sub>2</sub> SO <sub>4</sub> )	Indirect UV at 205 nm	Water analysis (well, tap, surface, mineral and waste)	[57]
Waters Novapak C <sub>18</sub> (150 X 3.9 mm) 4 $\mu$ m.	Potassium hydrogenphthalate 0.4 mM pH 4.9	Br <sup>-</sup> , NO <sub>3</sub> <sup>-</sup> , Cl <sup>-</sup> , NO <sub>2</sub> <sup>-</sup> , SO <sub>4</sub> <sup>2-</sup>	Permanent coating with 1 mM cetylpyridinium Cl in 10 % MeOH	Indirect UV at 254 nm	Inorganic anions in wine together with carboxylic acids.	[58]
Hamilton PRP-1 (150 X 4.1 mm) 10 $\mu$ m	0.1 mM Ru (II) complex with 1,10-phenanthroline or 2,2-bipyridine + 0.1 mM succinate buffer at pH 6.1	NO <sub>3</sub> <sup>-</sup> , Cl <sup>-</sup> , NO <sub>2</sub> <sup>-</sup> , SO <sub>4</sub> <sup>2-</sup> , ClO <sub>3</sub> <sup>-</sup> , BF <sub>4</sub> <sup>-</sup> , F <sup>-</sup> , HPO <sub>4</sub> <sup>2-</sup> , H <sub>2</sub> AsO <sub>4</sub> <sup>2-</sup> , CrO <sub>4</sub> <sup>2-</sup>	Dynamic modification	Direct and indirect Vis at 445 nm and fluorescence (phen: Ex: 465 nm, Em: 600 nm; bpy: Ex: 460 nm, Em: 580 nm)	-	[59]
Hamilton PRP-1 (150 X 4.1 mm) 5 $\mu$ m	3% MeOH + 5 mM TBA-Phosphate, pH 7.6	Selenite, selenate and trimethylselenonium	Dynamic modification	ICP-MS	Selenium species in urine	[60]
Hamilton RP-1 (150 X 4.1 mm) 10 $\mu$ m	0.01 mM Ru(phen) <sub>3</sub> (ClO <sub>4</sub> ) <sub>2</sub> + (0.02-0.1) mM sodium tartrate	Br <sup>-</sup> , NO <sub>3</sub> <sup>-</sup> , Cl <sup>-</sup> , Br <sup>-</sup>	Dynamic modification	Indirect fluorometric detection (Ex: 447 nm, Em: 261 nm)	-	[61]
Kaseisorb LC ODS (150 X 4.6 mm)	10:90 and 20:80 ACN/H <sub>2</sub> O with 0.2 mM phthalate and 7 mM TPA-OH	Polythionates	Dynamic modification	Suppressed conductivity	Hot spring water	[62]

## 1.8 Detection methods for ion-exchange and ion-interaction chromatography.

### 1.8.1 Conductivity detection.

Conductivity detection has received widespread use in IC because it is a universal method of detection, since all ions are conducting. A conductivity detector essentially consists of two electrodes across which a potential is applied, and the current conducted by the solution which passes between the electrodes is measured. The extent to which a particular ion conducts in solution is termed the *limiting equivalent ionic conductance* ( $\lambda$ ) and is specific for each ion extrapolated to infinite dilution<sup>1</sup>. It is given by the following equation:

$$\lambda_i = \frac{eFz_i}{\eta r} \quad \text{Equation 1-12}$$

where  $e$  is the electronic charge,  $F$  is the Faraday constant,  $z_i$  is the number of charges on the ion,  $\eta$  is the viscosity and  $r$  is the ionic radius. A list of limiting equivalent ionic conductances for common anions and cations is given in Table 1-3. From the equation it is clear that large multiply charged ions can have the same limiting equivalent ionic conductance as small singly charged ions. This is important since multiply charged ions can be powerful competing ions in an eluent, but can lead to high background conductances unless the ionic radius is also large. Therefore, in the case of anion exchange chromatography, large multiply charged anions such as phthalate and citrate are suitable competing ions for sensitive detection. Sensitive conductivity detection is most suited to anions and cations of strong acids and bases such as chloride, sulphate, nitrate, sodium and potassium. Ions of weak acids and bases such as phthalate, acetate and triethylamine are only detected with adequate

---

<sup>1</sup> Direct proportionality between the conductivity of an ionic solution and its concentration can be lost as the concentration increases because of possible formation of ion-pairs due to ion-ion interactions leading to a decrease in the effective conductivity of the solution. However, by measuring the conductance of an ion in solution extrapolated to infinite dilution, concentration effects are not an issue. At the analyte concentrations typically found in IC, conductivity is generally proportional to conductivity.

sensitivity when the mobile phase is such that they are appreciably dissociated. Anions with pKa values below pH 6, show good sensitivity for conductivity detection because as analyte dissociation increases, so does sensitivity. Conversely, anions with pKa's above 7.0 generally result in poor signal to noise ratios.

The change in conductivity ( $\Delta G$ ) as a solute is eluted is dependant on the concentration of the solute ( $C_S$ ) and also the degree of ionization of the solute (for anions derived from strong acids the degree of ionization will be high; however for weak acids it can become an important factor and control of eluent pH is therefore more critical). The change in conductivity ( $\Delta G$ ) is also proportional to the difference between the limiting equivalent ionic conductances of the solute ( $S$ ) and the eluent competing ion ( $E$ ).

$$\Delta G = \frac{(\lambda_{S^-} - \lambda_{E^-}) C_S}{10^{-3} K} \quad \text{Equation 1-13}$$

(Note:  $K$  is the *cell constant* and is given by  $L/A$ , the distance that the two cell electrodes are placed from each other divided by the cross-sectional area of the electrodes. The measured conductivity of any given electrolyte solution will be larger for cells of a large cross-sectional which are placed close together). In the case of anion exchange chromatography, the cationic counterion of the solute is not considered since this is unretained and is eluted in the void. Similar reasoning follows for cation exchange chromatography.

**Table 1-3.** Limiting equivalent ionic conductances for anions and cations at 25 °C. Reproduced from Dionex CD20 Conductivity detector operator's manual, Document No. 034854, Revision 03, February 1996 and also from P.R.Haddad, P.E. Jackson, *Ion Chromatography: Principles and Applications*, J. Chromatogr. Library, Vol.46, Elsevier, Amsterdam, 1990.

Anion	$\lambda_{-}(\text{S.cm}^2.\text{eq}^{-1})$	Cation	$\lambda_{+}(\text{S.cm}^2.\text{eq}^{-1})$
OH <sup>-</sup>	198	H <sub>3</sub> O <sup>+</sup>	350
Fe(CN) <sub>6</sub> <sup>4-</sup>	111	Rb <sup>+</sup>	78
Fe(CN) <sub>6</sub> <sup>3-</sup>	101	Cs <sup>+</sup>	77
CrO <sub>4</sub> <sup>2-</sup>	85	K <sup>+</sup>	74
CN <sup>-</sup>	82	NH <sub>4</sub> <sup>+</sup>	73
SO <sub>4</sub> <sup>2-</sup>	80	Pb <sup>2+</sup>	71
Br <sup>-</sup>	78	Fe <sup>3+</sup>	68
I <sup>-</sup>	77	Ba <sup>2+</sup>	64
Cl <sup>-</sup>	76	Al <sup>3+</sup>	61
C <sub>2</sub> O <sub>4</sub> <sup>2-</sup>	74	Ca <sup>2+</sup>	60
CO <sub>3</sub> <sup>2-</sup>	72	Sr <sup>2+</sup>	59
NO <sub>3</sub> <sup>-</sup>	71	CH <sub>3</sub> NH <sub>3</sub> <sup>+</sup>	58
PO <sub>4</sub> <sup>3-</sup>	69	Cu <sup>2+</sup>	55
ClO <sub>4</sub> <sup>-</sup>	67	Cd <sup>2+</sup>	54
SCN <sup>-</sup>	66	Fe <sup>2+</sup>	54
ClO <sub>3</sub> <sup>-</sup>	65	Mg <sup>2+</sup>	53
Citrate <sup>3-</sup>	56	Co <sup>2+</sup>	53
HCOO <sup>-</sup>	55	Zn <sup>2+</sup>	53
F <sup>-</sup>	54	Na <sup>+</sup>	50
HCO <sub>3</sub> <sup>-</sup>	45	Phenylethylammonium <sup>+</sup>	40
CH <sub>3</sub> COO <sup>-</sup>	41	Li <sup>+</sup>	39
Phthalate <sup>2-</sup>	38	N(C <sub>2</sub> H <sub>5</sub> ) <sub>4</sub> <sup>+</sup>	33
C <sub>2</sub> H <sub>5</sub> COO <sup>-</sup>	36	Benzylammonium <sup>+</sup>	32
Benzoate <sup>-</sup>	32	Methylpyridinium <sup>+</sup>	30
Octanesulphonate	29	Tetrabutylammonium	19.1

IC analyses using conductivity detection can be divided between non-suppressed and suppressed detection modes. Non-suppressed conductivity detection

can be operated in *direct* or *indirect* modes. In *direct* conductivity detection, the analyte ion has a higher limiting equivalent ionic conductance than the eluent competing ion such that there is an increase in measured conductivity as the analyte enters the conductivity cell. Suitable eluents for *direct* conductivity detection are organic acids such as phthalate, citrate or benzoate for anions, or organic bases such as benzylamine for cations. In *indirect* conductivity detection, the limiting equivalent ionic conductance of the eluent competing ion is higher than that of the analyte such that there is a decrease in measured conductivity as the analyte enters the detector cell. Typical eluents are hydroxide eluents for anions and mineral acids ( $\text{HNO}_3$ ) for cations.

There is an inherent limit to the sensitivity which can be achieved by non-suppressed chromatography. Since the measured conductivity of a solution is the sum of the individual contributions of all the ions in the solution multiplied by their concentration, the response from analyte anions can often be overwhelmed by the response of the eluent ions. The basis of suppression is to suppress or ideally eliminate the background conductivity of the eluent while increasing the conductivity of the analyte species. This will maximise the difference in limiting equivalent ionic conductances of the analyte from the suppressed eluent and therefore maximise the change in measured conductivity upon elution of an analyte ion. A suppressor device (either a membrane type or a packed column type) is placed between the column and the detector such that after suppression of the column effluent, the background conductivity measured by the detector is much reduced. The first types of suppressor were of a packed column design. In the case of anion exchange chromatography, the packed column suppressor was packed with a cation exchange resin in the hydrogen form. As the eluent (for example, sodium hydroxide) flowed across this resin,  $\text{H}^+$  ions from the resin were exchanged for  $\text{Na}^+$  ions in the eluent such that the highly conducting hydroxide ion ( $\lambda_- = 198 \text{ S.cm}^2.\text{equiv}^{-1}$ ) was neutralised to water. In addition, if an anion in the sodium form (for example, chloride) was eluted from the column, the conductance of the sample was increased by virtue of the replacement of sodium ions ( $\lambda_+ = 50 \text{ S.cm}^2.\text{equiv}^{-1}$ ) with hydrogen ions ( $\lambda_+ = 350 \text{ S.cm}^2.\text{equiv}^{-1}$ ).

**Eluent suppression:**  $\text{Resin-H}^+ + \text{Na}^+\text{OH}^- \leftrightarrow \text{Resin-Na}^+ + \text{H}_2\text{O}$

**Analyte signal enhancement:**  $\text{Resin-H}^+ + \text{Na}^+\text{Cl}^- \leftrightarrow \text{Resin-Na}^+ + \text{H}^+ + \text{Cl}^-$

In the case of cation exchange, the packed column suppressor contains an anion exchange resin in the  $\text{OH}^-$  form which supplies  $\text{OH}^-$  to the acidic eluent, neutralising it to water and replacing the anionic counterion of the analyte with  $\text{OH}^-$ .

**Eluent suppression:**  $\text{Resin-OH}^- + \text{H}^+\text{Cl}^- \leftrightarrow \text{Resin-Cl}^- + \text{H}_2\text{O}$

**Analyte signal enhancement:**  $\text{Resin-OH}^- + \text{Na}^+\text{Cl}^- \leftrightarrow \text{Resin-Cl}^- + \text{OH}^- + \text{Na}^+$

The improvement in sensitivity is somewhat less for analyte ions of weak acids or bases due to decreased ionization at the neutral pH of the mobile phase following suppression.

Membrane suppressors were developed to replace packed column suppressors due to a number of disadvantages of the latter. Packed column suppressors had to be regenerated periodically by passing an appropriate solution (such as  $\text{H}_2\text{SO}_4$  for the  $\text{H}^+$  form suppressor or  $\text{NaOH}$  for the  $\text{OH}^-$  form suppressor) to displace the accumulated eluent cations/anions. Also, the packed column suppressor introduced significant extra column band broadening resulting in a loss of chromatographic efficiency.

A membrane suppressor provides  $\text{H}^+$  ions (in the case of anion exchange) or  $\text{OH}^-$  ions (in the case of cation exchange) to the eluent by electrolysis of water via two electrodes as illustrated in Figure 1-20. The eluent flows through a central chamber which is bound on either side by flat sheets of ion-exchange material in a sandwich arrangement. Regenerant flows in a countercurrent direction on the opposite sides of the ion-exchange screens. The fact that the membrane suppressor is constructed of flat sheets of membrane as opposed to a packed bed of resin greatly increases the surface area available for exchange between eluent and regenerant ions. In addition, the volume of the eluent chamber is very small ( $< 50 \mu\text{L}$ ) so that band broadening is minimised.

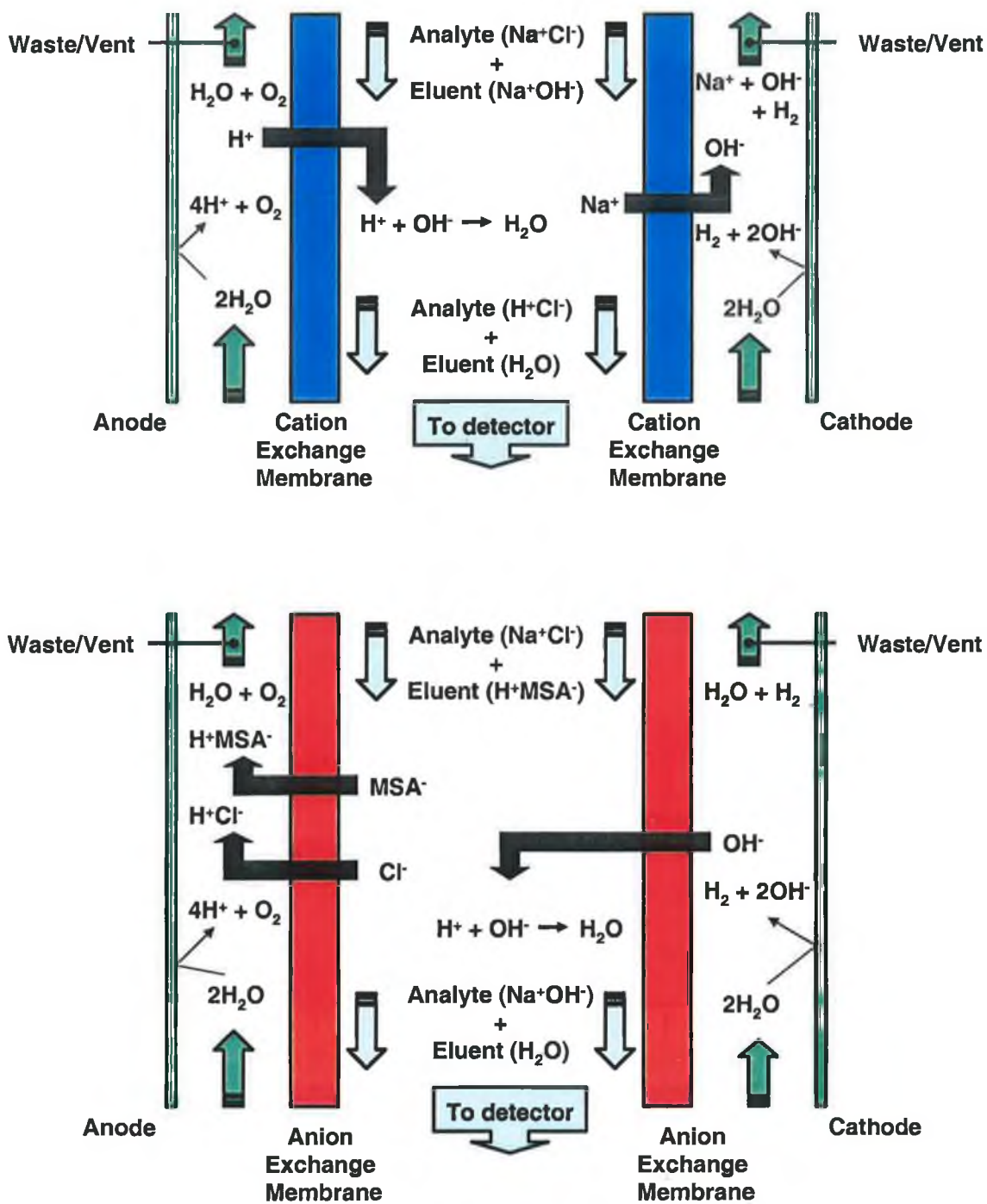


**Figure 1-20.** Mechanism of suppression in suppressed IC. The upper figure illustrates the suppression mechanism occurring inside a Dionex anion self regenerating suppressor (ASRS) using sodium hydroxide as the mobile phase for the determination of anions (in this case, chloride with sodium as counter-ion). The lower figure illustrates the suppression mechanism occurring inside a Dionex cation self regenerating suppressor (CSRS) using methanesulphonic acid as the mobile phase for the determination of cations (in this case, sodium with chloride as counter-ion).

When a suppressor is used in anion exchange chromatography, sodium salts of weak acids are generally used because they are converted to the neutral acid form in the suppressor. Because of the neutral pH of the mobile phase after suppression, it is important to use salts from acids with a high  $pK_a$  such that re-dissociation is minimised, thereby keeping background conductivity low. Sodium hydroxide is an excellent candidate since hydroxide is neutralised in the suppressor to water. A carbonate/bicarbonate buffer is another alternative, being suppressed to weakly conducting carbonic acid ( $pK_a = 6.2$ ). Other suitable mobile phases for suppressed anion chromatography include the sodium salts of boric acid (borax/tetraborate,  $pK_a = 9.2$ ) and o-cyanophenol ( $pK_a = 6.9$ ) [24]. For suppressed cation exchange chromatography, methanesulphonic acid is commonly used as an eluent.

#### 1.8.1.1 Effect of temperature upon conductivity detection.

Ion mobility and therefore conductivity are greatly affected by temperature. A 2 % conductance change is observed for each degree of temperature change over the range 10 °C to 25 °C [64], and therefore temperature fluctuations can affect the sensitivity and reproducibility of conductivity detection in IC.

#### 1.8.2 Spectrophotometric detection.

In anion exchange chromatography in which spectrophotometric detection is used, the change in absorbance during elution of a solute anion is described by Equation 1-10:

$$\Delta A = \left( \epsilon_{S^{x-}} - \frac{x}{y} \epsilon_{E^{y-}} \right) C_s m \quad \text{Equation 1-14}$$

where  $\epsilon_s^{x-}$  is the molar absorptivity of the solute ion,  $\epsilon_E^{y-}$  is the molar absorptivity of the eluent ion,  $x$  and  $y$  are the charges on the solute and eluent ions respectively,  $C_s$  is the concentration of the (dissociated) solute and  $m$  is the cell pathlength. The equation assumes that the solute is completely dissociated (in the case of anions, from HS to give  $H^+$  and  $S^-$  of which only  $S^-$  absorbs). In this instance, the change in

absorbance is due to the displacement of an equimolar amount of  $E^-$  from the eluent to give a solute peak, with a concentration of  $C_s$  at its maximum.

Spectrophotometric detection can be operated in direct or indirect mode. In direct spectrophotometric detection, ions which absorb to a greater extent than the eluent will result in a positive value of  $\Delta A$ . Examples of anions determined using this mode of detection include nitrate, nitrite, bromate, bromide, iodate and benzoate. The advantage of direct UV detection of anions is that interferences from anions with low molar absorptivities such as chloride, sulphate and phosphate can be reduced or eliminated. Suitable eluents for this mode of detections should be UV transparent at the wavelength chosen and include NaCl, NaOH,  $Na_2SO_4$ ,  $KH_2PO_4$  and carbonate/bicarbonate eluents. Most metal ions do not show strong enough molar absorptivities to be determined using direct spectrophotometric detection with the exception of copper (II), cerium (III), nickel (II) and cobalt (II). However, some cations can be detected in the UV range after complexation with a suitable ligand such as EDTA or  $Cl^-$ , both of which ligands form anionic complexes.

In indirect spectrophotometric detection, ions which absorb less than the eluent will result in a negative value for  $\Delta A$ , yielding an inverted peak at the detector. The polarity of the detector output may be reversed to give a positive peak on the data recorder used. Again, sensitivity will be maximised when the difference between the molar absorptivities of the solute and the eluent ion is large. The wavelength at which the eluent ion's absorptivity is highest is generally chosen. It is important, however, that the concentration of the eluent ion is not so high as to generate an excessively high background absorbance resulting in increased baseline noise. However, as will be discussed further in Chapter 6, (Section 6.3.2), a compromise must be made between sensitivity (low eluent ion concentration) and fast analysis times (higher eluent ion concentrations).

In the case of anion exchange chromatography with indirect UV detection, the following equation describes the change in absorbance due to elution of an anionic analyte and allows some conclusions to be made:

$$\Delta A = -\frac{x}{y} \varepsilon_{E^y} C_s m \quad \text{Equation 1-15}$$

where  $\Delta A$  is the change in absorbance,  $\varepsilon_{E^y}$  is the molar absorptivity of the eluent ion,  $x$  and  $y$  are the charges on the solute and eluent ions respectively,  $C_s$  is the concentration of the (dissociated) solute and  $m$  is the cell pathlength. The sensitivity of indirect UV detection increases as the ratio of the charge on the solute ( $x$ ) to the charge on the eluent ion ( $y$ ) is increased. Therefore, multi-charged eluents are not ideal.

For anion analysis, eluents such as p-hydroxybenzoate, phthalate, nitrate, pyromellitate etc are suitable. The pH of an aromatic acid eluent such as phthalate can be an important parameter affecting sensitivity. The use of alkaline pH's can cause a reduction in sensitivity because  $\text{OH}^-$  will then begin to compete with phthalate to elute solute anions. The elution of an anion due to the equimolar displacement of  $\text{OH}^-$  from the eluent does not cause an appreciable change in absorbance relative to when phthalate is displaced by the solute during elution. However, since phthalate is fully dissociated at alkaline pH's it is less prone to produce system peaks (as will be discussed later), and so again a compromise must be made. Ideally, aromatic acids should be used which are deprotonated at pH values  $< 7.0$ .

For indirect UV detection of cations, inorganic species such as copper (II), cobalt (II), nickel (II) and cerium (III) or aromatic amines have been used as eluents. For the same reasons as discussed for anions, UV absorbing aromatic amines should not be used at acidic pH's because  $\text{H}^+$  will compete very effectively with the protonated amine to be the principle competing eluent ion, resulting in a very small absorbance change and hence signal, at the detector. Only amines which are protonated at roughly neutral pH's should be used such as 1,4-phenylenediamine ( $\text{pK}_{a1} = 6.16$ ) or 2-methylpyridine ( $\text{pK}_a = 5.92$ ) [64].

### 1.8.2.1 System peaks.

Aromatic carboxylic acid salts when used as eluents in anion-exchange chromatography commonly give rise to system peaks, although system peaks are not exclusively confined to such eluents. System peaks are problematic since they can often co-elute with an analyte peak. They arise due to a disturbance of the equilibrium established between the eluent and the stationary phase upon injection of an analyte anion. Generally, one system peak known as the *injection peak* occurs early in the chromatogram. It arises due to the displacement of adsorbed eluent ions from the stationary phase at the head of the column by an injected analyte anion. A band of displaced eluent anions and unretained analyte cationic counter-ions will move down the column and produce a detector response, since the composition of this band is different to that of the bulk eluent. The retention time of this *injection peak* remains constant, regardless of the pH of the bulk eluent, or the concentration of the injected analyte. The conductance of the *injection peak* is proportional to the concentration of the injected solute.

In contrast, a second system peak can occur later in the chromatogram, and generally tends to elute at the characteristic retention time of the neutral eluent species. Haddad and Jackson [64] have proposed that a weak carboxylic acid eluent such as phthalate for example, will comprise of neutral undissociated phthalic acid as well as dissociated phthalate. The neutral eluent species will be hydrophobically bound to the unfunctionalised hydrophobic regions of an anion exchanger. Upon injection of a solute, this equilibrium is disturbed, and a system peak will be observed later in the chromatogram. The retention time of this peak is dependant on the nature of the eluent itself (phthalate, p-hydroxybenzoate etc), the pH and concentration of the eluent, and the type of stationary phase used. The height of the system peak depends on the eluent pH and also the pH of the injected sample, along with the concentration and volume of injected solute. Haddad and Jackson [64] have observed that system peaks can be reduced to just the injection peak by adjusting the pH of the eluent such that it is fully dissociated, thereby eliminating hydrophobic interactions between the neutral eluent species and the stationary phase.

## 1.9 References.

- [1]. M. Dong, *Today's Chemist at Work* 9 (2000) 46.
- [2]. "Fast LC", *Perkin Elmer Technical Bulletin* (1996).
- [3]. V.R. Meyer, "Practical high performance liquid chromatography" 1993 Wiley 298.
- [4]. D.B. Gomis, N.S. Nunez, E.A. Garcia, M.B. Jasanada, M.D.G. Alvarez, *Anal. Chim. Acta.* 498 (2003) 1.
- [5]. J. Macek, P. Ptacek, J. Klima, *J. Chromatogr. A* 755 (2001) 279.
- [6]. K. Yu, M. Balogh, *LCGC* 19 (January 2001) 60.
- [7]. M.W. Dong, J.R. Gant, *LCGC* 2 (1984) 294.
- [8]. K. Heinig, J. Henion, *J. Chromatogr. B* 732 (1999) 445.
- [9]. J. Zweigenbaum, J. Henion, *Anal. Chem.*, 72 (2000) 2446.
- [10]. N.D. Danielson, J.J. Kirkland, *Anal. Chem.* 59 (1987) 2501.
- [11]. H. Moriyama, M. Anegayama, Y. Kato, *J. Chromatogr. A* 729 (1996) 81.
- [12]. T. Issaeva, A. Kourganov, K. Unger, *J. Chromatogr. A* 846 (1999) 13.
- [13]. J.J. Kirkland, F.A. Truszkowski, C.H. Dilks Jr., G.S. Engel, *J. Chromatogr. A* 890 (2000) 3.
- [14]. F. Gerber, M. Krummen, H. Potgeter, A. Roth, C. Siffrin, C. Spöndlin, *J. Chromatogr. A* 1036 (2004) 127.
- [15]. K. Cabrera, D. Lubda, K. Sinz, C. Schaefer, *Application Note, Am. Lab.* (February 2001) 40.
- [16]. H. Minakuchi, K. Nakanishi, N. Soga, N. Ishizuka, N. Tanaka, *Anal. Chem.* 68 (1996) 3498.
- [17]. H. Minakuchi, K. Nakanishi, N. Soga, N. Ishizuka, N. Tanaka, *J. Chromatogr. A* 762 (1997) 135.
- [18]. N. Ishizuka, H. Minakuchi, K. Nakanishi, N. Soga, N. Tanaka, *J. Chromatogr. A* 797 (1998) 133.
- [19]. H. Minakuchi, N. Ishizuka, K. Nakanishi, N. Soga, N. Tanaka, *J. Chromatogr. A* 828 (1998) 83.
- [20]. N. Tanaka, H. Kobayashi, K. Nakanishi, H. Minakuchi, N. Ishizuka, *Anal. Chem.* (2001) 421A.

- [21]. N. Tanaka, H. Kobayashi, N. Ishizuka, H. Minakuchi, K. Nakanishi, K. Hosoya, T. Ikegami, *J. Chromatogr. A* 965 (2002) 35.
- [22]. M. Motokawa, H. Kobayashi, N. Ishizuka, H. Minakuchi, K. Nakanishi, H. Jinnai, K. Hosoya, T. Ikegami, N. Tanaka, *J. Chromatogr. A* 961 (2002) 53.
- [23]. N. Ishizuka, H. Kobayashi, H. Minakuchi, K. Nakanishi, K. Hirao, K. Hosoya, T. Ikegami, N. Tanaka, *J. Chromatogr. A* 960 (2002) 85.
- [24]. P. Hatsis, C.A. Lucy, *Anal. Chem.* 75 (2003) 995.
- [25]. S. Apers, T. Naessens, K. van Den Stern, F. Cuyckens, M. Claeys, L. Pieters, A. Vlietinck, *J. Chromatogr. A* 1038 (2004) 107.
- [26]. D. Lubda, K. Cabrera, W. Kraas, C. Schaefer, D. Cunningham, *LCGC* 19 (December 2001) 1186.
- [27]. K. Cabrera, G. Wieland, D. Lubda, K. Nakanishi, N. Soga, H. Minakuchi, K. Unger, *Trends Anal. Chem.* 17 (1998) 50.
- [28]. F. C. Leinweber, D. Lubda, K. Cabrera, U. Tallerek, *Anal. Chem.* 74 (2002) 2470.
- [29]. A.M. van Nederkassel, A. Aerts, A. Dierick, D.L. Massart, Y. Vander Heyden, *J. Pharm. Biomed. Anal.* 32 (2003) 233.
- [30]. K. Pihlainen, E. Sippola, R. Kostianen, *J. Chromatogr. A* 994 (2003) 93.
- [31]. D.V. McCalley, *J. Chromatogr. A* 965 (2002) 51.
- [32]. P. Hatsis, C.A. Lucy, *Analyst* 127 (2002) 451.
- [33]. J. Zweigenbaum, K. Heinig, S. Steinborner, T. Wachs, J. Henion, *Anal. Chem.* 71 (1999) 2294.
- [34]. B. Yan, J. Zhao, J.S. Brown, J. Blackwell, P.W. Carr, *Anal. Chem.* 72 (2000) 1253.
- [35]. ZirChrom Separations, Technical Bulletin No. 154.
- [36]. F.D. Antia, Cs. Horvath, *J. Chromatogr.* 435 (1988) 1.
- [37]. G. Mayr, T. Welsch, *J. Chromatogr. A* 845 (1999) 155.
- [38]. J. Chong, P. Hatsis, C.A. Lucy, *J. Chromatogr. A* 997 (2003) 161.
- [39]. ZirChrom Separations, Technical Bulletin No. 271.
- [40]. ZirChrom Separations, Technical Bulletin No. 279.
- [41]. ZirChrom Separations, Technical Bulletin No. 235.
- [42]. P. Hatsis, C.A. Lucy, *J. Chromatogr. A* 920 (2001) 3.
- [43]. P. Hatsis, C.A. Lucy, *Analyst* 126 (2001) 2113.

- [44]. M.C. Gennaro, S. Angelino, *J. Chromatogr. A* 789 (1997) 181.
- [45]. J. Zou, S. Motomizu, H. Fukutomi, *Analyst* 116 (1991) 1399.
- [46]. Y. Michigami, K. Fujii, K. Ueda, Y. Yamamoto, *Analyst* 117 (1992) 1855.
- [47]. Y. Miura, A. Kawaoi, *J. Chromatogr. A.*, 884 (2000) 81.
- [48]. J. Xu, M. Tin, T. Takeuchi, T. Miwa, *Anal. Chim. Acta.* 276 (1993) 261.
- [49]. M.C. Bruzzoniti, E. Mentasti, C. Sarzanini, *J. Chromatogr. A.*, 770 (1997) 51.
- [50]. F.G.P. Mullins, G.F. Kirkbright, *Analyst* 109 (1984) 1217.
- [51]. P.G. Rigas, D.J. Pietrzyk, *Anal. Chem.* 58 (1986) 2226.
- [52]. B.A. Bidlingmeyer, C.T. Santasania, F.V. Warren Jr., *Anal. Chem.* 59 (1987) 1843.
- [53]. Y. Michigami, Y. Yamamoto, K. Ueda, *Analyst* 114 (1989) 1201.
- [54]. B. Maiti, A.P. Walvekar, T.S. Krishnamoorthy, *Analyst* 114 (1989) 731.
- [55]. M.C. Gennaro, P.L. Bertolo, A. Cordero, *Anal.Chim. Acta.* 239 (1990) 203.
- [56]. K. Ito, Y. Ariyoshi, H. Sunahara, *Anal.Chem.* 63 (1991) 273.
- [57]. X. Jun, J.L.F.C. Lima, M. Conceicao, M.C.B.S.M. Montenegro, *Analyst* 120 (1995) 2469.
- [58]. X. Jun, J.L.F.C. Lima, M.C.B.S.M. Montenegro, *Anal. Chim. Acta.*, 321 (1996) 263.
- [59]. P.G. Rigas, D.J. Pietrzyk, *Anal. Chem* 60 (1988) 1650.
- [60]. K.L. Yang, S.J. Jiang, *Anal. Chim. Acta* 307 (1995) 109.
- [61]. Y.S. Fung, W.M. Tam, *Anal. Chim. Acta* 326 (1996) 67.
- [62]. Y. Muira, A. Saitoh, T. Koh, *J. Chromatogr. A* 770 (1997) 157.
- [63]. Dionex CD20 Conductivity detector operator's manual, Document No. 034854, Revision 03, February 1996.
- [64]. P.R.Haddad, P.E.Jackson, *Ion Chromatography: Principles and Applications*, *J. Chromatogr. Library*, Vol.46, Elsevier, Amsterdam, 1990.

## 2 Fast Separation of UV-Absorbing Anions Using Ion-interaction Chromatography.

### 2.1 Introduction.

Many studies have been reported on the use of alkylammonium salts for ion-interaction chromatography for the determination of both organic and inorganic anions. There exists a wide range of alkylammonium salts of varying hydrophobicity such that dynamic exchange capacities can be controlled across a wide range, allowing anion determinations in sample matrices of varying complexity and ionic strength.

Mullins and Kirkbright [1] separated iodate, nitrite, bromide, nitrate and iodide on a 250 X 5 mm i.d. Spherisorb C<sub>18</sub> (5 µm) column and a mobile phase of 10 mM cetyltrimethylammonium chloride buffered to pH 6.8 with 10 mM phosphate buffer, in 35 % acetonitrile. With a flow rate of 1.5 ml/min the runtime was ~ 18 minutes. Bidlingmeyer *et al.* [2] used an eluent of 0.4 mM tetrabutylammonium and salicylate at pH 4.62 with a Resolve C<sub>18</sub> Radial Pack 5 µm column of dimensions (100 mm X 8 mm I.D.). Phosphate, chloride, nitrite, bromide, nitrate, iodide, sulphate and thiosulphate were separated in 25 minutes with a flow rate of 2.0 ml/min. Both direct conductivity detection and indirect UV detection at 288 nm were used with an injection volume of 20 µL to yield detection limits<sup>1</sup> of 120 µg/L (chloride), 1,240 µg/L (bromide), 280 µg/L (nitrite) and 740 µg/L (nitrate).

A Spherisorb ODS-2 RP-18 (5 µm) 250 X 4.0 mm I.D. column was used by Gennaro *et al.* [3] to resolve nitrate from nitrite with a view to the analysis of these anions in lagoon water. The eluent was 5 mM octylammonium phosphate; using a flow rate of 0.8 ml/min, both peaks were resolved within 26 minutes. Direct UV detection at 230 nm was used such that high chloride levels in the samples did not cause an interference; for example nitrite could be detected at 5 µg/L even in the presence of up to 0.70 M chloride.

---

<sup>1</sup> Signal to noise ratio = 5

Later, Zou *et al.* [4] used tetrabutylammonium ions as ion-interaction reagent and naphthalene-1,5-disulphonate as a UV absorbing counter-ion to separate chloride, bromide, nitrate and sulphate within 20 minutes. The mobile phase used was 0.3 mM TBA and 0.2 mM 1,5-NDS in 5 % MeOH, pH 4.3. With a 150 X 4.6 mm I.D. Yokogawa SIL-C<sub>18</sub> column (particle size 5 µm) and a flow rate of 1.0 ml/min, determinations of these anions could be made in the low µg/L range of 2.6, 9.5, 2.6 and 7.5 µg/L for chloride, bromide, nitrate and sulphate respectively, using an injection volume of 20 µL and indirect UV detection at 300 nm. The method was applied to the analysis of river, tap, rain and sea water samples.

Tetrabutylammonium hydroxide was also used at a concentration of 3.0 mM by Xu *et al.* [5] in an eluent which also contained (15:85) MeOH/H<sub>2</sub>O, 60 mM phosphate buffer pH 5.5 and 0.1 mM EDTA. Using a 150 X 6 mm I.D. Shim-Pack CLC-C<sub>8</sub> (5 µm) analytical column and a flow rate of 1.0 ml/min, the separation time was faster than the methods discussed previously, with nitrite, thiosulphate, iodide, sulphide and thiocyanate all baseline resolved within 8 minutes.

Padaruskas and Schwedt [6] separated phosphate, chloride, nitrite, bromide, nitrate, chromate, sulphate, molybdate and Cr (III) in under 13 minutes using 1 mM TBA, 0.5 mM *trans*-1,2-diaminecyclohexane-*N,N,N',N'*-tetraacetic acid (DCTA) pH 6.5 in 2 % acetonitrile at a flow rate of 1.0 ml/min. The column used was a Nucleosil 5C<sub>18</sub> 250 X 4 mm I.D. column. The method was applied to the analysis of building materials (mortar) and leather extracts for chromium species.

In this work, ion-interaction chromatography is carried out on a short 30 x 4.6 mm I.D. analytical column, packed with a 3 µm particle size, ODS stationary phase, with the aim of developing fast chromatographic separations of UV absorbing inorganic ions using only moderate flow rates, direct UV detection and most importantly, non-specialist HPLC instrumentation.

## 2.2 Experimental.

### 2.2.1 Equipment.

A Dionex DX500 ion chromatograph (Dionex Corporation, Sunnyvale, CA, USA), comprising of a GP50 gradient pump, LC25 chromatography oven, an AD20 absorbance detector and a CD20 conductivity detector was used. The UV cell used throughout this work had a volume of 9  $\mu\text{L}$  and an optical pathlength of 10 mm (0.002 inches). The UV cell used in this work was also fitted with a 10  $\mu\text{L}$  heat exchanger which was bypassed to further reduce extra column band broadening. The conductivity cell used throughout this work had a volume of 1.0  $\mu\text{L}$ . The shortest possible length of 0.010 inch I.D. PEEK tubing was used from the injector to the column and from the column to the detector unless otherwise specified. Detection was by direct UV at 214 nm during initial system optimisation, with a wavelength of 225 nm subsequently used for nitrate and nitrite determinations. The analytical column used was a Phenomenex Hypersil, 3  $\mu\text{m}$  particle size, 30 mm x 4.6 mm I.D. column (Macclesfield, Cheshire, U.K.). The injection loop used was approximately 2  $\mu\text{L}$  for the optimisation studies and increased to 25  $\mu\text{L}$  for the separation of iodate and iodide and to 50  $\mu\text{L}$  bromide/bromate and nitrate/nitrite determinations. Data acquisition was at a rate of 10 Hz with processing of chromatograms performed using a PeakNet 6.0 chromatography workstation (Dionex). RMS noise was used for all S/N determinations as calculated by the chromatography software used.

### 2.2.2 Reagents and chromatographic conditions.

For preparation of the mobile phase, the water used was obtained from a Millipore MilliQ water purification system (Millipore, Bedford, MA, USA), tetrabutylammonium hydroxide (TBA-OH) was supplied by Aldrich, (Aldrich, Milwaukee, WI, USA) as a 50 % w/v solution in water, and methanol was obtained from Labscan (Labscan Limited, Stillorgan, Dublin, Ireland). The optimised mobile phase for the separation of eight anions consisted of 50 mM TBA-OH in 10 % aqueous MeOH, titrated to pH 6.2 using dilute HCl. For the optimised separation of the five early eluting anions the mobile phase consisted of 20 mM TBA-OH in 20 %

aqueous MeOH, titrated to pH 6.2 using dilute HCl. All mobile phases were degassed and filtered using 0.45  $\mu\text{m}$  filters before use. The flow rates used were 2.5 mL/min and 2.0 mL/min respectively. Column temperature was set at 45 °C for the separation of eight anions and ambient for all other separations.

Stock standard solutions of concentration 1000 mg/L were prepared monthly and working standards prepared from each respective stock solution. Iodate, iodide, nitrite, nitrate, thiosulphate and benzoate standards were prepared from their respective sodium salts (Aldrich, Milwaukee, WI, USA). Bromide and bromate standards were prepared from their respective potassium salts (Aldrich, Milwaukee, WI, USA).

## **2.3 Results and discussion.**

### **2.3.1 Mobile phase optimization.**

For simplicity, the test mix of anions that were to be used in this study was kept to those that exhibit a significant absorbance in the UV region. As this study was specifically focused upon developing fast separations, it was decided to try to keep the analytical instrumentation as simple as possible, therefore suppressed conductivity or post-column reaction detection were not considered. A number of the anions chosen to be included within this test mixture also happened to be currently receiving considerable interest in the fields of environmental monitoring and water analysis. These include anions such as nitrate, nitrite, bromide and bromate, some of which are known for their hazardous effects upon human health. Three other anions, namely iodide, thiosulphate and benzoate were also added to the test mix, since they are known to exhibit differing selectivities to the above set of inorganic ions when carrying out conventional ion-interaction chromatography. In the case of benzoate there is also a secondary hydrophobic based interaction with the ODS stationary phase and thus retention times would be expected to be considerably greater for this particular anion. Therefore, the test mix used for mobile phase optimisation was as

follows: nitrate, nitrite, iodide (iodate added later), bromide, bromate, thiosulphate and benzoate.

As discussed in Chapter 1, Section 1-7, when choosing the ion-interaction reagent it was important to consider that in general, changing reagent to a longer or shorter chain IIR is not necessarily the only way to effect a selectivity change. That is, in general one can obtain the same results with a high concentration of a short chain IIR as with a lower concentration of a long chain IIR. Minor changes in concentration of IIR below levels of about 10 mM can cause relatively large changes in system performance, whereas concentrations higher than about 100 mM can cause solubility problems (depending on the hydrophobicity of the IIR and the % organic modifier present). Therefore, in order to stay within a workable concentration range, tetrabutylammonium chloride was chosen for subsequent dynamically coated work.

When choosing the organic modifier, two solvents were considered; acetonitrile and methanol. Acetonitrile can offer advantages over the use of methanol, since it can sometimes provide an alternative chromatographic selectivity relative to methanol. Also it offers advantages in the sensitivity of detection since it absorbs at lower wavelengths than methanol. (See Table 2-1). However, for this work, methanol was chosen as the organic modifier because acetonitrile is notorious for its poor solubility characteristics when mixed with salts and buffers, relative to methanol.

**Table 2-1.** *UV transmittance of acetonitrile and methanol. [7]*

<u>ACETONITRILE</u>		<u>METHANOL</u>	
<b>Wavelength (nm)</b>	<b>Max. Absorbance</b>	<b>Wavelength (nm)</b>	<b>Max. Absorbance.</b>
190	1.000	205	1.000
200	0.050	225	0.160
225	0.010	250	0.020
250	0.005	300	0.005
350	0.005	400	0.005

One of the advantages of fast chromatographic separations is that full method optimisations can be carried out in much shorter times. In this study, two parameters were chosen for optimisation, namely the concentration of the IIR, (TBA-Cl) and the concentration of organic modifier, (MeOH). The mobile pH was kept constant in these experiments at 6.2 (for the test mixture of anions, pH was unlikely to have a major effect upon selectivity in the region of 3-7). The main reason for the use of this pH was in order to protect the silica packing against extremes of pH. The column used in this work was a Phenomenex Hypersil, 3  $\mu\text{m}$  particle size, 30 mm x 4.6 mm I.D. column (Macclesfield, Cheshire, UK) and was suitable for use between pH 2 and 8. Below pH 2, the silylether bond attaching the bonded phase to the silica support is unstable, and at pH values over pH 8, the actual silica packing dissolves, creating a void at the head of the column.

Firstly the independent effect that mobile phase MeOH concentration had upon the retention of the test mixture of anions was examined and can be seen in Figure 2-1. The concentration of ion-interaction reagent was held constant, at 20 mM TBA-Cl. The reduction in retention of all the anions is as expected in an ion-interaction model, where the IIR is a hydrophobic cationic species. By increasing the concentration of organic solvent in the mobile phase the dynamic equilibrium of IIR established between the mobile and stationary phases is shifted towards the mobile phase and the effective capacity of the column is reduced. The retention of the less hydrophilic anions, particularly benzoate, is obviously more drastically affected by the concentration of MeOH, as secondary reversed-phase interactions are also reduced.

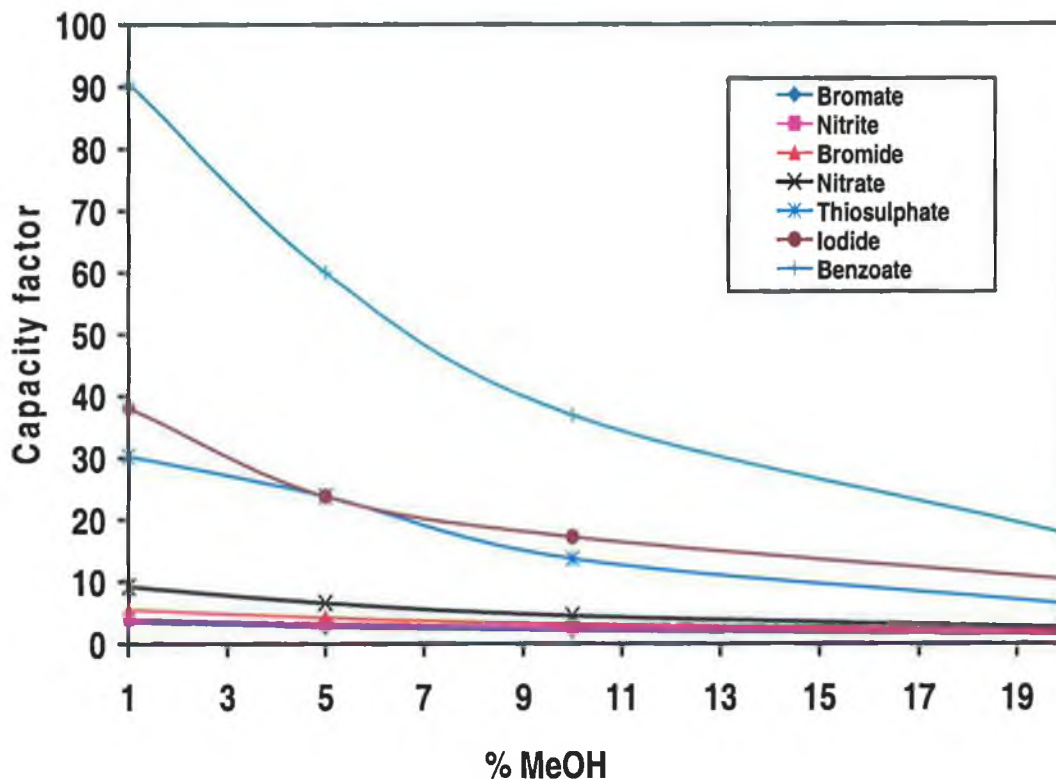


**Figure 2-1.** Effect of % MeOH upon the retention of UV absorbing anions. Other conditions: Column: Phenomenex Hypersil 3  $\mu\text{m}$  30 mm x 4.6 mm I.D. Mobile phase: 20 mM TBA-Cl, pH 6.2. Flow rate: 1.0 mL/min. Loop volume: 2  $\mu\text{L}$ , Detection: direct UV at 214 nm.

The independent effect of TBA-Cl concentration upon retention of the test mixture of anions was also examined. Figure 2-2 and Figure 2-3 show the effect upon the retention of the test anion mixture of varying the IIR concentration within a mobile phase containing 20 % MeOH. For the sake of completion, two extra data sets were generated by preparation of two extra mobile phases, 0.5 mM TBA-Cl in 20 % MeOH and 2 mM TBA-Cl in 20 % MeOH. It is clear from Figure 2-2 that there is a rapid increase in retention for all anions from 0 – 5 mM TBA-Cl, as the dynamic ion-exchange capacity of the column is increased and the surface adsorption sites become saturated. As the concentration of the IIR is increased above 5 mM, there is a clear levelling off in retention, followed by significant reductions in retention, particularly for thiosulphate and benzoate. As can be seen from Figure 2-2, thiosulphate is particularly sensitive to TBA-Cl concentration, as selectivity changes from thiosulphate > benzoate > iodide at 2 mM TBA-Cl, to benzoate > thiosulphate > iodide at 5-30 mM TBA-Cl, to benzoate>iodide>thiosulphate at 50 mM TBA-Cl.

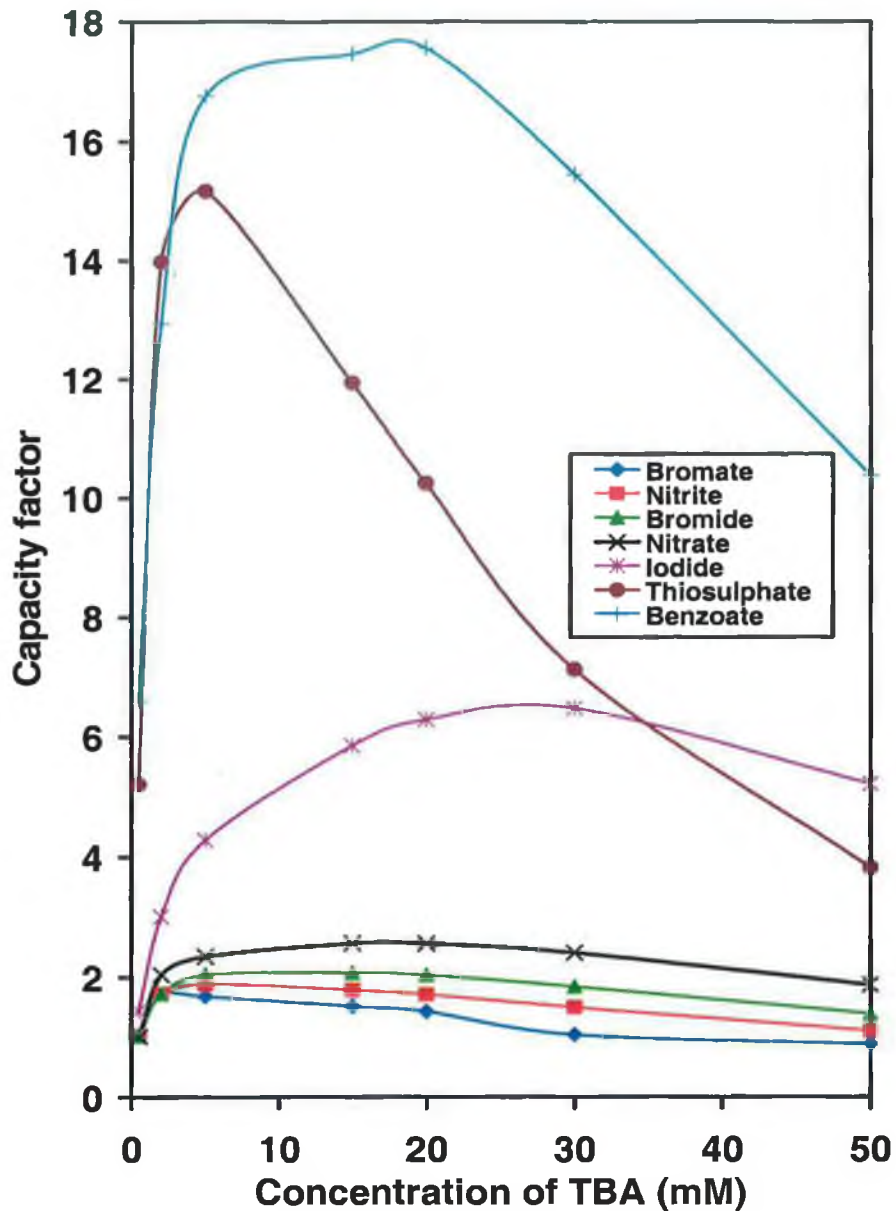


**Figure 2-2.** Effect of IIR concentration upon the retention of UV absorbing anions. Other conditions: Column: Phenomenex Hypersil 3  $\mu\text{m}$  30 mm x 4.6 mm I.D. Mobile phase: 20 % MeOH, pH 6.2. Flow rate: 1.0 mL/min. Loop volume: 2  $\mu\text{L}$ , Detection: direct UV at 214 nm.

In general, the trends shown are again typical of an ion-interaction mechanism, with the maximum retention being achieved at the point where the stationary phase surface becomes saturated with the IIR. After this point further addition of the IIR to the mobile phase causes a reduction in retention due to the increased concentration of the IIR counter-ion, in this case chloride.

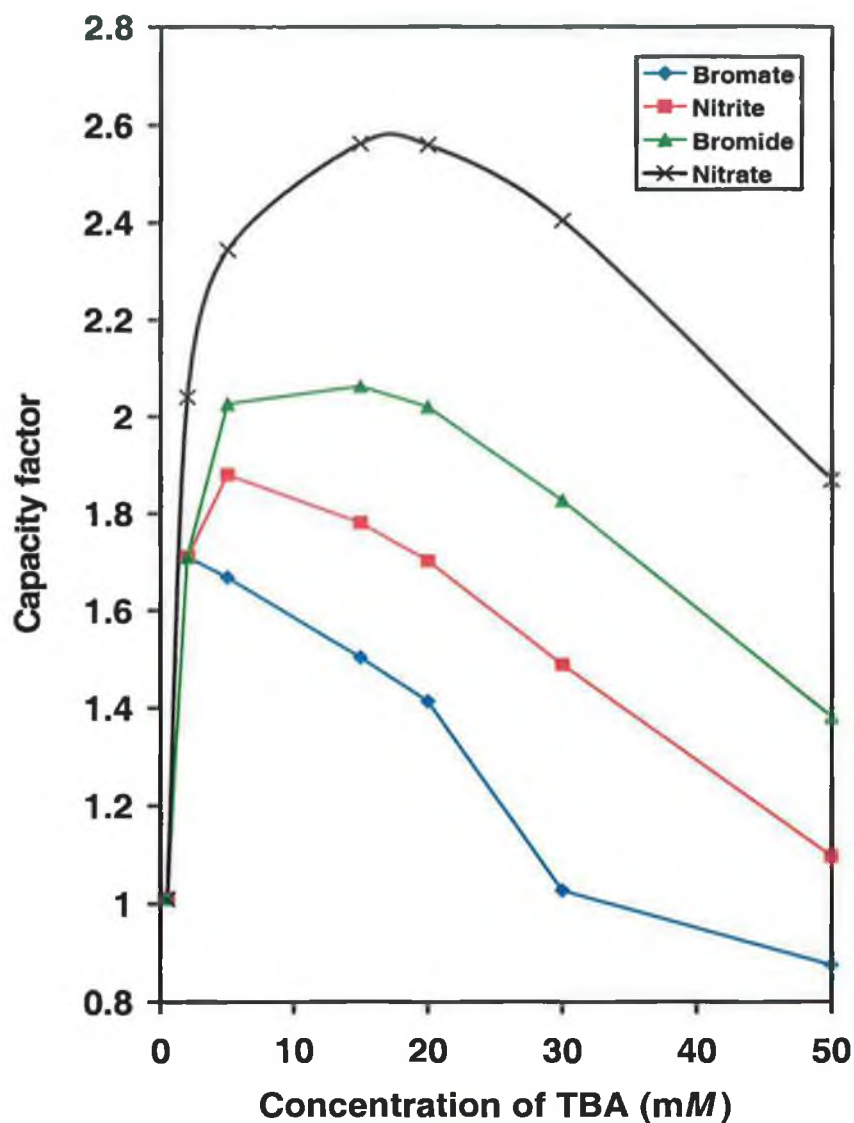


**Figure 2-3.** Effect of IIR concentration upon the retention of weakly retained UV absorbing anions. Conditions as in Figure 2-2.

Having considered the retention behaviour of the test mix of anions with respect to changes in % MeOH concentration and TBA-Cl concentration (mM) in the mobile phase, an experimental space incorporating 5 mM to 50 mM TBA-Cl and 1 % to 20 % MeOH was considered reasonable, with 20 mobile phase combinations prepared from within these limits. The test mix of anions was as follows: bromate (100 mg/L), nitrite (25 mg/L), bromide (150 mg/L), nitrate (25 mg/L), thiosulphate (75 mg/L), iodide (25 mg/L) and benzoate (100 mg/L).

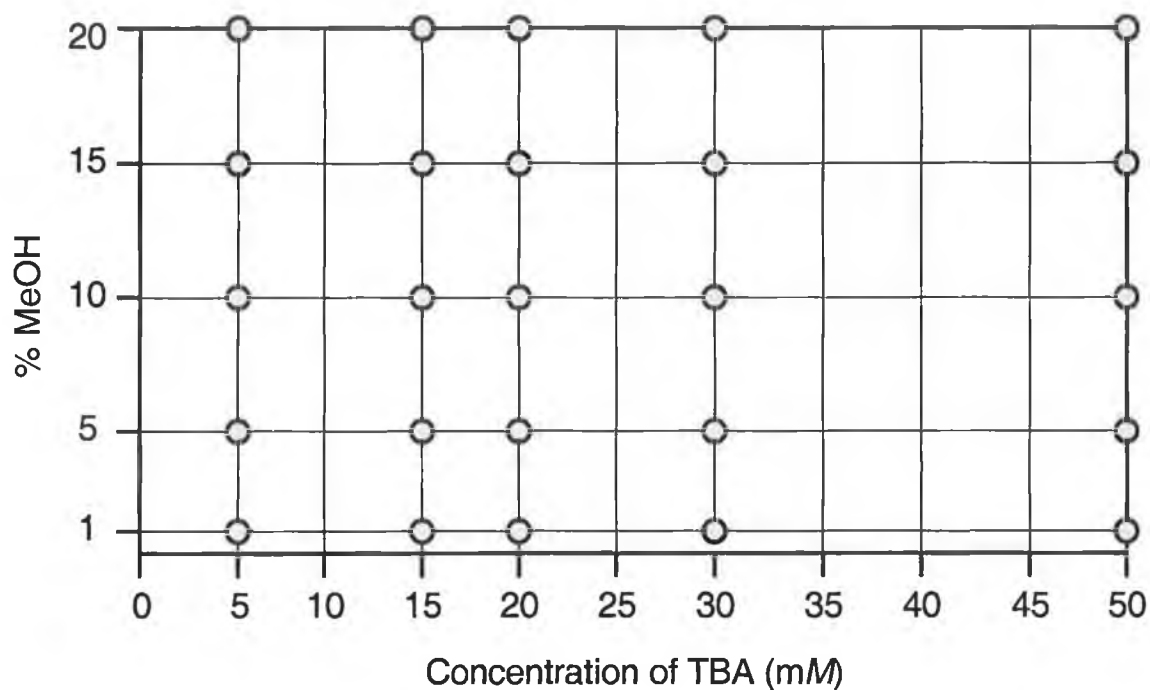


**Figure 2-4.** Schematic showing the test mobile phases within the chosen experimental search area. Each green symbol represents a mobile phase preparation with the concentrations of methanol and TBA indicated.

Injection of the test anion mixture was carried out using each of the 20 mobile phase preparations at a flow rate of 1 mL/min and ambient (~22 °C) column temperature. The resultant chromatograms were evaluated using the normalised resolution product,  $R$ , calculated using Equation 2-1, where  $R_s(i,i-1)$  is the resolution between adjacent peaks and  $n = \text{no. of analytes}$ .  $R_s(i,i-1)$  was calculated using Equation 2-2 where  $W_{50\%} = \text{peak width at half height}$ . The normalised resolution product criterion is at maximum when all  $R_s$  values are equal, that is, when all peaks are distributed evenly over the length of the chromatogram. A value of  $R= 0$  indicates a worst-case separation in which there are two or more co-eluting peaks [8].

$$R = \prod_i^{n-1} \frac{R_s(i,i-1)}{\frac{1}{n-1} \sum R_s(i,i-1)} \quad \text{Equation 2-1.}$$

$$R_s = \frac{1.18(t_{next} - t_{ret})}{W_{50\%next} + W_{50\%ret}}$$

Equation 2-2.

A three dimensional response surface plot showing the combined effects of IIR concentration and % MeOH upon the normalised resolution product,  $R$ , was constructed for the test mixture of anions. (The surface was constructed on Sigma Plot Version 4.0, which allows the user to rotate the surface in 3 dimensions and view from different angles in order to visually determine those mobile phases with maximum  $R$  value). This is shown in Figure 2-5. The data shown was obtained without the inclusion of iodate to the test mix. Seven ions were included in the initial “test mix” for the purposes of mobile phase optimisation. Once the optimum mobile phase was determined, an eight analyte, iodate, was added to the test mix and found to be well resolved from all other anions and so did not negatively affect the response surface shown. Therefore, although iodate was not included as an eight parameter in the mathematical calculation of  $R$ , the normalised resolution product, it is assumed that the mobile phase chosen as optimum, remains optimum for all eight anions notwithstanding that it was determined based on an initial test mix of seven anions.

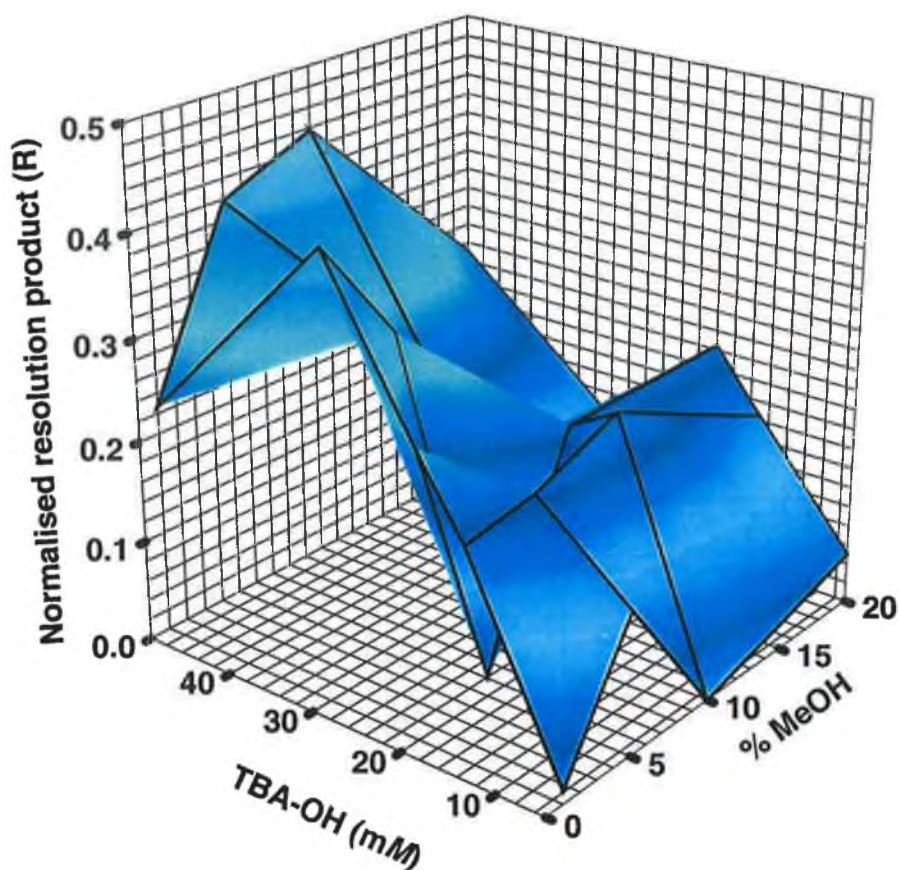


**Figure 2-5.** Response surface for mobile phase optimisation showing normalised resolution production ( $R$ ) as a function of mobile phase IIR concentration and % MeOH for a standard mixture of bromate, nitrite, bromide, nitrate, thiosulphate, iodide and benzoate.

As can be seen from Figure 2-5, two regions of maximum overall resolution are evident, namely 50 mM TBA-Cl in 5-10 % MeOH and 30 mM TBA-Cl in 1-5 % MeOH. However, the mobile phases with the higher IIR concentration led to overall run times of less than half that of those containing the lower IIR concentration. Thus, the optimum conditions for the separation of the test mixture was found to be 50 mM TBA-Cl in 10 % MeOH, as this resulted in both the highest  $R$  value and shortest total run time. Under these conditions all eight anions could be baseline resolved in under 11 min. The corresponding chromatogram for the test mix of anions is shown in Figure 2-6, which shows that there is a clear difference in selectivities shown

between what can be termed the more hydrophilic anions, iodate, bromate, nitrite, bromide and nitrate, and the less hydrophilic anions, thiosulphate, iodide and benzoate.

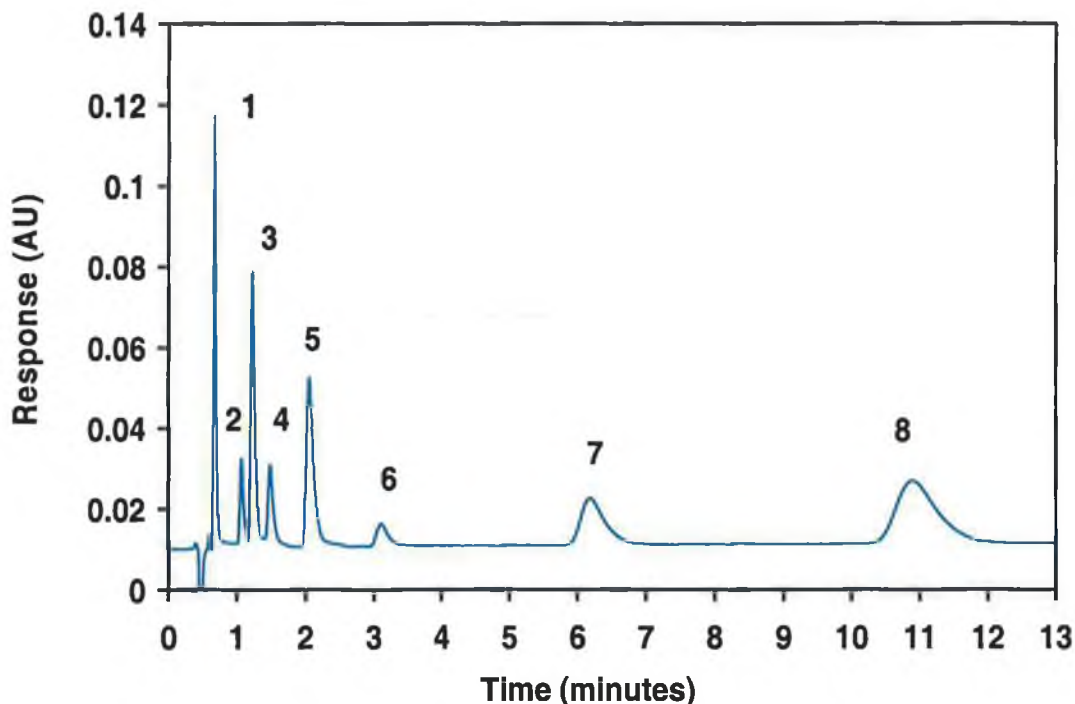


**Figure 2-6.** Optimised mobile phase for determination of eight UV absorbing anions by ion-interaction chromatography on a short 3 cm 3  $\mu\text{m}$  column. Column: Phenomenex Hypersil 3  $\mu\text{m}$  30 mm x 4.6 mm I.D. Mobile phase: 50 mM TBA-Cl, 10 % MeOH, pH 6.2, Column temperature: ambient. Flow rate: 1.0 mL/min. Injection volume: 2  $\mu\text{L}$ . Detection: 214 nm. Peaks: [1] iodate (25 mg/L), [2] bromate (100 mg/L), [3] nitrite (25 mg/L), [4] bromide (150 mg/L), [5] nitrate (25 mg/L), [6] thiosulphate (75 mg/L), [7] iodide (25 mg/L) and [8] benzoate (100 mg/L).

Therefore, a further calculation of the normalised resolution product,  $R$ , for the weakly retained anions was made to determine the optimum mobile phase for their separation. The “weakly retained” test mix was as follows: bromate (100 mg/L), nitrite (25 mg/L), bromide (150 mg/L), nitrate (25 mg/L). Again, the data shown was obtained without the inclusion of iodate to the test mix. The subsequent inclusion of iodate showed it was found to belong to this “weakly retained” subgroup and was well resolved from the remaining anions under all conditions, therefore not negatively affecting the response surface shown. The resolution surface plot for the weakly retained anions is shown as Figure 2-7. As can be seen from Figure 2-7, excellent resolution of the weakly retained subgroup of anions was possible when the

IIR was present at greater than 20 mM with 20 % MeOH. As the concentration of IIR above 20 mM had little effect on reducing retention times of this subgroup of anions, and also to limit reagent consumption, the optimum mobile phase was concluded to be 20 mM TBA-Cl in 20 % MeOH. This resulted in the baseline resolution of iodate, bromate, nitrite, bromide and nitrate in just over 2 min shown in Figure 2-8 (again, at a nominal flow rate of 1.0 ml/min and ambient column temperature).

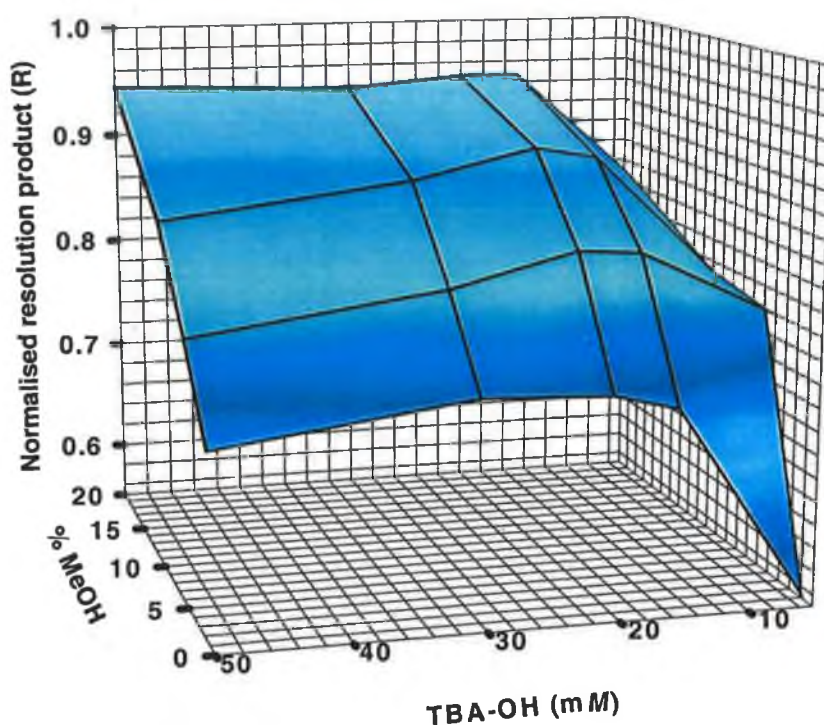


**Figure 2-7.** Response surface for mobile phase optimisation showing normalised resolution production ( $R$ ) as a function of mobile phase IIR concentration and % MeOH for a standard mixture of bromate, nitrite, bromide and nitrate, the weakly retained subgroup of anions.

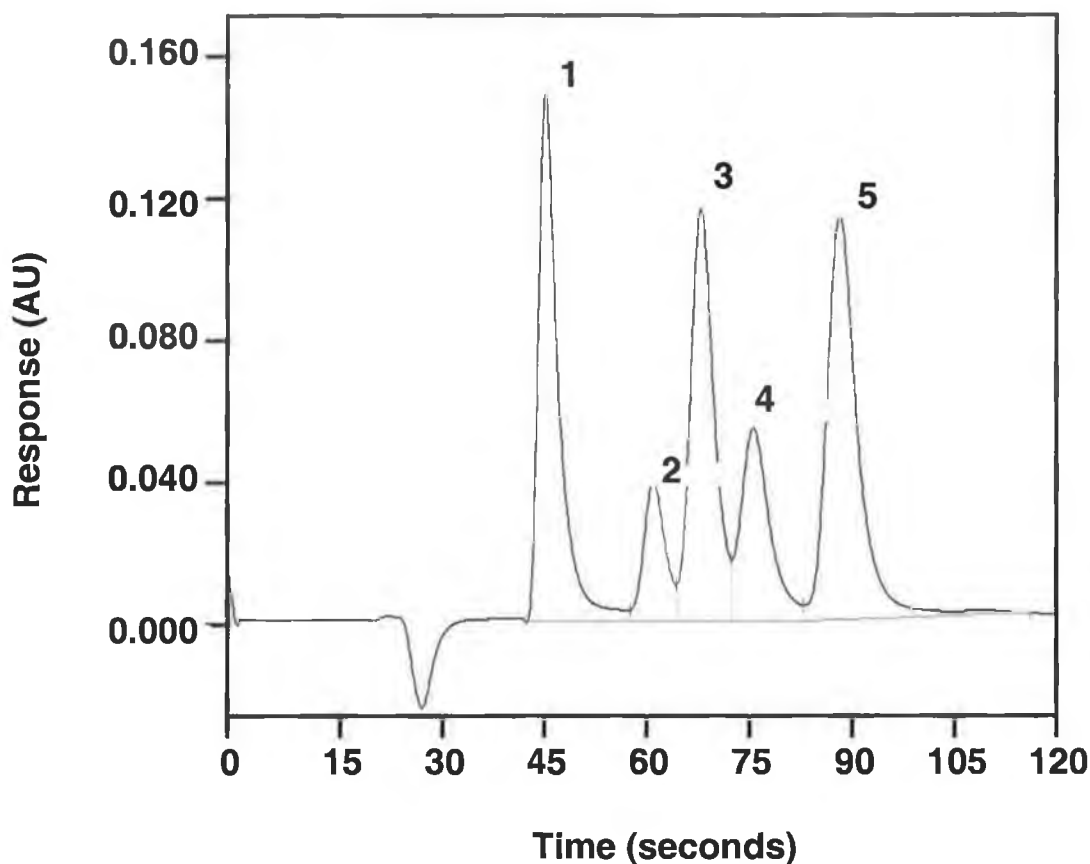


**Figure 2-8.** Optimised mobile phase for determination of five “weakly retained” UV absorbing anions by ion-interaction chromatography on a short 3 cm 3  $\mu\text{m}$  column. Column: Phenomenex Hypersil 3  $\mu\text{m}$  30 mm x 4.6 mm I.D. Mobile phase: 20 mM TBA-Cl, 20 % MeOH, pH 6.2, Column temperature: ambient. Flow rate: 1.0 mL/min. Injection volume: 2  $\mu\text{L}$ . Detection: 214 nm. Peaks: [1] iodate (25 mg/L), [2] bromate (100 mg/L), [3] nitrite (25 mg/L), [4] bromide (150 mg/L), [5] nitrate (25 mg/L).

### 2.3.2 Optimization of column temperature.

The effect of column temperature was determined by varying the column oven compartment temperature from ambient (22 °C) to 45 °C. The LC25 column compartment used was an air-bath type. It operates in a similar fashion to a GC column oven, with the entire column and connecting tubing suspended in a heated air current, which is circulated by a fan. Results are displayed in Figure 2-9. As can be seen from the figure, the two subgroups of anions again behaved somewhat differently, with temperature having little effect upon the retention of the weakly

retained anions (including thiosulphate), but resulting in a considerable shortening of the retention times of the less hydrophilic anions, iodide and benzoate. This was as expected since the retention mechanism for these late eluting anions is part electrostatic interaction and part hydrophobic interaction with the ODS stationary phase (particularly benzoate). An increase in temperature increases solute solubility in the mobile phase thereby leading to reduced retention, and also it increases the rate of hydrophobic interactions.

A second reason for using elevated column temperatures is to reduce overall column back-pressure, (generated by the smaller stationary phase particles used (3  $\mu\text{m}$ ), which is directly proportional to the viscosity of the mobile phase. Column back-pressure was successfully reduced by  $\sim 200$  psi by the use of elevated temperatures. The early eluting anions are mainly retained through electrostatic interactions, which are less affected by temperature fluctuations. Therefore, the optimum column temperature for separation of all eight anions was chosen as  $45\text{ }^{\circ}\text{C}$  with total runtime reduced by some 1.8 minutes, as illustrated in Figure 2-10, which can be directly compared with Figure 2-6.

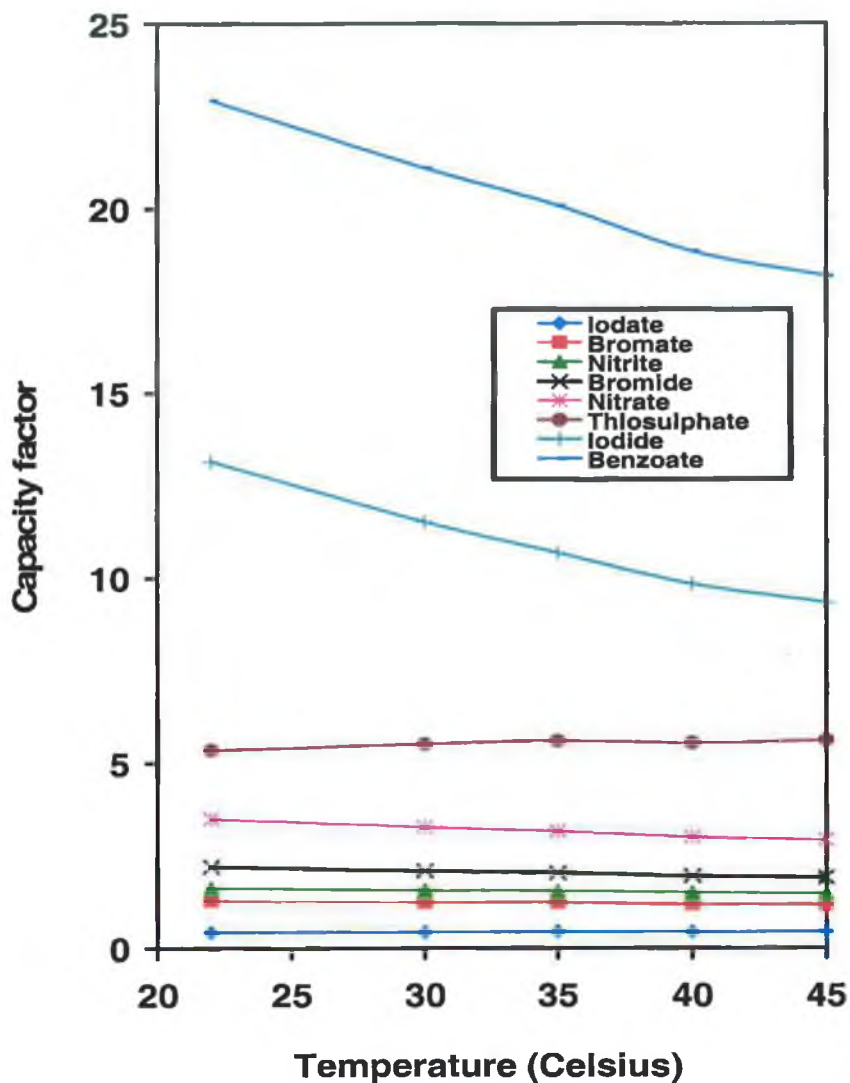


**Figure 2-9.** Effect of temperature upon the retention of UV absorbing anions in ion-interaction chromatography on a short 3 cm 3  $\mu$ m column. Column: Phenomenex Hypersil 3  $\mu$ m 30 mm x 4.6 mm I.D. Mobile phase: 50 mM TBA-Cl in 10% MeOH, pH 6.2. Flow rate: 1.0 ml/min. Loop volume: 2  $\mu$ L. Detection: Direct UV at 214 nm. Test mix: nitrate (25 mg/L), nitrite (25 mg/L), iodide (25 mg/L), bromide (150 mg/L), bromate (100 mg/L), thiosulphate (75 mg/L) and benzoate (100 mg/L).

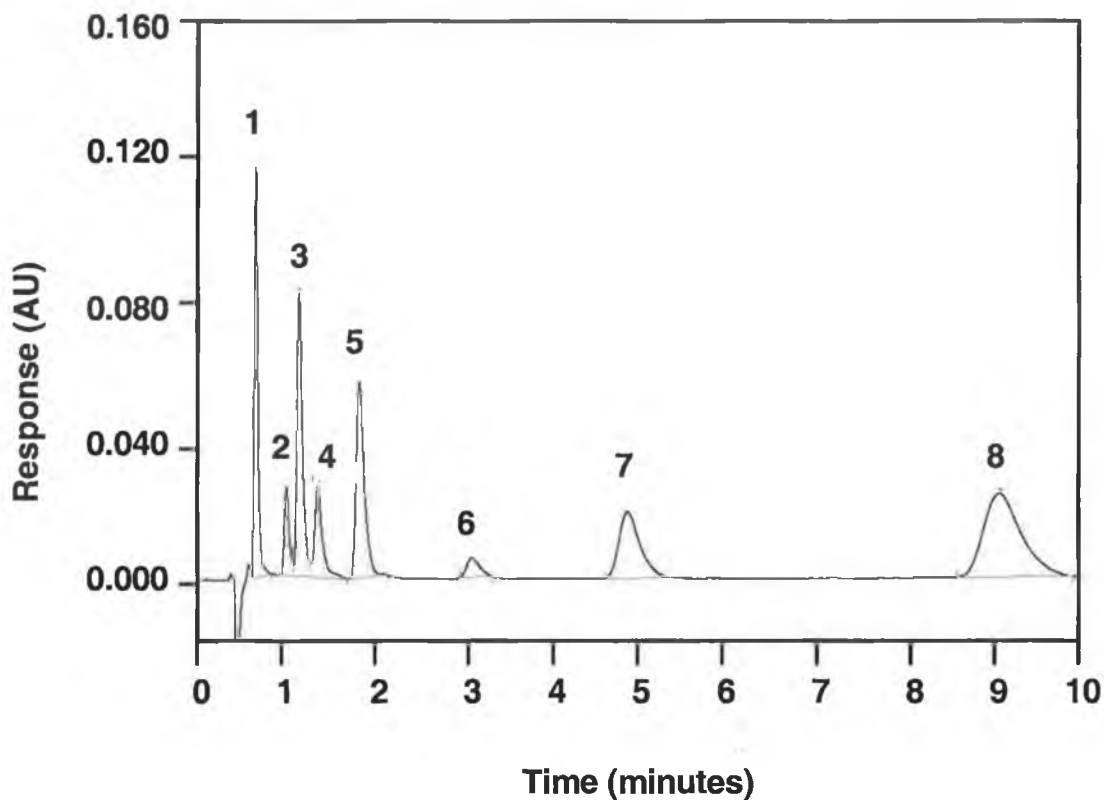


**Figure 2-10.** Separation of eight anions by ion-interaction chromatography on a short 3 cm 3  $\mu\text{m}$  column at the optimum column temperature. All conditions as in Figure 2-6 except column temperature: 45  $^{\circ}\text{C}$ . Peaks: [1] iodate (25 mg/L), [2] bromate (100 mg/L), [3] nitrite (25 mg/L), [4] bromide (150 mg/L), [5] nitrate (25 mg/L), [6] thiosulphate (75 mg/L), [7] iodide (25 mg/L) and [8] benzoate (100 mg/L).

However, since no significant improvements in either resolution or analysis time were noted for the weakly retained anions, which are mainly retained by electrostatic interactions, and are less affected by temperature fluctuations, further work looking at just this subgroup was carried out at ambient temperature. Figure 2-11, shows that the normalised resolution product (R) is little affected by temperature for the weakly retained group but decreases slightly for all seven analytes as is to be expected by inspection of Figure 2-9.

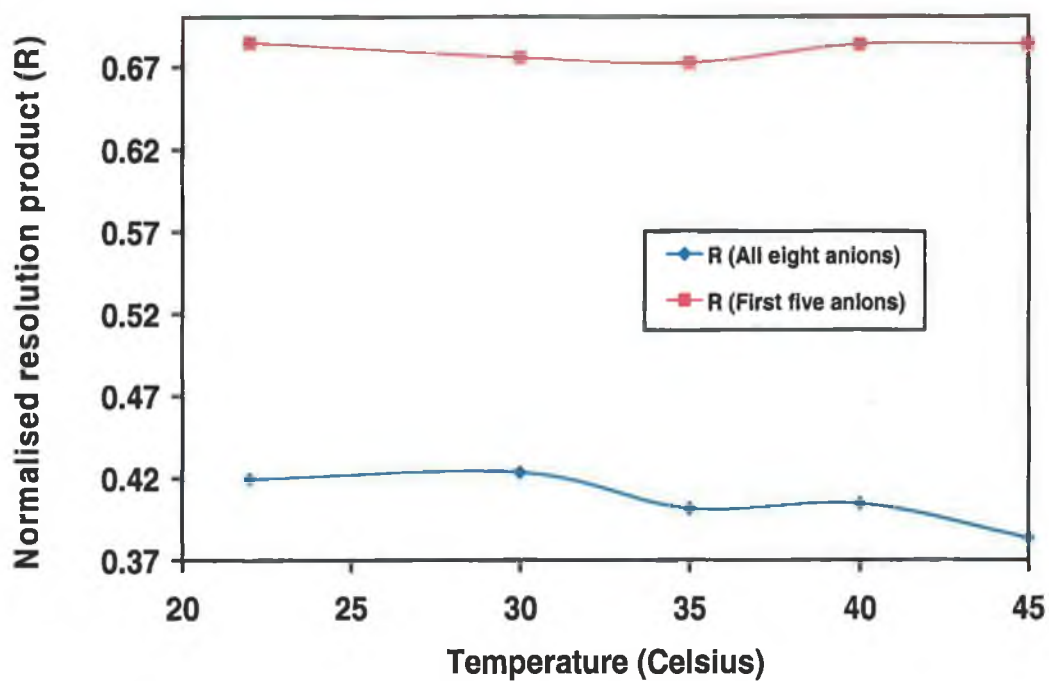


**Figure 2-11.** *Effect of temperature in ion-interaction chromatography upon the normalised resolution product for a test mixture of eight UV absorbing anions and for the “weakly retained subgroup”. Other mobile phase conditions: Mobile phase: 50 mM TBA-Cl, 10 % MeOH, pH 6.2. Flow rate: 1.0 mL/min. Injection volume: 2  $\mu$ L. Detection: 214 nm.*

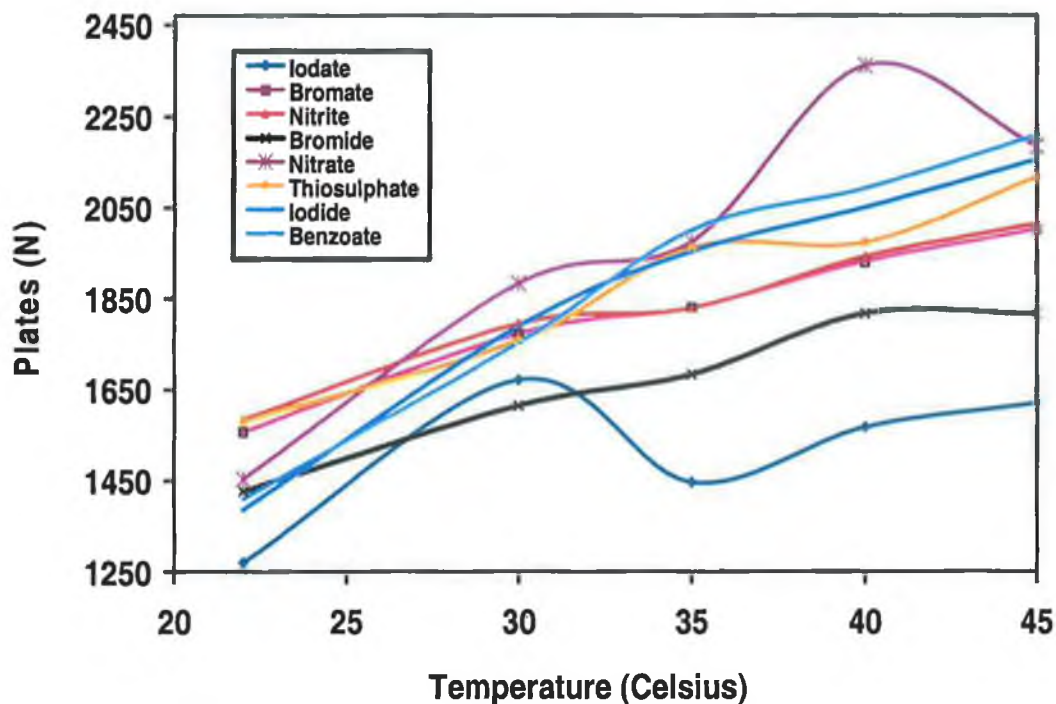


**Figure 2-12.** Effect of temperature upon the separation efficiency of a test mixture of eight UV absorbing anions in ion-interaction chromatography. Other mobile phase conditions: Mobile phase: 50 mM TBA-Cl, 10 % MeOH, pH 6.2. Flow rate: 1.0 mL/min. Injection volume: 2  $\mu$ L. Detection: 214 nm.

### 2.3.3 Effect of flow rate.

The effect of mobile phase flow rate upon both efficiency and normalised resolution product,  $R$ , was determined. For the first five eluting anions (iodate, bromate, nitrite, bromide, nitrate), peak efficiency in terms of theoretical plate number,  $N$ , was calculated at 1.0 ml/min, 1.5 ml/min and 2.0 mL/min using the EP standard formula shown in Equation 2-3.

$$N = 5.54 \left( \frac{T_R}{W_{1/2}} \right)^2 \quad \text{Equation 2-3.}$$

where  $T_R$  is the retention time of the peak, and  $W_{1/2}$  is the peak width at half-height. The average number of theoretical plates for the first five anions was found to be 61,600 plates/m at 1.0 ml/min, 71,800 plates/m at 1.5 mL/min, and 63,133 plates/m

at 2.0 ml/min. (See Figure 2-13). The effect of flow rate upon resolution of these five anions was found to be insignificant. Therefore, as efficiency was only marginally affected and resolution remained the same, a flow rate of 2.0 mL/min was concluded optimum.

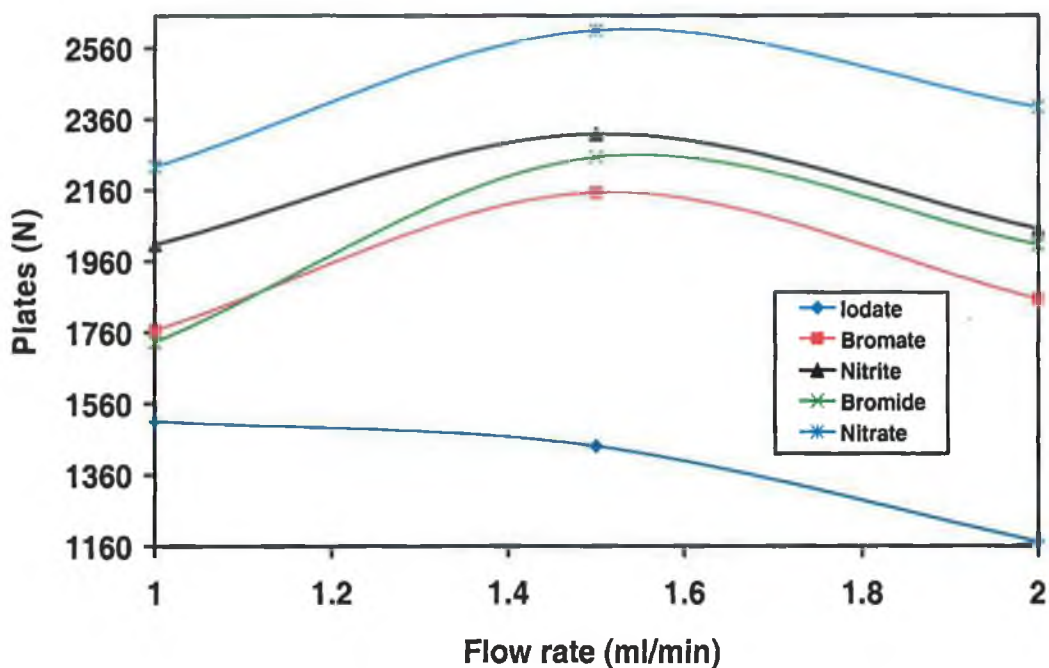


**Figure 2-13.** Effect of flow rate upon the separation efficiency of a test mixture of “weakly retained” anions in ion-interaction chromatography. All other chromatographic conditions as in Figure 2-8.

Figure 2-14 shows the chromatogram obtained from the injection of iodate, bromate, nitrite, bromide and nitrate, under the optimised mobile phase conditions developed earlier, at a flow rate of 2.0 mL/min. As can be seen from Figure 2-14 all five anions can be separated in under 50 sec, with the actual separation window for the five anions being only 28 sec.

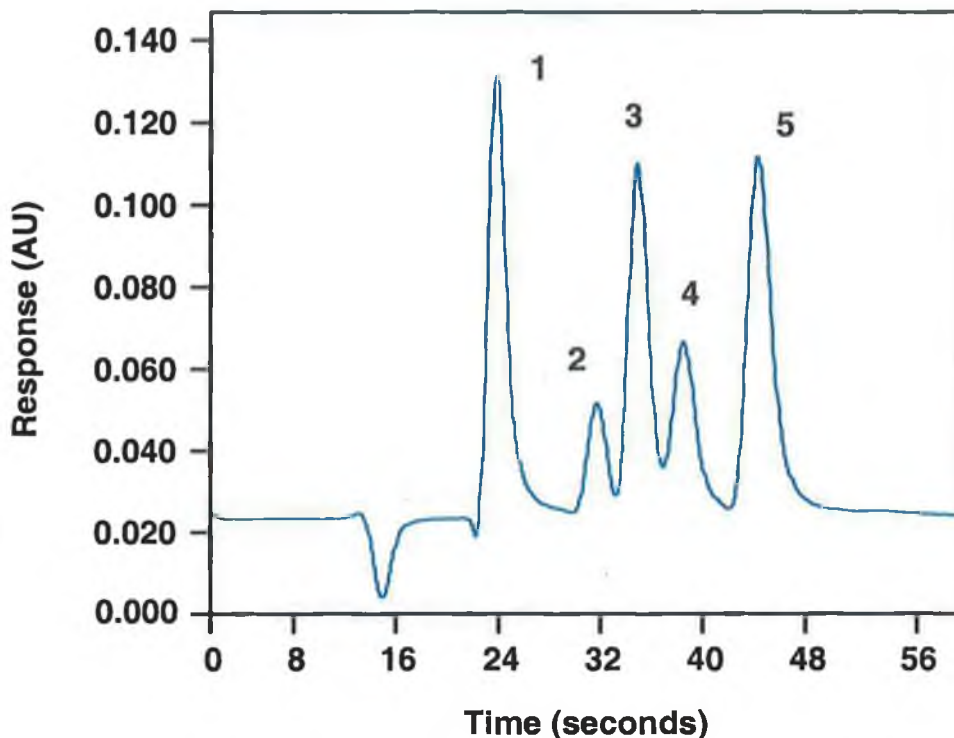


**Figure 2-14.** Optimised separation of five inorganic UV-absorbing anions by fast ion-interaction chromatography on a short 3 cm 3  $\mu\text{m}$  column. Mobile phase: 20 mM TBA-Cl, 20 % MeOH, pH 6.2. Flow rate: 2.0 mL/min. Injection volume: 2  $\mu\text{L}$ . Column temperature: ambient. Detection: 214 nm. Peaks: [1] iodate (23.7 sec), [2] bromate (32.0 sec), [3] nitrite (35.4 sec), [4] bromide (39.2 sec), [5] nitrate (45.3 sec).

For the separation of the complete group of test anions a higher flow rate of 2.5 mL/min was possible, without excessive back pressure (approx. 1500 psi), due to the increased column temperature, set at 45 °C. This flow rate once more had only a slight effect upon the overall efficiency (Figure 2-15) and actually improved the peak symmetry of iodide and benzoate. This resulted in a separation in 4.4 mins with a subsequent compromise in resolution (Figure 2-16) although all analytes remain baseline resolved. The optimum chromatogram<sup>2</sup> is shown below as Figure 2-17.

<sup>2</sup> At this flow rate column pressure exceeded 1500 psi. In order to maintain column performance, backpressures were limited to 1500-1700 psi

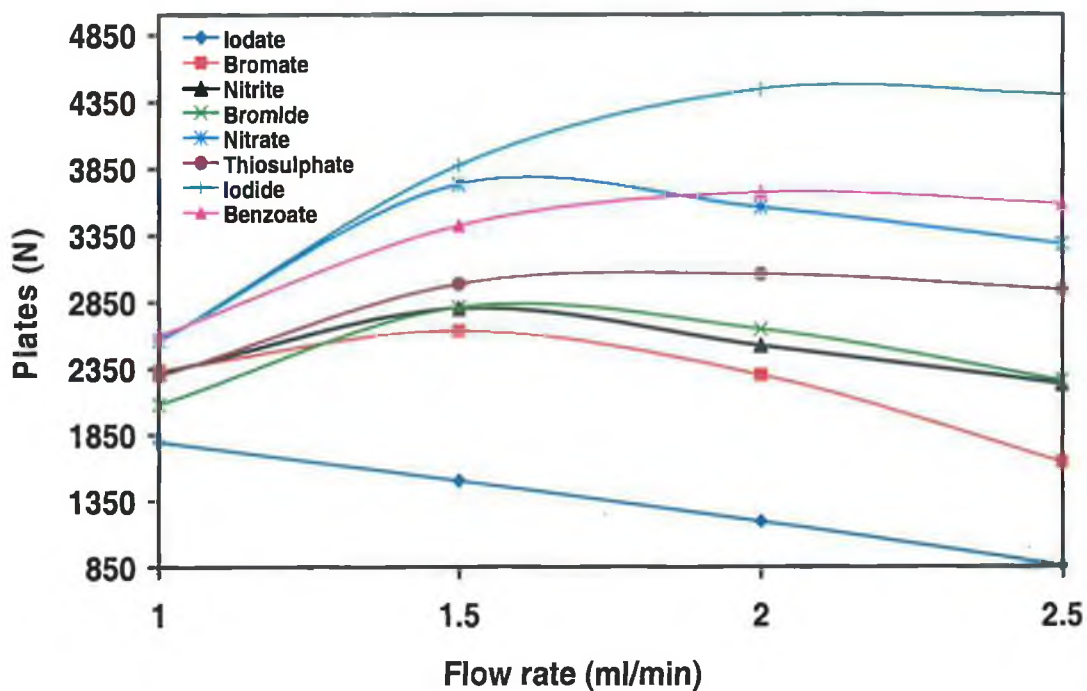


**Figure 2-15.** Effect of flow rate upon the separation efficiency of a test mixture of eight UV absorbing anions by ion-interaction chromatography on a short 3 cm 3  $\mu\text{m}$  column. Conditions: Mobile phase: 50 mM TBA-Cl, 10 % MeOH, pH 6.2. Column temperature: 45  $^{\circ}\text{C}$ . Injection volume: 2  $\mu\text{L}$ . Detection: 214 nm.

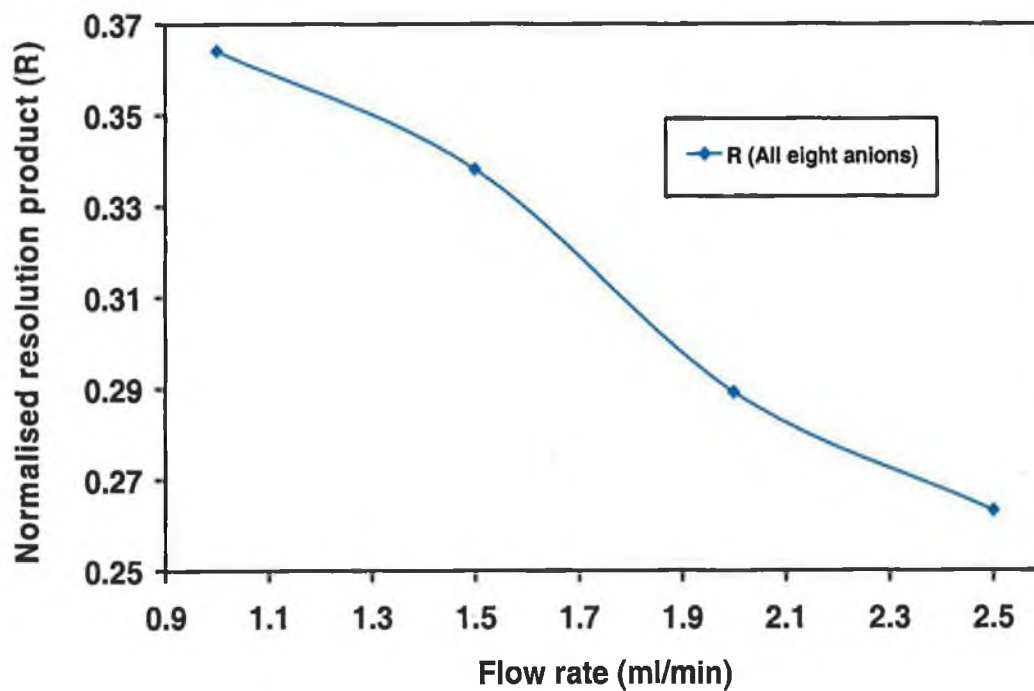


**Figure 2-16.** Effect of flow rate upon the normalised resolution product of a test mixture of eight UV absorbing anions in ion-interaction chromatography. Conditions: Mobile phase: 50 mM TBA-Cl, 10 % MeOH, pH 6.2. Column temperature: 45  $^{\circ}\text{C}$ . Injection volume: 2  $\mu\text{L}$ . Detection: 214 nm.

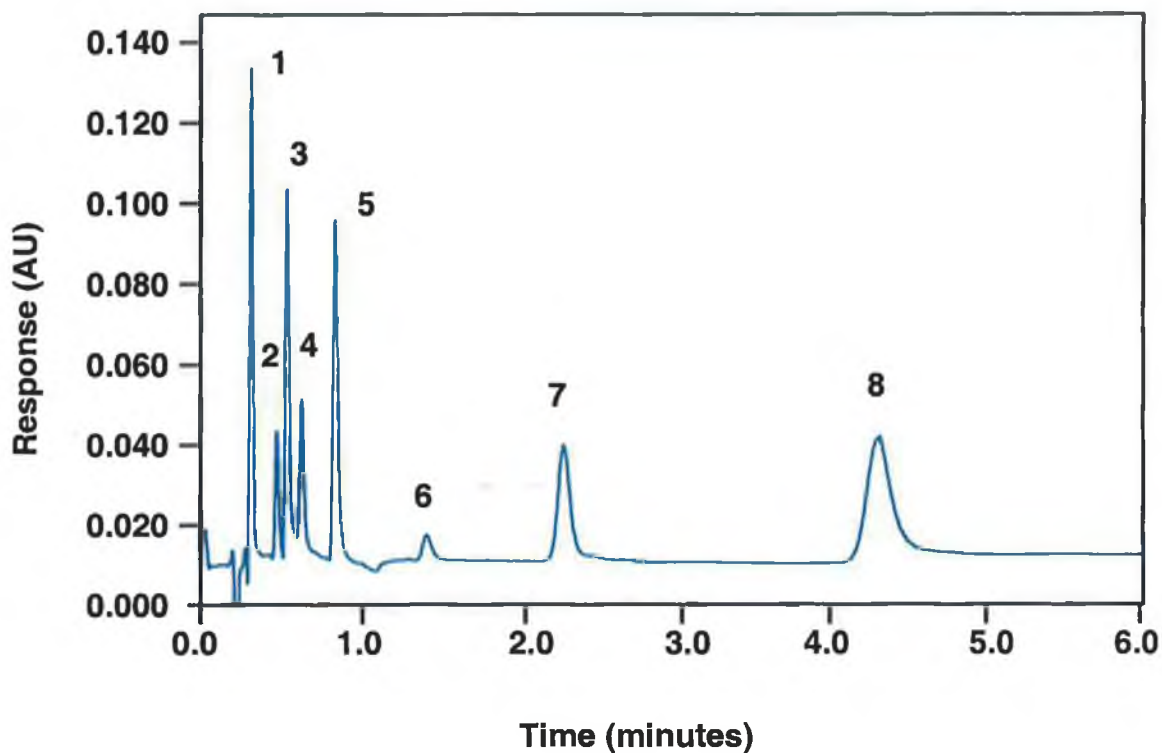


**Figure 2-17.** Optimised separation of eight UV absorbing anions by fast ion-interaction chromatography on a short 3 cm 3  $\mu\text{m}$  column. Mobile phase: 50 mM TBA-Cl, 10 % MeOH, pH 6.2. Column temperature: 45  $^{\circ}\text{C}$ . Flow rate: 2.5 mL/min. Injection volume: 2  $\mu\text{L}$ . Detection: 214 nm. Peaks: [1] iodate (25 mg/L), [2] bromate (100 mg/L), [3] nitrite (25 mg/L), [4] bromide (150 mg/L), [5] nitrate (25 mg/L), [6] thiosulphate (75 mg/L), [7] iodide (25 mg/L) and [8] benzoate (100 mg/L).

#### 2.3.4 Data acquisition in rapid chromatography.

With the use of a small column, the result is a higher, sharper peak than would be obtained on an equivalent 25 cm column. In addition, the faster runtimes results in less band broadening, and therefore, narrower peaks. Therefore, the data acquisition rate was set to 10 Hz for this work. Figure 2-18 below illustrates that the peak in question (bromide), is very well defined, and indeed would remain so, even if the sampling rate was reduced to 5 Hz.

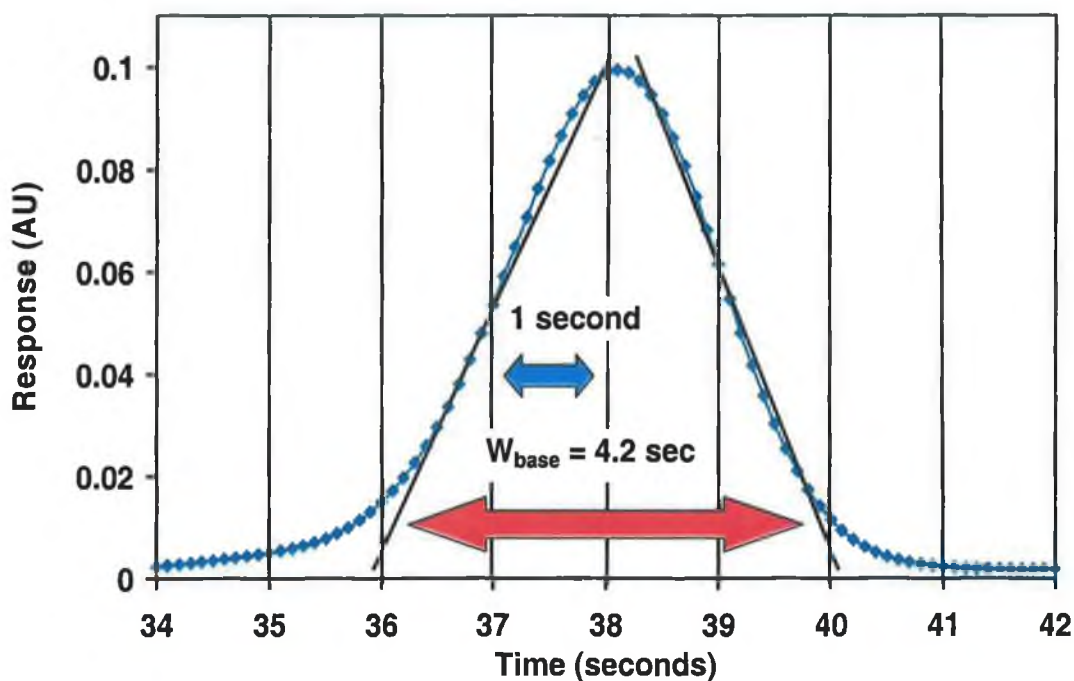


**Figure 2-18.** Data acquisition rate for a rapidly eluting peak (bromide) by fast ion-interaction chromatography on a short 3 cm 3  $\mu\text{m}$  column. Chromatographic conditions as in Figure 2-14.

### 2.3.5 Speciation studies.

Simple inorganic speciation methods are particularly important in the monitoring of environmental processes and also in the analysis of natural and treated waters. It was clear from the earlier experiments that the rapid separation of a number of inorganic anion pairs was possible using the developed ion-interaction method. Therefore, the conditions required for the rapid separation of nitrite and nitrate, bromide and bromate and iodide and iodate were determined. For nitrite and nitrate, and bromide and bromate, the conditions used in Figure 2-14 were again considered optimum. These conditions resulted in the separation of bromate and bromide in under 42 sec and the separation of nitrite and nitrate in under 50 sec. As the detection method used in the determination of nitrite and nitrate was simple UV absorbance at 225 nm<sup>3</sup> there was no interference from common anions such as chloride, sulphate, carbonate and phosphate. Detector sensitivity, although good for nitrite and nitrate (see Chapter 3), was not sufficient for the determination of bromate

<sup>3</sup> See Section 3.3.1 for wavelength optimisation studies.

in water samples at trace levels, such as those set by the USEPA and illustrated in Table 2-2. Nevertheless, the rapid separation of bromate and bromide achieved in this work is over eight times faster than the bromate/bromide separation achieved by Maiti *et al.* [9] who also used ion-interaction chromatography. With a 25 cm X 4.6 mm I.D. Zorbax C<sub>18</sub> (5 μm) column and a mobile phase of acetonitrile/water (35:65), 2 mM cetylpyridinium bromide and 10 mM phosphate buffer, bromate and bromide were separated in 4.86 and 5.91 minutes respectively with a flow rate of 1 ml/min.

**Table 2-2. USEPA drinking water regulations.**

<b>USEPA National Primary Drinking Water Regulations (EPA 815-F-99-004)</b>				
<i>Contaminant</i>	<i>MCLG<sup>1</sup> (mg/L)</i>	<i>MCL<sup>2</sup> (mg/L) TT<sup>3</sup></i>	<i>Potential Health Effects</i>	<i>Common sources.</i>
<i>Fluoride</i>	4.0	4.0	Bone disease. Children may get mottled teeth.	Water additive which promotes strong teeth; erosion of natural deposits; discharge from fertiliser and aluminium factories.
<i>Nitrate</i>	10	10	"Blue baby syndrome" in infants under 6 months – life threatening without immediate medical attention. Symptoms: infant looks blue and has shortness of breath.	Runoff from fertiliser use; leaching from septic tanks, sewage; erosion of natural deposits.
<i>Nitrite</i>	1	1	See Nitrate	See Nitrate
<i>Bromate</i>	0.010	0.010	Carcinogen	Disinfectant by-product due to ozonation of water.
<b>USEPA National Secondary<sup>4</sup> Drinking Water Regulations (EPA 815-F-99-004)</b>				
<i>Contaminant</i>	<i>Guideline (mg/L)</i>		<i>Effect</i>	
<b>Chloride</b>	250.0		Taste/odour	
<b>Fluoride</b>	2.0		Taste/odour	
<b>Sulphate</b>	250.0		Taste/odour	

<sup>1</sup> Maximum Contaminant Level Goal (MCLG) – The maximum level of a contaminant in drinking water at which no known or anticipated adverse affect on the health of persons would occur, and which allows for an adequate margin of safety. MCLG's are non-enforceable public health goals.

<sup>2</sup> Maximum Contaminant Level. (MCL) – The maximum permissible level of a contaminant in water which is delivered to any user of a public water system. MCL's are enforceable standards.

<sup>3</sup> Treatment Technique – An enforceable procedure or level of technical performance which public water systems must follow to ensure control of a contaminant.

<sup>4</sup> A National Secondary Drinking Water Regulation is a non-enforceable guideline regarding contaminants that may cause cosmetic effects (such as taste, odour or colour). Some states in the USA choose to adopt them as enforceable standards.

A rapid separation of iodate and iodide was possible by reducing the concentration of IIR added to the mobile phase. It is clear from the chromatogram shown in Figure 2-6, that iodate belonged to the subgroup of weakly retained hydrophilic anions, whereas the selectivity of the method for iodide was considerably greater. Figure 2-2 shows how the retention of iodide decreased sharply with a decrease in concentration of TBA-Cl in the mobile phase. Therefore, a mobile phase containing 0.5 mM TBA-Cl in 20 % MeOH was used to reduce the retention time of iodide, with the retention of iodate remaining unaffected. Using these conditions the separation of iodate and iodide was possible in under 40 seconds. Figure 2-19, Figure 2-20 and Figure 2-21 show the rapid separations of iodate/iodide, bromate/bromide and nitrate/nitrite.

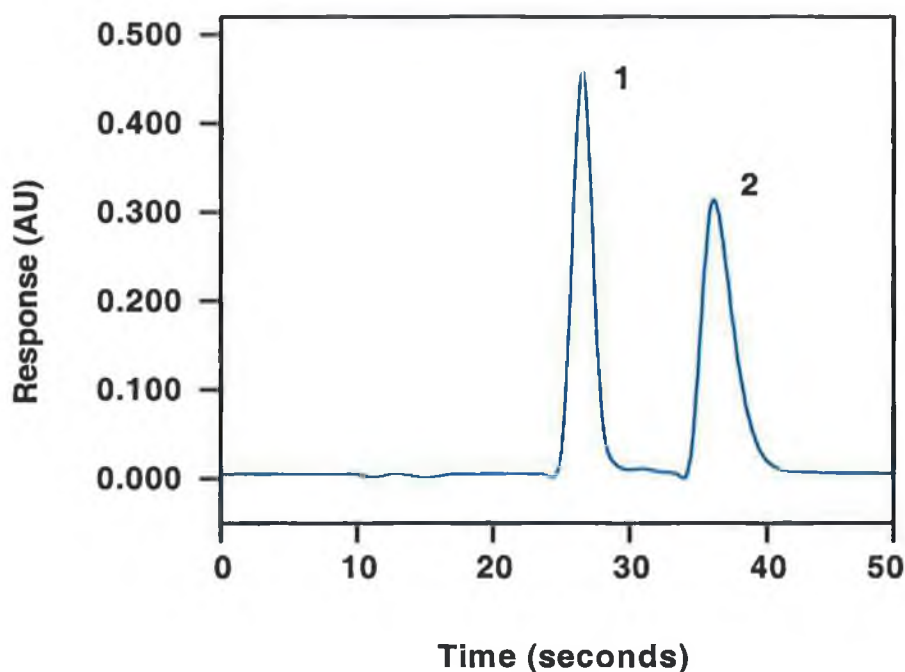


**Figure 2-19.** Ultra-fast separation of iodate and iodide by ion-interaction chromatography on a short 3 cm 3  $\mu\text{m}$  column. Mobile phase: 0.5 mM TBA-Cl in 20 % MeOH, pH 6.2. Flow rate: 2.0 ml/min, Column temperature: ambient. Injection volume: 25  $\mu\text{L}$ . Detection: 225 nm. Peaks: [1] iodate, [2] iodide.

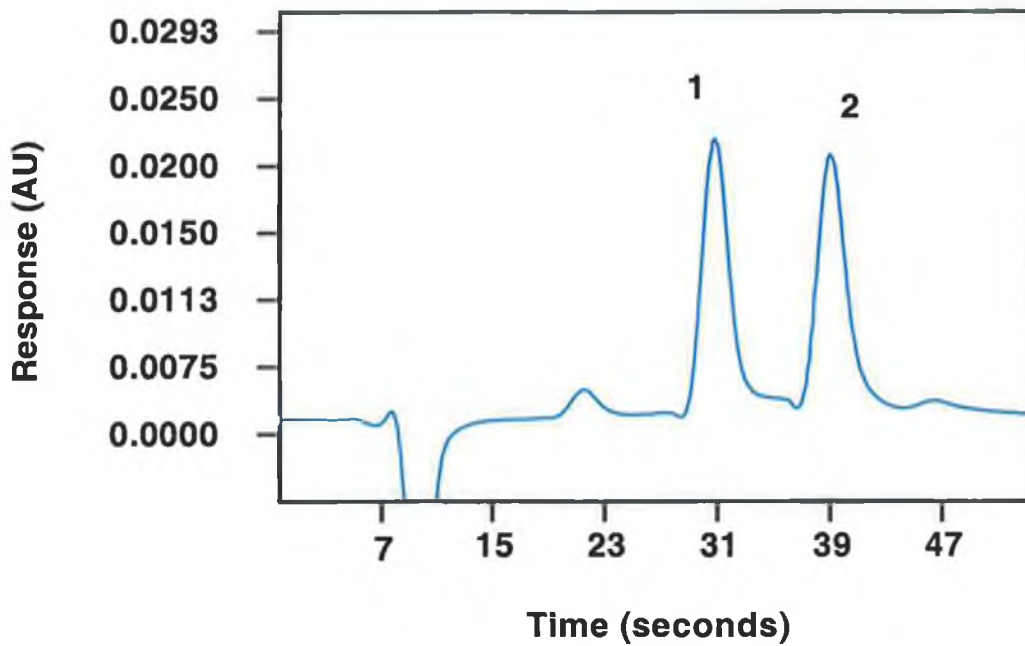


**Figure 2-20.** Ultra-fast separation of 5 mg/L bromate and bromide by ion-interaction chromatography on a short 3 cm 3  $\mu$ m column. Chromatographic conditions as in Figure 2-14 with an injection volume of 50  $\mu$ L. Peaks: [1] bromate, [2] bromide.

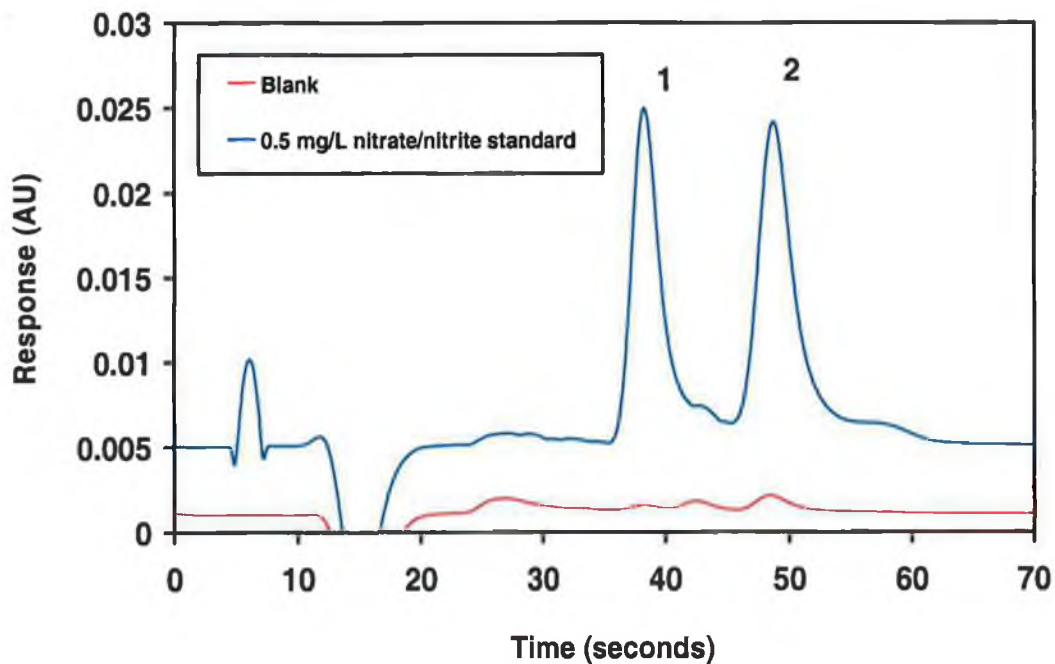


**Figure 2-21.** Ultra-fast separation of nitrite and nitrate by ion-interaction chromatography on a short 3 cm 3  $\mu$ m column. Chromatographic conditions as in Figure 2-14 with an injection volume of 50  $\mu$ L. Peaks: [1] nitrite, [2] nitrate.

## 2.4 Conclusions.

In this work, fast-chromatography, previously predominantly confined to reversed-phase separations was successfully applied to anion analysis using ion-interaction chromatography on a short (30 x 4.6 mm) 3  $\mu\text{m}$  ODS column. The separation efficiencies ( $> 50,000$  plates/m) and resolution achieved compare very favourably with similar separations performed on columns of more traditional length and analysis times have been significantly reduced. For example, the use of an optimised mobile phase containing 20 mM TBA-Cl and 20 % methanol resulted in the baseline separation of five important anions (iodate, bromate, nitrite, bromide and nitrate) in a separation window of just 28 seconds, with a total analysis time of  $< 50$  seconds. Possible applications include rapid screening of samples for particular UV absorbing anions (for example, nitrate and nitrite in drinking water) without interference from other common matrix anions such as chloride, sulphate and phosphate. This would allow rapid on-line monitoring of flowing systems, a possibility that will be illustrated in Chapter 3.

## 2.5 References.

- [1]. F.G.P. Mullins, G.F. Kirkbright, *Analyst* 109 (1984) 1217.
- [2]. B.A. Bidlingmeyer, C.T. Santasania, F. V. Warren, *Anal. Chem.* 59 (1987) 1843.
- [3]. M.C. Gennaro, P.L. Bertolo, A. Cordero, *Anal. Chim. Acta.* 239 (1990) 203.
- [4]. J. Zou, S. Motomizu, H. Fukutomi, *Analyst* 116 (1991) 1399.
- [5]. J. Xu, M. Xin, T. Takeuchi, T. Miwa, *Anal. Chim. Acta.* 276 (1993) 261.
- [6]. A. Padaruskas, G. Schwedt, *Talanta* 42 (1995) 693.
- [7]. Labscan Limited, Stillorgan, Dublin, Ireland.
- [8]. K.L. Ng, B. Paull, P.R. Haddad, K. Tanaka, *J. Chromatogr. A* 850 (1999) 17.
- [9]. B. Maiti, A.P. Walvekar, T.S. Krishnamoorthy, *Analyst* 114 (1989) 731.

### **3 Rapid online determination of nitrate and nitrite in drinking water using ion-interaction liquid chromatography.**

#### **3.1 Introduction.**

Nitrate and nitrite levels in our natural waters are important indicators of water quality. Nitrate and nitrite are both intimately involved in the overall nitrogen cycle of soil and higher plants; in natural systems both species are produced in the nitrification process in which ammonia is oxidized by certain soil bacteria [1]. Leaching of nitrate from fertilizers added to soils can also result in elevated levels of nitrate in ground and surface waters. Nitrogenous solutes such as ammonia, nitrate and nitrite are thought to play a major role in limiting phytoplankton primary production in oceanic surface waters over short time scales [2]. Nitrite can be formed during the biodegradation of nitrate, ammonical nitrogen and other nitrogenous organic matter, and is an important indicator of fecal pollution of natural water systems. In addition, nitrite is readily oxidised to nitrate by dissolved oxygen thus decreasing oxygen levels in water. The acceptable daily intake recommended by the World Health Organization is 220 mg nitrate for an adult person of about 60 kg. For nitrite the recommended acceptable daily intake is 8 mg [3].

When nitrate contaminated water supplies are used as a source for drinking water adverse human health effects are also of great concern. Relative to nitrites, nitrates are compounds of lower toxicity, representing a danger only when ingested in excessive doses or when converted to nitrites. Nitrites, however, can have several adverse effects upon human health. For example, the *in vivo* reaction between nitrite and secondary or tertiary amines produces N-nitrosamines, which are potential carcinogens, mutagens and/or teratogens. In addition, nitrite interacts with blood pigment to cause methaemoglobinemia, especially in infants (aka 'blue baby syndrome'). This condition limits the blood's ability to carry oxygen from the lungs to the rest of the body. To guard against the above effects the US EPA have set the MCL (maximum contaminant level) for nitrate in drinking water at 10 mg/L.

Nitrate and nitrite salts are also added to certain foods during processing (meats, some fish and dairy products) such that a microbiological preservative effect is attained. For example, nitrite provides specific protection against *Clostridium botulinum* [4]. During meat curing processes, nitrite is added to speed curing and the formation of the required colours and flavours [5].

There are a number of analytical methodologies applicable to nitrate/nitrite quantification based upon either spectrophotometric, [1,2,4] [6-14], electrophoretic [3,5] [15-19] or chromatographic techniques [20-22]. Based upon the former, numerous flow injection analysis (FIA) methods have been developed, each exhibiting the benefits that FIA has to offer in terms of versatility, high sample throughput, high degree of reproducibility and ease of automation. The majority of FIA methods based on spectrophotometric detection involve the well known Griess reaction between nitrite and an aromatic primary amine under acidic conditions [1,4] [6-10]. The aromatic primary amine usually used is sulphanilamide [1,4,6] [8-10], but sulphapyridine [1], sulphathiazole [1], 3-nitroaniline [7] and aniline [2] have also been used. The resulting diazonium cation is coupled with a coupling agent to form a stable, pinkish azo dye that is measured colourimetrically at wavelengths ranging from 510 nm to 555 nm depending on the experimental conditions used. The coupling agent used is usually N-(1-naphthyl)ethylenediamine dihydrochloride [4] [6-10] but 1-naphthol-4-sulphonate [1] and imidazole [2] have also been used. In all cases, the resulting azo dyes were found to be stable in aqueous solution even after standing for over 90 minutes, with the relative changes in absorbance with time being < 0.2 %. Also, the diazotization reagents in the absence of nitrite are colourless and the reaction with nitrite is instantaneous at room temperature.

To achieve simultaneous determination of both analytes (nitrate and nitrite), using flow injection analysis the sample is usually split, producing two peaks. One sample zone merges with the reagents directly and produces the first peak, which corresponds to the total nitrite in the sample; the other sample zone passes through a reduction column first, where nitrate is reduced to nitrite, then merges with the reagents

and produces the second signal. Each channel has a different residence time in the FIA manifold, and therefore two peaks are obtained which correspond to nitrite, or nitrite plus nitrate. Subtracting the area of peak #1 from peak #2 gives the total nitrate present in the sample.

Kojlo and Gorodkiewicz [6] used the Griess reaction in an FIA manifold to simultaneously determine nitrate and nitrite in natural waters. The workers reported the use of a portion of the sample loop as a reduction column, whereby part of the sample loop was filled with copperized cadmium. A peak with a shoulder on the ascending part of the analytical signal was produced. The height of the shoulder corresponded to the concentration of nitrite in the sample, and the maximum of the peak correlated with the sum of both anions. Detection limits were relatively high at 0.1 mg/L for nitrite and 0.5 mg/L for nitrate. Sample throughput was 22 samples/hour.

Ahmed *et al.* [7] reacted nitrite with 3-nitroaniline and coupled the resulting diazonium cation with N-(1-naphthyl)ethylenediamine dihydrochloride resulting in considerably lower detection limits of 1 µg/L for nitrite and 10 µg/L for nitrate, and a sampling rate of 30 samples/hour. The method was successfully applied to the analysis of sausage, flour, cheese, beer and soil samples.

The Griess reaction was used by Pinho *et al.* [4] to analyse liver pate samples for nitrate and nitrite, with detection limits of 10 µg/L for nitrite and 100 µg/L for nitrate. Sample throughput was 40 samples/hour. Gabriel *et al.* [8] achieved detection limits of 56 µg/L for nitrate and 15 µg/L for nitrite. The sampling frequency of the system was 180 samples/day. The system was set up to monitor real time fluctuations in nitrate/nitrite levels in a waste water treatment plant which operated on a 24 hour basis, leaving the actual sample rate at only 7.5 samples/hour. Cerda *et al.* [9] used an automated sequential injection system involving a sandwich arrangement in which the sample zone was placed between two Griess reagent zones. Nitrite was determined at the sample front by direct reaction with the Griess reagent to produce the coloured azo dye, while nitrate was similarly determined at the tail of the injected sample plug after

previous reduction to nitrite. The same reaction product was formed at the two interfaces between the sample and reagent and thus spectrophotometric measurements were made at a single wavelength. Injection volumes of 1,800  $\mu\text{L}$  were used such that the central part of the sample plug did not overlap with the Griess reagent on either side thus acting as a separation zone between the reaction products at both extremes and allowing complete peak resolution. Detection limits were 4.6  $\mu\text{g/L}$  for nitrite and 27.6  $\mu\text{g/L}$  for nitrate. The sampling rate was very low at only 10 samples/hour.

An on-chip micro-flow analysis of nitrate was developed by Petsul *et al.* [10] in which the flow manifold took the form of 115  $\mu\text{m}$  X 300  $\mu\text{m}$  channels wet etched in borosilicate glass. Conventional pumping methods involving moving parts were not used. Instead, reagents and sample solutions were pumped using an electro-osmotic flow, established by applying a voltage of 50 V across the sampling reservoir (in which nitrate standards and samples were placed) to the waste reservoir. An *in situ* miniature copperized cadmium reduction column was immobilized in micro-porous silica frit located in the sample introduction reservoir. The nitrite produced on leaving the reduction frit was detected using the diazo-coupling Griess reaction which was monitored *in situ* using a micro-spectrometer. Limits of detection for nitrate were 26  $\mu\text{g/L}$ , however the precision using a 310  $\mu\text{g/L}$  standard was quite high at 8.3 %. The sampling rate was 30 samples/hour.

Detection limits as low as 1  $\mu\text{g/L}$  for nitrite and 0.75  $\mu\text{g/L}$  for nitrate using the Griess reaction were obtained by Horita *et al.* [1] who used column pre-concentration on naphthalene supported with an ion-pair of tetradecyldimethylammonium and iodide. The azo dye formed was retained on the naphthalene adsorbent and was subsequently dissolved from the column with 5 ml of dimethylformamide (DMF) and determined spectrophotometrically. Since the azo dye was dissolved from the column along with the naphthalene adsorbent in 5 ml DMF, the method was characterized by the fact that the solid adsorbent in the column could only be used for a single determination.

The Griess reaction has also been used with fluorescence detection as reported by Masserini and Fanning [2] who analysed seawater for nitrate and nitrite. The workers capitalized on the fluorescence of the  $\pi$  electrons within the bond between the two nitrogen atoms within the diazonium cation formed via the reaction between an acidified nitrite sample and an aromatic primary amine. Reverse flow injection analysis (rFIA) was used to correct for background fluorescence from leachates and naturally occurring dissolved organic matter. rFIA is a modification of traditional FIA methodologies in which the sample (seawater) acts as the carrier while a fixed volume of reagent is injected. In this work, rFIA allowed a background signal to be established prior to the injection of reagent. Once the seawater's background fluorescence reached a plateau, the reagent was injected to produce a fluorescent signal proportional to the nitrite present in the sample. The throughput of the instrumentation was 18 samples/hour with detection limits of 0.2  $\mu\text{g/L}$  and 0.4  $\mu\text{g/L}$  for nitrite and nitrate.

Common interferences in most azo dye methods are Cu (II), Fe (III), Cr (VI) and sulphate requiring the use of masking agents. Examples of masking agents used for interfering metals [1] are  $\text{NH}_4\text{F}$  for Fe (II), triethanolamine for Fe (III), EDTA for  $\text{Mn}^{2+}$  and sodium tartrate for Co (II).

Although the Griess reaction has had widespread acceptance in the determination of nitrate and nitrite, it is also accepted that the reagents involved in this methodology are carcinogenic. Alternatives to the Griess reaction have been proposed, offering equivalent sensitivity. Guerrero *et al.* [11] utilized the intense violet colour produced by the reaction of nitrite with 3,6-diamino acridine (proflavin sulphate) in acidic media. Detection limits for nitrate were as low as 0.075  $\mu\text{g/L}$  with a sample throughput of 24 samples/hour.

The oxidizing effect of nitrite on iodide ion to produce tri-iodide was investigated by Gil Torro *et al.* [12]. The tri-iodide thus formed was detected biamperometrically in excess iodide by using a flow cell furnished with two platinum electrodes polarized at 100 mV. Limits of detection and throughput for nitrite and nitrate

were 25 and 50  $\mu\text{g/L}$  and 27 and 25 samples/hour respectively. Concentrations of  $\sim 1$   $\text{mg/L}$  of oxidizing cations such as Fe (III) and Cu (II) produced considerable errors, however, and these effects were minimized by preparation of the iodide solution in  $\text{Na}_2\text{EDTA}$ .

Zhi-Qi *et al.* [13] used the catalytic effect of nitrite on the oxidation of naphthol green B (NGB) by potassium bromate in phosphoric acid medium. The effect was discolouration of NGB with the decrease in absorbance being directly proportional to the nitrite concentration. Detection limits of 0.5  $\mu\text{g/L}$  and 2.5  $\mu\text{g/L}$  were achieved for nitrite and nitrate respectively. Up to 30 samples could be analysed per hour.

Nitrite is known to have a catalytic effect on the oxidation of galloyanine by bromate in acidic media causing a decrease in the absorbance of the system at 530 nm. Ensafi and Kazemzadeh [14] utilized this effect in an FIA system for determination of nitrite and nitrate in food and water samples by splitting the flow of sample through a reduction column containing copperized cadmium. The sampling rate of analysis was 20 samples/hour and detection limits were 1  $\mu\text{g/L}$  and 2  $\mu\text{g/L}$  for nitrite and nitrate respectively.

A major disadvantage common to all the FIA methods discussed is that a portion of the sample must be passed through a reductor assembly such that nitrate is reduced to nitrite. Reduction of nitrate to nitrite is generally achieved using a heterogeneous reduction process with copperized cadmium [1,2,4] [6-11] [14] or cadmium coated zinc [13], but Gil Torro *et al.* [12] reported the use of UV irradiation with a low pressure 8 W mercury lamp for photochemical reduction. In all cases where reducing metals have been used, workers have reported problems with the stability of the reduction column, with effects such as incomplete reduction primarily observed. All workers using cadmium particles as a reducing agent reported that the presence of copper (usually coated onto the cadmium particles using a solution of  $\text{CuSO}_4$  to produce "copperized cadmium") as a catalyst dramatically increased the response, providing quantitative reduction with a short contact time. Ahmed *et al.* [7] reported the incorporation of a

copper column before the copperized cadmium column in the reaction manifold, resulting in a five fold increase in lifetime for the copperized cadmium column.

Nevertheless, all workers reported the need for periodic regeneration of the reduction column by replacing the ammonium chloride buffer solution<sup>1</sup> with an EDTA-CuSO<sub>4</sub> solution to provide new copper to regenerate the external coating of the cadmium granules, and EDTA to avoid the precipitation of Cd(OH)<sub>2</sub> and Cu(OH)<sub>2</sub>. Gabriel *et al.* [8] reported the sieving of the cadmium reductant particles prior to packing the reduction column to achieve an optimum particle size; but ultimately found that the repetitive running of the regeneration cycle not only decreased the sampling rate but also shortened the lifetime of the column due to the gradual breakdown of the cadmium granules in to smaller particles due to compaction from a continuous one way flow.

A further disadvantage of the use of cadmium reducing columns is that the wastes contain highly toxic and polluting metals. As an alternative Gil Torro *et al.* [12] described the use of UV irradiation for reduction of nitrate to nitrite in the 200-300 nm region, where the PTFE tubing used in the reaction coil was found to be UV transparent. The sample (a nitrate or nitrite solution) was circulated through a PTFE tube (697 cm long X 0.8 mm I.D. X 1.4 mm O.D.) coiled around the low pressure mercury lamp located at the inlet of the sample loop.

Analytical methods based upon separation methods are predominantly those employing either ion chromatography (IC) or capillary zone electrophoresis (CZE). A number of methods for nitrate and nitrite determinations using CZE have been proposed for water samples of varying complexity in recent years [15] [17-19]. Capillary zone electrophoresis offers a number of advantages such as high separation efficiency, short run-times, low reagent costs and feasibility in selectivity manipulation.

---

<sup>1</sup> The rate of reduction of nitrate to nitrite in the copperized cadmium column increased in the presence of ammonium chloride.

The technique lends itself particularly well to the analysis of waters due to the minimal sample preparation steps required. Guan *et al.* [15] developed an electrophoretic separation of nitrate and nitrite for analysis of tap and river waters, demonstrating that a large concentration of nitrate did not adversely affect the quantification of a small amount of spiked nitrite. A tetraborate/cetyltrimethylammonium chloride electrolyte was used with a 50 cm X 50  $\mu\text{m}$  I.D. capillary and a separation voltage of -10 kV. Runtimes for nitrate and nitrite in tap and river water were 7.0 minutes, with detection limits of 0.4 mg/L for both anions.

Okemgbo *et al.* [18] used hexamethonium bromide as an electro-osmotic flow modifier in a pH 9.2 borate buffer with a 50 cm X 50  $\mu\text{m}$  I.D. capillary and a separation voltage of -22 kV to resolve nitrate and nitrite in under 3 minutes. Detection limits of 3.8  $\mu\text{g/L}$  (nitrite) and 2.0  $\mu\text{g/L}$  (nitrate) were obtained using a gravity injection time of 3 minutes, essentially increasing total runtimes to 6 minutes.

Fukushi *et al.* [17] used CE to analyze more complex sample matrices such as seawater for nitrate and nitrite by using an artificial seawater as carrier solution. This eliminated the interference of high concentrations of the chloride ion in seawater and therefore regardless of the salinity of the samples, peak area and migration time reproducibilities were within 3 %. A 100  $\mu\text{m}$  I.D. capillary was used to extend the optical path length such that limits of detection were 40  $\mu\text{g/L}$  and 70  $\mu\text{g/L}$  for nitrate and nitrite respectively. However, in terms of high-speed analysis, the runtime of just under 15 minutes was relatively slow. Migration times were 13 minutes for nitrite and 14 minutes for nitrate.

In stark contrast is the work of Melanson and Lucy [19] in which a shortened capillary (7 cm to detector), higher voltages and low pH values (to reduce the mobility of nitrite); resulted in a separation of nitrate and nitrite in under 12 seconds. Total runtime (pre-rinse, injection and separation) was less than one minute resulting in a sample throughput of up to 60 samples per hour. Detection limits were 6.2  $\mu\text{g/L}$  and 46  $\mu\text{g/L}$  for nitrate and nitrite using electrokinetic injection and 0.62 mg/L (nitrate) and 0.46 mg/L

(nitrite) for hydrodynamic injection. Melanson and Lucy observed that electrokinetic injection was limited to low conductivity samples, with hydrodynamic injection being more suited to higher conductivity samples such as seawater.

The third instrumental technique suggested to date for nitrate/nitrite analysis is HPLC. Chromatographic methods for nitrate and nitrite are usually based upon the use of IC. Ion chromatography has been used to determine nitrate and nitrite in a range of biological fluids; these methods will be discussed in Chapter 4. A number of detection modes have been found to be applicable for these methods as discussed in Chapter 4; direct UV detection, suppressed conductivity detection, fluorescence detection and a post-column diazotization coupling reaction (Griess reaction).

To date, no studies have been published relating to the rapid determination of nitrate and nitrite in water samples by IC. As discussed previously, the majority of rapid nitrate and nitrite determinations have been with FIA methodologies. The US EPA's recommended method for the determination of inorganic anions in drinking water samples (Method 300.1) uses IC with suppressed conductivity detection [23]. A Dionex AS9-HC 25 cm X 2.0 mm anion exchange column is used with a 9 mM Na<sub>2</sub>CO<sub>3</sub> eluent and a flow rate of 0.4 ml/min. The conductivity of the eluent is suppressed using an ASRS-I suppressor in external source electrolytic mode at a current of 100 mA. Using an injection volume of 10 µL, detection limits of 1 µg/L for nitrite and 8 µg/L for nitrate are achieved, but the method suffers in terms of total analysis times, which if the sample also contains common anions, such as sulphate and phosphate, can be of the order of 15 minutes<sup>2</sup>.

In this work, to illustrate the potential of rapid chromatographic methods for use in drinking water monitoring applications, a rapid on-line ion-interaction chromatographic system was developed and used for the continuous analysis of a flowing drinking water sample stream for nitrate and nitrite. Samples were analysed at a

---

<sup>2</sup> Phosphate and sulphate elute at 12 and 13.5 minutes respectively, however EPA Method 300.1 recommends a method total analysis time of 25 minutes.

rate of 1 injection per minute with the chromatographic system exhibiting both efficiency and sensitivity comparable with standard IC methods.

## **3.2 Experimental.**

### **3.2.1 Equipment.**

The ion chromatograph and analytical column described in Chapter 2 were also used in this work. For the analysis of discrete river and tap water samples, 0.45  $\mu\text{m}$  swinny filters (Gelman Laboratories Michigan, USA) were used for sample filtration prior to injection. The injection loop used was 50  $\mu\text{L}$  with detection by direct UV at 225 nm. For the on-line experiments a peristaltic pump (Gilson Minipuls 312, Villiers, France) was employed to deliver a constant sample stream to the injection port and an in-line 0.45  $\mu\text{m}$  nylon membrane filter added (Gelman Laboratories Michigan, USA) (shown schematically as Figure 3-7). The PeakNet 6.0 software controlling the system was set up to inject a sample every 60 seconds, beginning data acquisition at time = 0 seconds and switching the injection loop back to 'load' position at time = 30 seconds, ready for the next injection at  $t = 60$  seconds. Comparative ion chromatographic experiments were carried out using a 25 cm X 4.6 mm AS17 anion exchange analytical column (Dionex) with UV detection at 227 nm.

### **3.2.2 Reagents.**

Mobile phase and chromatographic conditions were as described in Chapter 2. The eluent used for the comparative analysis of validation samples was 15 mM NaOH, prepared from a 50 % w/w NaOH solution supplied by Aldrich, (Aldrich, Milwaukee, WI, USA). The flow rate used was 1.0 ml/min. Standard solutions used were as described in Chapter 2.

### **3.3 Results and discussion.**

The work detailed in Chapter 2, illustrated that fast-chromatography, previously predominantly confined to reversed-phase separations could be successfully applied to anion analysis using ion-interaction chromatography. The separation efficiencies and resolution achieved, compared very favourably with similar separations performed on columns of more traditional length and analysis times were significantly reduced. Comparisons of retention data versus changing MeOH/TBA-Cl concentrations indicated that the separation mechanism mirrored a pattern which would be achieved on a column of conventional length. Therefore, previously well-established ion-interaction models were shown to be applicable, even when such a short column was used. Due to the rapid run times achievable on such a short column, the mobile phase could be completely optimized to obtain the highest resolution of a selected group of UV absorbing anions in only a few hours. Using these conditions, the total analysis time was under 50 seconds, which indicated that the method had considerable potential for the rapid screening of water samples for these particular analytes. The optimized fast ion-interaction separation of iodate, bromate, nitrite, bromide and nitrate previously shown in Chapter 2 is illustrated again in Figure 3-1.

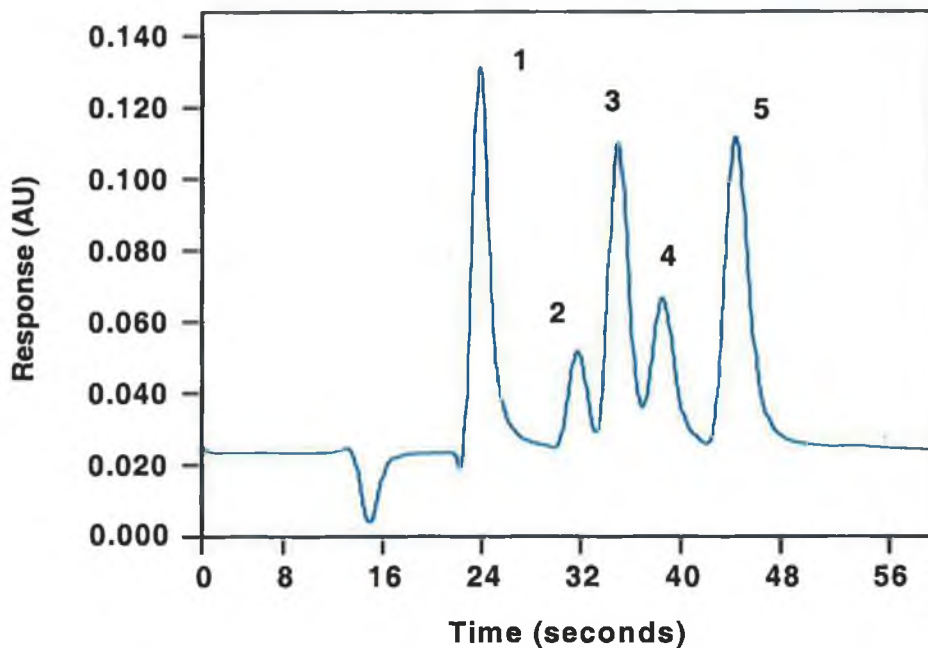


**Figure 3-1.** Rapid separation of five inorganic UV-absorbing anions by ion interaction chromatography on a short 3  $\mu\text{m}$   $\text{C}_{18}$  column. Column: Phenomenex Hypersil, 3  $\mu\text{m}$  particle size, 30 mm x 4.6 mm I.D., Mobile phase: 20 mM TBA-Cl, 20 % MeOH, pH 6.2. Flow rate: 2.0 mL/min. Injection volume: 2  $\mu\text{L}$ , Column temperature: ambient, Detection: Direct UV at 214 nm. Peaks: [1] iodate (23.7 sec), [2] bromate (32.0 sec), [3] nitrite (35.4 sec), [4] bromide (39.2 sec), [5] nitrate (45.3 sec).

### 3.3.1 Determination of nitrate/nitrite in water samples.

To illustrate how the methodology developed here has real application potential, the method was briefly applied to the determination of nitrite and nitrate in both drinking water and a local freshwater river sample. The optimum detection wavelength was determined for nitrate and nitrite by injecting a 5 mg/L standard mix across a range of wavelengths and plotting the peak height vs wavelength, (see Figure 3-2). In addition, the baseline noise was determined across this wavelength range, when a water blank was injected, and compared to the injection of mobile phase (Figure 3-3). It was found that the baseline noise for a water blank approached the theoretical optimum (a situation in which all standards are actually made up in mobile phase) at 225 nm. It was concluded

that although peak height in itself, was not optimum at 225 nm, the overall  $S/N$  ratio for an analyte would be maximised at this wavelength.

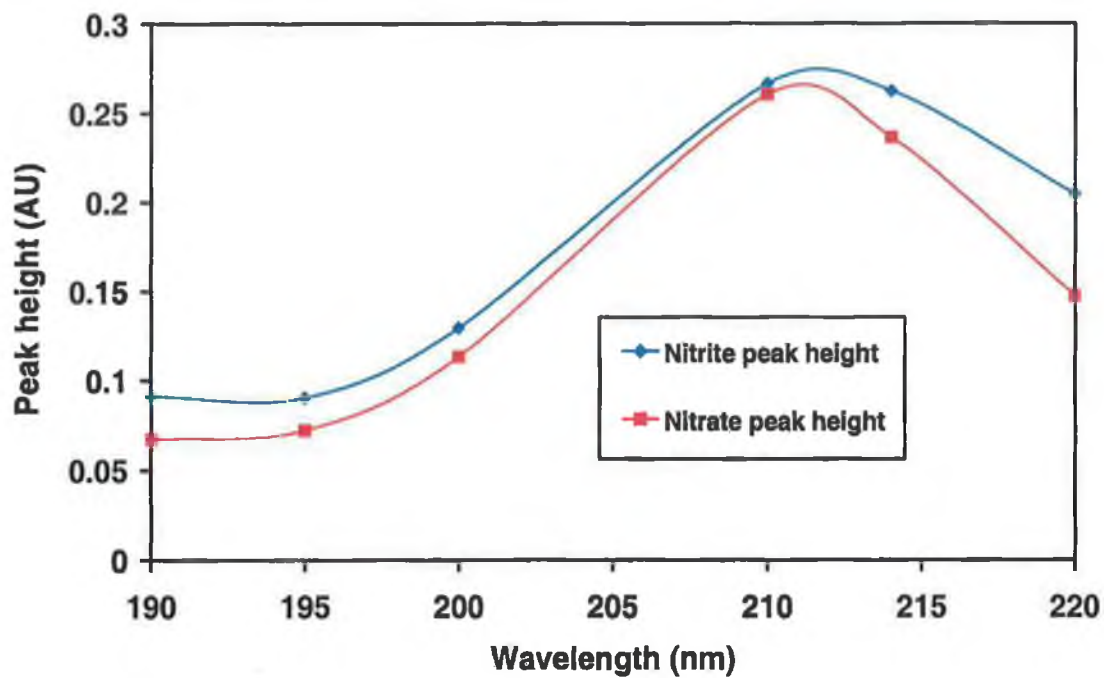
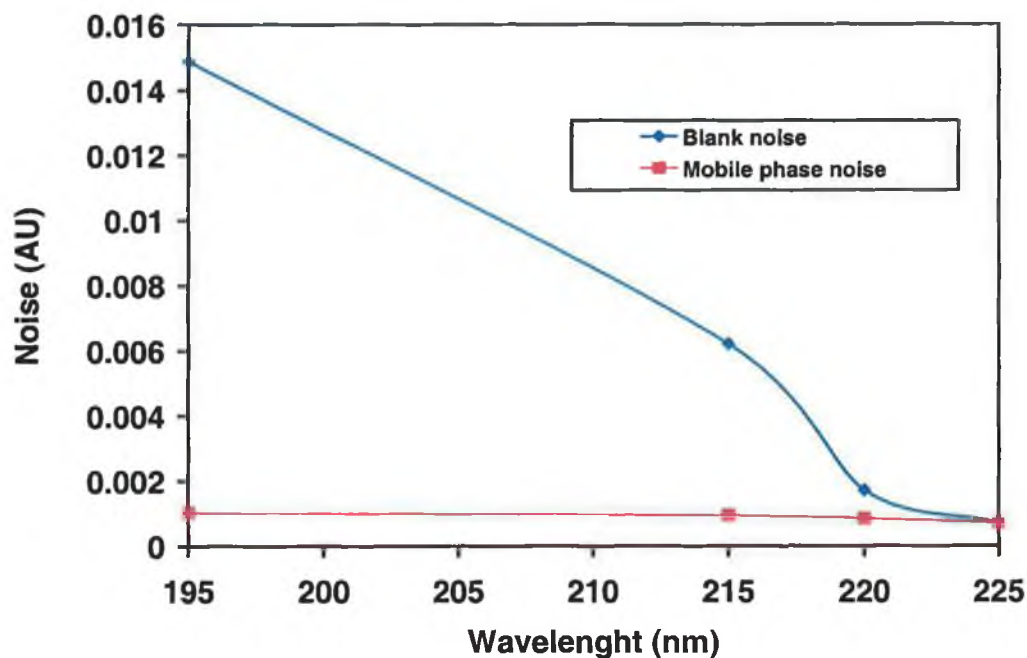


Figure 3-2. Optimisation of detector wavelength for the determination of nitrate and nitrite by fast ion interaction chromatography. Chromatographic conditions as in Figure 3-1.



**Figure 3-3.** Comparison of noise generated by the injection of a water blank compared with a mobile phase blank by ion interaction chromatography. Conditions are as in Figure 3-1. Noise measured from 45 seconds to 120 seconds.

Two samples, one of tap water and one from a freshwater river, were obtained, treated only to filtration (0.45  $\mu\text{m}$ ), and then analysed using the developed method. The injection volume was increased to 50  $\mu\text{L}$  to improve sensitivity<sup>3</sup>. The resultant chromatograms from the injection of a standard and blank solution, and the two samples, both spiked and unspiked, are shown in Figure 3-4, Figure 3-5 and Figure 3-6. As can be seen from the figures, neither the tap water nor freshwater sample matrix caused any interference with the separation of nitrite and nitrate. Both anions were crudely quantified in the two samples, by an approximate correlation of sample peak areas with a 0.5 mg/L and 5 mg/L mixed nitrate and nitrite standard, ran on the same day. The tap water sample was shown to contain ~3.4 mg/L nitrate, with no nitrite peak being detectable. In the freshwater river sample nitrate was present at a lower concentration of

<sup>3</sup> See Section 3.3.3.3 for further information.

just ~0.6 mg/L, but a peak for nitrite was clearly present indicating a concentration of ~0.07 mg/L.

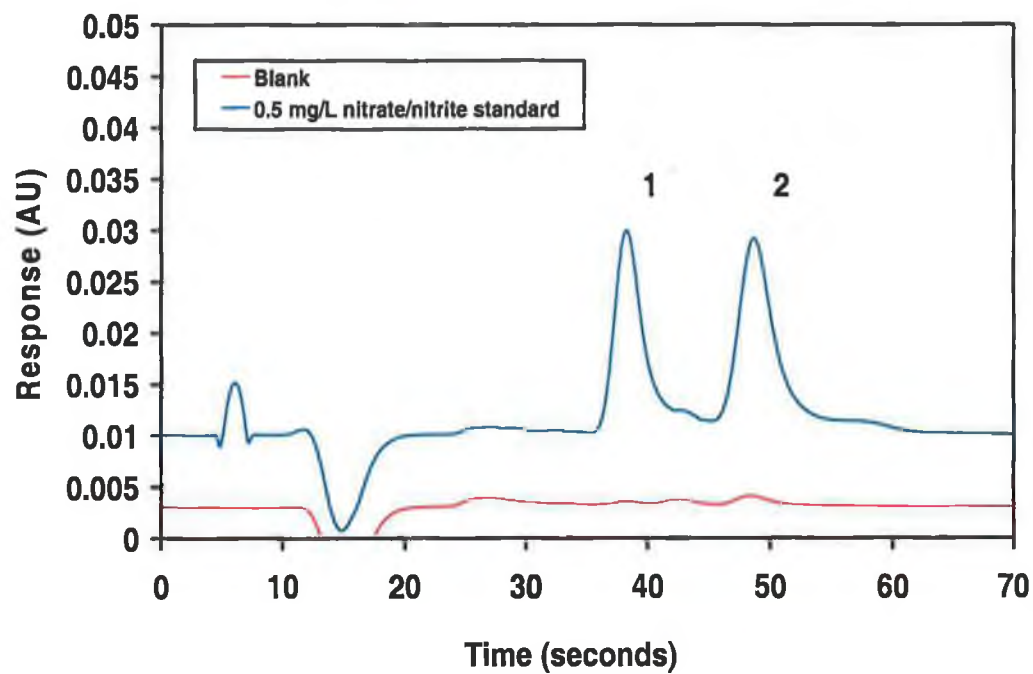


**Figure 3-4.** Rapid determination of nitrate/nitrite by ion interaction chromatography on a short 3  $\mu\text{m}$   $\text{C}_{18}$  column. Chromatographic conditions are as in Figure 3-1 except: Detector wavelength: 225 nm, Loop volume: 50  $\mu\text{L}$ . Peaks: [1] nitrite, [2] nitrate.

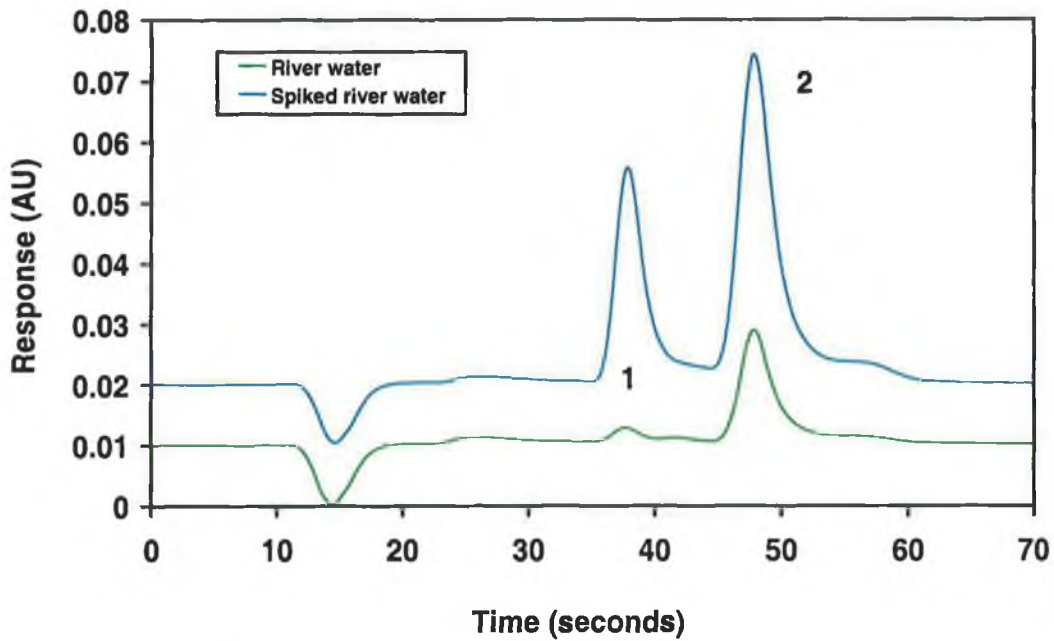


Figure 3-5. Rapid determination of nitrate/nitrite levels in river water by ion interaction chromatography on a short  $3\ \mu\text{m}\ C_{18}$  column. Chromatographic conditions are as in Figure 3-4. Peaks: [1] nitrite, [2] nitrate.

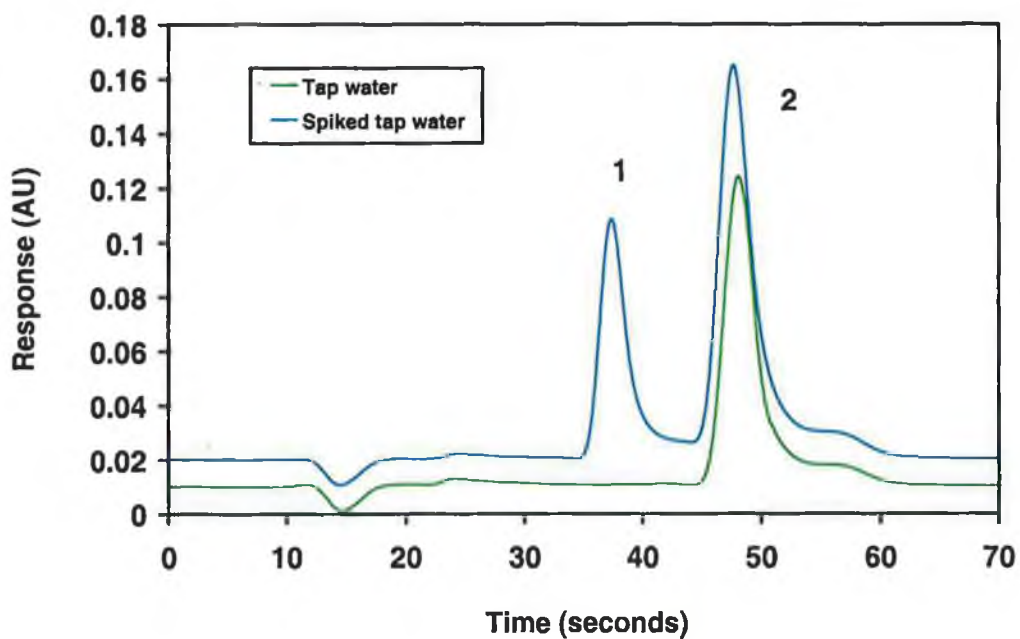


Figure 3-6. Rapid determination of nitrate/nitrite levels in tap water by ion interaction chromatography on a short  $3\ \mu\text{m}\ C_{18}$  column. Chromatographic conditions are as in Figure 3-4. Peaks: [1] nitrite, [2] nitrate.

The rapid separation of nitrate and nitrite compares well with similar chromatography developed by Maiti *et al.* [24] who separated both anions using a 25 cm X 4.6 mm I.D. 5  $\mu$ m Zorbax ODS column and a mobile phase of acetonitrile/water (35/65); 2 mM cetylpyridinium bromide and 10 mM phosphate buffer with direct UV detection at 222 nm. However, runtimes were over six times longer than this current work, with retention times of 4.6 minutes and 5.6 minutes for nitrite and nitrate.

### 3.3.2 On-line determination of nitrate and nitrite in drinking water.

The determination of nitrate and nitrite in both natural waters and treated drinking waters is one of the most common analyses carried out on a daily basis by water treatment companies and environmental agencies, often on large numbers of individual samples. The advantage of instrumental methods based upon either FIA or IC is that either can (i) be used with an auto-sampler when dealing with large numbers of samples or (ii) be readily configured to run on-line and monitor a flowing sample stream. In this study, simultaneous determination of nitrate and nitrite has been shown to be possible in the same time range as that of traditional FIA techniques, and offers a clear advantage in terms of reduced sample-handling time, and simplified instrumentation, with conventional HPLC equipment used throughout.

An example of high sample throughput is the high speed analysis developed by Heinig and Henion [25] who detailed an IC-MS-MS analysis of five benzodiazepines in human urine in under 15 seconds. The feasibility of injecting 240 samples per hour was investigated by filling a 10 mL syringe pump with urine extract and pumping at a rate of 120  $\mu$ L/min to keep the 5  $\mu$ L sample loop filled at all times. This allowed injections to be made automatically at discrete time intervals via a programmable Rheodyne valve.

In this work a similar experimental setup is detailed. Basic IC equipment, incorporating the above fast ion-interaction chromatography, was set-up to continuously sample and analyze, unattended, a dynamic flowing drinking water stream. The system was configured as shown in Figure 3-7. Tap water was allowed to flow into the sink, at

the base of which; a turbulent pool of water (described hereafter as the "sample reservoir") drained to waste. The peristaltic pump was used to deliver a continuous sample stream from this reservoir, to the injection loop such that the loop was constantly filled when in the "load" position. Sample preparation prior to injection was by means of a simple swinny syringe filter assembly, fitted with 0.45  $\mu\text{m}$  nylon membrane filter and positioned in the sample flow path just before the Rheodyne injection valve assembly. The software controlling the chromatographic system was configured to inject a sample every 60 seconds, beginning data acquisition at time = 0 seconds and switching the injection loop back to the "load" position at time = 30 seconds, such that the next sample could be injected. The injection valve was connected in such a way as to allow the injection of standard solutions at any desired point within the sampling period for system calibration.

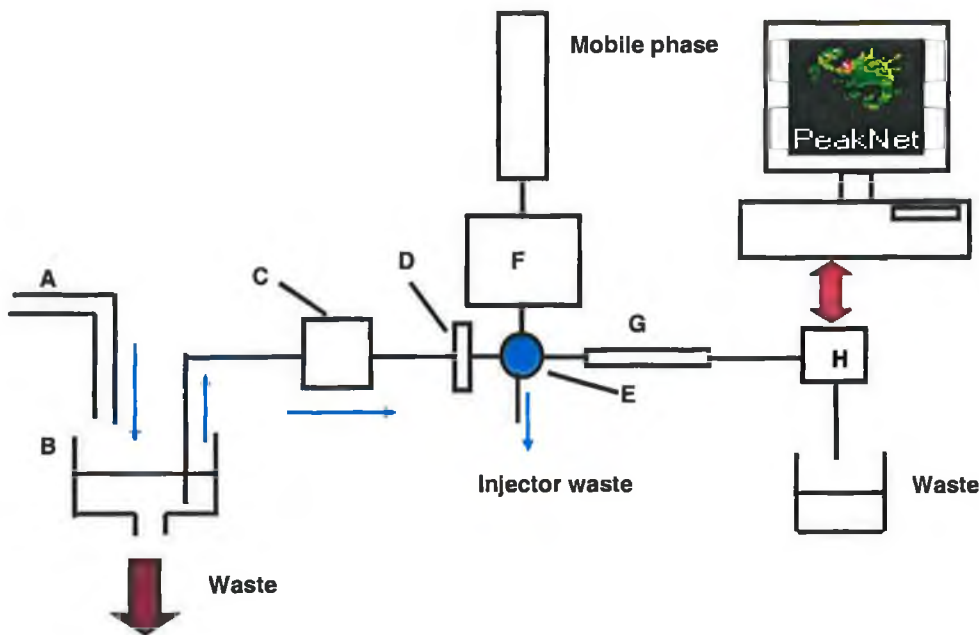


**Figure 3-7.** Instrumental set-up for online analysis of tap water by fast ion interaction chromatography. Key: A (tap), B (reservoir/sink), C (peristaltic pump), D (membrane filter), E (automated Rheodyne valve), F (HPLC pump), G (analytical column), H (UV-Vis detector).

To test the performance of the system it was left to monitor the drinking water stream unattended for an hour, analysing a total of 60 discrete samples. During this trial

period both nitrite and nitrate were crudely added to the dynamic sample reservoir to test the response of the system to rapid changes in the concentrations of the two analytes. Nitrite was added at 20 minutes and nitrate added at 40 minutes. The sample stream was also sampled at 10 minute intervals for comparative analyses (see Section 3.3.3.5). Figure 3-8 illustrates the results of this trial, showing the concentrations of nitrate and nitrite against sampling time. Each point represents an analyte concentration determined from each of the 60 individual chromatograms. As would be expected from a single tap water supply, the concentrations of the two analytes did not vary significantly over the 1 hour period. There was no detectable nitrite, and the nitrate concentration was steady at between 7.5 and 8.0 mg/L. However, the two points at which the sample stream was spiked with nitrite and nitrate can be clearly seen. The system responds rapidly to real-time changes in concentration and equally rapidly returns to the original concentrations, illustrating how such a system would identify short-term concentration changes that could otherwise be missed.

For example, a similar set up was employed by Gabriel *et al.* [8] who used an unattended FIA manifold to continuously sample and analyze samples for nitrate and nitrite from biological reactors in a waste water treatment plant. The FIA manifold incorporated the Griess reaction and a copperized cadmium reductor column for conversion of nitrate to nitrite. A small portion of filtered sample was fed into the FIA manifold while the rest was fed back into the reactor. The maximum unattended deployment time was four days to refill the carrier reservoir, and the filtration devices had to be cleaned every eight days.

Gabriel *et al.* observed that if a plant operates correctly, then its nitrite concentration rarely reaches 1 mg/L. However, an excessive load of ammonium inhibits the biological oxidation of nitrite to nitrate so that the former may build up in the reactor at concentrations well above the usual levels. During validation of the system, this process was modeled by monitoring the response of the system to a sudden increase in the concentration of ammonium, demonstrating that the system could successfully monitor online, the dynamics of a waste water treatment plant over time. The results

allowed real-time control of the plant in order to maximize the removal of ammonium nitrogen and to avoid operating problems that would be detected with considerable delay at an unmonitored plant.

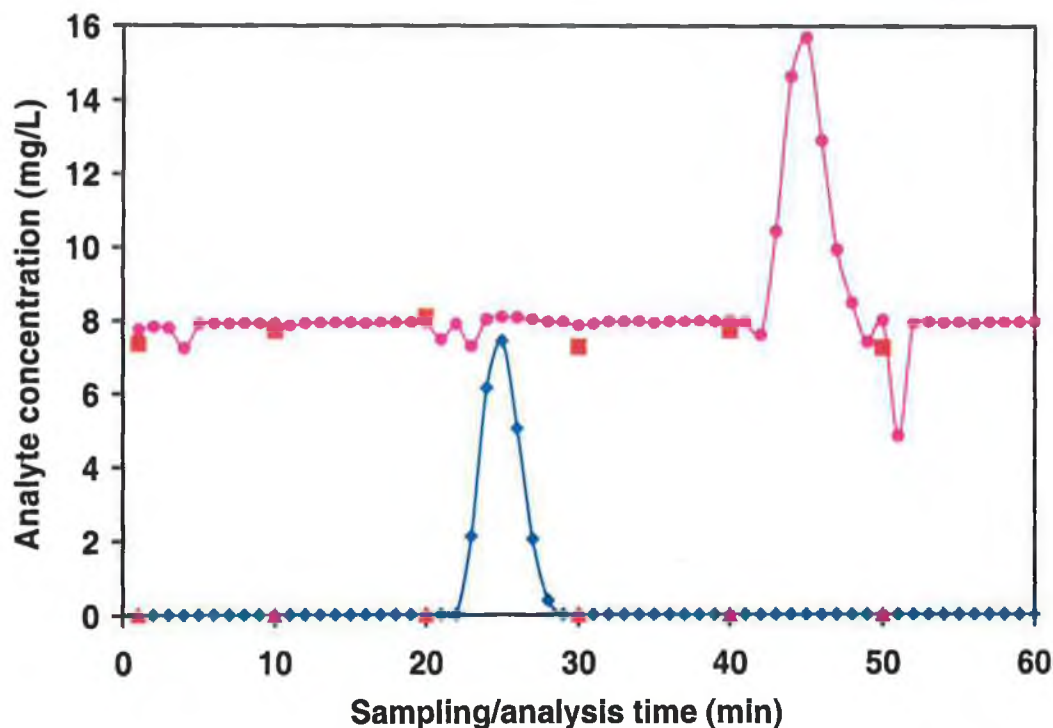
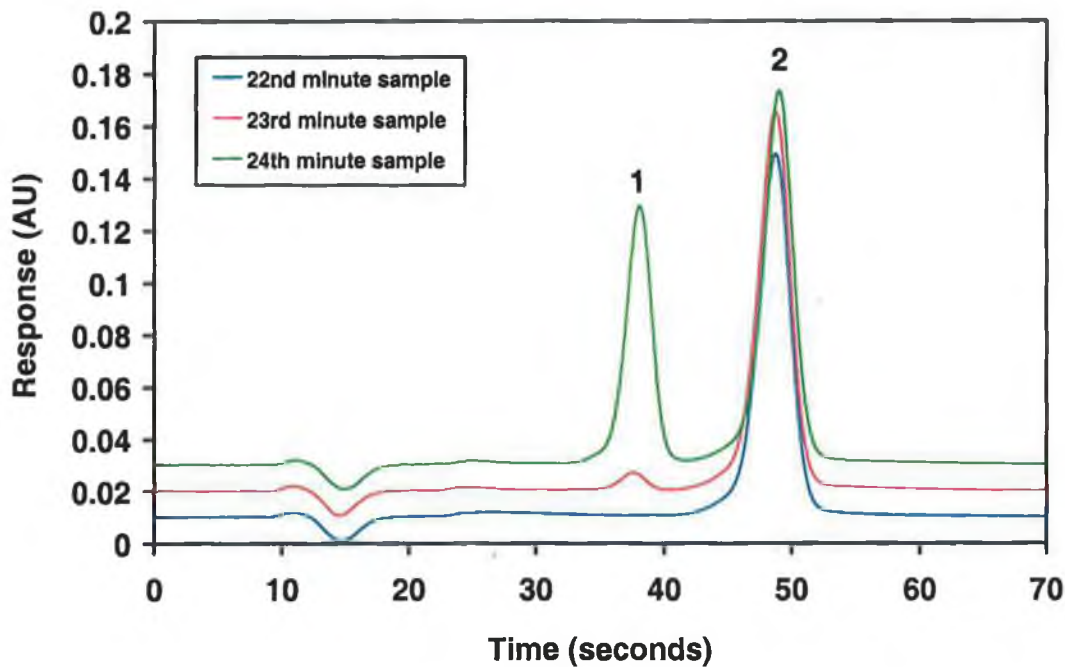


Figure 3-8. Plot of nitrate and nitrite concentration versus sampling/analysis time. (• = nitrate, ◆ = nitrite, ■ = nitrate determination by ion-exchange, ▲ = nitrite determination by ion-exchange. Chromatographic conditions are as in Figure 3-4.

Typical chromatograms obtained during the above on-line trial can be seen in Figure 3-9. Here, three chromatograms are overlaid, showing the concentrations of nitrite and nitrate present in the three samples taken at time 22, 23 and 24 minutes. As can be seen from the chromatograms shown, the tap water samples resulted in no interfering peaks from other matrix anions such as chloride and sulphate, and even after 60 consecutive injections there was no sign of any interfering peaks that may have been retained for longer. The two peaks are also well resolved from both each other and a small system peak that elutes at 0.4 minutes, with the signal clearly returning to baseline well before 1 minute is up.



**Figure 3-9.** *Overlay of chromatograms collected 22, 23 and 24 minutes into the sampling period. There is a clear increase in nitrite concentration due to the crude nitrite spike added to the sampling reservoir. Chromatographic conditions are as in Figure 3-4. Peaks: [1] nitrite, [2] nitrate.*

In terms of sample rate per hour the fast ion-interaction method detailed here compares very favourably with the current range of analytical methods available for simultaneous nitrite and nitrate determinations. Table 3-1 shows some of the most recent methods published for nitrate and nitrite determinations and their maximum sample throughput per hour. As can be seen from the table, the developed fast ion-interaction method can analyze more samples per hour than the FIA based methods and matches the rate of the ultra-rapid CE method developed by Melanson and Lucy [19] However, the method described here has the added advantage in that it can be used to monitor flowing sample streams.

**Table 3-1.** Comparison of sample throughput for the analysis of nitrate and nitrite for various instrumental analytical methodologies.

<b>Technique</b>	<b>Sample throughput (samples/hour)</b>	<b>Reference.</b>
<b>FIA</b>	22	[6]
	30	[7]
	40	[4]
<b>CZE</b>	10	[18]
	60	[19]
<b>IC</b>	4	[26]
	7.5	[27]
<b>Fast IC (this work)</b>	60	

### 3.3.3 Analytical performance characteristics.

#### 3.3.3.1 System precision.

To determine system precision, a single homogenous tap water sample containing a slightly lower concentration of nitrate (3.9 mg/L) was taken and put in place of the flowing sample reservoir. This single sample was then repeatedly injected 30 times. The results obtained are shown as Figure 3-10. As can be seen the method proved highly reproducible, with the system precision being 0.53 % for peak area (shown as nitrate concentration) and 0.42 % for peak retention time. Therefore, if for monitoring purposes the “minimum quantifiable change” (MQC) is defined as ten times the % RSD, at the above sample concentration, changes as small as  $\pm 0.2$  mg/L could be quantifiably identified. The highly reproducible peak retention time is also essential for monitoring purposes as it allows the software to accurately identify and integrate the peak automatically, thus permitting the use of ‘real time’ trending software to be used in monitoring applications.

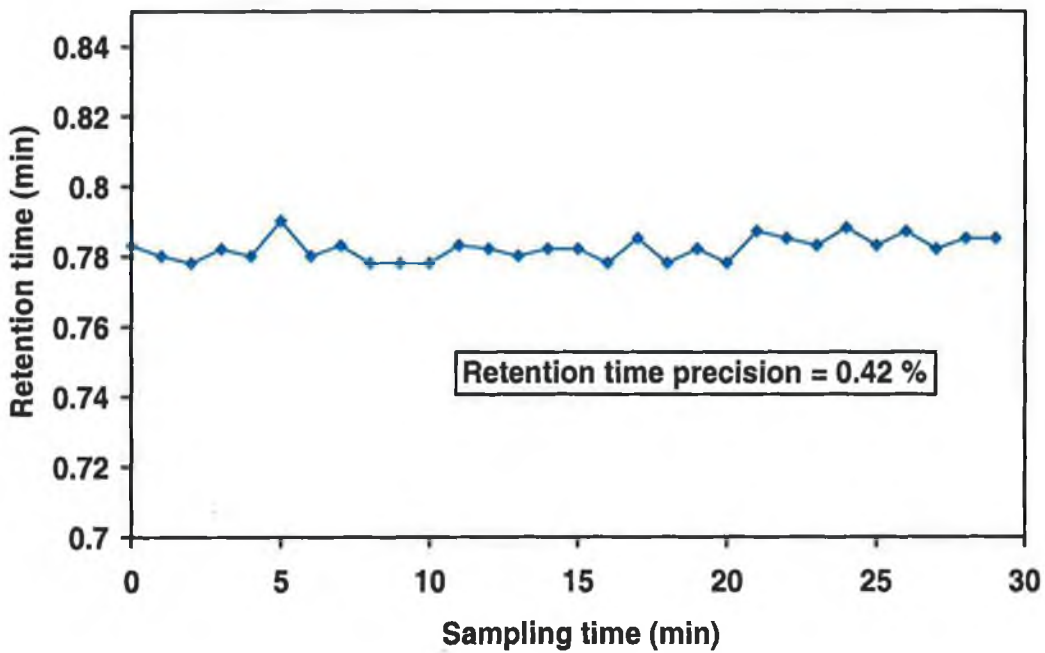
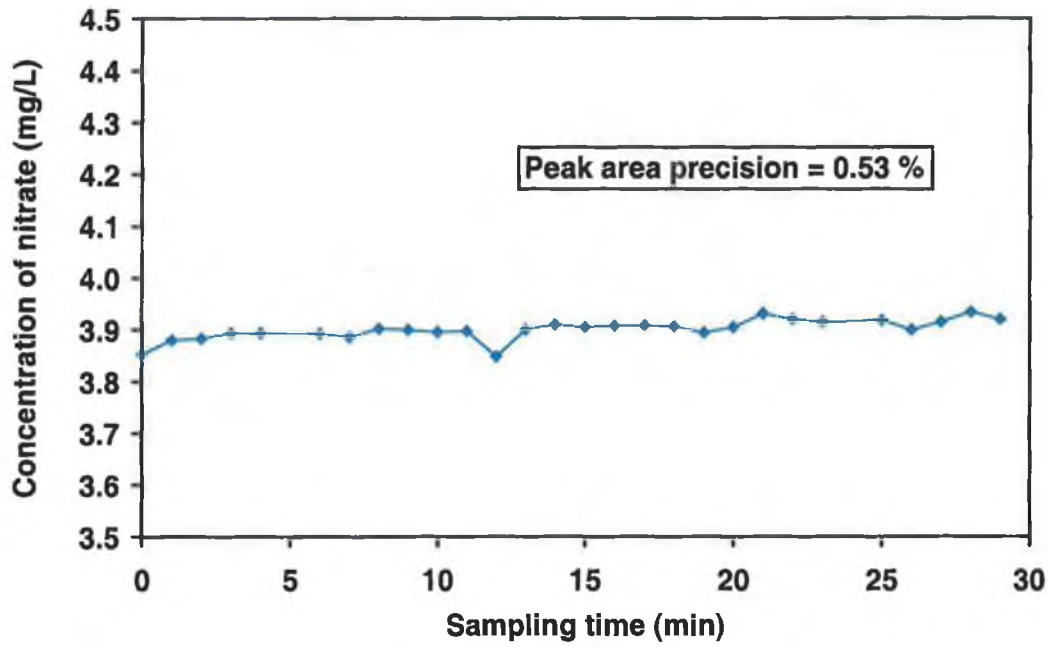


Figure 3-10. Determination of system precision by thirty consecutive injections of a 3.9 mg/L nitrate standard. The upper figure represents area precision and the lower figure represents retention time precision. Chromatographic conditions are as in Figure 3-4.

### 3.3.3.2 Detector linearity.

Detector linearity was investigated in two ways. The method was checked for linearity and found to be linear over the concentration range of interest for both nitrite and nitrate (four standards were prepared in the range 1.0 mg/L – 25.0 mg/L),  $R^2 > 0.9990$  for nitrite and  $R^2 > 0.9980$  nitrate, (n=3).

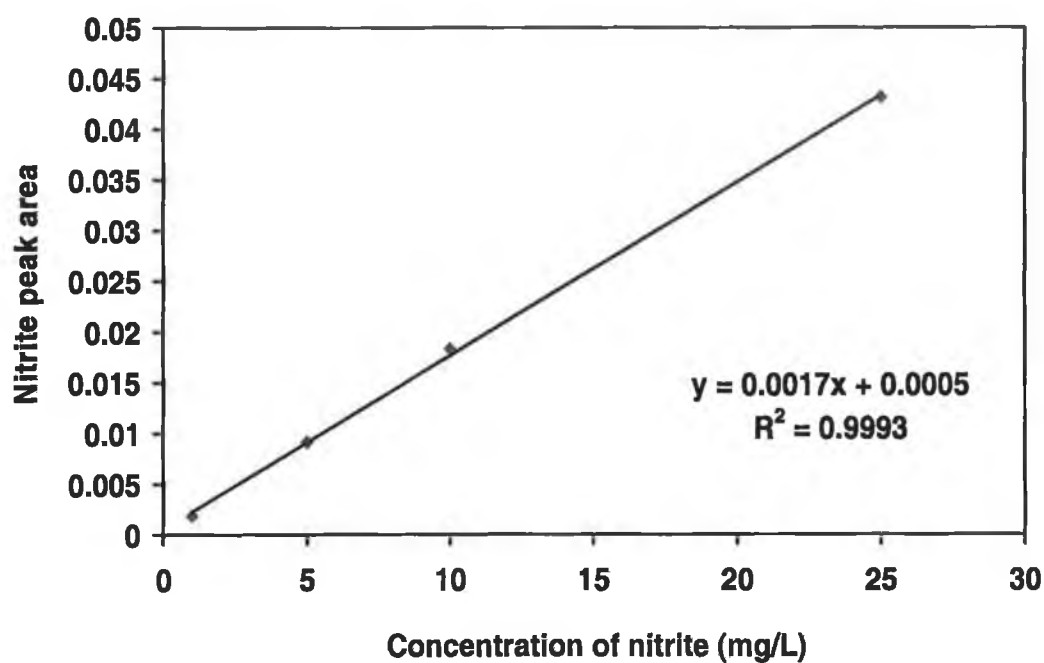


Figure 3-11. Linearity study for nitrite by fast ion interaction chromatography.

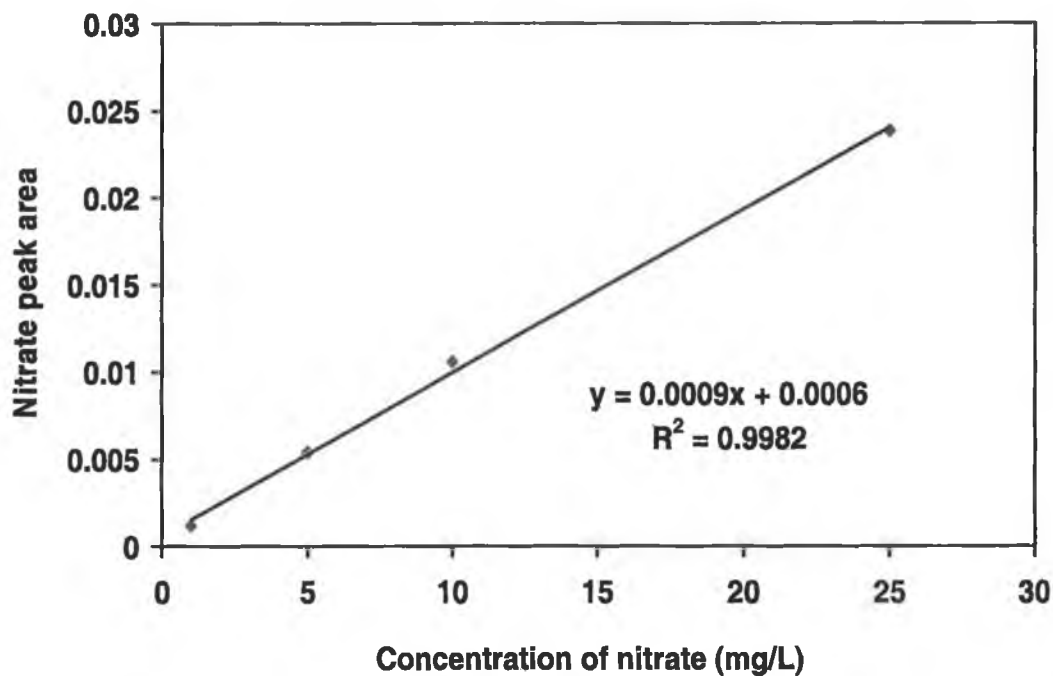


Figure 3-12. Linearity study for nitrate by fast ion interaction chromatography.

Secondly, as is likely to be the case in most water samples, the linearity of trace nitrite in the presence of excess nitrate was determined. A real tap water sample containing 5 mg/L nitrate was spiked with 20, 40, 100 and 200  $\mu\text{g/L}$  nitrite. The linearity for nitrite in the above sample was again  $R^2 > 0.9999$  ( $n = 3$ ).

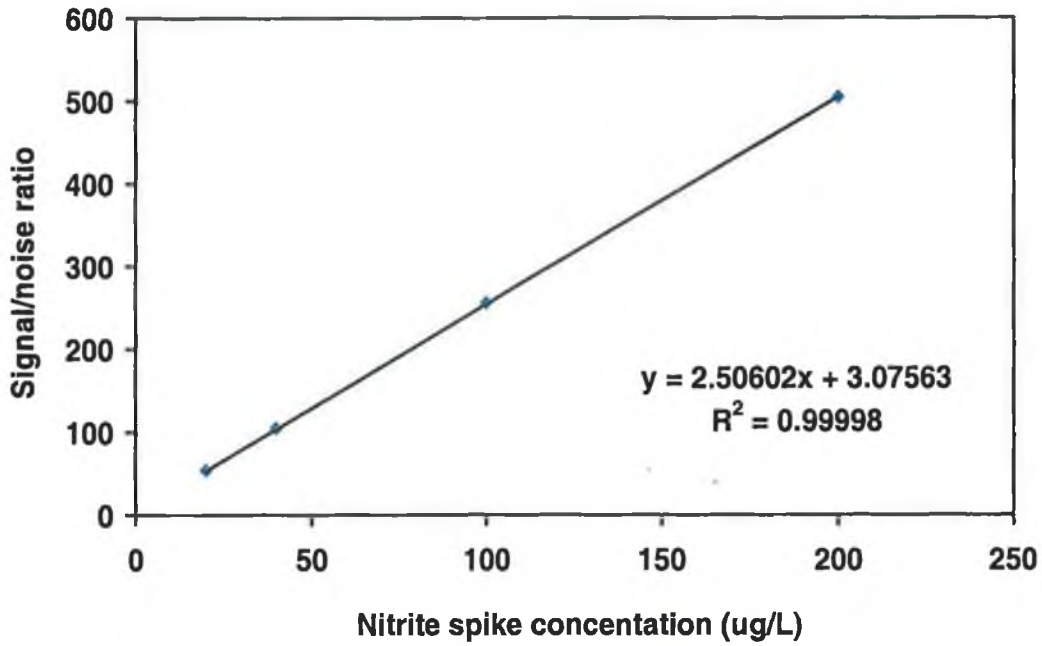


Figure 3-13. Linearity study for  $\mu\text{g/L}$  nitrite spikes in a 5 mg/L nitrate matrix by fast ion interaction chromatography.

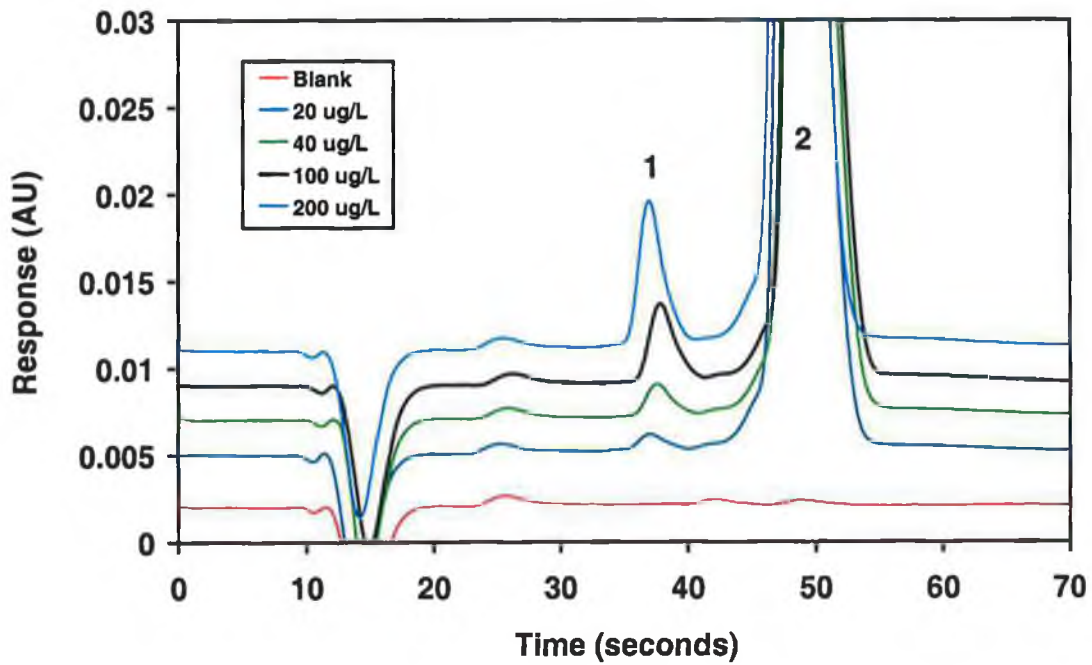
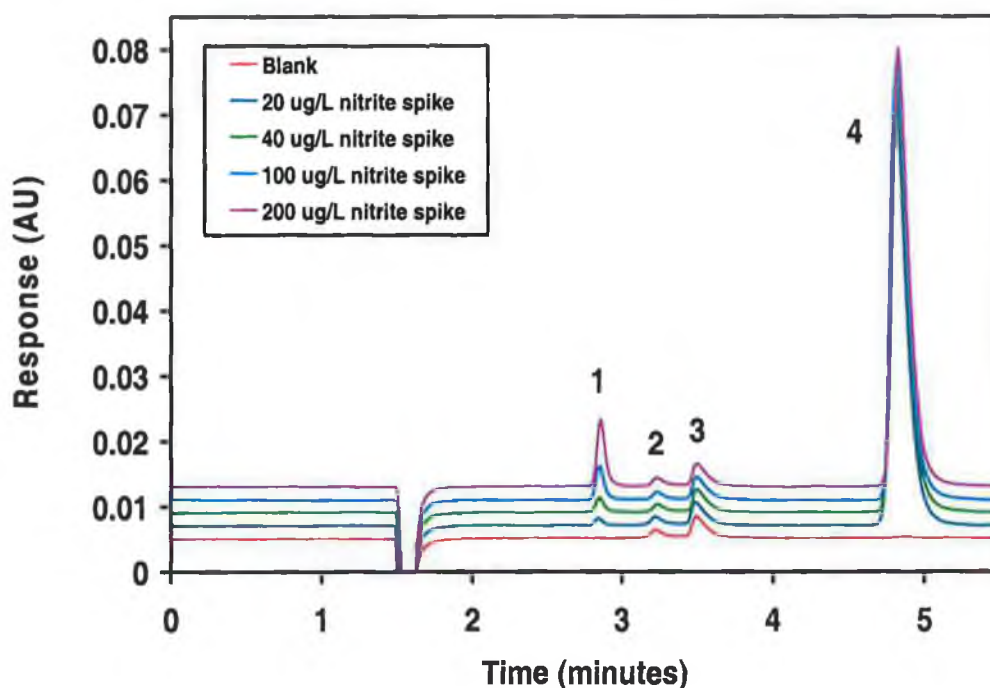


Figure 3-14. Overlay of  $\mu\text{g/L}$  nitrite spikes in a 5 mg/L nitrate matrix by fast ion interaction chromatography. Chromatographic conditions are as in Figure 3-4. Peaks: [1] nitrite, [2] nitrate.

Figure 3-14 shows the overlaid chromatograms obtained from the injections of the above spiked samples. Also shown in Figure 3-15 are chromatograms obtained for the above spiked samples using a conventional size AS17 anion exchange column with a hydroxide eluent. As can be seen from the chromatograms shown, even at such high ratios nitrite is still well resolved from the nitrate peak and the separation is complete is less than  $1/5^{\text{th}}$  the time of the conventional column. In terms of efficiency, the short column method also compares favourably with the conventional column, with an average of 63,100 plates/m compared to 53,540 plates/m respectively.



**Figure 3-15.** Overlay of  $\mu\text{g/L}$  nitrite spikes in a  $5 \text{ mg/L}$  nitrate matrix on a  $25 \text{ cm}$  anion exchange column. Chromatographic conditions: Column: Dionex AS17  $25 \text{ cm} \times 4.6 \text{ mm}$ , Eluent:  $15 \text{ mM NaOH}$ , Flow rate:  $1.0 \text{ ml/min.}$ , Loop size:  $50 \mu\text{L}$ , Detection wavelength:  $227 \text{ nm}$ . Peaks: [1] nitrite, [2,3] impurities in laboratory water, [4] nitrate.

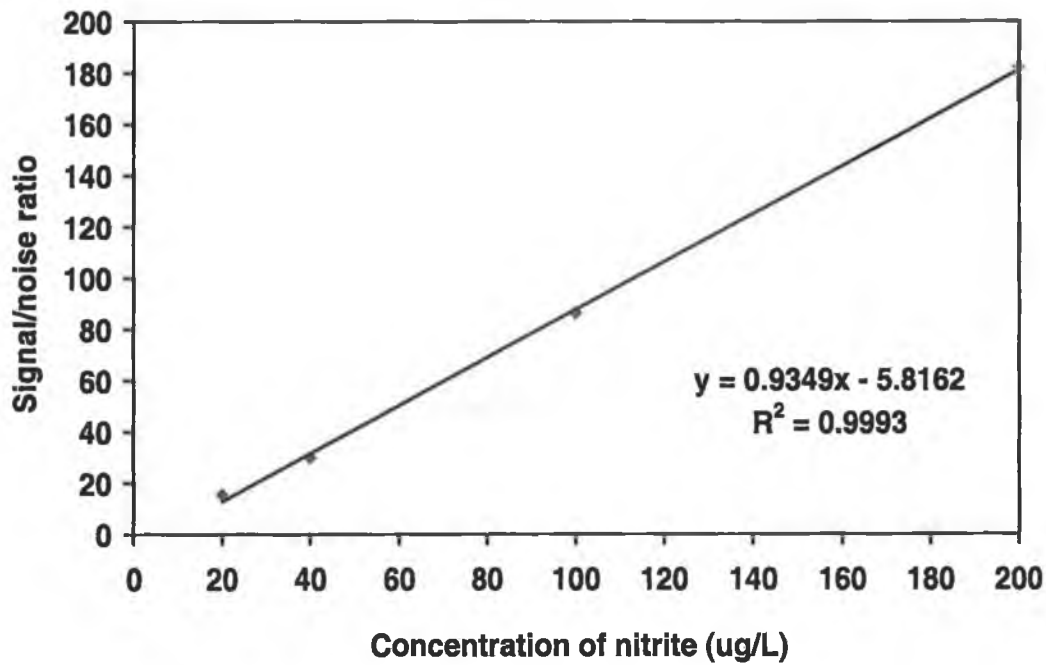


Figure 3-16. Linearity study for  $\mu\text{g/L}$  nitrite spikes in a 5 mg/L nitrate matrix on a conventional (25 cm) anion exchange column. Conditions as in Figure 3-15.

### 3.3.3.3 Sensitivity.

To increase method sensitivity the injection volume had been increased to 50  $\mu\text{L}$  (see Figure 3-4). Despite this rather large injection volume, particularly for such a short column, neither peaks shapes or resolution were noticeably affected.

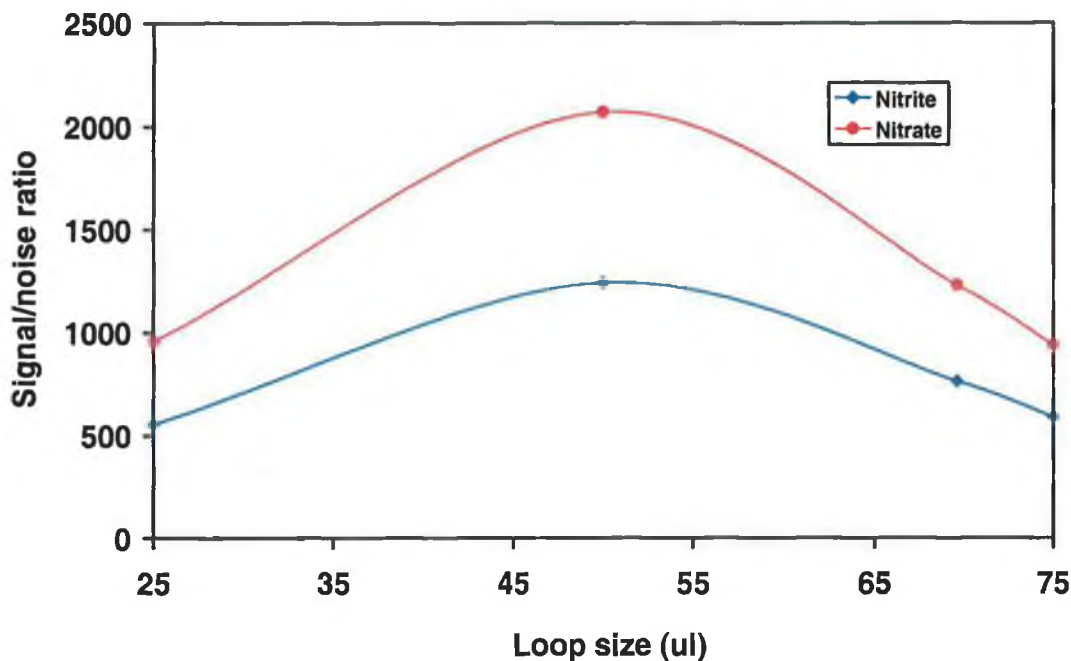


Figure 3-17. Optimization of injection volume for the determination of nitrate and nitrite by fast ion interaction chromatography. Conditions as in Figure 3-4.

Detection limits were calculated using peak height equivalent to three times the baseline noise and found to be  $3 \mu\text{g/L}$  for nitrite and  $7 \mu\text{g/L}$  for nitrate. Absolute detection limits were  $0.15 \text{ ng}$  and  $0.35 \text{ ng}$  (based upon  $50 \mu\text{L}$  injection volume and an S/N ratio of three). The nitrate detection limit was slightly higher due to the present of a small system peak which partially co-eluted with nitrate and made integration difficult at concentrations  $< 10 \mu\text{g/L}$ . However, detection limits were low enough for the method to be useful for the monitoring of drinking water and freshwater samples, and are comparable to those obtained by the USEPA Method 300.1<sup>4</sup> which uses anion-exchange chromatography with suppressed conductivity detection ( $1 \mu\text{g/L}$  for nitrite and  $8 \mu\text{g/L}$  for nitrate)

Figure 3-18 and Figure 3-19 shows the two sets of chromatograms obtained for standard solutions of nitrite ( $25 \mu\text{g/L}$ ) and nitrate ( $25 \mu\text{g/L}$ ) at concentrations close to the method detection limits. The two sets of chromatograms show how the sensitivities of

the two methods were very similar, with the peak heights for 25  $\mu\text{g/L}$  nitrite equal to  $1.2 \times 10^{-3}$  AU using the fast ion-interaction method and  $1.3 \times 10^{-3}$  AU using the conventional anion exchange method.

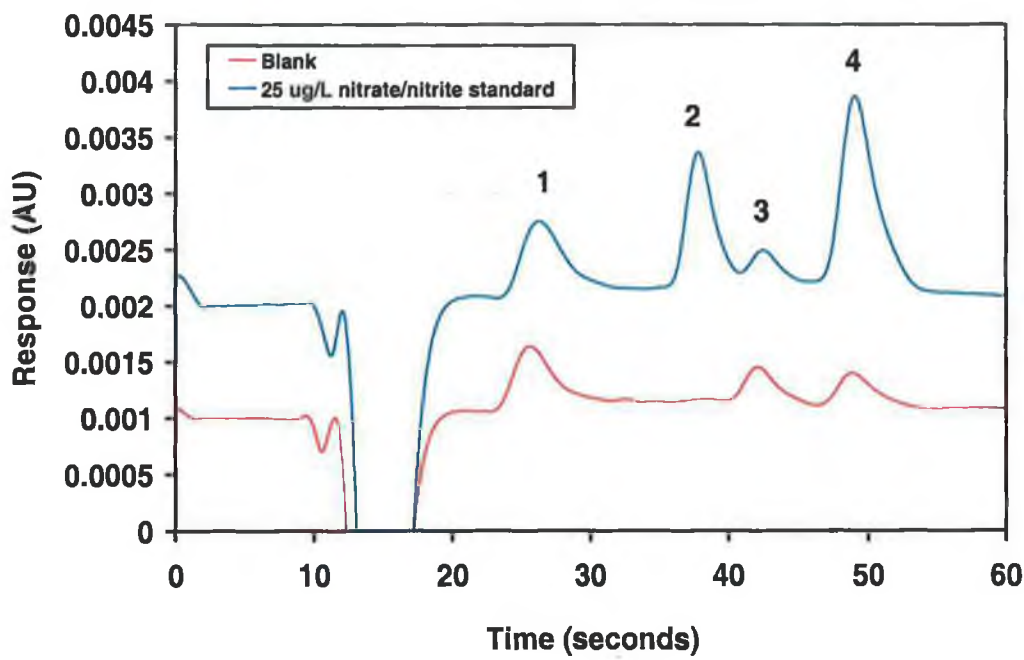
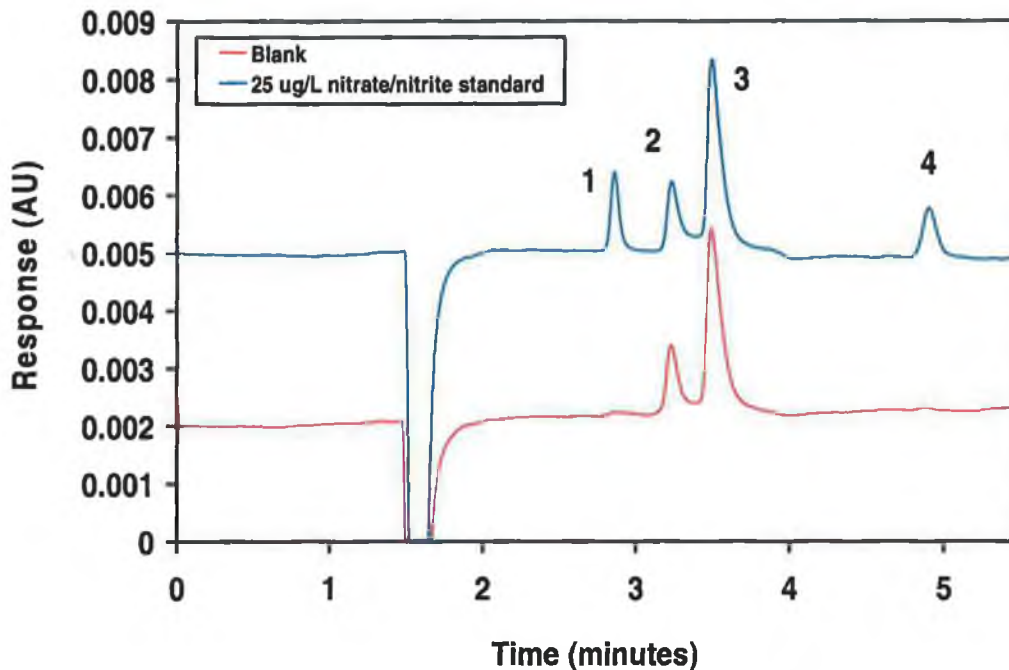


Figure 3-18. Chromatogram showing overlays of a blank, with a standard containing 25  $\mu\text{g/L}$  nitrate and nitrite determined by fast ion-interaction chromatography. Chromatographic conditions are as in Figure 3-4. Peaks: [1,3] system peaks, [2] nitrite, [4] nitrate.

<sup>4</sup> Method 300.1 "Determination of inorganic anions in drinking water by ion chromatography".



**Figure 3-19.** Chromatogram showing overlays of a blank, with a standard containing 25 µg/L nitrate and nitrite determined by anion exchange chromatography. Conditions as in Figure 3-15. Peaks: [1] nitrite, [2,3] unidentified impurities in laboratory water, [4] nitrate.

#### 3.3.3.4 Interferences.

Possible interferences were also investigated. Common anions that gave no detector response and also had no effect upon the chromatography (at concentrations expected in drinking waters) included, chloride, sulphate, phosphate, formate and acetate. Less common UV absorbing anions which were retained and did give a detector response but were baseline resolved from the nitrite and nitrate peaks included, iodate (0.40 min), bromate (0.54 min), bromide (0.67 min), iodide (3.1 min), thiocyanate (~3.5 min), thiosulphate (~5.0 min) and benzoate (~8.5 min). Of the above only bromide may be expected to be present in drinking water but at concentrations well below that of nitrate.

### 3.3.3.5 System accuracy/comparative analysis.

Finally, to determine accuracy, the samples taken during the on-line trial were analysed by a conventional anion exchange method for nitrite and nitrate concentration. The column used was a 25 cm AS17 anion exchange column, with 15 mM NaOH used as eluent. The flow rate was 1.0 ml/min, with a loop volume of 50  $\mu$ L. Initially, suppressed conductivity detection was used, and a good separation of chloride, bromide, nitrate, nitrite, sulphate and phosphate was achieved. However, since it was only necessary to determine nitrate and nitrate for the purposes of validation of the online flow work; and since the runtime of 35 minutes was quite long, direct UV detection was subsequently used. This resulted in no interference from other non-UV absorbing anions, likely to be present in the samples, such as chloride, sulphate, carbonate, and phosphate.

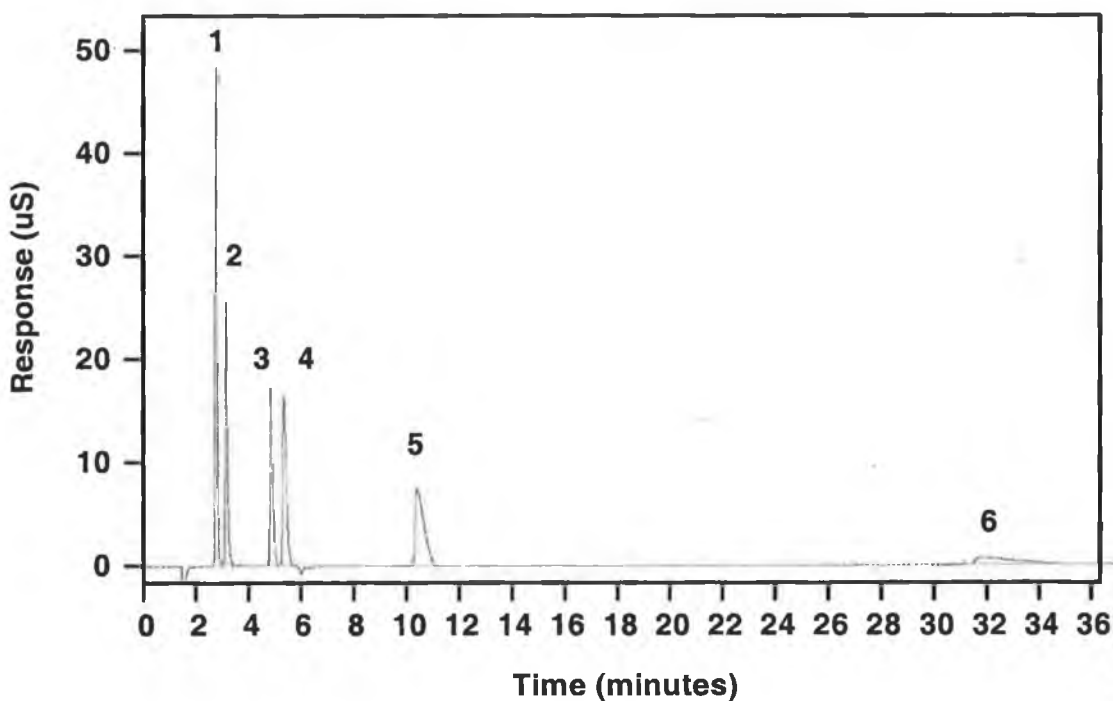


**Figure 3-20.** Separation of common inorganic anions by anion exchange chromatography with suppressed conductivity detection. Chromatographic conditions: Column: Dionex AS17 25 cm X 4.6 mm, Eluent: 15 mM NaOH, Flow rate: 1.0 ml/min., Loop size: 50  $\mu$ L, Detection: Suppressed conductivity at 100 mA in the recycling mode. Peaks: [1] chloride, [2] nitrite, [3] bromide, [4] nitrate, [5] sulphate, [6] phosphate.

The optimum detection wavelength was determined by injecting a 5 mg/L nitrate/nitrite standard over a range of wavelengths and plotting the signal to noise ratio for both anions against the wavelength. A detection wavelength of 227 nm was considered optimum.

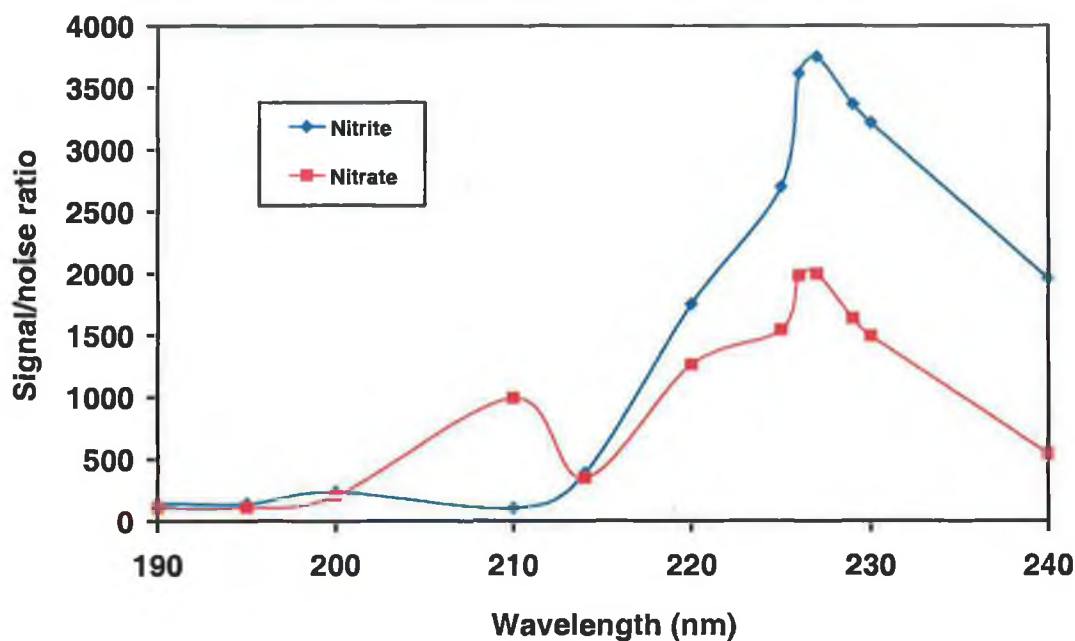
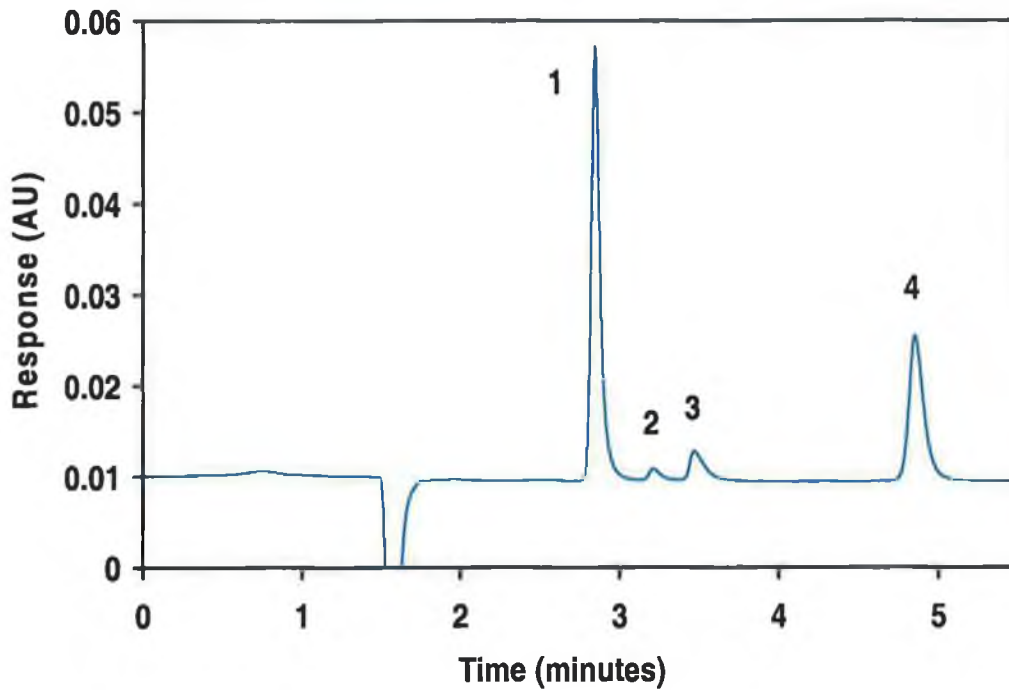


Figure 3-21. Determination of optimum detection wavelength for nitrite/nitrate analysis by anion exchange chromatography. Conditions as in Figure 3-15.

Validation of this anion exchange method involved determination of system precision, by using six consecutive injections of a 1 mg/L nitrate/nitrite standard. System precision for peak area was 2.85 % for nitrite, and 1.82 % for nitrate. System precision for retention times was 0.21 % for nitrite and 0.20 % for nitrate.



**Figure 3-22.** Separation of 1.0 mg/L nitrate and nitrite by anion exchange chromatography. Chromatographic conditions as in Figure 3-15. Peaks: [1] nitrite, [2,3] system peaks, [4] nitrate.

Figure 3-22 illustrates the optimum anion exchange separation of a 1 mg/L nitrate/nitrite standard. The method was checked for linearity and found to be linear over the concentration range of interest for both nitrite and nitrate (four standards were prepared in the range 1.0 mg/L – 25.0 mg/L),  $R^2 > 0.9993$  for nitrite and  $R^2 > 0.9999$  nitrate.

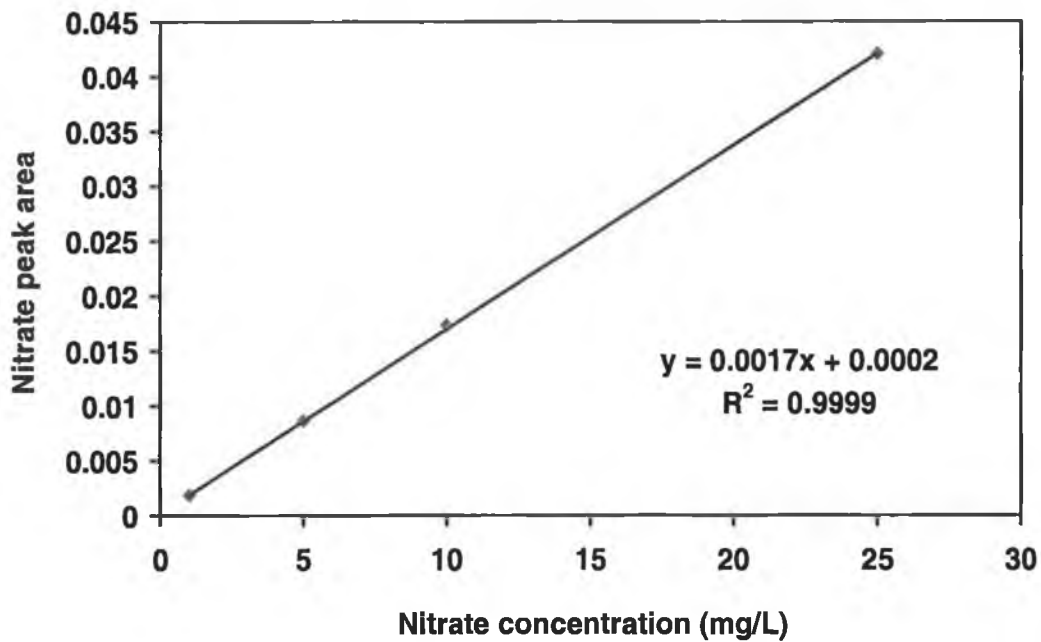


Figure 3-23. Linearity of nitrate on an anion exchange AS17 column.

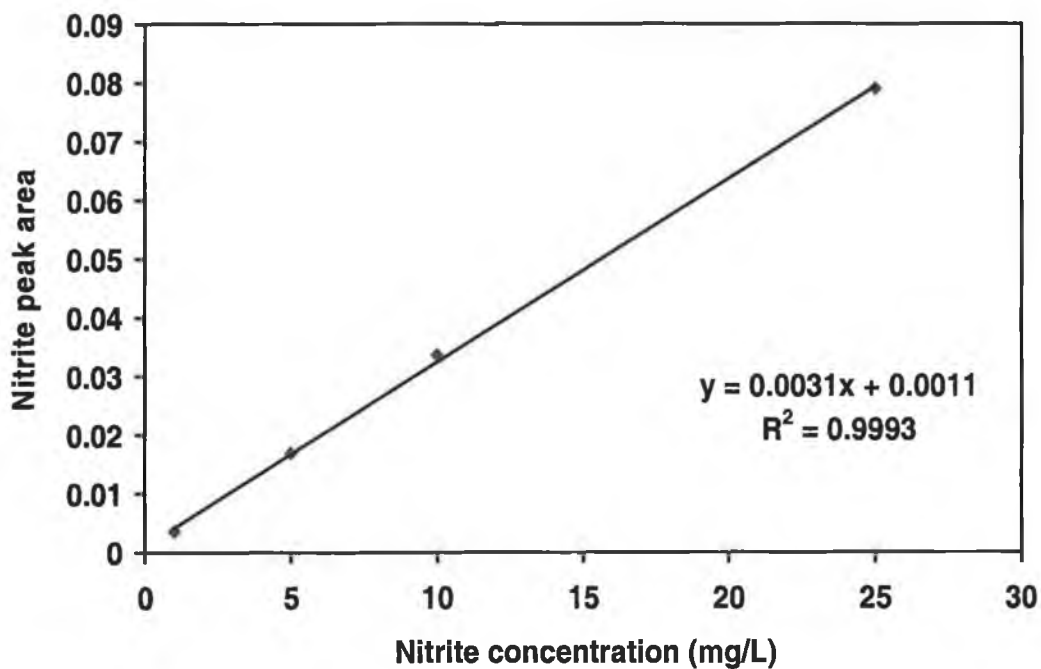
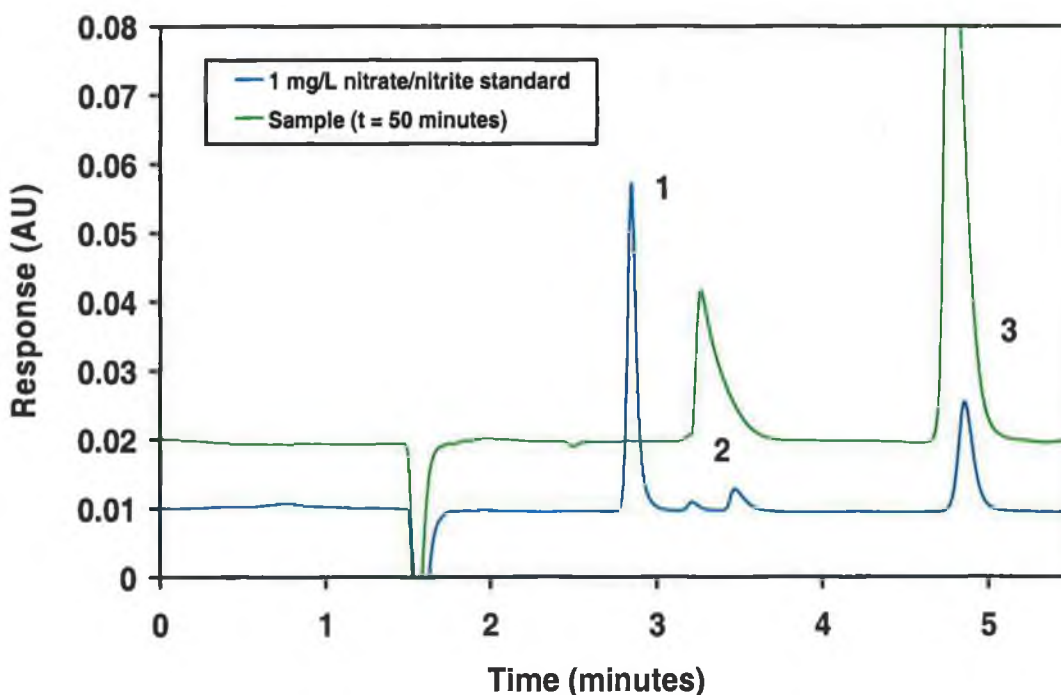


Figure 3-24. Linearity of nitrite on an anion exchange AS17 column.

Figure 3-25 below, shows the determination of nitrate and nitrite in the validation sample collected after 50 minutes. As seen with the on-line ion-interaction method (Figure 3-8), no nitrite was present in any of the 6 samples taken. However, the concentration of nitrate found matched that determined using ion-interaction extremely well. The concentrations determined for nitrate using the two methods were found to be within 1 and 5 % of each other, with the concentrations found using the conventional anion exchange method plotted as individual points within Figure 3-8. Clearly, the method described herein can respond more rapidly to sudden changes in analyte concentration relative to conventional methods. These traditional methods involve longer runtimes and therefore, more widely spaced sampling intervals are more practical, such that such rapid spikes may go undetected.



**Figure 3-25.** Overlay of the analysis of a validation sample taken at 50 minutes with a 1 mg/L nitrate and nitrite standard, on a 25 cm anion exchange column. Chromatographic conditions as in Figure 3-15. Peaks: [1] nitrite, [2] system peaks, [3] nitrate.

### 3.4 Conclusions.

A simple ion-interaction chromatographic method for the fast determination of nitrite and nitrate at trace concentrations in water samples has been developed. Using a short 3.0 cm x 4.6 mm 3  $\mu\text{m}$  ODS analytical column together with a mobile phase containing 20 mM of the ion-interaction reagent tetrabutylammonium chloride (TBA-Cl), nitrite and nitrate have been readily separated from each other and other common UV absorbing anions in under 50 sec. The method was briefly applied to the rapid analysis of river water and tap water samples for nitrate and nitrite determinations. With the addition of a peristaltic pump and in-line filter, the developed method was subsequently configured for continuous monitoring of nitrate and nitrite concentrations in tap water. Up to 60 analyses per hour could be carried out using the on-line system, which matches the analysis rate possible with traditional FIA based methods. Standard analytical performance criteria were evaluated with detection limits of 3  $\mu\text{g/L}$  and 7  $\mu\text{g/L}$  obtained for nitrite and nitrate respectively. Results obtained using the fast ion-interaction method compared well to those obtained using a conventional ion chromatographic method.

### 3.5 References.

- [1]. K. Horita, G. Wang, M. Satake, *Anal. Chim. Acta.* 350 (1997) 295.
- [2]. R.T. Masserini Jr., K.A. Fanning, *Marine Chem.* 68 (2000) 323.
- [3]. M. Jimidar, C. Hartmann, N. Cousement, D.L. Massart, *J. Chromatogr. A* 706 (1995) 479.
- [4]. O. Pinho, I.M.P.L.V.O. Ferreira, M. Beatriz, P.P. Oliveira, M.A. Ferreira, *Food. Chem.* 62 (1998) 359.
- [5]. P.A. Marshall, V.C. Trenerry, *Food Chem.* 57 (1996) 339.
- [6]. A. Kojlo, E. Gorodkiewicz, *Anal. Chim. Acta.* 302 (1995) 283.
- [7]. M.J. Ahmed, C.D. Stalikas, S.M. Tzouwara-Karayanni, M.I. Karayannis, *Talanta* 43 (1996) 1009.
- [8]. D. Gabriel, J. Baeza, F. Valero, J. Lafuente, *Anal. Chim. Acta.* 359 (1998) 173.

- [9]. A. Cerda, M.T. Oms, R. Forteza, V. Cerda, *Anal. Chim. Acta.* 371 (1998) 63.
- [10]. P.H. Petsul, G.M. Greenway, S.J. Haswell, *Anal. Chim. Acta.* 428 (2001) 155.
- [11]. R.S. Guerrero, C.G. Benito, J.M. Calatayud, *Talanta* 43 (1996) 239.
- [12]. I. Gil Torro, J.V.G. Mateo, J.M. Calatayud, *Anal. Chim. Acta.* 366 (1998) 241.
- [13]. Z. Zhi-Qi, G. Lou-Jun, Z. Han-Ying, L. Qian-Guang, *Anal. Chim. Acta.* 370 (1998) 59.
- [14]. A.A. Ensafi, A. Kazemzadeh, *Anal. Chim. Acta.* 382 (1999) 15.
- [15]. F. Guan, H. Wu, Y. Luo, *J. Chromatogr. A* 719 (1996) 427.
- [16]. A.A. Okemgbo, H.H. Hill, S.G. Metcalf, M.A. Bachelor, *J. Chromatogr. A* 844 (1999) 387.
- [17]. K. Fukushi, K. Tada, S. Takeda, S. Wakida, M. Yamane, K. Higashi, K. Hiroy, *J. Chromatogr. A* 838 (1999) 303.
- [18]. A.A. Okemgbo, H.H. Hill, W.F. Siems, S.G. Metcalf, *Anal. Chem.* 71 (1999) 2725.
- [19]. J.E. Melanson, C.A. Lucy, *J. Chromatogr. A.* 884 (2000) 311.
- [20]. F.G.P. Mullins, G.F. Kirkbright, *Analyst* 109 (1984) 1217.
- [21]. M.C. Gennaro, P.L. Bertolo, A. Cordero, *Anal. Chim. Acta.* 239 (1990) 203.
- [22]. K. Ito, Y. Ariyoshi, F. Tanabiki, H. Sunahara, *Anal. Chem.* 63 (1991) 273.
- [23]. USEPA Method 300.1 "Determination of inorganic anions in drinking water by ion chromatography".
- [24]. B. Maiti, A.P. Walvekar, T.S. Krishnamoorthy, *Analyst* 114 (1989) 731.
- [25]. K. Heinig, J. Henion, *J. Chromatogr. B* 732 (1999) 445.
- [26]. M.N. Muscara, G. de Nucci, *J. Chromatogr. B* 686 (1996) 157.
- [27]. M.I.H. Helaleh, T. Korenaga, *J. Chromatogr. B* 744 (2000) 433.

## **4 Determination of urinary thiocyanate, nitrate and nitrite using fast ion-interaction chromatography.**

### **4.1 Introduction.**

#### 4.1.1 Thiocyanate in biological fluids.

Low concentrations of thiocyanate are usually found in urine, due mainly to the subject's diet. This may be through ingestion of certain vegetables containing glucosinolates (cabbage / turnip etc), or foods that actually contain levels of inorganic thiocyanate such as milk and cheese. Higher levels of thiocyanate are found where thiocyanate has been directly administered to treat thyroid conditions, or where sodium nitroprusside (used as a hypotensive agent) is metabolised to contribute to urinary thiocyanate. At high concentrations, thiocyanate can lead to vertigo and unconsciousness, and as such is an important biochemical parameter to consider when studying such conditions.

However, despite the above natural and medical sources of thiocyanate, the majority of studies based on analysis of this anion in urine have actually been performed due to the usefulness of thiocyanate as an important biomarker for inorganic cyanide [1]. Once absorbed into the body cyanide has a very high affinity for iron in the ferric (trivalent) state, and as such binds to and inhibits the activity of cytochrome oxidase, thereby inhibiting mitochondrial respiration. Renal elimination of low levels of cyanide from the body is accomplished by its conversion to thiocyanate by the enzyme, rhodanese (EC 2.8.1.1), which is found in the mitochondria of liver and kidney cells. Inorganic cyanide (CN<sup>-</sup>) can enter the system in a number of ways, including for example, certain topically applied cosmetics that contain alkyl and arylalkyl-cyanides as fragrance ingredients [2]. There is the possibility that such topically applied cosmetics can undergo percutaneous absorption and possible conversion *in vivo* to inorganic cyanide. Potter and Smith [1] quantified thiocyanate levels in rat urine samples, after oral administration of an organonitrile (benzyl cyanide) which was suspected to release inorganic cyanide and convert to thiocyanate *in vivo*. Results indicated that there was a marked increase in

background levels of urinary thiocyanate after the oral administration of benzyl cyanide, demonstrating that thiocyanate is a useful biomarker for inorganic cyanide.

However, a much more significant source of cyanide to the body is tobacco smoke. Increased levels of thiocyanate are therefore mainly present in the human body as a metabolic degradation product of compounds in tobacco smoke that contain cyanide. Chinaka *et al.* [2] found that the concentrations of inorganic cyanide in blood were not very different between smokers and non-smokers. However, thiocyanate concentrations in the blood of smokers (mean, 3.2 mg/L) were clearly higher than they were in the blood of non-smokers (mean, 0.6 mg/L). The blood samples from smokers were taken 30-60 minutes after smoking, and the results indicate that the cyanide from cigarette smoke is immediately metabolised to thiocyanate in vivo. Michigami *et al.* [3] found that serum levels of thiocyanate was up to seven times higher in smokers than that of non-smokers.

It should be noted, however, that when cyanide exposure exceeds the cyanide-to-thiocyanate conversion rate, other metabolic pathways of cyanide come in to play, resulting in the formation of other cyanide metabolites such as 2-aminothiazoline-4-carboxylic acid [2]. Also, the thiocyanate produced by the rhodanese-catalysed reaction can undergo other fates besides renal elimination such that recovery figures for thiocyanate from urine would need to be amended. Nevertheless, many studies have demonstrated the usefulness of urinary thiocyanate as an important biomarker for the generation of inorganic cyanide in the body. Since tobacco smoke has been shown to be a major contributor to production of cyanide in vivo, levels of urinary thiocyanate can be used to distinguish between smokers and non-smokers and to effectively evaluate and characterise smoking behaviour [4-8].

Thiocyanate has been determined in a range of biological samples (blood, serum, urine and saliva) by a number of analytical methodologies. Spectrophotometric methods based on the formation of a highly coloured product have been reported. Bendtsen and Hansen [9] reported the reaction of thiocyanate with 2-(5-bromo-2-pyridylazo)-5-diethylaminophenol, which, in an acidic medium in the presence of the strong oxidising agent, dichromate, produced an intensely coloured product. Since the reaction product formed was unstable, flow injection

analysis was used to monitor the kinetically transient signal that was obtained. The detection limit of the method was found to be 203  $\mu\text{g/L}$ , with no significant interferences observed, even with a 1000-fold excess of inorganic cyanide. The rapid reaction time allowed a sampling rate of 60 samples/hour, and the method was successfully applied to the determination of thiocyanate in saliva samples, in which a clear difference was noted between smokers and non-smokers.

Ensafi and Tajebakhsh-E-Ardakany [6] developed a spectrophotometric method involving just the use of a simple UV-Vis spectrophotometer. The rapid oxidation of azide by iodine in the presence of trace amounts of thiocyanate was monitored after a fixed reaction time by measuring the change in absorbance at 348 nm. The experimental limit of detection for thiocyanate was very low at 0.3  $\mu\text{g/L}$ , but the method suffered from interferences from  $\text{Cu}^{2+}$ ,  $\text{SO}_3^{2-}$  and  $\text{S}^{2-}$ . These interferences required the sample to be first passed through a cation exchange resin in the sodium form for removal of  $\text{Cu}^{2+}$ , followed by a 10 minute reaction with hydrochloric acid and nitrogen gas to remove  $\text{SO}_3^{2-}$  and  $\text{S}^{2-}$  before sample analysis. Nevertheless, urine samples of smokers and non-smokers were successfully analysed using this method.

More recently Zhang *et al.* [5] determined trace thiocyanate in urine and saliva of smokers and non-smokers using a fluorimetric method, based on the inhibiting effect of thiocyanate on the oxidation of rhodamine 6G by potassium bromate in acidic medium. The detection limit for thiocyanate was 0.09  $\mu\text{g/L}$ , which is an order of magnitude lower than that achieved in earlier work by Ensafi and Tajebakhsh-E-Ardakany [6]. However, each of these spectrophotometric methods are time consuming and laborious to perform, with some involving the use of harmful reagents.

The separation techniques applied to thiocyanate determinations in biological samples include gas chromatography [7,10] capillary electrophoresis [4] and liquid chromatography, with the liquid chromatographic methods generally being based upon some mode of ion chromatography [2,3,8].

Where gas chromatography has been used, a derivatisation step has been performed initially, and the derivatives obtained, subsequently analysed

quantitatively by gas chromatography. Funazo *et al.* [7] determined cyanide and thiocyanate recoveries added to human urine samples by quantitatively methylating cyanide and thiocyanate with dimethyl sulphate to form acetonitrile and methyl thiocyanate respectively. The resulting acetonitrile or methyl thiocyanate was extracted into ethyl acetate and determined by gas chromatography using flame thermionic detection. Good linear calibration curves were obtained in the ranges of 0.25 to 10.0 mg/L for thiocyanate which was considered low enough to detect the anion in biological samples (urine). The recovery of thiocyanate added to human urine samples was over 90 %.

Later, Kage *et al.* [10] used pentafluorobenzyl bromide as a derivatisation reagent and tetradecyldimethylbenzylammonium chloride as the phase transfer catalyst. The derivatisation products pentafluorobenzyl cyanide and pentafluorobenzyl thiocyanate were eluted off the column in ~ 3.5 minutes and ~8 minutes respectively. The column was a glass 2.1 m X 3.1 mm I.D. tube packed with 5 % OV-225 on Uniport HP, 60-80 mesh. The temperatures of the column, injection port and detector were kept at 170 °C, 220 °C and 220 °C respectively. Nitrogen was used as the carrier gas at a flow rate of 30 ml/min. The detection limit of thiocyanate was 0.17 mg/L and the method was used to determine the blood levels of two victims who had died from cyanide poisoning. The thiocyanate levels of the victims was twice that of smokers but were lower than that of cyanide. This observation can be explained due to the sudden death of the victims, where there was little time for inorganic cyanide to be metabolised to thiocyanate before death.

Analysis of thiocyanate in biological fluids (serum, urine and saliva) by capillary electrophoresis was reported by Glatz *et al.* [4]. The determinations were performed in a fused silica capillary, 64.5 cm (56 cm effective length) X 75 µm) using 0.1 M β-alanine-HCl (pH 3.50) as a background electrolyte, separation voltage 18 kV (negative polarity), temperature of capillary 25 °C and direct UV detection at 220 nm. The runtime was 10 minutes which included a 3 minute capillary flush cycle. The detection limit for thiocyanate was 41 µg/L.

Michigami *et al.* [3] determined thiocyanate in human serum samples collected from smokers and non-smokers by ion chromatography using a TSK-gel IC

anion-SW (50 X 4.6 mm i.d.) column and a phosphate eluent with direct UV detection at 195 nm. Detection limits for thiocyanate were 5 µg/L.

An alternative approach that has been investigated is the use of ion-interaction liquid chromatography, performed on a conventional C<sub>18</sub> reversed phase column. For example, Michigami *et al.* [8] developed an analytical method for thiocyanate in urine on a short 5 cm ODS Capcell Pak column permanently coated with cetyldimethylamine. Using direct UV detection, a detection limit for thiocyanate of 20 µg/L was achieved. However, despite the use of a short analytical column, the retention time of thiocyanate with a citrate eluent was still rather long at 16 minutes, with a total runtime of > 30 minutes due to a late eluting peak in the urine sample.

Chinaka *et al.* [2] used direct UV detection at 210 nm for thiocyanate analysis in blood samples. The separation was performed on a TSK-gel IC anion-SW (50 X 4.6 mm I.D.) using a 10 mM phosphate buffer (pH 6.1) – methanol (1:1, v/v) eluent at 1.0 ml/min. Detection limits of 4.9 µg/L were achieved.

#### 4.1.2 Nitrate and nitrite in biological fluids.

It is known that nitric oxide (NO) has a number of diverse physiological roles within the body, particularly in the cardiovascular, immune and nervous systems [11]. In the nervous system, NO modifies neurotransmission in the peripheral and central nervous systems. NO is also one of the ultimate effector molecules in the host defence against many intra and extra-cellular pathogens. Therefore, NO is also generated as part of an immune response by virtue of its cytotoxic behaviour, being a free radical<sup>1</sup>. Because NO is a free radical molecule released by cells in picomolar to nanomolar ranges and has a very short half life (< 5 seconds), a direct measurement of its production is difficult. In oxygenated aqueous solution NO is rapidly oxidised to nitrite [12], which in turn is nearly completely further oxidised to nitrate. Thus the analysis of nitrite and nitrate, the stable products of NO oxidation is often performed to estimate NO synthesis in biological systems and cell cultures.

---

<sup>1</sup> The NO free radical molecule has one unpaired electron.

Cigarette smoke is an excellent source of NO (up to 500 mg/L) [11] However, heavy smoking is paradoxically linked with lower serum NO<sub>x</sub> levels (nitrite and nitrate combined), and so unlike thiocyanate, analysis of biological fluids for nitrite and nitrate with a view to evaluating smoking behaviour can yield contradictory results.

However, the levels of these anions in biological fluids are important to determine for other reasons, as discussed by Ellis *et al.* [11] in a comprehensive review from a clinical biochemistry perspective. Their review discusses the analytical methodologies for analysis of nitrite and nitrate in biological fluids such as colorimetric methods, fluorimetry, capillary electrophoresis, gas chromatography, gas chromatography-mass spectrometry, and high performance liquid chromatography. The review also comprehensively discusses the correlation between elevated nitrate/nitrite levels in the body, and certain clinical conditions, such as urinary tract infections, gastrointestinal diseases, suppressed immune system responses, hypertension, renal and cardiovascular diseases, organ transplant rejection, respiratory diseases and nervous system disorders.

The harmful effects of high levels of ingested nitrate and nitrite were previously discussed in Chapter 3. Also previously discussed in Chapter 3 were the studies which have been performed on a wide range of foodstuffs [13-18] which indicate that vegetables including beets, celery, and leafy vegetables such as lettuce and spinach are rich in nitrate. In western diets assessed by survey [11], the average adults daily intake of nitrite (0.1 mg) is much lower than that of nitrate (80 mg). In certain countries however, the mean daily intake may be as high as 8.7 mg nitrite and (in vegetarians) as high as 194 mg nitrite. Despite the fact that dietary nitrite is low relative to nitrate, and in general, levels of nitrate are higher than nitrite in biological fluids<sup>2</sup>, salivary nitrite can nevertheless be produced by microbial reduction of nitrate in the oral cavity, advancing the production of carcinogenic nitroso compounds discussed previously. This reason suggests the need for accurate control and monitoring of nitrite and nitrate levels in human saliva [19-21].

---

<sup>2</sup> Levels of nitrite are lower in biological fluids due to its oxidation to nitrate in vivo.

Maiti *et al.* [21] used an ion-interaction methodology to determine nitrate and nitrite in saliva samples. Cetylpyridinium bromide above the critical micellar concentration was used as a modifier in an acetonitrile mobile phase, with direct UV detection at 222 nm. Nitrite was found in saliva samples from six volunteers within the range 3 – 9 mg/L. As expected, higher levels of nitrate were found in the saliva samples over the range 18 – 49 mg/L.

Michigami *et al.* [19] later used a TSK gel ODS-80T<sub>M</sub> column which was coated with cetylpyridinium chloride. The mobile phase employed was 1 mM citrate/2.5 % methanol (pH 6.5). Using a flow rate of 1.0 ml/min and direct UV detection at 210 nm, sulphate, bromide, nitrite and nitrate were separated, with nitrite eluting after ~ 6 minutes, and nitrate after ~14 minutes. Detection limits for nitrite and nitrate were very low, at 5 µg/L and 8 µg/L respectively. In all saliva samples subsequently analysed, nitrite levels were lower than nitrate levels, but overall nitrite/nitrate ratios ranged from 1:3 to 1:64, demonstrating that some volunteers in the study had markedly higher nitrite levels relative to nitrate, reflecting differing degrees of bacterial activity in the oral cavity.

More recently, Helalah and Korenaga [20] used a 200 mm X 4 mm Ion Pac AS12A column with a 2.7 mM Na<sub>2</sub>CO<sub>3</sub> – 0.3 mM NaHCO<sub>3</sub> eluent and suppressed conductivity detection, to determine nitrite and nitrate levels in saliva samples. Retention times were faster than the methods discussed previously at 4.1 minutes and 7.6 minutes respectively, but detection limits were higher at 15 µg/L and 34 µg/L respectively. Again, nitrite levels were lower than nitrate levels in all samples. The method developed by Maiti *et al.* [21] which is discussed above, was used as a reference method by these workers, and excellent correlation between the two results was achieved.

As well as monitoring nitrate and nitrite levels in saliva, urine levels are also monitored, since both anions are excreted in the kidneys<sup>3</sup>, nitrate is excreted as such, or after its conversion to urea. Nitrite concentrations in urine are usually only a small fraction (< 5 %) of nitrate concentrations, reflecting in part the dietary intakes of

---

<sup>3</sup> Like thiocyanate, it should be noted that nitrite and nitrate undergo other fates besides renal excretion.

these ions and also their bioreactivity [11]. Usually, nitrate and nitrite levels in urine are stable in the absence of microbial activity. However, nitrite can be produced from urinary nitrate by bacterial nitrate reductase. Therefore, elevated urinary nitrite may assist in the diagnosis of urinary tract infections, and test strips for this purpose have been available for many years.

A number of workers have developed methodologies for determination of nitrate and nitrite in urine samples. As discussed previously, Michigami *et al.* [19] developed a separation of nitrate, nitrite, sulphate and bromide and successfully applied it to determination of nitrate and nitrite in saliva. The same separation was also applied to urine samples. The nitrate peak was free from interferences in all samples, but nitrite could only be detected in a few instances.

Later, Muscara and de Nucci [22] developed an anion exchange chromatographic method with a post-column diazotization-coupling reaction between nitrite and the Griess reagent. The column used was a Spherisorb SAX, 250 mm X 4.6 mm 5  $\mu\text{m}$  column, with a mobile phase of 0.06 M  $\text{NH}_4\text{Cl}$  pH 2.8 and a flow rate of 0.7 ml/min. The post column reactions first involved the reduction of nitrate to nitrite on a copper-plated cadmium powder filled column (placed after the analytical column), followed by the formation of the diazo-compound after reaction with the Griess reagent. The runtime for urine samples was relatively long, however, with retention times for nitrite and nitrate of ~10 minutes and ~15 minutes respectively. In addition, the instrumentation was quite complex, requiring three separate pumps for the anion exchange mobile phase, the Cd/Cu column carrier solution and finally the Griess reagent.

Li *et al.* [23] used the derivatisation of nitrite with 2,3-diaminonaphthalene (DAN) under acidic conditions to yield the highly fluorescent 2,3-naphthotriazole (NAT), which was subsequently separated on a 5  $\mu\text{m}$   $\text{C}_8$  column (150 mm X 4.6 mm) with a 15 mM sodium phosphate buffer (pH 7.5) containing 50 % MeOH (flow rate, 1.3 ml/min). For the analysis of nitrate in urine, the nitrate was initially converted to nitrite using nitrate reductase before reacting with DAN to form NAT. Detection limits were very low at 0.6  $\mu\text{g/L}$  for nitrate and nitrite, but the reduction of nitrate to nitrite had a required incubation period of 1 hour, with the subsequent

reaction with DAN requiring a further ten minutes, before injection onto the HPLC column.

The work described in this chapter reports on the use of a simple ion-interaction liquid chromatographic method to obtain a rapid separation of nitrate, nitrite and thiocyanate, and its application to the analysis of urine samples. In particular, it is demonstrated in this work that the analysis of urine samples taken from non-smokers, moderate smokers and heavy smokers for thiocyanate is a useful means of evaluating smoking behaviour.

## **4.2 Experimental.**

### 4.2.1 Equipment.

The ion chromatograph and analytical column described in Chapter 2 were also used in this work, but with the additional use of a Phenomenex Kingsorb, 3  $\mu\text{m}$  C<sub>18</sub>, 30 mm x 4.6 mm I.D. column (Macclesfield, Cheshire, U.K). The injection loop used was 25  $\mu\text{L}$  with by direct UV at 230 nm. Urine samples were centrifuged using a Biofuge 13 centrifuge (Heraeus, Germany).

### 4.2.2 Reagents and chromatographic conditions.

The reagents used for mobile phase preparation were as described in Chapter 2. The optimised mobile phase consisted of 10 mM TBA-OH in 20 % aqueous MeOH, titrated to pH 6.0 using 85 % phosphoric acid (Riedel de Haen, Germany). The flow rate used was 1.0 ml/min with column temperature set at 45 °C. Standard solutions were prepared as described in Chapter 2, with thiocyanate standards prepared from their respective sodium salts (Aldrich, Milwaukee, WI, USA).

### 4.2.3 Sample pre-treatment.

Analyses of biological fluids represent a difficult analytical task. Such complex matrices require special sample pre-treatment for successful separation by

ion-chromatography because of high protein concentrations and high ionic strengths. Ultrafiltration [23] has been used for preparation of protein free samples. However, special filtration membranes are rather expensive and require long periods of centrifugation. Precipitation with acetonitrile is a simple, rapid and effective way of removing serum proteins. Since the concentration of proteins in urine from healthy<sup>4</sup> individuals is many times lower in comparison with serum [4], the possibility of direct injection of urine after dilution has been tested [4,7]. However, when analysing saliva and urine samples, most workers [5,9] [18-20] also incorporate a centrifugation step to remove solid matter, with subsequent dilution of the supernatant. Other workers [8] have used a 0.45  $\mu\text{m}$  filter in addition to centrifugation and dilution steps, and Muscara and de Nucci [22] passed six-fold diluted urine samples, through an ODS silica column and 400  $\mu\text{L}$  of effluent subsequently injected onto the column.

In this work, urine samples were collected after getting up in the morning from a non-smoker, moderate smoker and heavy smoker. Samples were centrifuged at 13,000 g for two minutes and stored at 4 °C until needed. Before injection onto the column, each sample was diluted 1 in 20 with deionised water. To remove organic interferences, 1 mL of sample was pushed through an SPE C<sub>18</sub> cartridge (Waters “Sep-Pak Light”, Waters Corporation, Milford, MA, USA), which had been preconditioned with 2 mL MeOH followed by 2 mL of deionised water. The sample was then injected onto the column through a 0.45  $\mu\text{m}$  nylon membrane filter from Gelman Laboratories (Michigan, USA). Saliva samples were also subjected to the same pre-treatment steps as the urine samples.

### **4.3 Results and discussion.**

#### **4.3.1 Preliminary studies of saliva analysis.**

Using an optimised mobile phase from previous work in Chapter 3, (20 mM TBA-OH in 20 % aqueous MeOH, titrated to pH 6.2 using dilute HCl) saliva

---

<sup>4</sup> Patients with proteinuria require sample treatment similar to that of serum.

samples were run on a Phenomenex Hypersil 3  $\mu\text{m}$  C<sub>18</sub>, 30 mm x 4.6 mm I.D. column. Following the sample preparation procedures as described, the supernatant was injected “neat” onto the column. The supernatant was also passed down a SPE C<sub>18</sub> cartridge to remove organic interferants and re-injected. Work on saliva analysis was not continued, because the viscous nature of the samples made them difficult to work with. However, Figure 4-1 illustrates the chromatography obtained and demonstrates the clear advantage of using the SPE C<sub>18</sub> cartridge to “clean up” the sample prior to injection. Further work involving the analysis of urine samples, therefore used similar sample preparation methodologies.

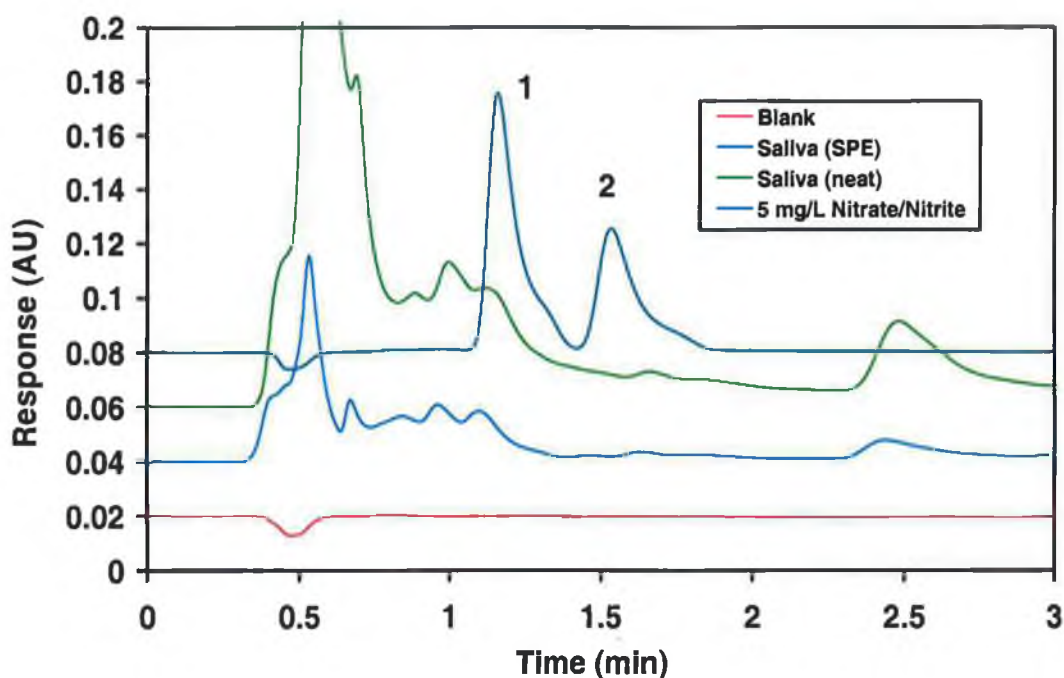


**Figure 4-1.** Comparison of sample preparation with, and without the use of C<sub>18</sub> SPE cartridges for saliva analysis by ion-interaction chromatography. Column: 30 mm X 4.6 mm Phenomenex Hypersil C<sub>18</sub> 3  $\mu\text{m}$  column. Mobile phase: 20 mM TBA-Cl in 20 % MeOH, pH 6.0, Flow rate: 1.0 ml/min. Loop size: 25  $\mu\text{L}$ . Column temperature: Ambient. Detection: Direct UV at 225 nm. Peaks: [1] nitrite, [2] nitrate.

#### 4.3.2 Mobile phase optimisation for analysis of urine.

Based on retention data collected in previous work in Chapter 2, tetrabutylammonium chloride (prepared by titrating a TBA-OH containing eluent with HCl) was initially chosen as the ion-pair reagent to use in this study, with methanol as organic modifier. An initial mobile phase preparation of 10 mM TBA-Cl

in 20 % MeOH, pH 6.0, (flow rate: 1.0 ml/min; column temperature: ambient) resulted in baseline separation of nitrate (1.4 min,  $k' = 1.8$ ) and nitrite (1.6 min,  $k' = 2.2$ ) with a retention time for thiocyanate of 6.5 minutes ( $k' = 12$ )

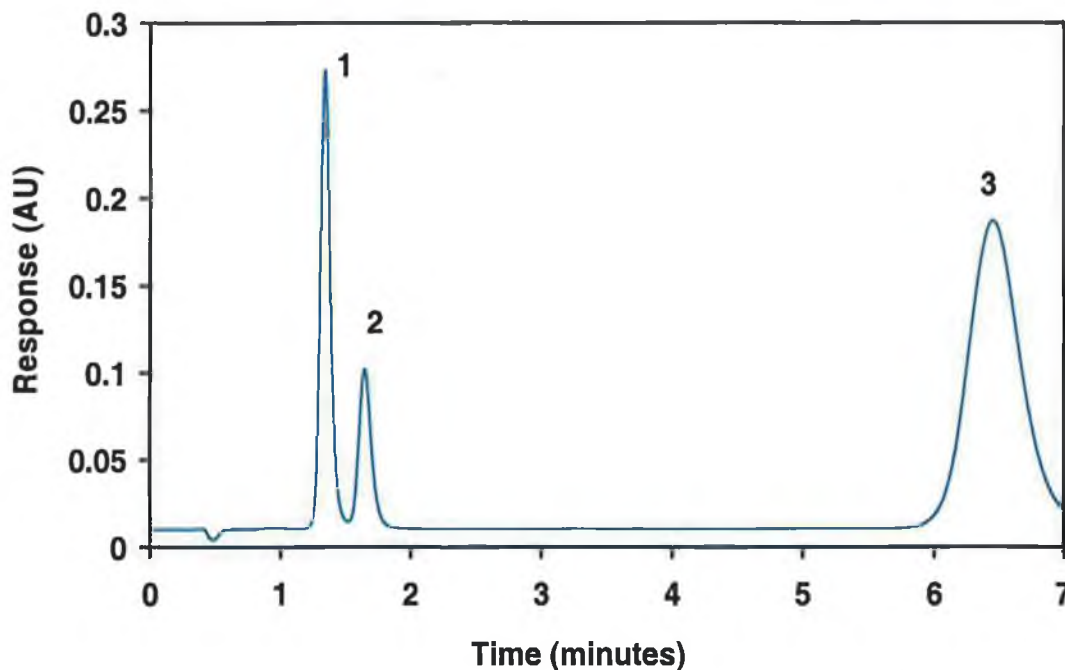


**Figure 4-2.** Initial mobile phase conditions for the separation of nitrate, nitrite and thiocyanate by ion interaction chromatography. Column: 30 mm X 4.6 mm Phenomenex Hypersil C<sub>18</sub> 3  $\mu$ m column. Mobile phase: 10 mM TBA-Cl in 20 % MeOH, pH 6.0, Flow rate: 1.0 ml/min. Loop size: 25  $\mu$ L. Column temperature: Ambient. Detection: Direct UV at 225 nm. Peaks: [1] 2.5 mg/L nitrite, [2] 2.5 mg/L nitrate, [3] 5 mg/L thiocyanate.

However, in an attempt to further reduce the retention time for thiocyanate and also add some buffering capacity to the eluent, the chloride counter ion was replaced with phosphate, by titrating the TBA-OH with phosphoric acid to pH 6.0. As phosphate has a greater eluting strength than chloride this change resulted in reduced retention times for all three anions, with thiocyanate now eluting at 5.8 minutes ( $k' = 10.6$ ) and nitrate and nitrite eluting at 1.1 and 1.3 minutes respectively ( $k' = 1.2$  and 1.6) (flow rate: 1.0 ml/min; column temperature: ambient). This observation is consistent with basic ion-pair theory. Phosphate, being divalent at pH 6.0 has a greater competing power with the analytes for charged sites on the stationary phase (relative to monovalent chloride); such that the dynamic equilibrium is shifted toward the mobile phase.

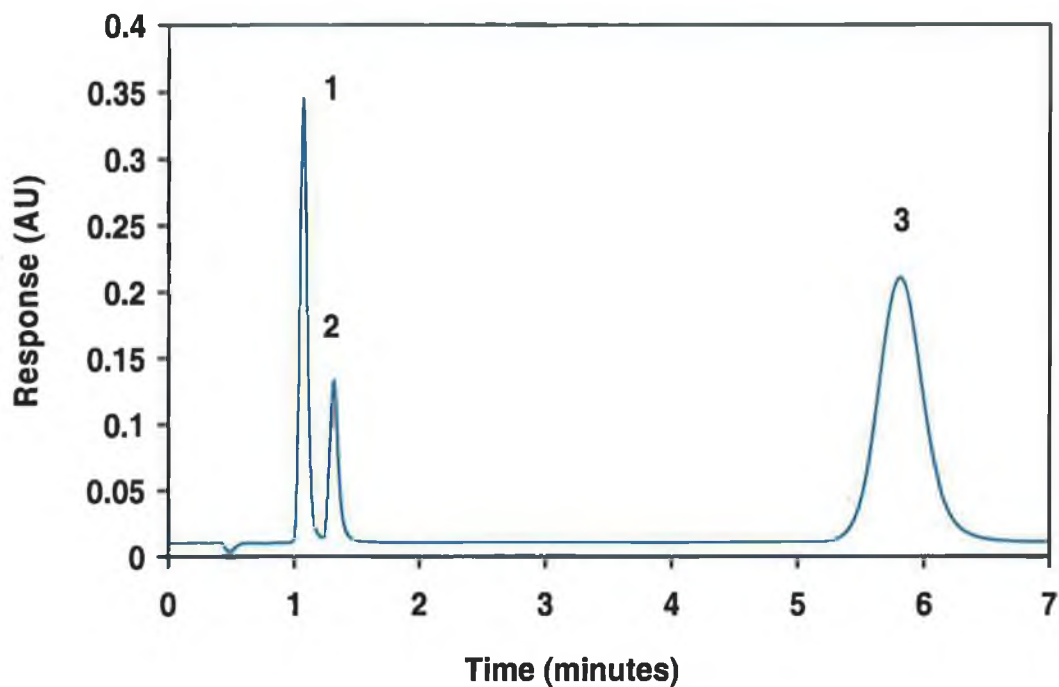


**Figure 4-3.** Chromatogram showing the analysis of nitrate, nitrite and thiocyanate by ion interaction chromatography with a mobile phase containing phosphate as a counter-ion. Column: 30 mm X 4.6 mm Phenomenex Hypersil C<sub>18</sub> 3  $\mu$ m column. Mobile phase: 10 mM TBA-phosphate in 20 % MeOH, pH 6.0, Flow rate: 1.0 ml/min. Loop size: 25  $\mu$ L. Column temperature: Ambient. Detection: Direct UV at 225 nm. Peaks: [1] 2.5 mg/L nitrite, [2] 2.5 mg/L nitrate, [3] 5 mg/L thiocyanate.

As thiocyanate is a less hydrophilic anion than nitrate and nitrite, it can be supposed that its retention was in part due to non-electrostatic interactions with the stationary phase. Therefore, a further reduction in the retention of thiocyanate relative to nitrate and nitrite should result if an increase in column temperature were investigated, as non-electrostatic interactions would be reduced. To test this assumption the column temperature was raised to 45 °C and used with the above eluent. The resultant optimum standard chromatogram is shown as Figure 4-4.

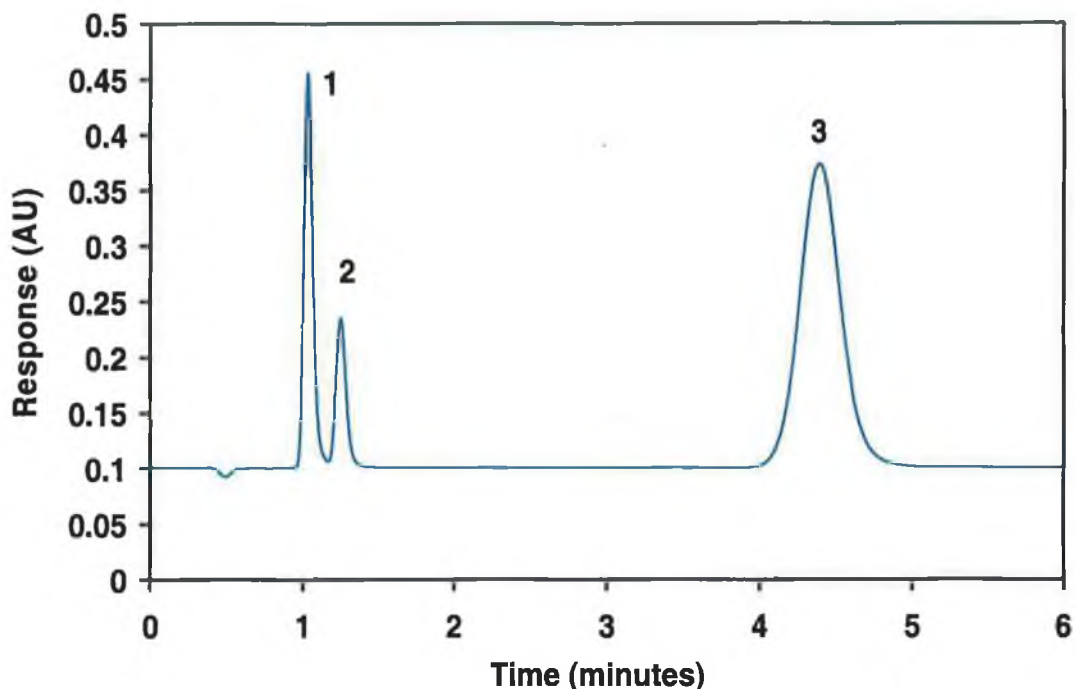


**Figure 4-4.** Optimised chromatographic conditions for the analysis of nitrate, nitrite and thiocyanate by ion interaction chromatography. Column: 30 mm X 4.6 mm Phenomenex Hypersil C<sub>18</sub> 3  $\mu$ m column. Mobile phase: 10 mM TBA-phosphate in 20 % MeOH, pH 6.0, Flow rate: 1.0 ml/min. Loop size: 25  $\mu$ L. Column temperature: 45 °C. Detection: Direct UV at 225 nm. Peaks: [1] 2.5 mg/L nitrite, [2] 2.5 mg/L nitrate, [3] 5 mg/L thiocyanate.

As can be seen from the figure, the increase in column temperature reduced the retention time of thiocyanate by approximately 1.5 minutes, down to 4.4 minutes ( $k' = 7.8$ ), without affecting the retention times or resolution of the nitrite and nitrate peaks. This separation is significantly faster than that achieved by Maiti *et al.* [21] who used a 25 cm X 4.6 mm I.D. 5  $\mu$ m Zorbax ODS column and a 35/65 acetonitrile/water mobile phase containing 2 mM cetylpyridinium bromide and 10 mM phosphate buffer at a flow rate of 1.0 ml/min. Nitrite, nitrate and thiocyanate were eluted in 6.0 minutes, 7.5 minutes and 16.9 minutes respectively. (In the present work, the total run time for the separation of all three analytes in the standard mixture shown in Figure 4-4 could be further reduced to under 2.5 minutes through the use of a 2.0 ml/min flow rate without a detrimental affect upon resolution or peak shape, although for complex biological matrices the use of the lower flow rate was more suitable due to the large number of matrix peaks likely to be present).

### 4.3.3 Optimisation of detection parameters

To optimise detection sensitivity a mixture of nitrate/nitrite (2.5 mg/L) and thiocyanate (5.0 mg/L) was injected at wavelengths ranging from 190 nm to 235 nm. Signal to noise ratios for each peak were plotted versus wavelength. The baseline noise was at a minimum above 215 nm (Figure 4-6), and the signal to noise ratio for  $\text{SCN}^-$  was at a maximum at 230 nm. This also corresponded to the optimal signal to noise value for nitrite. The optimum response for nitrate was obtained at 220 nm, although as nitrate is present at higher levels than thiocyanate in urine, 230 nm was used as the detection wavelength.

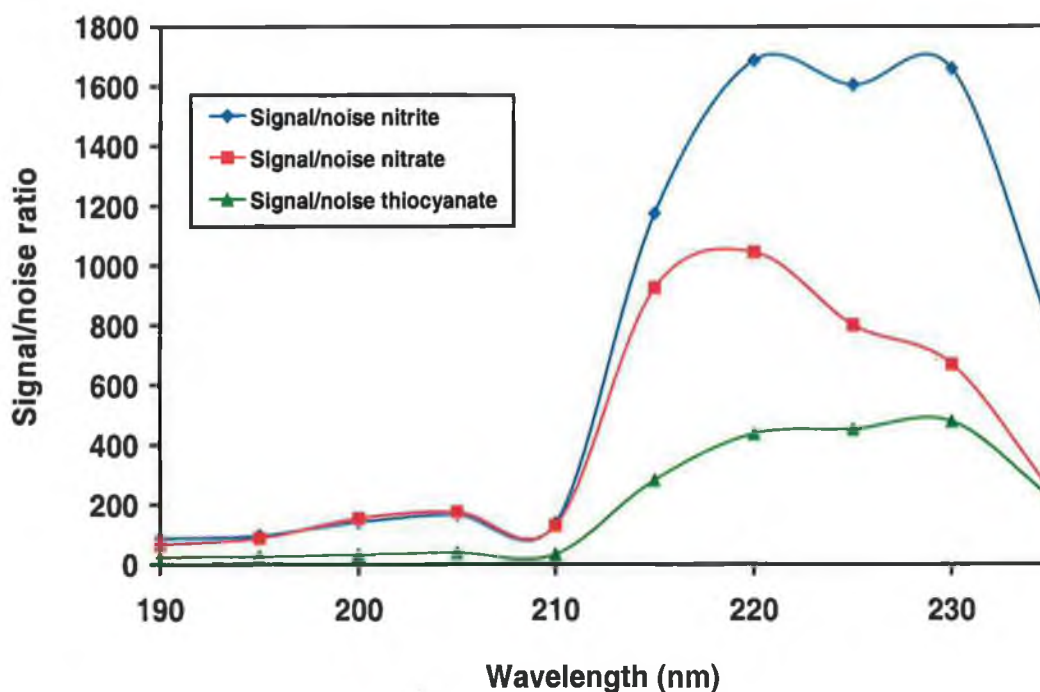


**Figure 4-5.** Optimisation of detector wavelength for the analysis of nitrate, nitrite and thiocyanate by ion interaction chromatography. Signal to noise ratios Vs wavelength are shown. All other conditions as in Figure 4-4.

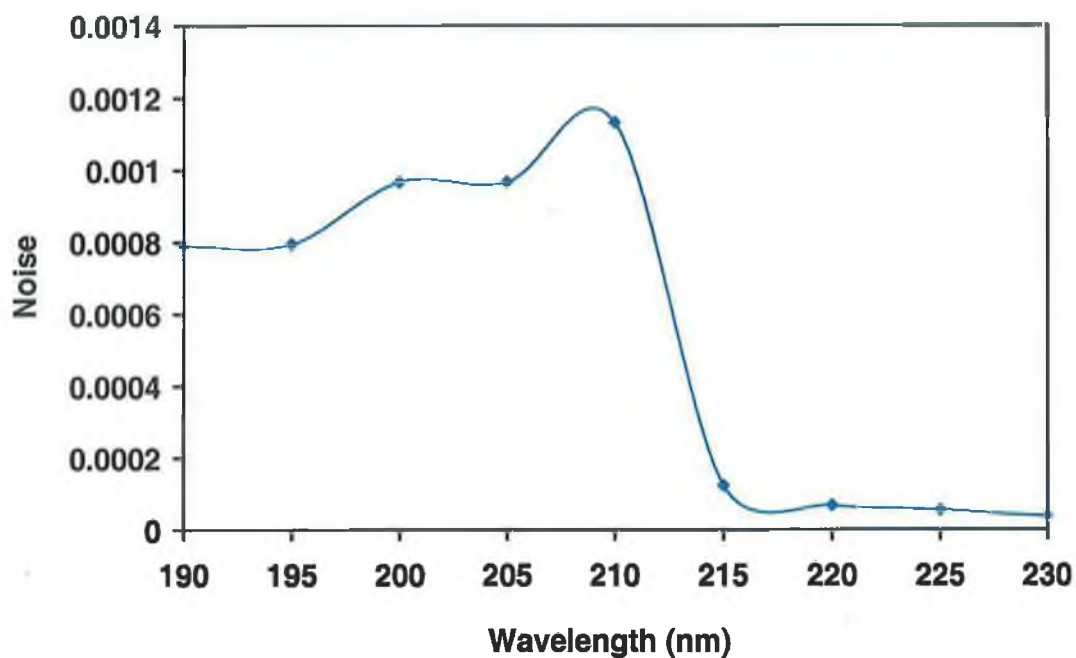


**Figure 4-6.** *Baseline noise versus detection wavelength for a TBA-phosphate/MeOH mobile phase. All other conditions as in Figure 4-4.*

#### 4.3.4 Precision, linearity and detection limits.

Method precision was determined by the repeat injection ( $n = 6$ ) of a standard mixture at a concentration of 5 mg/L nitrite, nitrate and thiocyanate. The resultant % RSD values for peak area were 0.87 % for nitrite, 1.44 % for nitrate and 1.10 % for thiocyanate.

**Table 4-1.** System precision study for nitrate, nitrite and thiocyanate by ion interaction chromatography.

Nitrite peak area	Nitrate peak area	SCN <sup>-</sup> peak area
0.004110	0.001879	0.002697
0.004110	0.001807	0.002624
0.004107	0.001866	0.002626
0.004110	0.001862	0.002663
0.004021	0.001838	0.002628
0.004098	0.001831	0.002663
<b>0.87 %</b>	<b>1.44 %</b>	<b>1.10 %</b>

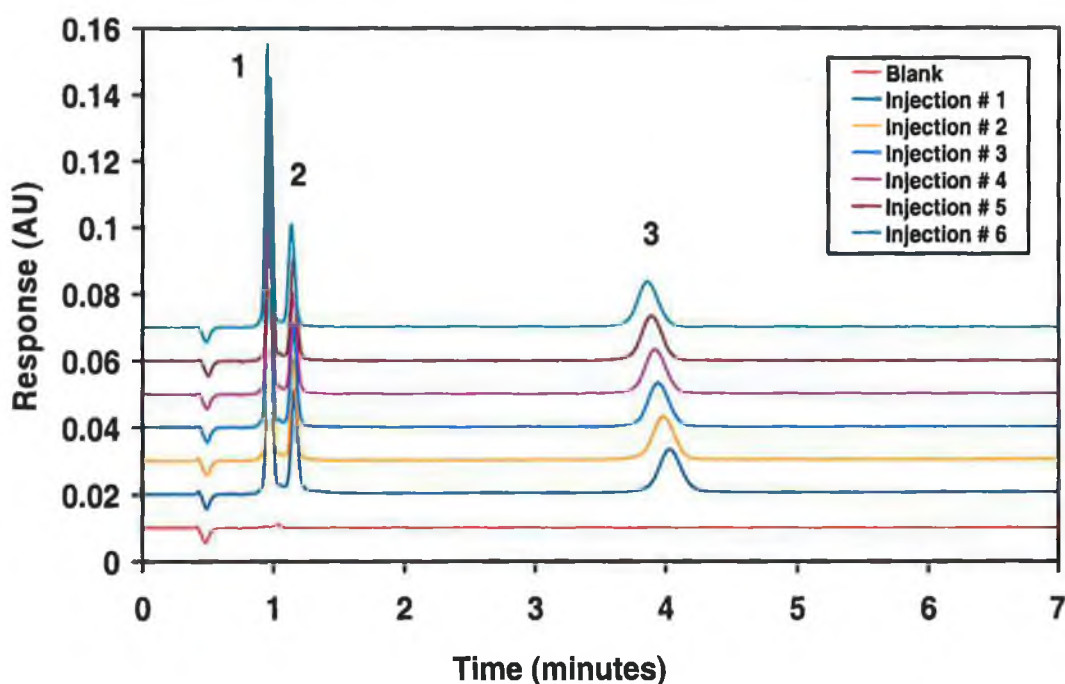


**Figure 4-7.** Overlay of six consecutive injections of a nitrate, nitrite and thiocyanate standard. Conditions as in Figure 4-4, with UV detection at 230 nm. Peaks: [1] nitrite, [2] nitrate, [3] thiocyanate.

Linearity standards were prepared as five separate concentrations over the range 0.5 mg/L to 10 mg/L and each standard injected in triplicate. Correlation coefficients obtained were  $R^2 = 0.9993$  for nitrite,  $R^2 > 0.9999$  for nitrate and  $R^2 > 0.9999$  for thiocyanate, illustrating that the method showed excellent linearity over the concentration range of interest.

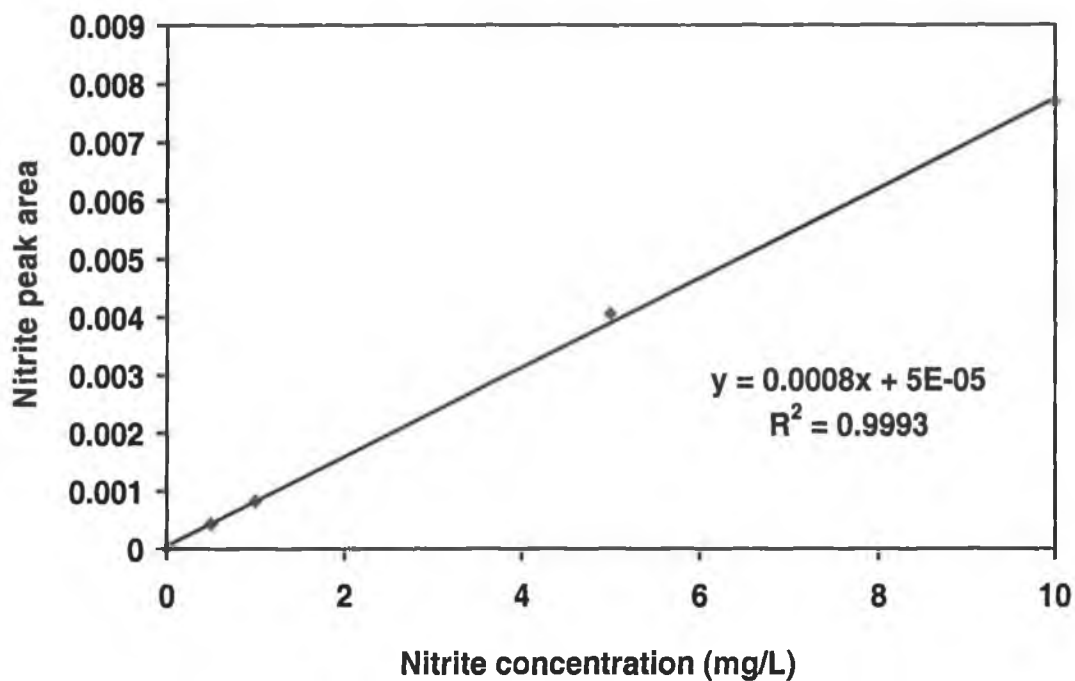


Figure 4-8. Linearity studies for the determination of nitrite by ion interaction chromatography.

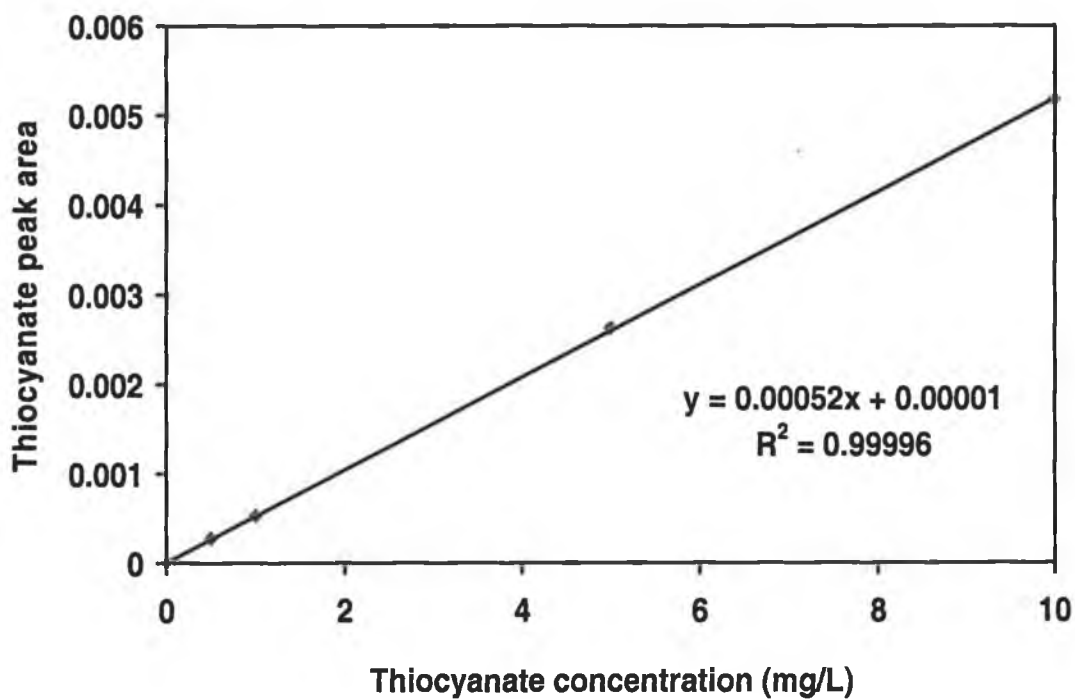


Figure 4-9. Linearity studies for the determination of thiocyanate by ion interaction chromatography.

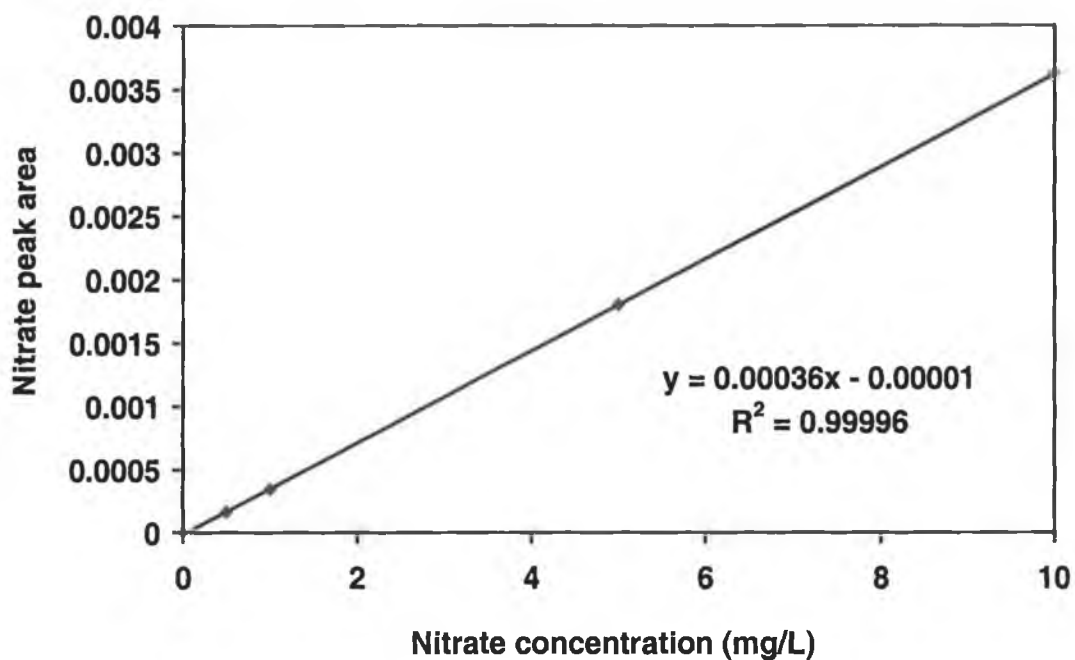
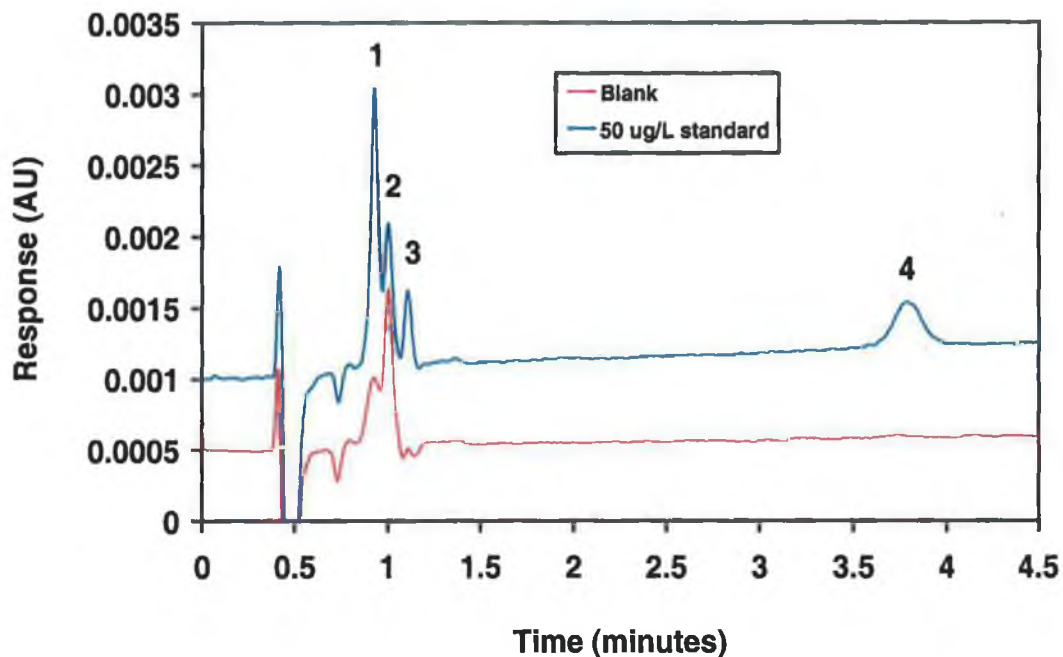


Figure 4-10. Linearity studies for the determination of nitrate by ion interaction chromatography.

Using a 25  $\mu\text{L}$  injection loop, limits of detection were found to be 23.7  $\mu\text{g/L}$  for nitrite, 76.9  $\mu\text{g/L}$  for nitrate and 21.4  $\mu\text{g/L}$  for thiocyanate. Noise values and peak heights were determined in triplicate and averaged. In the case of nitrate and nitrite, the peak heights of co-eluting system peaks were measured in triplicate in a deionised water blank, then averaged and taken to represent system “noise” for  $s/n$  ratio calculations. In the case of thiocyanate, baseline noise was measured from 3.5 minutes to 4.5 minutes in the blank.



**Figure 4-11.** Sensitivity studies for the determination of nitrite, nitrate and thiocyanate by ion interaction chromatography. The figure shows a 50  $\mu\text{g/L}$  standard mix overlaid with a blank. Conditions as in Figure 4-4, with UV detection at 230 nm. Peaks: [1] nitrite, [2] contaminant in laboratory water, [3] nitrate, [4] thiocyanate.

Improved detection limits were possible with the use of larger injection volumes. Loop sizes of 25, 50 and 75  $\mu\text{L}$  were studied by injecting the same standard mix as above. Increasing the injection volume up to 75  $\mu\text{L}$  caused retention times to increase for standard solutions as shown in Figure 4-12, but had no deleterious effect on peak shape or efficiency. However, a 25  $\mu\text{L}$  loop was chosen for use with real samples to reduce potential fouling of the short column due to the complex nature of the sample.

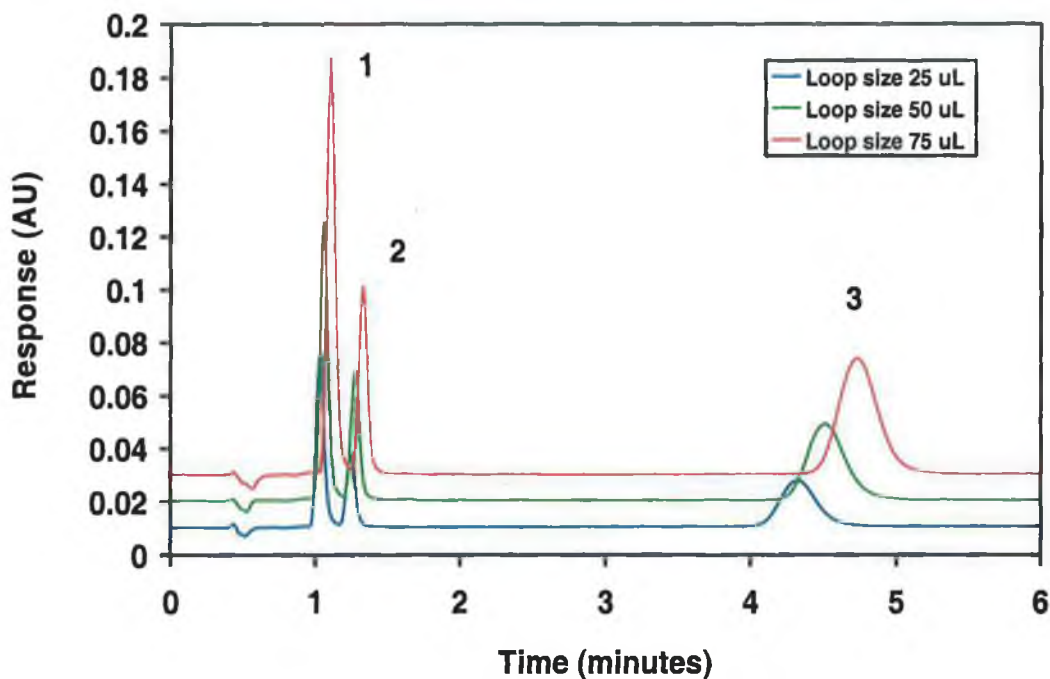


**Figure 4-12.** Effect of increased injection volume upon the separation of nitrate, nitrite and thiocyanate. Conditions as in Figure 4-4, with UV detection at 230 nm. Peaks: [1] nitrite, [2] nitrate, [3] thiocyanate.

#### 4.3.5 Analysis of real samples.

Urine samples were collected from a non-smoker (male), moderate smoker (female - 10 to 20 cigarettes per day) and heavy smoker (male - 30 to 40 cigarettes per day) in order to demonstrate the effectiveness of this method as a means of evaluating smoking behaviour. Samples were analysed against a standard curve for each of the three analytes respectively (five point standard curves could be constructed in under an hour with each standard injected in duplicate). The runtime for samples was extended to 10 minutes due to a late eluting sample matrix peak at ~ 9 minutes. Nitrate and thiocyanate peaks, which were evident in all samples, displayed shorter retention times compared to an injection of the relevant standard. This was presumably due to the high ionic strength of the sample resulting in blocking of stationary phase sites leading to probable 'self elution'. It was found that analyte sensitivity was not affected by the analytes being present in the diluted urine matrix. Figure 4-13 shows the chromatogram obtained from the analysis of a urine sample taken from a heavy smoker. Overlaid is the same sample spiked with

thiocyanate. As can be seen from the two chromatograms, thiocyanate is clearly well resolved from all major matrix peaks, the majority of which elute in under 2 minutes. Although the exact profile of individual urine samples will vary, there was no interference from matrix peaks for any of the samples studied, indicating the method is generally applicable for this particular sample type. Levels of thiocyanate found in the samples were 6.5 mg/L, 11.4 mg/L and 29.9 mg/L in the non-smoker, moderate smoker and heavy smoker samples respectively.

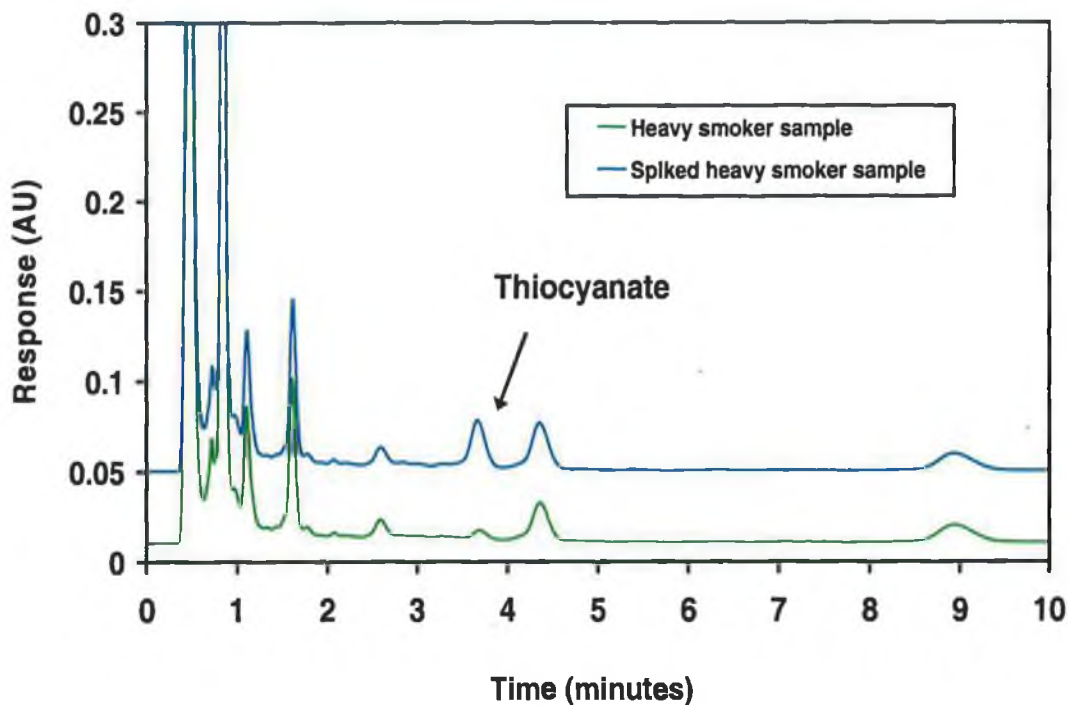


**Figure 4-13.** Analysis of urine for thiocyanate by ion interaction chromatography on a short 3  $\mu\text{m}$   $\text{C}_{18}$  column. Lower trace: Sample (heavy smoker) diluted 1/20. Upper trace: Sample (heavy smoker) diluted 1/20 and spiked with thiocyanate. Conditions as in Figure 4-4, with UV detection at 230 nm.

Also shown in Figure 4-14 and Figure 4-15 are expanded views of the thiocyanate spike (Figure 4-14) and of the thiocyanate peak in each diluted sample type (Figure 4-15). Figure 4-15 shows a clear increase in peak height for thiocyanate in each sample, indicating that the method can be used to evaluate smoking behaviour.

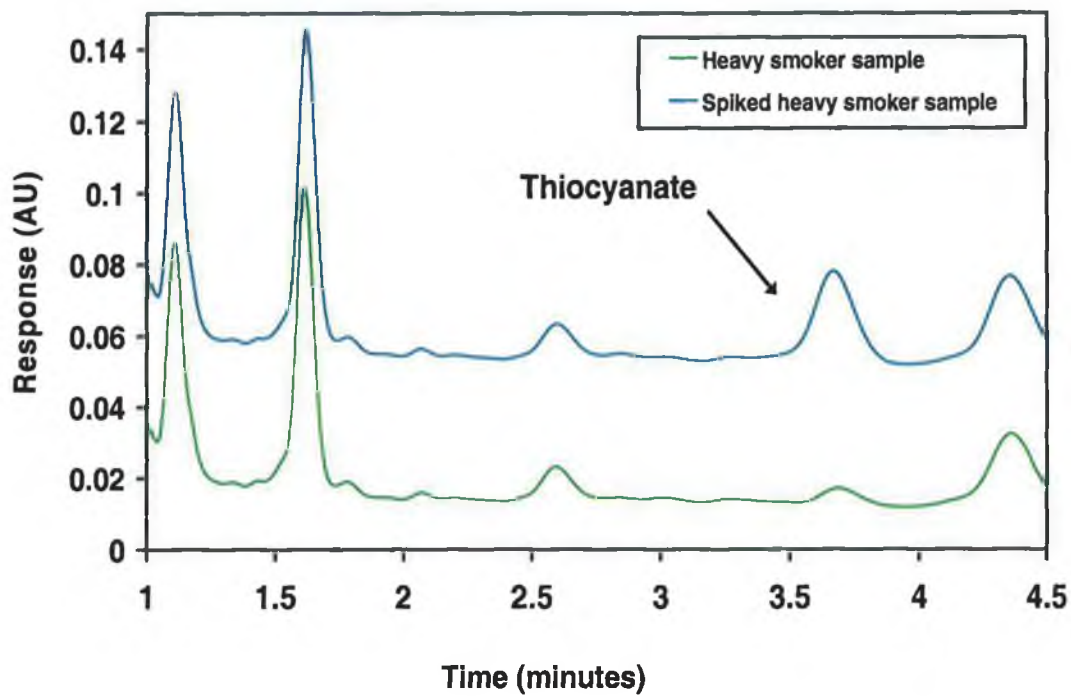


Figure 4-14. Expanded view of Figure 4-13.

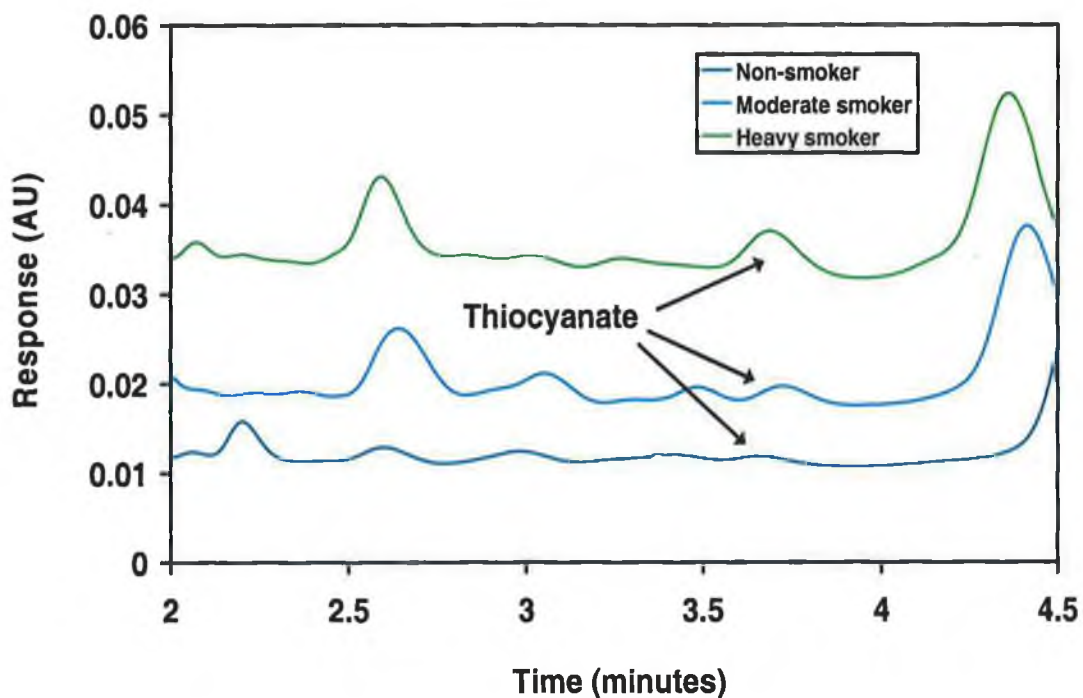
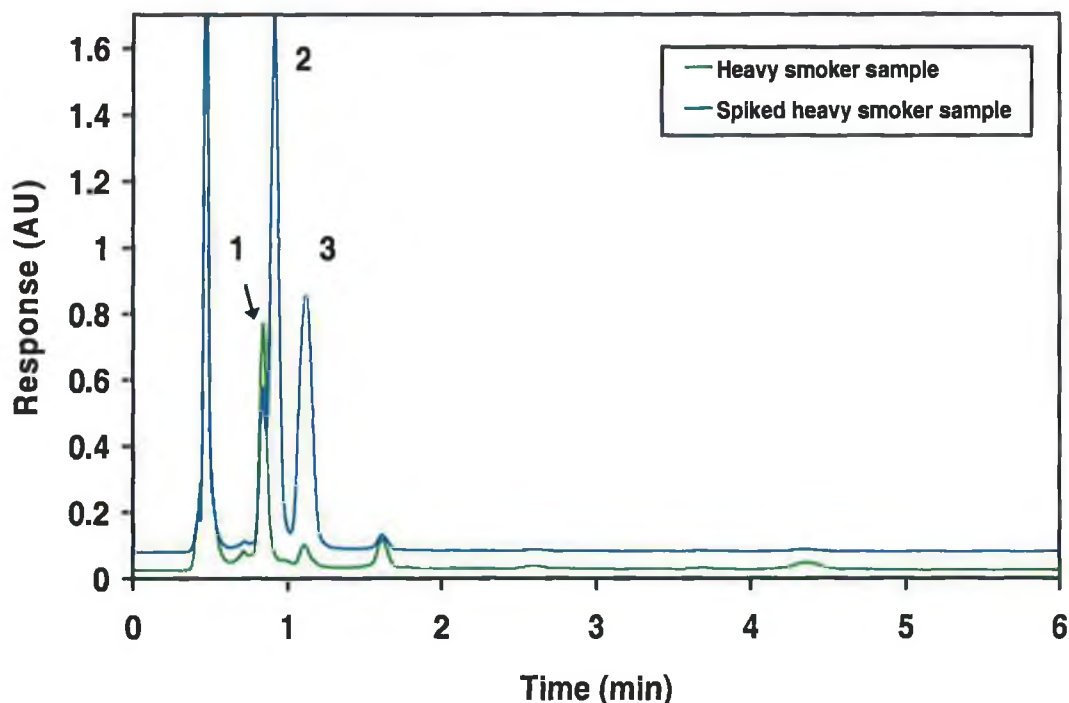


Figure 4-15. Overlay of the thiocyanate peak in the analysis of each of the three urine samples.

The ability of the method to also simultaneously determine nitrite and nitrate in the above samples is illustrated in Figure 4-16. The figure shows overlaid urine

sample chromatograms, one of which has been spiked with both nitrite (Peak 2) and nitrate (Peak 3). The reduction in size of Peak 1 is simply due to the dilution of the spiked sample.



**Figure 4-16.** Analysis of urine for nitrate and nitrite by ion interaction chromatography. Lower trace: Sample (heavy smoker) diluted 1/20. Upper trace: Sample (heavy smoker) diluted 1/20 and spiked with nitrate and nitrite. Conditions as in Figure 4-4, with UV detection at 230 nm. Peaks: [1] unidentified sample matrix peak, [2] nitrite, [3] nitrate.

As can be seen nitrate is well resolved from nitrite (none of which was detected in any of the real samples) which partially co-elutes with a sample matrix peak (Peak 1). It should be noted that the partial coelution of nitrite with the sample matrix peak would make the quantitative determination of low levels of nitrite difficult, although the presence of nitrate in the sample would be clearly seen. Levels of nitrate found in the samples were 141 mg/L, 259 mg/L and 223 mg/L in the non-smoker, moderate smoker and heavy smoker samples respectively. At this point, to avoid any confusion, it is pertinent to note that unlike thiocyanate, the urine samples were *not* analysed for nitrite and nitrate as a means of evaluating smoking behaviour. Rather the analysis of urine samples for nitrate and nitrite can be used as an indicator of *other* separate clinical conditions such as urinary tract infections. Therefore, a clear advantage of this method is that it can be used *both* to characterise inorganic

cyanide metabolism (through analysis of thiocyanate in smokers' urine) and to monitor urinary nitrate and nitrite levels.

Table 4-2 details the results obtained for thiocyanate determinations. The results obtained in this brief study are compared to urinary thiocyanate levels determined in alternative studies (chromatographic/electrophoretic) and analysis times are also compared. The results obtained in this study compare well with average values found previously and the faster runtime of this method compared to other methods is also demonstrated.

**Table 4-2.** Typical urinary thiocyanate levels (mg/L) as determined by different analytical methodologies.

Reference	Analytical method	Thiocyanate (non-smoker)	Thiocyanate (smoker)	Total runtime
[8]	Ion-interaction chromatography	2.39 mg/L	12.72 mg/L	30 min.
[4]	Capillary electrophoresis	4.87 mg/L	12.56 mg/L	10 min.
This work	Ion-interaction chromatography	6.50 mg/L	29.90 mg/L	10 min.

#### 4.3.6 Additional spike linearity data and working range studies.

Further to the work described above, a separate set of spike linearity and working range experiments were also conducted to supplement the results obtained thus far. The aim of these studies was to examine the linearity of nitrate, nitrite and thiocyanate spikes in a real urine sample. Optimised chromatographic conditions were used as before, but an earlier shift in retention times<sup>5</sup> for all three analytes was noted as shown in Table 4-3.

<sup>5</sup> Despite the earlier shift in retention times, resolution of 1.5 was still maintained between nitrite and nitrate.

**Table 4-3.** Effect of  $C_{18}$  stationary phase type on the retention of nitrate, nitrite and thiocyanate in ion interaction chromatography.

Anion	Hypersil 3 $\mu\text{m}$ $C_{18}$		Kingsorb 3 $\mu\text{m}$ $C_{18}$	
	Retention time	Capacity factor ( $k'$ )	Retention time	Capacity factor ( $k'$ )
Nitrite	1.1 min	1.2	0.6 min	0.92
Nitrate	1.3 min	1.6	0.7 min	1.23
Thiocyanate	4.4 min	7.8	2.1 min	5.46

The only chromatographic condition that was changed from the original optimised chromatography was that a Phenomenex Kingsorb 3  $\mu\text{m}$   $C_{18}$  column was used instead of a Phenomenex Hypersil 3  $\mu\text{m}$   $C_{18}$  column. The other dimensions of both columns were identical (3.0 cm X 4.6 mm I.D., 3  $\mu\text{m}$  particle size). The reason that this study was performed on a Kingsorb stationary phase rather than a Hypersil (as was initially used), was that it was anticipated that since Kingsorb stationary phases are a newer column technology relative to Hypersil, that the Kingsorb column could offer greater mechanical stability. Kingsorb silica particles have a smoother surface, reducing the effect of the particle shearing off into smaller particles over time. It was assumed that both columns having  $C_{18}$  phases would produce essentially equivalent separations. Upon further investigation, it was found that the two stationary phases actually differed in several respects as detailed in Table 4-4.

**Table 4-4.** Characteristics of Hypersil and Kingsorb  $C_{18}$  stationary phases.

$C_{18}$ phase type	Pore size	Surface area	% Carbon load
Hypersil	120 (Å)	170 ( $\text{m}^2/\text{g}$ )	10 %
Kingsorb	90 (Å)	425 ( $\text{m}^2/\text{g}$ )	18 %

Given the higher surface area and increased carbon loading, it would be expected that the Kingsorb column would give longer retention than the Hypersil column, since more ion-interaction reagent would be adsorbed onto the column, resulting in a higher overall dynamic exchange capacity. The opposite effect was

observed however, with longer retention on the Hypersil column. A possible explanation due to the decreased carbon loading, is that the Hypersil phase should have more exposed silanol groups which have been shown to act as weak cation exchange sites, which can influence the ion-interaction separation of both anions and cations [24].

Adsorbed IIR tends to be spaced evenly over the stationary phase due to repulsion effects, and it was initially anticipated that much of the Hypersil stationary phase would remain unmodified by the IIR, relative to a Kingsorb stationary phase which has a higher carbon loading. Smith *et al.* [24] found, however, that tetra-alkylammonium salts were retained on silica based reversed-phase columns by two types of interaction; the first being hydrophobic interactions between the C<sub>18</sub> chains and the hydrophobic chain of the IIR, and the second interaction being ion-exchange between the tetra-alkylammonium group and H<sup>+</sup> at the free SiOH sites within the stationary phase.

It has been found in this current work that a C<sub>18</sub> stationary phase containing more exposed silanol groups (Hypersil) relative to another (Kingsorb) will have a higher dynamic exchange capacity, resulting in more retention. The same observations were made by Gennaro *et al.* [25] who used an eluent of 5 mM octylammonium phosphate (pH 6.4) to determine nitrate and nitrite in sea water samples. Two different columns were employed, a Hibar LiChrosorb and a Spherisorb ODS-2. The former had a carbon load of 22 % and the latter had a carbon load of 12 %. The retention times noted for the Spherisorb column were generally much longer than those achieved on the Hibar LiChrosorb column of higher carbon load, with the same mobile phase and flow rate.

Figure 4-17 shows a proposed mechanism whereby the Hypersil column with increased numbers of exposed silanol groups results in an overall higher dynamic exchange capacity. The upper section of the figure represents the Kingsorb stationary phase, where the majority of interactions between the IIR (in black) and the stationary phase are through hydrophobic interactions with the C<sub>18</sub> chains (in green). In contrast, the lower section of the figure represents the Hypersil phase. This phase has fewer C<sub>18</sub> chains for the hydrophobic interactions described above, but it has

more exposed silanol groups. These silanol groups could be involved in electrostatic interactions with one side of the spherical micelles of the tetra-alkylammonium IIR formed in solution. The other side of the spherical micelle provides additional ion-exchange sites for analyte anions, such that overall, the Hypersil column has a higher dynamic exchange capacity.

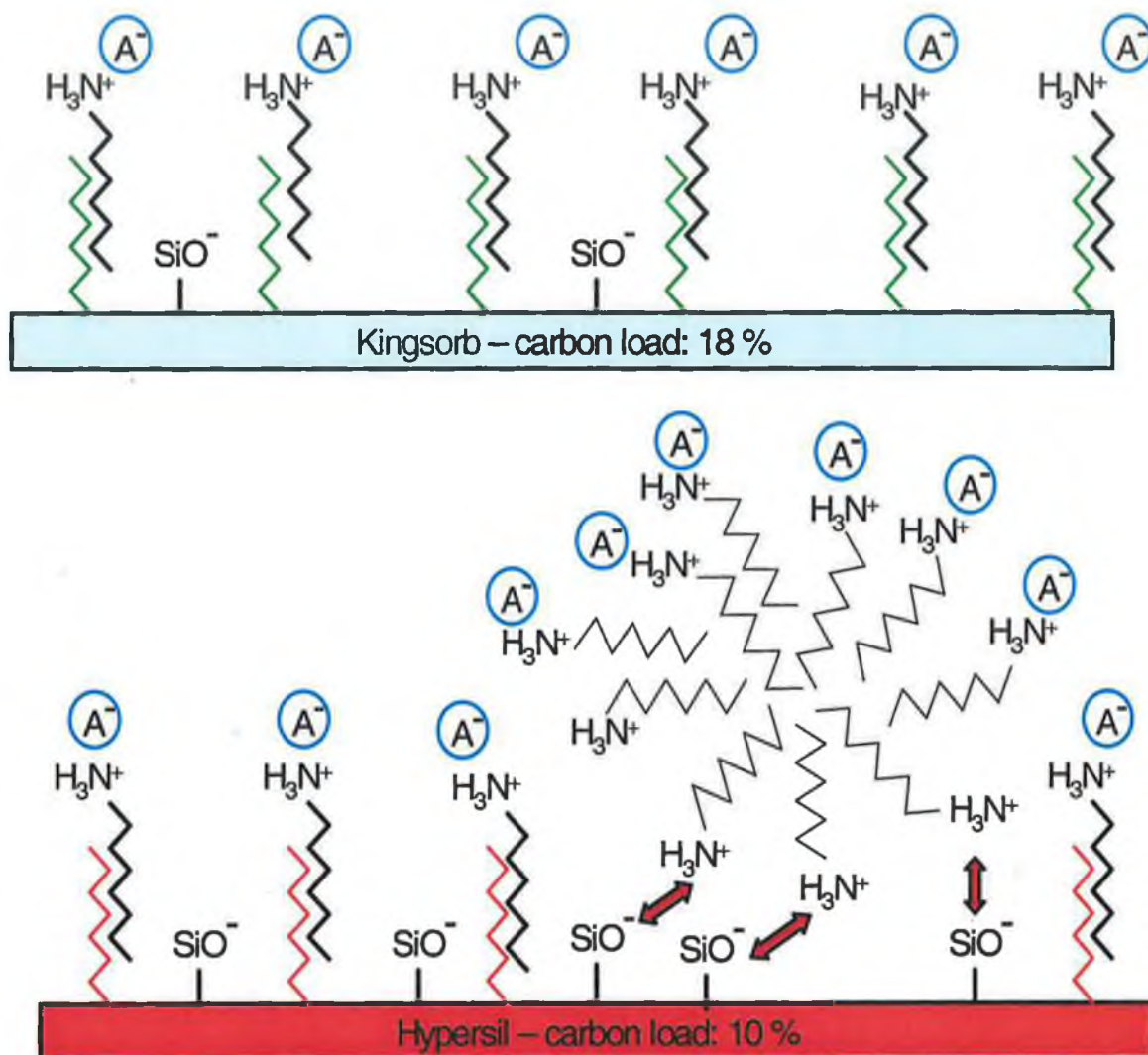


**Figure 4-17.** Proposed mechanism resulting in increased retention of nitrate, nitrite and thiocyanate on a 3 μm Hypersil stationary phase relative to a 3 μm Kingsorb stationary phase. The upper figure represents the Kingsorb silica phase (in green), with IIR (in black) hydrophobically bound to the C<sub>18</sub> chains (in green). Analyte anions (in blue) are retained by electrostatic interactions. The lower figure represents the Hypersil silica phase (in red), with IIR (in black) hydrophobically bound to the C<sub>18</sub> chains (in red). Despite the fact that there are less C<sub>18</sub> chains, micelles of IIR are also electrostatically bound to exposed silanol groups, increasing the overall dynamic exchange capacity.

Spike samples were prepared such that each contained the raw (centrifuged) sample of a medium smoker, at a dilution ratio of 1/40. A total of six standards were prepared as detailed in Table 4-5. Figures in parentheses represent the spike concentration when extrapolated in the raw undiluted sample. Standard addition curves for both nitrate and nitrite (n=5) were constructed over the range 0-10 mg/L. Acceptable correlation coefficients were obtained,  $R^2 = 0.9979$  for nitrite and  $R^2 = 0.9982$  for nitrate. For thiocyanate a standard addition curve over the range 0-5 mg/L was constructed (n=5). For this curve, a correlation coefficient of  $R^2 = 0.9956$  was obtained. From the standard addition work carried out, nitrate and nitrite spikes were linear up to 10 mg/L (representing up to 400 mg/L in the raw undiluted samples) and thiocyanate spikes were linear up to 5 mg/L (representing up to 200 mg/L in the raw undiluted samples) This was deemed sufficient to cover the concentrations of the two anions likely to be present in the majority of samples.

**Table 4-5.** Spike linearity studies for nitrate, nitrite and thiocyanate on a short column by ion interaction chromatography.

<b>Standard number</b>	<b>Nitrite added (mg/L)</b>	<b>Nitrate added (mg/L)</b>	<b>Thiocyanate added (mg/L)</b>
Blank-unspiked (1/40)	0 (0)	0 (0)	0 (0)
#1 (1/40)	2 (80)	2 (80)	0 (0)
#2 (1/40)	4 (160)	4 (160)	0.5 (20)
#3 (1/40)	8 (320)	8 (320)	1.0 (40)
#4 (1/40)	10 (400)	10 (400)	2.0 (80)
#5 (1/40)	12 (480)	12 (480)	5.0 (200)

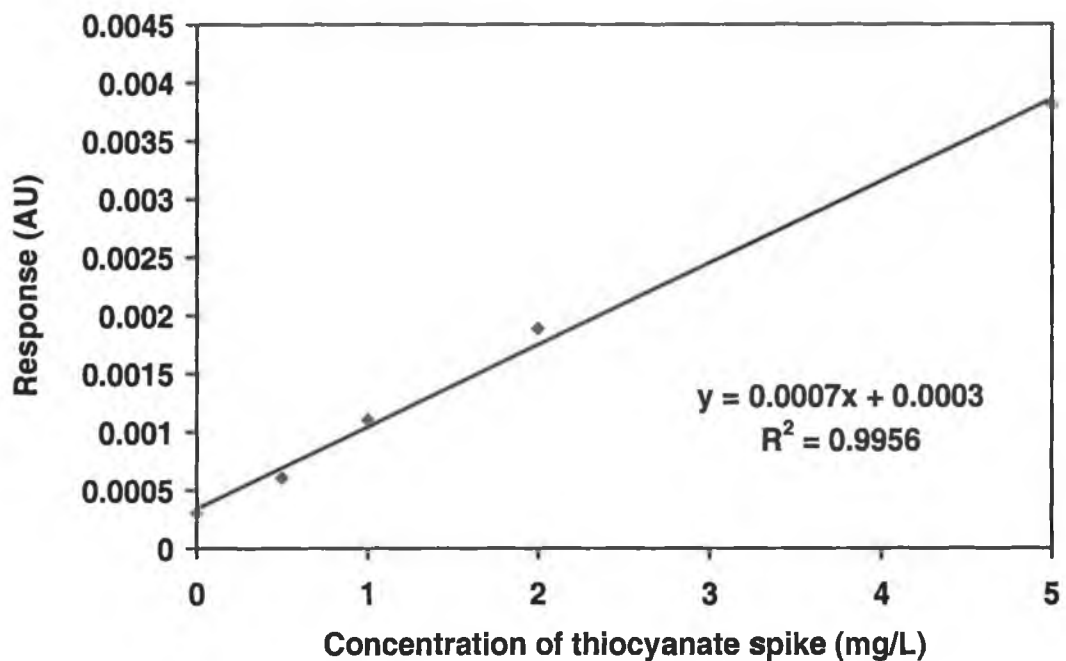


Figure 4-18. Thiocyanate spike linearity study on a short column by ion interaction chromatography.

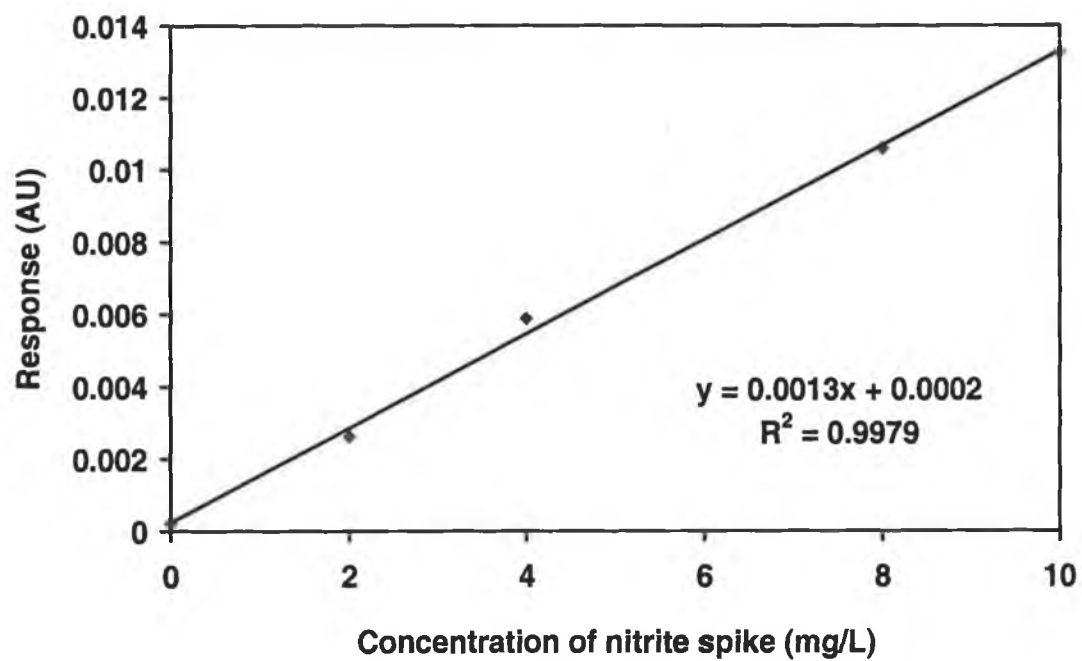


Figure 4-19. Nitrite spike linearity study on a short column by ion interaction chromatography.

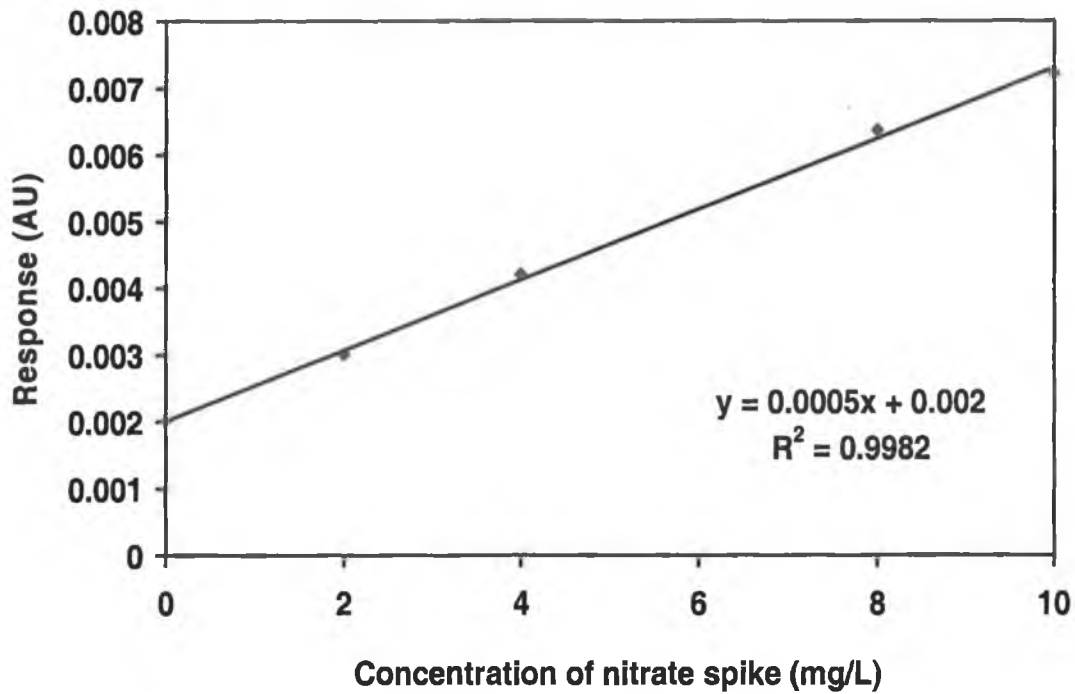


Figure 4-20. Nitrate spike linearity study on a short column by ion interaction chromatography.

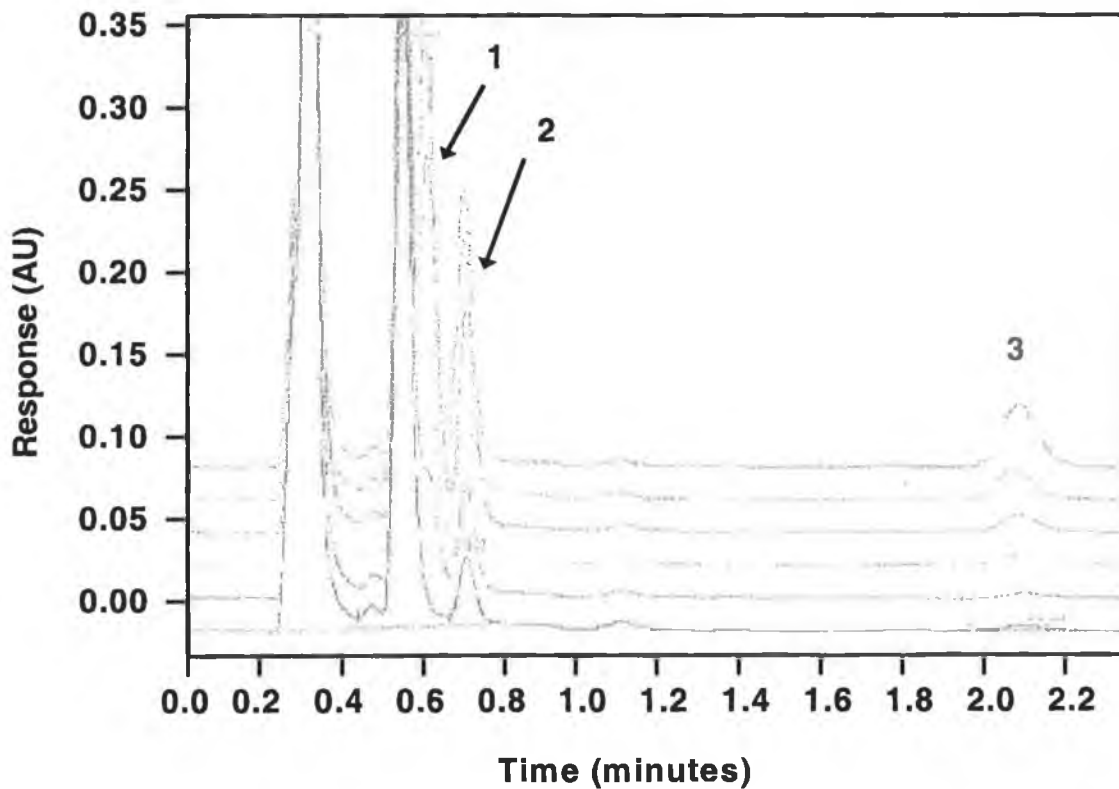


Figure 4-21. Overlay of nitrate, nitrite and thiocyanate linearity spikes in a single urine sample diluted 1/40. Conditions as in Figure 4-4 except for the column used: Phenomenex Kingsorb C<sub>18</sub> (3 μm) 30 mm X 4.6 mm. Detection: UV detection at 230 nm. Peaks: [1] nitrite, [2] nitrate, [3] thiocyanate.

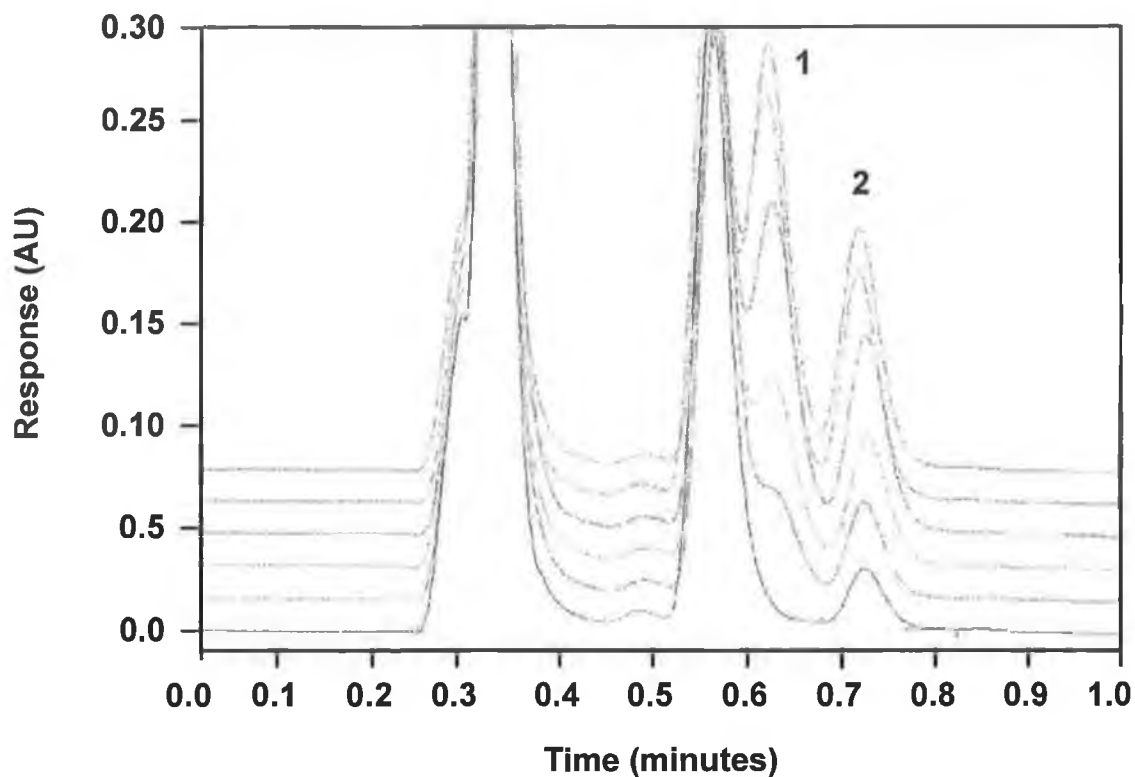


Figure 4-22. Expanded view of Figure 4-21 showing nitrate and nitrite linearity spikes. Conditions as in Figure 4-21. Peaks: [1] nitrite, [2] nitrate.

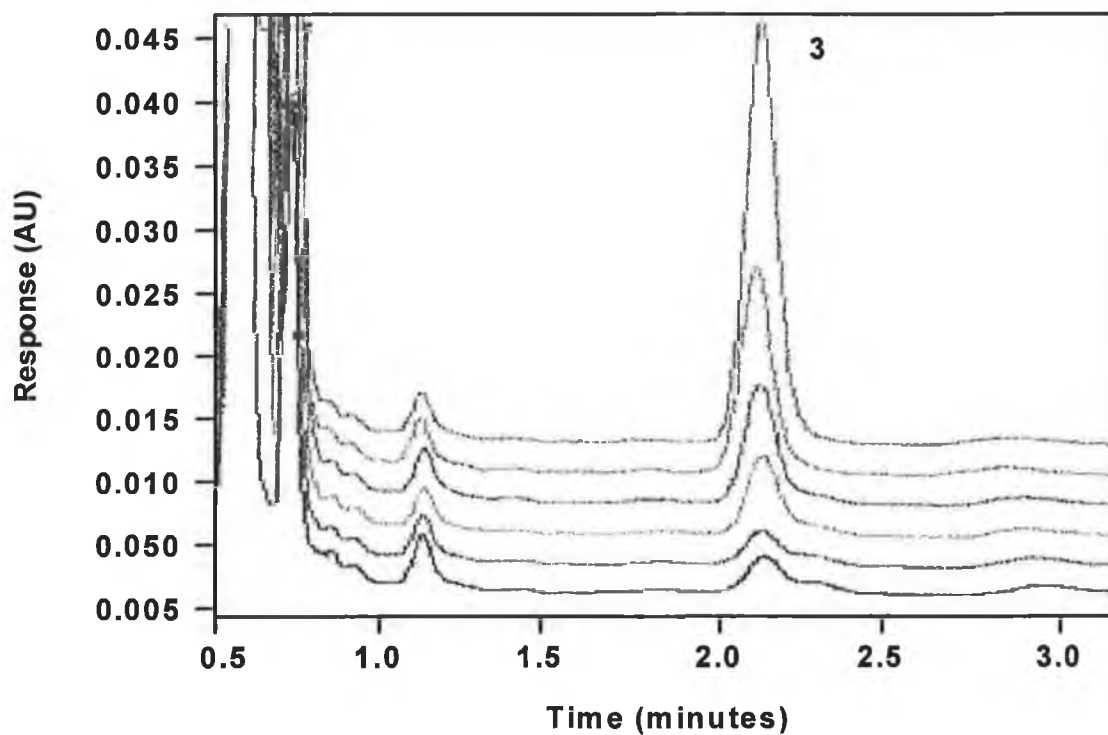


Figure 4-23. Expanded view of Figure 4-21 showing thiocyanate linearity spikes. Conditions as in Figure 4-21.

#### 4.3.7 Comparative analysis using anion exchange chromatography.

A section of work was also performed on a 25 cm Dionex AS17 anion exchange column with a view to illustrating the advantage of using a short C<sub>18</sub> column for ion-interaction chromatography, over the use of anion exchange chromatography on a column of more standard length. Jackson *et al.* [26] recently studied the analysis of perchlorate in ground waters by anion exchange chromatography. They reported on the difficulty of anion-exchange analysis of “polarizable” ions such as perchlorate; a subgroup to which thiocyanate also belongs. Cotton *et al.* [27] describe polarizability as “*The ease with which polar character can be induced. Technically this is the size of the electric dipole moment that is induced by a given electric field*”. As such, these anions have “hydrophobic” character and usually have a small hydrated radius. Ions of a smaller solvated size show greater binding affinity than larger ions as discussed by Haddad and Jackson [28] since a smaller ion is more easily accommodated in the resin pores. Thus the higher degree of cross-linking in conventional PS-DVB exchange resins, the greater the preference of the resin for ions of a smaller hydrated size.

Therefore such anions are strongly retained on conventional anion-exchange resins and are difficult to elute from conventional anion exchange resins, typically exhibiting poor peak shape. Mobile-phase additives (MeOH or p-cyanophenol), are often used to minimise adsorption and improve peak shape. Alternatively the use of specialist hydrophilic ion-exchange columns are required to address these problems. One such column, the Ionpac AS16 [29] by Dionex which is a more hydrophilic column than previous columns used for determination of polarisable anions (for example the Ionpac AS11), which therefore minimizes any adsorption interactions with the stationary phase resulting in improved chromatographic efficiency.

The following study was performed for the purposes of comparison with the methodology using ion-interaction chromatography discussed previously. The following anion-exchange method illustrates that despite adequate sensitivity, precision and linearity achieved on a conventional anion exchange column, the runtime is nonetheless slower than that achieved on the 3 cm C<sub>18</sub> column using rapid ion-interaction chromatography. In addition to this, expensive anion-exchange

columns can become easily fouled when dealing with complex biological samples, and so the use of a short inexpensive reversed phase column is an obvious advantage.

#### 4.3.7.1 Mobile phase optimisation.

An Ionpac AS17 was the only column available in the laboratory for this work. As suggested by Jackson *et al.* [26] a mobile phase of 35 mM NaOH was prepared and a nitrite/nitrate/thiocyanate standard mix injected with a flow rate of 1.0 ml/min. The relatively long retention time of thiocyanate (approx. 26 minutes) and its poor peak shape is consistent with that predicted by Jackson *et al.* who instead used an Ionpac AG11 and an Ionpac AS11 which is more hydrophilic than the AS17, and resulted in shorter retention times for thiocyanate (approximately 12 minutes). It was not possible to improve peak shape and retention times in this work by using a more specialised column such as the Ionpac AS11, due to its prohibitive expense for this work. The two-fold decrease in retention of thiocyanate when using a specialised AS11 column relative to a conventional AS17 column demonstrates that rapid, efficient anion-exchange separations are not possible without using expensive hydrophilic columns.

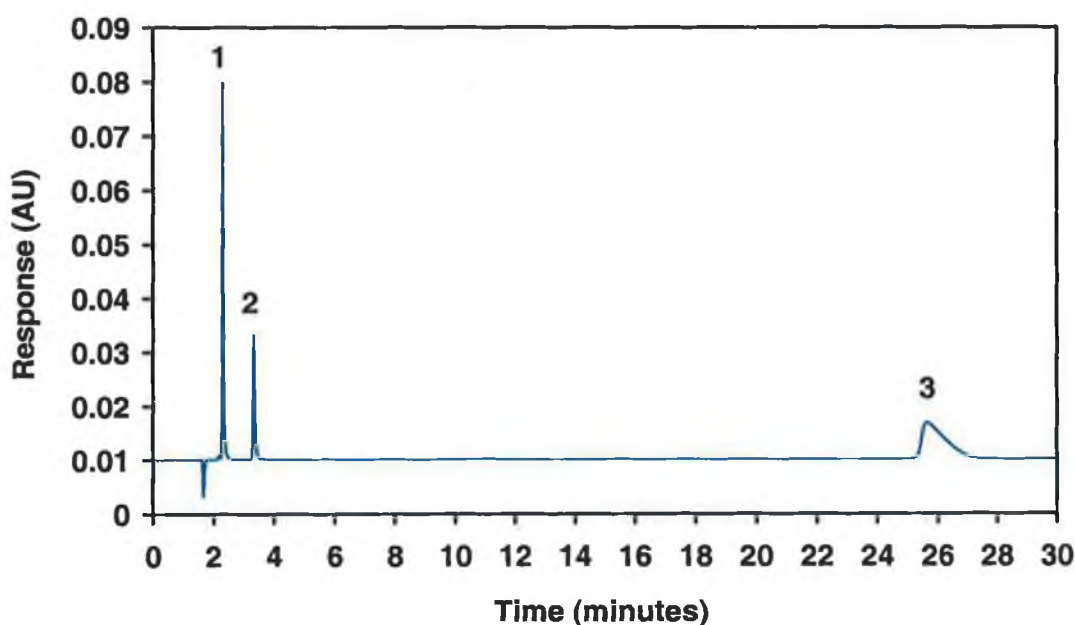


**Figure 4-24.** Initial separation of a nitrite/nitrate/thiocyanate standard mix on an anion exchange column. Conditions: Column: Dionex AS17 25 cm X 4.6 mm, Mobile phase: 35 mM NaOH, Flow rate: 1.0 ml/min, Injection volume: 25  $\mu$ L, Detection: 230 nm. Peaks: [1] nitrite, [2] nitrate, [3] thiocyanate.

#### 4.3.7.2 System precision.

System precision was determined by injecting a 5 mg/L nitrate/nitrite/thiocyanate mix six times, and reporting the % RSD of the peak areas for each peak. The % RSD's for nitrate, nitrite and thiocyanate were 2.80 %, 1.26 % and 0.40 % respectively.

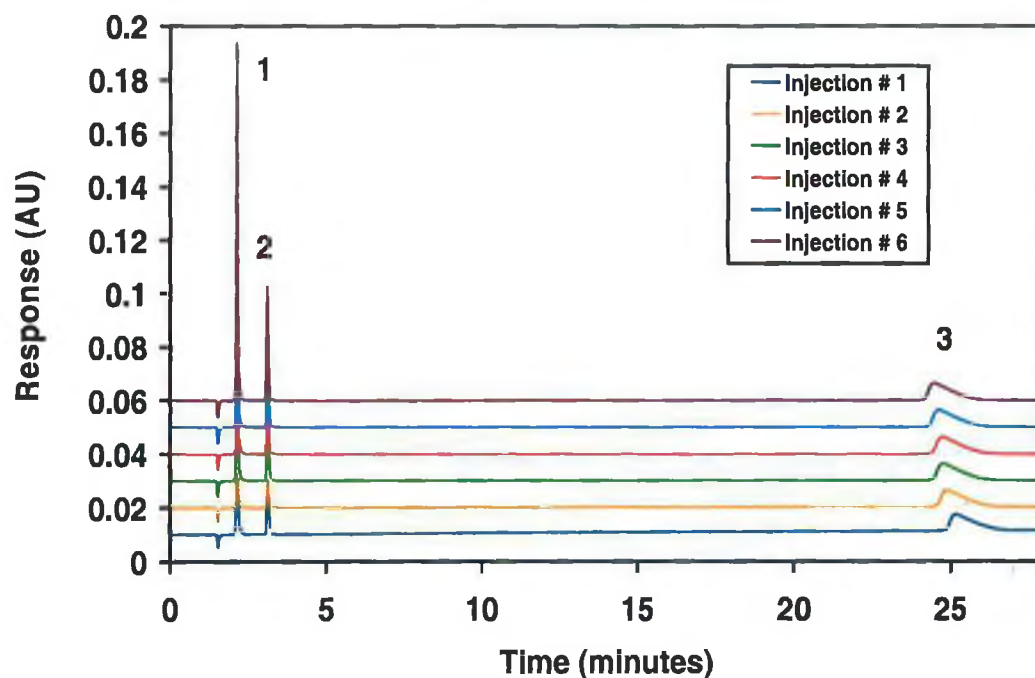


Figure 4-25. Overlay of consecutive injections of a nitrate, nitrite and thiocyanate standard on an anion exchange column. Conditions as in Figure 4-24. Peaks: [1] nitrite, [2] nitrate, [3] thiocyanate.

#### 4.3.7.3 Linearity studies.

Standards were prepared over the range 0.5 mg/L and 10 mg/L. Correlation coefficients were  $\geq 0.9999$  for each anion.

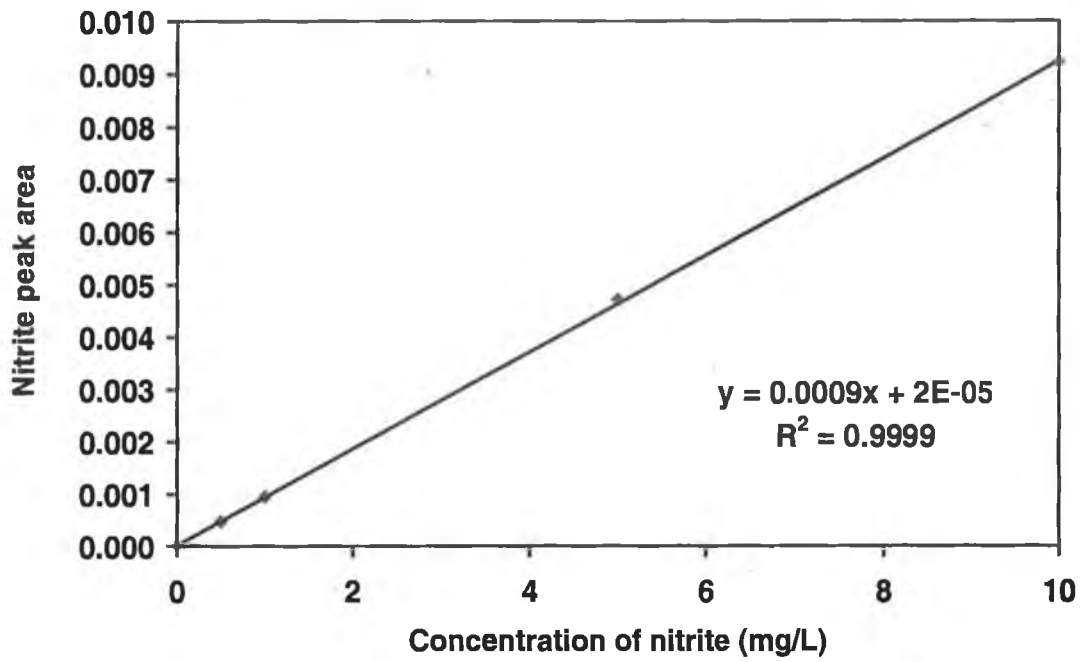


Figure 4-26. Nitrite linearity study on an AS17 anion exchange column.

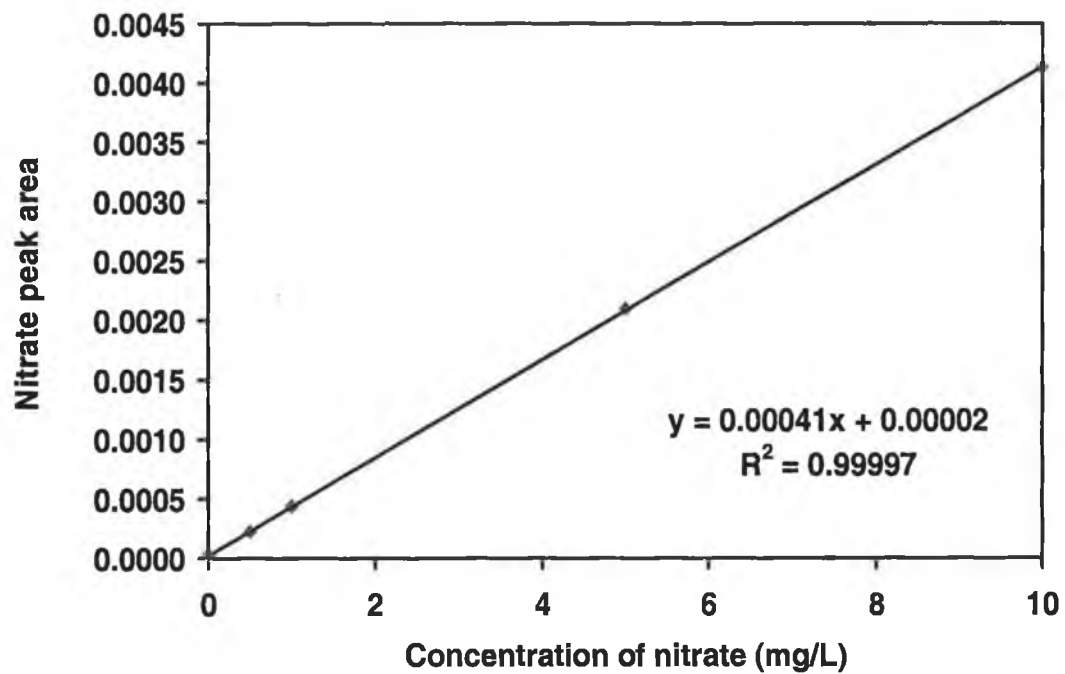


Figure 4-27. Nitrate linearity study on an AS17 anion exchange column.

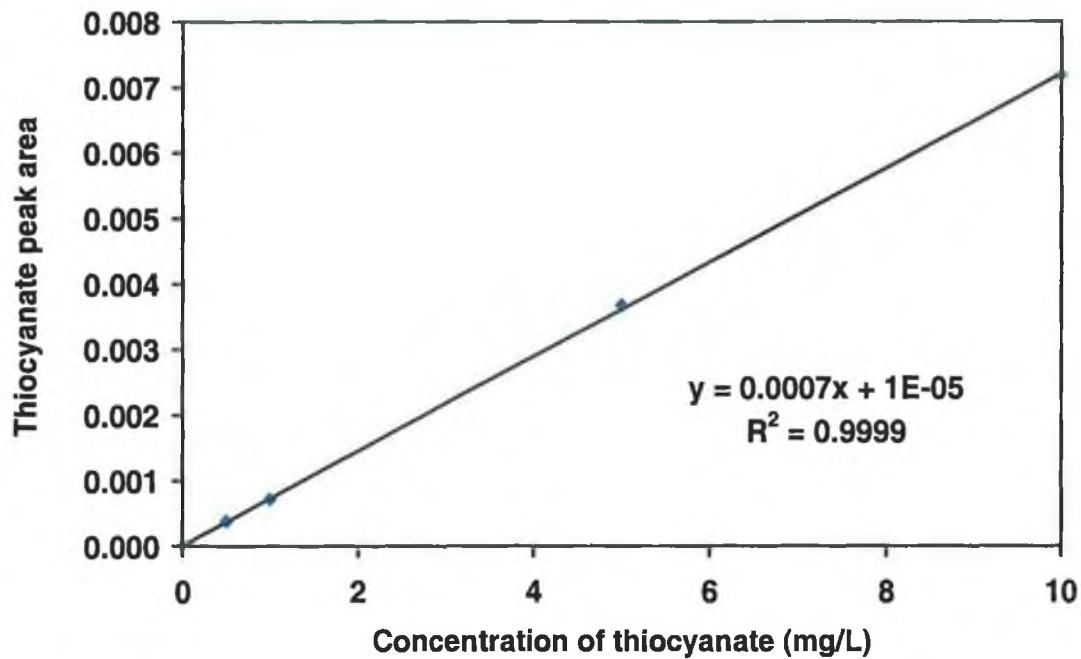


Figure 4-28. Thiocyanate linearity study on an AS17 anion exchange column.

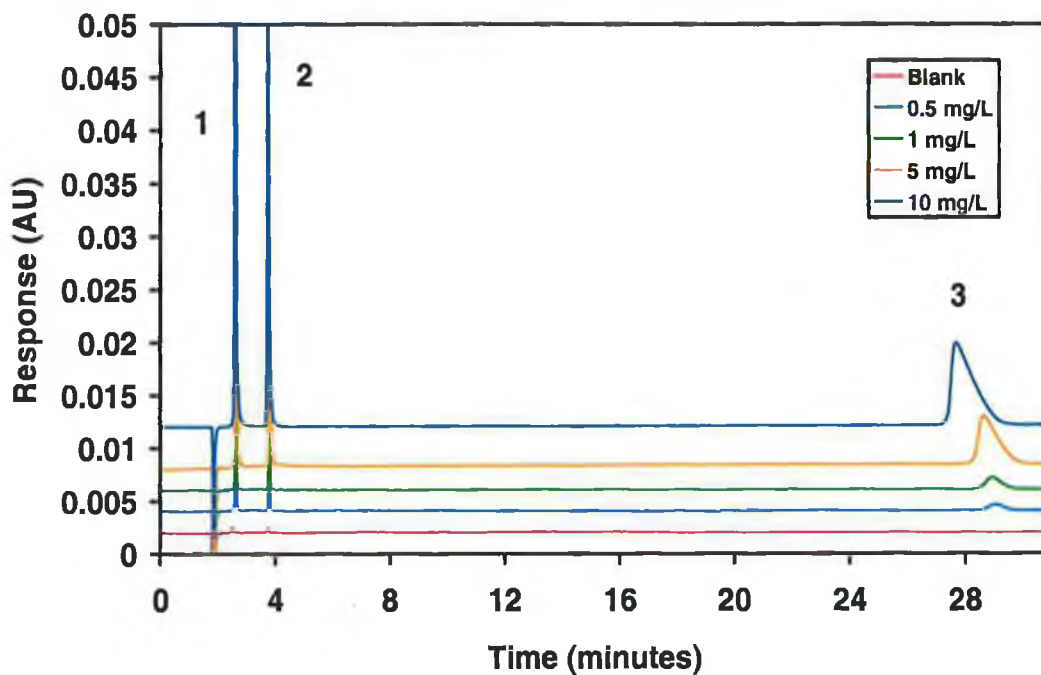
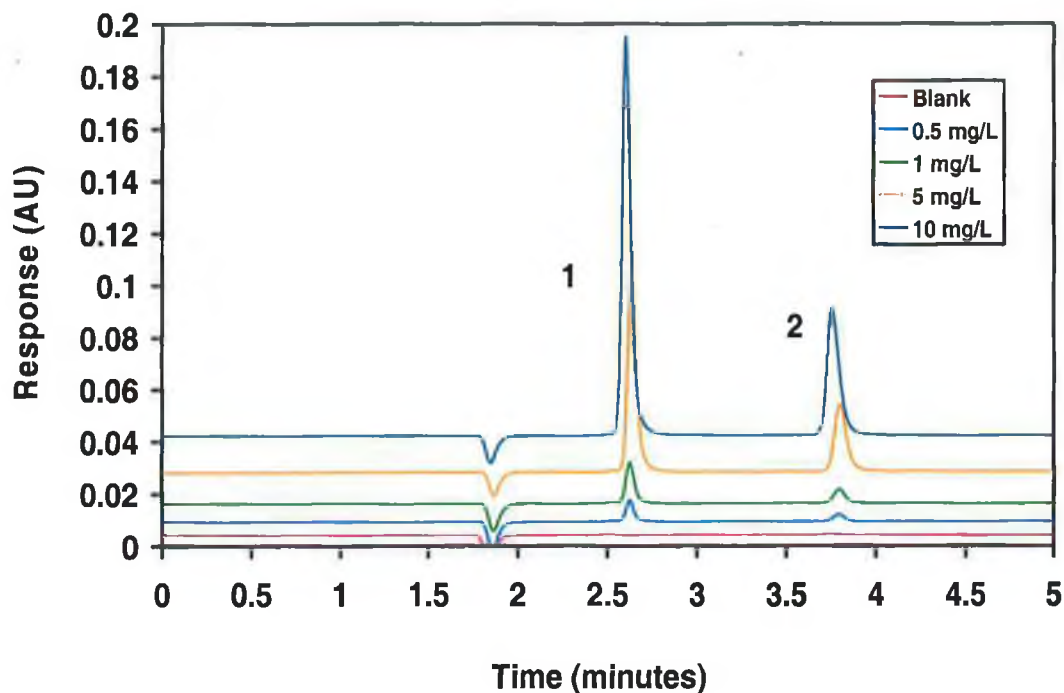


Figure 4-29. Overlay of nitrate, nitrite and thiocyanate linearity standards on an AS17 anion exchange column. Chromatographic conditions as in Figure 4-24. Peaks: [1] nitrite, [2] nitrate, [3] thiocyanate.



**Figure 4-30.** Expansion of Figure 4-29 showing an overlay of nitrite and nitrate linearity standards on an AS17 anion exchange column.

#### 4.3.7.4 Sensitivity.

Using a 25  $\mu\text{L}$  loop, limits of detection were determined for nitrite, nitrate and thiocyanate. Peak heights were measured in triplicate, as were noise determinations in the blank. Limits of detection were 5  $\mu\text{g/L}$  for nitrite, 54.3  $\mu\text{g/L}$  for nitrate, and 117.7  $\mu\text{g/L}$  for thiocyanate, assuming a signal/noise ratio of  $\geq 3$ . It should be noted that the quality of the water used in the laboratory varied from day to day throughout this study, and so co-eluting system peaks with nitrate and nitrite were unavoidable. However, in the case of nitrate, since levels of this anion are likely to be present at much higher levels in the samples analysed, this was not considered a major concern. In the case of nitrate and nitrite, noise values were determined by measuring the peak heights of the co-eluting system peaks. For thiocyanate, noise values were measured in the blank from 20 minutes to 28 minutes.

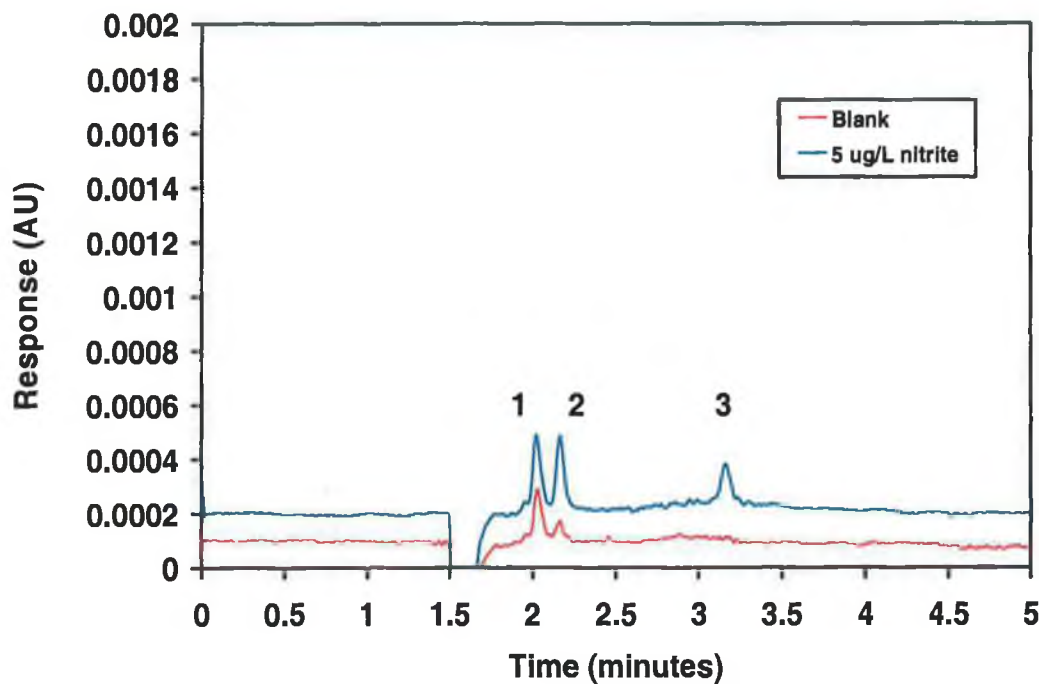


**Figure 4-31.** Sensitivity study for a 5 µg/L nitrite standard determination by anion exchange chromatography. Chromatographic conditions as in Figure 4-24. Peaks: [1] system peak, [2] nitrite, [3] nitrate.

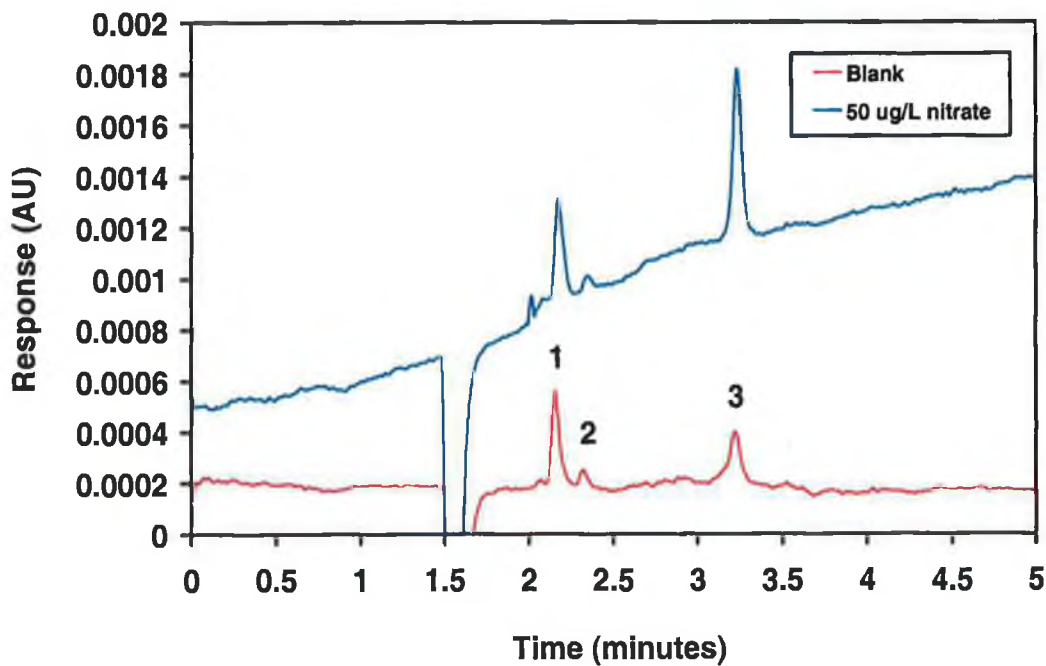


**Figure 4-32.** Sensitivity study for a 50 µg/L nitrate standard determination by anion exchange chromatography. Chromatographic conditions as in Figure 4-24. Peaks: [1] system peak, [2] nitrite, [3] nitrate.

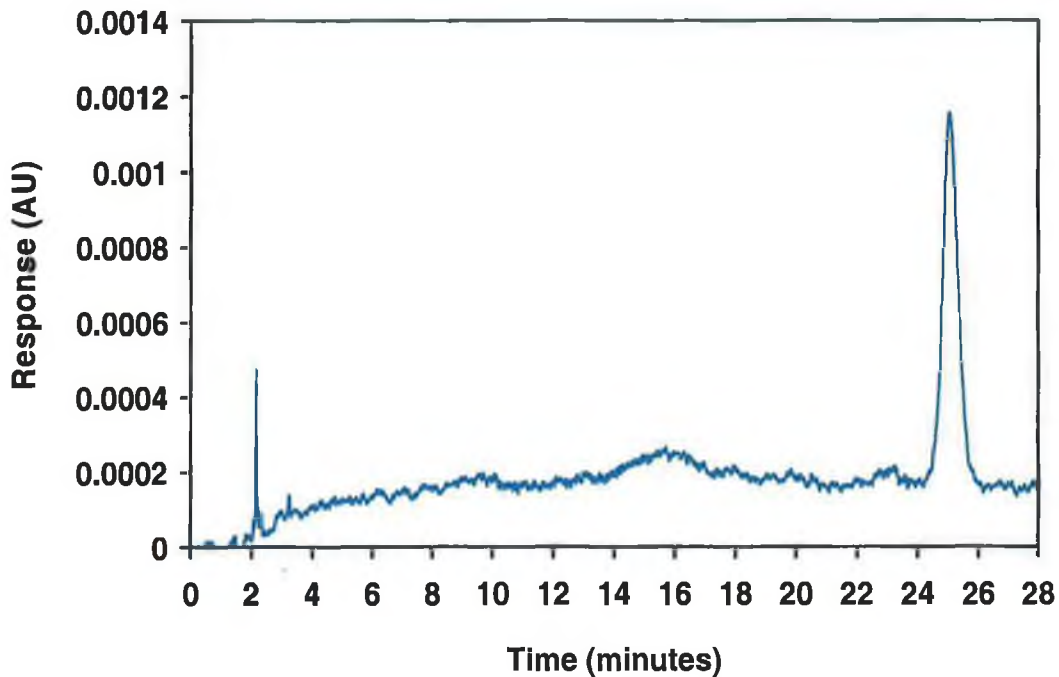


**Figure 4-33.** Sensitivity study for a 500 µg/L thiocyanate standard determination by anion exchange chromatography. Chromatographic conditions as in Figure 4-24.

#### 4.3.7.5 Analysis of real samples; thiocyanate spike linearity.

Urine samples were subjected to the same sample pre-treatment steps as described previously and injected, using the chromatographic conditions described in Figure 4-24. Figure 4-34 illustrates an overlay of a urine sample from a heavy smoker, diluted 1/40 and spiked with increasing concentrations of thiocyanate. The 1/40 urine dilution was spiked with thiocyanate over the range 0.7 mg/L to 5 mg/L, representing concentrations of thiocyanate in the raw, undiluted sample of 28 mg/L to 200 mg/L, and was found to be linear, with a correlation coefficient of > 0.9990.

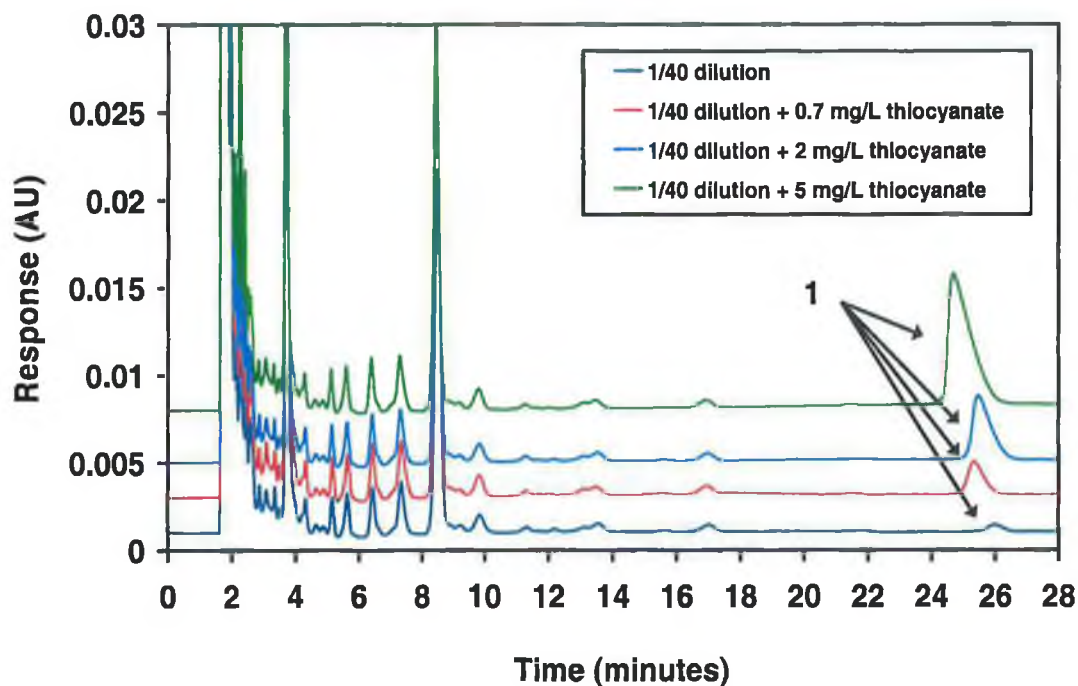


Figure 4-34. Analysis of a heavy smokers' urine sample by anion exchange chromatography diluted 1/40 and spiked with thiocyanate. Chromatographic conditions as in Figure 4-24.

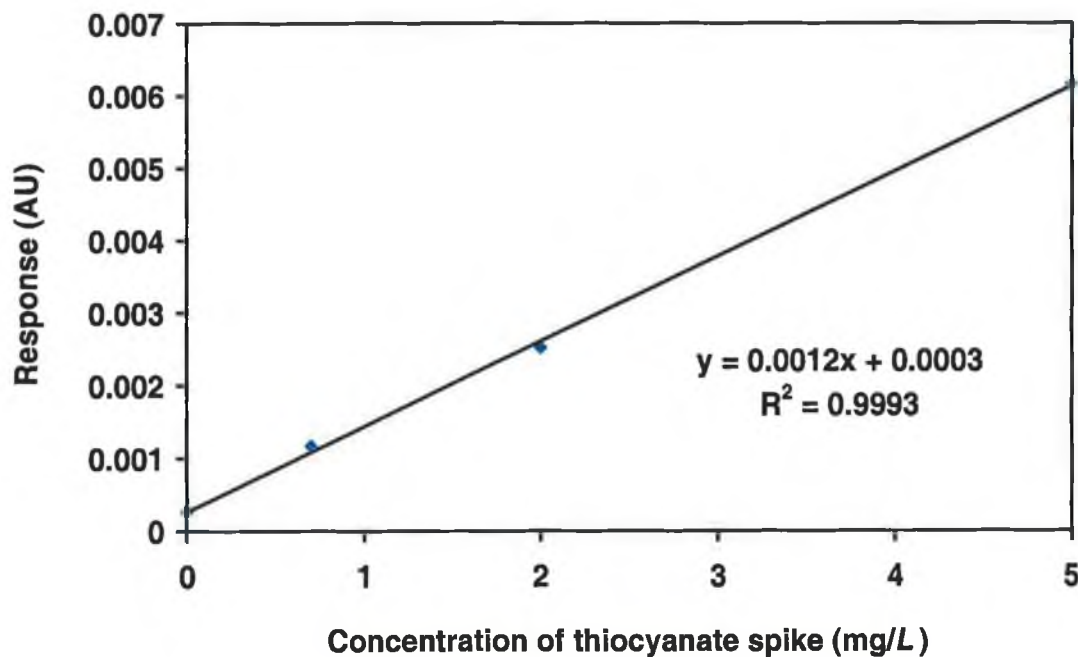
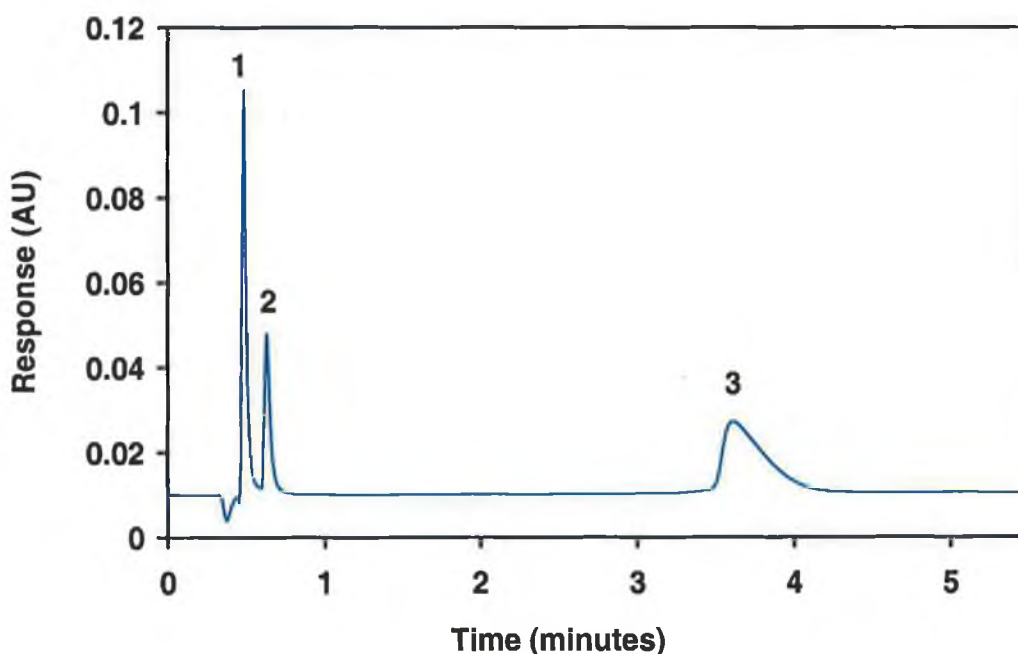


Figure 4-35. Thiocyanate standard addition linearity study for a heavy smokers' urine sample diluted 1/40 as determined by anion exchange chromatography. Chromatographic conditions as in Figure 4-24.

#### 4.3.7.6 Use of an AG17 guard column to reduce analysis times.

In an attempt to reduce the runtime of the anion-exchange separation achieved on the AS17 column, an AG17 guard column was used to separate the anion mix with a mobile phase of 35 mM NaOH in 1 % MeOH. Good resolution between nitrite and nitrate was achieved, and the total runtime was under 5 minutes. However, the thiocyanate peak still displayed some tailing. Further studies with this guard column separation were not advanced, not least because the high ionic strength of the urine samples may have caused difficulties due to the reduced column length. However, the preliminary separation shown in Figure 4-36 demonstrates nevertheless that faster separations are possible by using short anion-exchange guard columns in place of longer analytical columns. When Figure 4-4 is compared with Figure 4-36, the poor peak shape for thiocyanate on the AG17 guard column is indicative however of the advantages of ion-interaction chromatography for rapid determination of thiocyanate.



**Figure 4-36.** Preliminary rapid separation of nitrite, nitrate and thiocyanate on an AG17 anion exchange guard column. Conditions: Column: Dionex AG17 5.0 cm X 4.6 mm, Mobile phase: 35 mM NaOH in 1 % MeOH, Flow rate: 1.0 ml/min, Injection volume: 25  $\mu$ L, Detection: 230 nm. Peaks: [1] nitrite, [2] nitrate, [3] thiocyanate.

#### 4.4 Conclusions.

A very simple, rapid and selective method for urinary nitrite, nitrate and thiocyanate determinations has been shown. The method uses only a short inexpensive analytical column, resulting in shorter runs times, allowing rapid method development, system calibration and sample analysis. Applied to urine samples taken from smokers and non-smokers, the method showed how the chromatography can be used to indicate the smoking behaviour of the donor through determination of thiocyanate. Nitrate was also well resolved from matrix interferants, such that the method could also be used for evaluation of other clinical conditions in which changes in nitrate levels are noted.

In addition, a comparative study was also performed on a conventional anion exchange column, demonstrating that despite comparable precision, sensitivity and linearity being achieved, runtimes were increased by a factor of three. The use of shorter anion-exchange columns (AG17) illustrated that the chromatographic efficiency obtained on the reversed phase column of comparable length was much improved due to the difference in stationary phase characteristics.

#### 4.5 References.

- [1]. J. Potter, R.L. Smith, A.M. Api, *Food. Chem. Toxicol.* 39 (2001) 141.
- [2]. S. Chinaka, N. Takayama, Y. Michigami, K. Ueda, *J. Chromatogr. B* 713 (1998) 353.
- [3]. Y. Michigami, T. Takahashi, F. He, Y. Yamamoto, K. Ueda, *Analyst* 113 (1988) 389.
- [4]. Z. Glatz, S. Novakova, H. Sterbova, *J. Chromatogr. A* 916 (2001) 273.
- [5]. G. Zhang, B. Li, J. Fan, S. Feng, *Talanta* 44 (1997) 1141.
- [6]. A.A. Ensafi, J. Tajebakhsh-E-Ardakany, *Anal. Letters* 28 (1995) 731.
- [7]. K. Funazo, M. Tanaka, T. Shono, *Anal. Chem.* 53 (1981) 1377.
- [8]. Y. Michigami, K. Fujii, K. Ueda, Y. Yamamoto, *Analyst* 117 (1992) 1855.
- [9]. A.B. Bendtsen, E. H. Hansen, *Analyst* 116 (1991) 647.
- [10]. S. Kage, T. Nagata, K. Kudo, *J. Chromatogr. B* 675 (1996) 27.

- [11]. G. Ellis, I. Adatia, M. Yazdanpanah, S.K. Makela, *Clin. Biochem.* 31 (1998) 195.
- [12]. S.A. Everett, M.F. Dennis, G. Tozer, V.E. Prise, P. Wardman, M.R.L. Stratford, *J. Chromatogr. A* 706 (1995) 437.
- [13]. P.A. Marshall, C. Trenerry, *Food Chem.* 57 (1996) 339.
- [14]. M. Jimidar, C. Hartmann, N. Cousement, D.L. Massart, *J. Chromatogr. A* 706 (1995) 479.
- [15]. I. Gil Torro, J.V. Garcia Mateo, J. Martinez Calatayud, *Anal. Chim. Acta.* 366 (1998) 241.
- [16]. M.J. Ahmed, C.D. Stalikas, S.M. Tzouwara-Karayanni, M.I. Karayannis, *Talanta* 43 (1996) 1009.
- [17]. O. Pinho, I.M.P.L.V.O. Ferreira, M.B.P.P. Oliveira, M. Ferreira, *Food Chem.* 62 (1998) 359.
- [18]. A.A. Ensafi, A. Kazemzadeh, *Anal. Chim. Acta.* 382 (1999) 15.
- [19]. Y. Michigami, Y. Yamamoto, K. Ueda, *Analyst* 114 (1989) 1201.
- [20]. M.I.H. Helaleh, T. Korenaga, *J. Chromatogr. B* 744 (2000) 433.
- [21]. B. Maiti, A.P. Walkevar, T.S. Krishnamoorthy, *Analyst* 114 (1989) 731.
- [22]. M.N. Muscara, G. de Nucci, *J. Chromatogr. B* 686 (1996) 157.
- [23]. H. Li, C.J. Meininger, G. Wu, *J. Chromatogr. B* 746 (2000) 199.
- [24]. R.L. Smith, Z. Iskandarani, D.J. Pietrzyk, *J. Liq. Chromatogr.* 7 (1984) 1935.
- [25]. M. C. Gennaro, P.L. Bertolo, A. Cordero, *Anal. Chim. Acta.* 239 (1990) 203.
- [26]. P.E. Jackson, S. Gokhale, T. Streib, J.S. Rohrer, C.A. Pohl, *J. Chromatogr. A* 888 (2000) 151.
- [27]. F.A. Cotton, G. Wilkinson, P.L. Gaus, *Basic Inorganic Chemistry*, 3<sup>rd</sup> edition, Wiley, 1995.
- [28]. P.R.Haddad, P.E.Jackson, *Ion Chromatography: Principles and Applications*, *J. Chromatogr. Library*, Vol.46, Elsevier, Amsterdam, 1990.
- [29]. *Dionex IonPac AS16 Product Information Bulletin*, Dionex Corporation, Sunnyvale, California, 1999.